UNIVERSIDADE FEDERAL DE MINAS GERAIS
Instituto de Ciências Biológicas
Programa de Pós-Graduação em Zoologia

Rafaela Velloso Missagia

MACROEVOLUTIONARY AND ECOLOGICAL PATTERNS OF THE MORPHOLOGICAL EVOLUTION OF AKODONTINE RODENTS

Belo Horizonte
2019

Rafaela Velloso Missagia

MACROEVOLUTIONARY AND ECOLOGICAL PATTERNS OF THE MORPHOLOGICAL EVOLUTION OF AKODONTINE RODENTS

Versão Final

Tese apresentada ao Programa de Pós-Graduação em Zoologia da Universidade Federal de Minas Gerais, como requisito parcial à obtenção do título de Doutor em Zoologia.

Orientador: Fernando Araújo Perini

Belo Horizonte
2019

043 Missagia, Rafaela Velloso.
Macroevolutionary and ecological patterns of the morphological evolution of akodontine rodents [manuscrito] / Rafaela Velloso Missagia. – 2019.

230 f. : il. ; 29,5 cm.

Orientador: Prof. Dr. Fernando Araújo Perini.
Tese (doutorado) – Universidade Federal de Minas Gerais, Instituto de Ciências Biológicas. Programa de Pós-Graduação em Zoologia.

1. Zoologia. 2. Morfologia (Animais). 3. Sigmodontinae. 4. Isótopos estáveis. I. Perini, Fernando Araújo. II. Universidade Federal de Minas Gerais. Instituto de Ciências Biológicas. III. Título.

CDU: 591

Ficha catalográfica elaborada pela bibliotecária Rosilene Moreira Coelho de Sá – CRB 6 - 2726

ATA DE DEFESA DE TESE DE DOUTORADO

Rafaela Velloso Missagia

Ao décimo quarto dia do mês de agosto do ano de dois mil e dezenove, às quatorze horas, na Universidade Federal de Minas Gerais, teve lugar a defesa de Doutorado da Pós-Graduação em Zoologia, de autoria da Doutoranda Rafaela Velloso Missagia intitulada: **"Macroevolutionary and ecological patterns of the morphological evolution of akodontine rodents"**. Abrindo a sessão, o Presidente da Comissão, Prof. Dr. Fernando Araújo Perini, após dar a conhecer aos presentes o teor das Normas Regulamentares do Trabalho Final, passou a palavra para a candidata para apresentação de seu trabalho.

Esteve presente a Banca Examinadora composta pelos membros: Adriano Pereira Paglia, Ana Paula Carmignotto, Lucilia Souza Miranda, Pablo Rodrigues Gonçalves, e demais convidados. Seguiu-se a arguição pelos examinadores, com a respectiva defesa da candidata.

Após a argüição, apenas os Srs. Examinadores permaneceram na sala para avaliação e deliberação acerca do resultado final, a saber: o trabalho foi:

- [x] Aprovado sem alterações
- [ ] Aprovado com alterações (observações em anexo)
- [ ] Reprovado

Nada mais havendo a tratar, a Presidente da Comisão encerrou a reunião e lavrou a presente ata, que será assinada por todos os membros participantes da Comissão Examinadora.

Belo Horizonte, 14 de agosto de 2019.

Comissão Examinadora	Assinatura
Prof. Dr. Adriano Pereira Paglia	
Profa. Dra. Ana Paula Carmignotto	
Prof. Dr. Fernando Araújo Perini (Orientador)	
Profa. Dra. Lucilia Souza Miranda	
Prof. Dr. Pablo Rodrigues Gonçalves	

In memory of my father, my biggest fan.

ACKNOWLEDGEMENTS

I thank my advisor for the idea that gave rise to this dissertation, and for his enthusiasm for each result of this work. Thank you, Fernando, for all that you have taught me during these years.

I am fortunate to have had the chance to meet and work with Bruce Patterson, who kindly received me at the Field Museum during my sandwich fellowship. Thank you for always being willing to talk about our work, for your guidance, and for giving me the opportunity to spend a few months working at the museum with you and so many amazing people. I cherish the memory of these months with endearment.

This dissertation would not have been possible without the financial support from CAPES, which funded my four years of doctorate, including six months of sandwich fellowship.I also thank the members of the evaluation comittee, and the staff and teachers of the UFMG Graduate course in Zoology.

This study, like many others, was only possible because of the people who work to maintain all scientific collections. In a world where scientific thinking has been increasingly devalued, their work is invaluable, and I am very grateful to the curators and staff of the mammalian collections of the Field Museum of Natural History, American Museum of Natural History, National Museum of Natural History, National Museum of the Federal University of Rio de Janeiro, Museum of Natural History of the Pontifical Catholic University of Minas Geraisand Center for Taxonomic Collections of the Federal University of Minas Gerais, which allowed me access to the material.

The opportunity to collaborate and discuss with others greatly improves the quality of our work. I was lucky to come across many people who somehow contributed to these results. Special thanks to Daniel Casali, who contributed immensely to Chapter 4, for his innumerous conversations on the subject. I am grateful to everyone who spent time at coffee breaks to discuss evolutionary processes, biomechanics, rodents, methods, and the science itself.

I am especially grateful for all the friends I have made in Belo Horizonte and Chicago over the last four years. To those at the Field Museum, thank you for welcoming me (especially our “Latin family”), and to those from Belo Horizonte, thank you for helping me feel at home.

No woman is an island, and I am grateful to all my friends outside academia for the shared beers.

To my parents, Zélia Missagia and Rogério Missagia, who always gave me love and support, and worked hard to give me the best conditions to get here. They taught me to do my best, be kind, and always celebrate when deserved. A toast to you, who will always be an inspiration to me.

To Rogério Velloso Missagia, thank you for being my big brother.

To João, the one with whom I can laugh at everything, with whom I share a life with all its exciting and not so exciting moments. Thank you for being by my side during all these years.

And, lastly, thank you, Ioiô, for keeping me company during the writing of this dissertation, you are the best cat in the world.

"'It's just like I always tell my daughter,' said the man. 'Stories are just stories. Life is complicated enough as it is. We have to plan for the real world. There's no room for the fantastic.''Exactly,' said the rat."

The Amazing Maurice and his Educated Rodents,

Terry Pratchett.

RESUMO

A história evolutiva da tribo Akodontini é caracterizada por uma radiação bem-sucedida na América do Sul. Eles são diversos em morfologia e tipos adaptativos, e particularmente ricos em espécies insetívoras. No entanto, os padrões macroevolutivos e ecológicos permanecem quase inexplorados no grupo. Coletamos um conjunto de dados morfológicos abrangentes e amostras de pelo de espécies de Akodontini para análises funcionais, ecológicas e macroevolutivas, e os resultados foram comparados entre as quatro linhagens principais de Akodontini. Através de uma descrição morfológica comparativa, mostramos que as características cranianas de *Blarinomys breviceps* refletem seus hábitos fossoriais e dieta insetívora. Fornecemos novos dados isotípicos para 47 espécies de roedores Akodontini, representando a primeira informação ecológica desse tipo para algumas delas. O conjunto de dados de isótopos estáveis foi analisado através de uma perspectiva macroecológica, fornecendo informações sobre a diversidade de nichos tróficos dentro do grupo. A distribuição de algumas espécies no espaço de nicho trófico corroborou os dados de conteúdo estomacal da literatura, e observou-se que os clados na tribo ocupam o espaço de nicho trófico de maneira semelhante, embora diferindo na sua diversidade trófica. Ao analisar a influência da dieta na morfologia, descobrimos que os traços funcionais da mandíbula refletem a ecologia alimentar dos roedores Akodontini. Enquanto as espécies herbívoras apresentam maiores vantagens mecânicas e forças de mordida para processar o material vegetal, as espécies insetívoras favorecem a velocidade sobre a força do aparelho mandibular, mais útil para capturar presas vivas. A linhagem mais antiga da tribo também é a mais diversa em ecologia e morfologia craniana, e compreende um conjunto de espécies que parecem ter adquirido uma morfologia especializada que corresponde, em parte, a diferentes hábitos alimentares. Em geral, a contingência histórica parece ter mais influência nos padrões de disparidade em tamanho e forma em Akodontini, com a ecologia alimentar tendo um papel secundário. Encontramos evidências de um padrão de evolução convergente em quatro linhagens de Akodontini, que apresentam uma forma semelhante do crânio, aparentemente em resposta à especialização à insetivoria.

Palavras-chave: evolução morfológica, Sigmodontinae, métodos comparativos, morfologia funcional, isótopos estáveis, nicho trófico, macroevolução.

ABSTRACT

The evolutionary history of Akodontini is characterized by a successful radiation in South America. They are diverse in adaptive types and morphology, and are particularly rich in soricine insectivorous species. However, macroevolutionary and ecological patterns remain mostly unexplored in the group. We collected a comprehensive morphological dataset and hair samples of Akodontini species for functional, ecological and macroevolutionary analyses, and the results were compared between the four main lineages of Akodontini. Through a comparative morphological description, we show that cranial characteristics of *Blarinomys breviceps* reflect its fossorial habits and insectivorous diet. We provided new isotopic data for 47 species of Akodontini rodents, representing the first ecological information of this kind for some of them. The stable isotopes dataset was analyzed from a macroecological perspective, and gave insights about the trophic niche diversity inside the group. The distribution of some species on the bivariate isospace corroborated stomach content data from the literature, and the clades whitin the tribe occupy the bi-plot in a similar way, although differing in trophic diversity. When analysing the influence of diet on morphology, we found that functional traits of the jaw reflect feeding ecology in akodontine rodents. While herbivorous species present higher mechanical advantages and bite forces to process plant material, insectivorous species favour speed over strength of the jaw apparatus, more useful for catching live prey. The oldest lineage within the tribe is also the most diverse in ecology and cranial morphology. Although not taxonomically rich, it comprises a set of species that appear to have acquired a specialized morphology corresponding, in part, to different feeding habits. In general, historical contingency seems to have more influence on the patterns of disparity in size and shape in Akodontini, with feeding ecology having a secondary role. We found evidence for a pattern of convergent evolution in four Akodontini lineages, which present a similar skull shape apparently in responseto specialization to an insectivorous diet.

Keywords: morphological evolution, Sigmodontinae, comparative methods, functional morphology, stable isotopes, trophic niche, macroevolution.

Summary

GENERAL INTRODUCTION

The order Rodentia is by far the most diverse among living mammals (Wilson and Reeder 2005, Hautier and Cox 2015). Rodents have a distinct skull morphology when compared with other mammals, mainly due to the long diastema separating the ever-growing developed incisors from the rest of the teeth, the longitudinal orientation of the glenoid fossa, and the position of the orbital cavity, dorsal to the check teeth (Wood 1965, Landry 1970, Turnbull 1970,Hautier and Cox 2015). Rodents also have a distinct architecture of masticatory muscles when compared with other mammals, with a highly developed masseter complex that appears in different conformations within the group (Wood 1965, Swanson et al. 2019). Several of these differences are associated with an increase in strength and change in the line of action of these muscles, which are optimized for gnawing at the incisors or chewing at the molars, depending ontheir conformation (Swanson et al. 2019). The high adaptability of rodents allowed the occupation of virtually all terrestrial environments around the world during their evolutionary history, and they are considered a "model-group" to study patterns of convergence and macroevolution (Hautier and Cox 2015).

The suborder Myomorpha Brants, 1855 differ from the others by presenting a morphology of the masticatory muscles that allows them to be efficient as generalist feeders (Cox et al. 2012), which may have contributed to their high diversity and wide geographical range (Lacher et al. 2016). Among myomorphs, Cricetidae G. Fischer, 1817 is one of the most diverse families, comprising approximately 700 species distributed on the Palearctic, Nearctic and Neotropical regions (Lacher et al. 2016). They are adapted to a wide range of environments and, together with Muridae Illiger, 1811, encompass a large part of the morphological variation among myomorph rodents (Alhajeri and Steppan 2018).

Among Cricetidae, the subfamily Sigmodontinae Wagner, 1843 is the most diversified group of mammals in South America (Wilson and Reeder 2005, D'Elía and Pardiñas 2015, Pardiñas et al. 2017). Estimates for their arrival from North America are usually between middle to late Miocene (~12 mya), before the complete closure of the Panamanian isthmus (Reig 1972, Leite et al. 2014, Maestri et al. 2019), and they are currently found from Tierra del Fuego to Central America (D'Elía and Pardiñas 2015). Most of its species are endemic to South America (D'Elía and Pardiñas 2015, Pardiñas et al. 2017), where they reach high diversity and occupy practically all terrestrial biomes, from tropical lowlands to temperate portions of the Andes (Maestri and

Patterson 2016). Sigmodontinae rodents have been divided into tribes with variable content over the years, according to different phylogenetic proposals (Smith and Patton 1999, Jansa and Weksler 2004, Weskler 2006, D'Elía et al. 2007, Leite et al. 2014, Teta et al. 2016). Currently, eleven tribes comprise most of the 106 known Sigmodontinae genera (D'Elía and Pardiñas 2015, Pardiñas et al. 2017, Cazzaniga et al. 2019).

The tribe Akodontini Cockerell and Printz 1914 (in Cockerell et al. 1914) is the second most diverse among Sigmodontinae (D'Elía and Pardiñas 2015). The first mention of the group included only the genus *Akodon* Meyen, 1833 (Cockerell et al. 1914), and Thomas (1916, 1918) and Tate (1932) were the first to recognize the morphological similarity between *Akodon* and some other Sigmodontinae genera. However, recurring disagreements regarding the content ofthe informal group of so-called "akodont rodents" (Reig 1987) led to different generic groupings over time (Tate 1932, Vorontzov 1959, Hopper and Musser 1964, Hershkovitz 1966, Smith and Patton 1991, 1993, 1999). Only more recently the availability of molecular data allowed the establishment of a more well supported phylogenetic hypotheses for Akodontini (D'Elía 2003, Leite et al. 2014, Leite et al. 2015, Maestri et al. 2017, 2019, Steppan and Schenk 2017).

According to the most recent phylogenies (Maestri et al. 2017, 2019, Steppan and Schenk 2017), four main lineages can be recognized within the tribe: one comprising the highly diverse genus *Akodon*, together with *Castoria* Pardiñas, Geise, Ventura and Lessa, 2016 and *Deltamys* Thomas, 1917*,* representing the majority of akodontine species; a second group including *Necromys* Ameghino, 1889, *Podoxymys* Anthony, 1929, *Thalpomys* Thomas, 1916, and *Thaptomys* Thomas, 1916, sister-group of the later; a third lineage comprising of the insectivore specialists *Oxymycterus* Waterhouse, 1837 and *Juscelinomys* Moojen, 1965, sister- group of the *Akodon* and *Necromys* lineages; and, lastly, a lineage comprising *Blarinomys* Thomas 1896, *Brucepattersonius* ,Hershkovitz, 1998, *Bibimys* Massoia, 1979, *Lenoxus* Thomas, 1909, *Kunsia* Hershkovtz, 1966, and *Scapteromys* Waterhouse, 1837 sister to all of the previous clades (Fig. 1).

The evolutionary history of Akodontini is characterized by a successful radiation and ecological versatility (Reig 1972, 1987, D'Elía and Pardiñas 2015), which allowed the occupation of a wide variety of habitats in South America (D'Elía and Pardiñas 2015, Maestri et al. 2019). Therefore, in addition to being one of the tribes with the greatest taxonomic diversity, akodontine rodents are also particularly diverse in adaptive types (Hershkovitz 1966, Reig 1972, 1987, D'Elía and Pardiñas 2015), including specialized fossorial genera (*Blarinomys*), the largest living

sigmodontines (*Kunsia*, *Gyldenstolpia* and *Scapteromys*), and more generalists vole-like cursorial rodents (some species of the *Akodon* and *Necromys* genera) (D'Elía and Pardiñas 2015)(Fig. 2). In Chapter 1 of this dissertation, we described the skull of the fossorial shrew mouse *Blarinomys breviceps*, comparing it with other Akodontini genera and focusing on aspects related to its insectivorous diet and underground mode of life.

Diet is usually defined as the most common resource consumed by an organism (Pineda-Munoz and Alroy 2014), and is an important feature of the natural history of a species. Due to its high impact on fitness, diet is often subject of high selective pressures (Pineda-Munoz and Alroy 2014), and information about feeding ecology can serve as basis for ecomorphology, adaptation and evolutionary studies (Pineda-Munoz and Alroy 2014, Davis and Pineda-Munoz 2016). Most rodents have an opportunistic diet, consuming seeds, leaves, and invertebrates, according to the availability of these resources in their habitat (Landry 1970, Meserve et al. 1988). However, some rodent species are remarkably specialized in their feeding ecology, ranging from strict leaf and seed eaters to invertebrate consumers (Verde Arregoitia 2016).

Direct evidence of small mammal diets is usually difficult to obtain due to their cryptic behavior, nocturnal habits, and small size, which prevent observations from being obtained in their natural environment. Because of that, stomach and fecal content analyses have been commonly used to access diet information for several rodent species (Pizzimenti and de Salle 1980, Ellis et al. 1998). However, rodent diets, especially in the Neotropics, are still poorly understood, and cumulative evidence is necessary for a better understanding of the trophic niche of a given species. More recently, stable isotope analysis is gaining relevance as a new approach to obtain ecological data. They record natural processes by measuring assimilated components on organic tissues, allowing researchers to infer the nature of consumed food resources (Crawford et al. 2008). While stomach content data can only inform about last ingested food items, stable isotope analyses time-averages over longer time periods and, depending on the tissue, can give information about food items consumed over the last weeks to months (Davisand Pineda-Munoz 2016). Furthermore, it is possible to gather stable isotope information from museum specimens, allowing access to a species diet information in a time span of decades, and across their entire distribution. However, since they are specimen-specific, these analyses are usually applied to community and population ecology studies, and are less commonly used in a macroevolutionary scale. Chapter 2 brings stable isotope information of 47 Akodontini species, analyzed in an explicitly phylogenetic context over

a macroevolutionary scale, with considerations about the diversity of trophic niche of the four main lineages of the tribe.

Morphological traits can, by themselves, provide evolutionary and phylogenetic insights (Wiens 2004). However, when considering ecological information, morphology can be used to address questions concerning adaptive factors (Fig. 3). Some rodents species are remarkably specialized for invertebrate consumption, and insectivorous species appeared repeatedly among myomorph rodents (Samuels 2009, Rowe et al. 2016). They have convergently evolved several morphological characteristics in skull, teeth, masticatory muscles, and digestive tract (Langer 2002, Samuels 2009, Rowe et al. 2016) that are known to improve their ability to feed on liveprey (Samuels 2009). Akodontini rodents present a great diversity of cranial morphologies andsizes, with a variety of more gracile soricine types contrasting with robust gopher-like species (Hershkovitz 1966, Reig 1987, D'Elía and Pardiñas 2015). This diversity may be related tofeeding ecology, since dietary pressures can affect some functional properties of the skull (Satoh1999, Fabre et al. 2018). In Chapter 3, we accessed the morphology of the jaw of akodontinerodents to establish if functional measures related to the action of different muscle groups can berelated to differences in bite force. Additionally, we tested possible correlations between thesetwo functional measurements and diet, represented by literature data and stable isotope values.We expected that variations on functional measures of the jaw would be correlated withdifferences in feeding behavior.

Although morphological diversity is often studied under an adaptational context, it is probably shaped by a combination of historical and ecological factors (Erwin 2007), and the incorporation of phylogenetic information becomes necessary to better understand morphological evolution. Considering the influence of diet on skull morphology (Samuels 2009),in Chapter 4 we aimed to evaluate if feeding ecology influences the rates of morphological evolution of the skull of Akodontini rodents. We also analyzed how the morphological disparity of the cranial complex of akodontine rodents is distributed along the phylogeny. We believe that answering these questions could help us to achieve a better understanding of the morphological evolution of the Akodontini tribe, particularly the influence of ecological and historical factors inshaping the morphological diversity observed in this group.

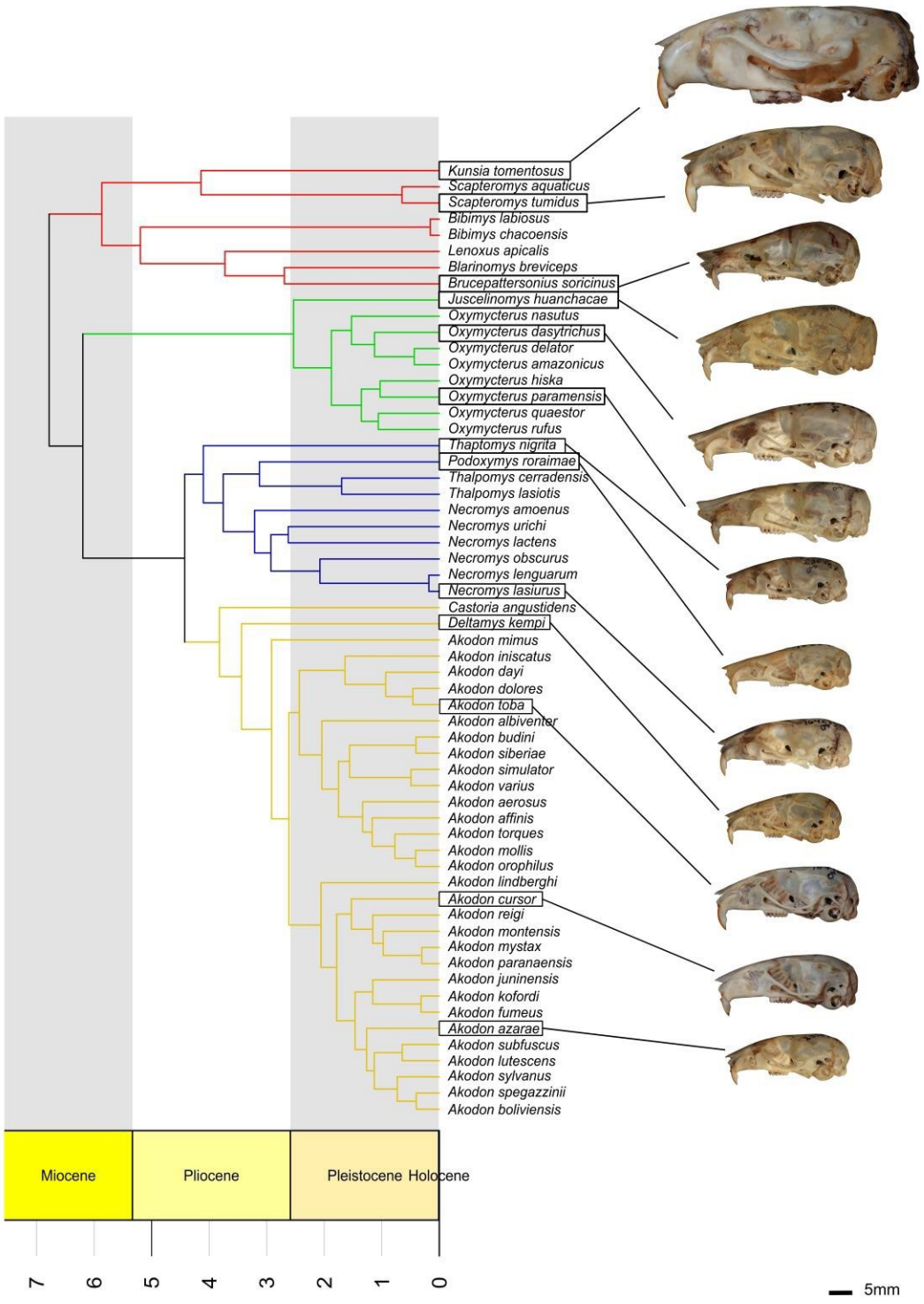

Figure 1. Phylogenetic hypothesis for Akodontini modified from Maestri et al. (2017), with different colors representing the four mains lineages. Skull of some species depicted on the right. Scale bar: 5mm.

Figure 2. Living specimens of Akodontini: (a) *Oxymycterus nasutus* (photo by Guilherme Grazzini); (b) *Necromys lasiurus* (photo by Shivani Raval); (c) *Scapteromys tumidus* (photo by Ricardo Roth); (d) *Kunsia tomentosus* (photo by Louise Emmons); (e) *Deltamys kempi* (photo by Ricardo Roth); (f) *Thaptomys nigrita* (photo by Ricardo Roth); (g) *Akodon montensis* (photo by Ricardo Roth); (h) *Juscelinomys hunchacae* (photo by Louise Emmons).

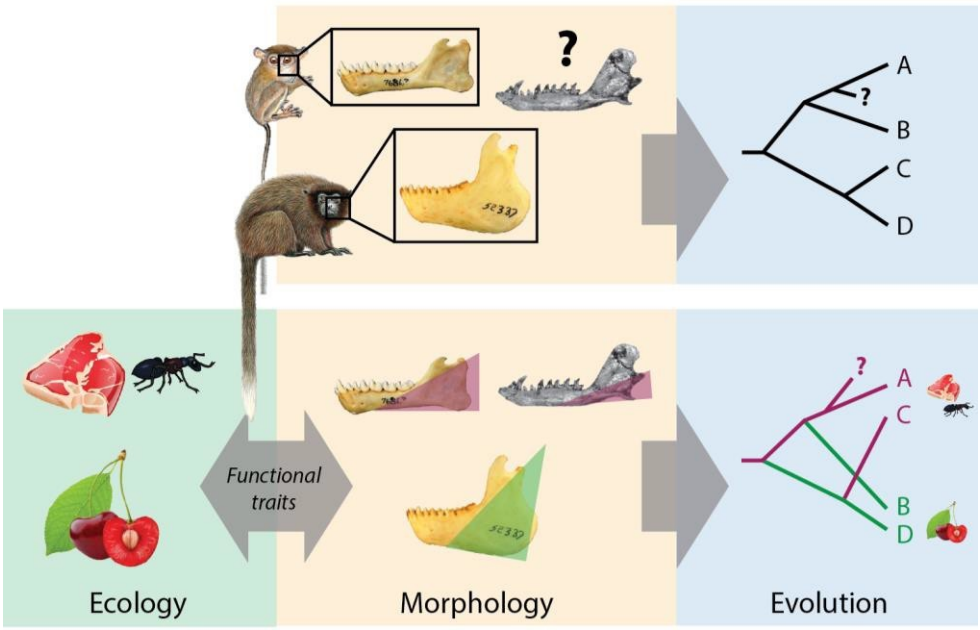

Figure 3. Besides information about phylogenetic relationships, morphological traits can give us insights on adaptive hypothesis about the influence of ecological traits on morphological evolution. Figure from Grossnickle (2018).

REFERENCES

Alhajeri, B.H. and Steppan, S.J., 2018. Ecological and ecomorphological specialization are not associated with diversification rates in muroid rodents (Rodentia: Muroidea). Evolutionary Biology, 45(3), pp. 268-286.

Cazzaniga, N.J., Cañón, C. and Pardiñas, U.F.J., 2019. The availability, authorships and dates of tribal names in the Sigmodontinae (Rodentia, Cricetidae) current classification. Bionomina, 15(1), pp. 37-50.

Cockerell, T.D.A., Miller, L.I. and Printz, M., 1914. The auditory ossicles of American Rodents. Bulletin of the American Museum of Natural History, 33(28), pp. 347–380.

Cox, P.G., Rayfield, E.J., Fagan, M.J., Herrel, A., Pataky, T.C. and Jeffery, N., 2012. Functional evolution of the feeding system in rodents. PLoS One, 7(4), p. E36299.

Crawford, K., Mcdonald, R.A. and Bearhop, S., 2008. Applications of stable isotope techniques to the ecology of mammals. Mammal Review, 38(1), pp. 87-107.

D'Elía, G., 2003. Phylogenetics of Sigmodontinae (Rodentia, Muroidea, Cricetidae), with specialreference to the akodont group, and with additional comments on historical biogeography. Cladistics, 19(4), pp. 307-323.

D'Elía, G., Pardiñas, U.F.J, Teta, P. and Patton, J.L., 2007. Definition and diagnosis of a new tribe of sigmodontine rodents (Cricetldae: Sigmodontinae), and a revised classification ofthe subfamily. Gayana, 71(2), pp. 187-194.

D'Elía, G. and Pardiñas, U.F.J., 2015. Tribe Akodontini Vorontsov 1959. Mammals of South America, Volume 2: Rodents, pp. 140-144. Chicago: University of Chicago Press.

Davis, M. and Pineda-Munoz, S., 2016. The temporal scale of diet and dietary proxies. Ecology and Evolution, 6(6), pp. 1883-1897.

Ellis, B.A., Mills, J.N., Glass, G.E., McKee Jr, K.T., Enria, D.A. and Childs, J.E., 1998. Dietary habits of the common rodents in an agroecosystem in Argentina. Journal of Mammalogy, 79(4), pp. 1203-1220.

Erwin, D.H., 2007. Disparity: morphological pattern and developmental context. Palaeontology, 50(1), pp. 57-73.

Fabre, A.C., Perry, J.M., Hartstone-Rose, A., Lowie, A., Boens, A. and Dumont, M., 2018. Do muscles constrain skull shape evolution in strepsirrhines? The Anatomical Record, 301(2), p. 291-310.

Grossnickle, D.M., 2018. Macroevolutionary Patterns and Dietary Adaptations in Early Cladotherian Mammals. Ph.D. dissertation, The University of Chicago.

Hautier, L. and Cox, P.G., 2015. Rodentia: a model order. Evolution of the Rodents Advances in Phylogeny, Functional Morphology and Development, pp. 1-18.

Hershkovitz, P., 1966. South American swamp and fossorial rats of the scapteromyine group (Cricetinae, Muridae) with comments on the glans penis in murid taxonomy. Zeitschrift für Säugetierkunde, 31, pp. 81-149.

Hooper, E.T. and Musser, G.G., 1964. The glans penis in Neotropical cricetines (family Muridae) with comments on classification of muroid rodents. Miscellaneous Publications, Museum of Zoology, University of Michigan, 123, pp. 1-57.

Jansa, S.A. and Weksler, M., 2004. Phylogeny of muroid rodents: relationships within and among major lineages as determined by IRBP gene sequences. Molecular Phylogenetics and Evolution, 31(1), pp. 256-276.

Lacher, T.E., Murphy, W.J., Rogan, J., Smith, A.T. and Upham, N.S., 2016. Evolution, phylogeny, ecology, and conservation of the Clade Glires: Lagomorpha and Rodentia. Handbook of the Mammals of the World, Volume 6: Rodents I, pp.15-26. Barcelona: Lynx Edicions.

Landry Jr, S.O., 1970. The Rodentia as omnivores. The Quarterly Review of Biology, 45(4), pp. 351-372.

Leite, R.N., Kolokotronis, S.O., Almeida, F.C., Werneck, F.P., Rogers, D.S. and Weksler, M., 2014. In the wake of invasion: tracing the historical biogeography of the South American cricetid radiation (Rodentia, Sigmodontinae). PLoS One, 9(6), p. E100687.

Leite, Y.L., Kok, P.J. and Weksler, M., 2015. Evolutionary affinities of the 'Lost World'mouse suggest a late Pliocene connection between the Guiana and Brazilian shields. Journal of Biogeography, 42(4), pp. 706-715.

Maestri, R., Monteiro, L.R., Fornel, R., Upham, N.S., Patterson, B.D. and de Freitas, T.R.O., 2017. The ecology of a continental evolutionary radiation: Is the radiation of sigmodontine rodents adaptive? Evolution, 71(3), pp. 610-632.

Maestri, R., Upham, N.S. and Patterson, B.D., 2019. Tracing the diversification history of a Neogene rodent invasion into South America. Ecography, 42(4), pp. 683-695.

Meserve, P.L., Lang, B.K. and Patterson, B.D., 1988. Trophic relationships of small mammals in a Chilean temperate rainforest. Journal of Mammalogy 69(4), pp. 721-730.

Pardiñas, U.F.J., Myers, P., León-Paniagua, L., Ordóñez-Garza, N., Cook, J., Kryštufek, B., Haslauer, R., Bradley, R., Shenbrot, G., Patton, J., 2017. Family Cricetidae. Handbook of the Mammals of the World, Volume 7: Rodents II, pp. 204-279. Barcelona: Lynx Edicions.

Pineda-Munoz, S. and Alroy, J., 2014. Dietary characterization of terrestrial mammals.Proceedings of the Royal Society B: Biological Sciences, 281(1789), p. 20141173.

Pizzimenti, J.J., and de Salle, R.O.B, 1980. Dietary and morphometric variation in some Peruvian rodent communities: the effect of feeding strategy on evolution. Biological Journal of the Linnean Society, 13(4), pp. 263-285.

Reig, O.A., 1972. The evolutionary history of the South American cricetid rodents. Ph.D. dissertation, University of London, London.

Reig, O.A., 1987. An assessment of the systematics and evolution of the Akodontini, with the description of new fossil species of Akodon (Cricetidae, Sigmodontinae). Fieldiana Zoology, 39, pp. 347-399.

Rowe, K.C., Achmadi, A.S. and Esselstyn, J.A., 2016. Repeated evolution of carnivory among Indo-Australian rodents. Evolution, 70(3), pp. 653-665.

Samuels, J.X., 2009. Cranial morphology and dietary habits of rodents. Zoological Journal of theLinnean Society, 156(4), pp. 864-888.

Smith, M.F. and Patton, J.L., 1991. Variation in mitochondrial cytochrome b sequence in natural populations of South American akodontine rodents (Muridae: Sigmodontinae). Molecular Biology and Evolution, 8(1), pp. 85-103.

Smith, M.F. and Patton, J.L., 1993. The diversification of South American murid rodents: evidence from mitochondrial DNA sequence data for the akodontine tribe. Biological Journal of the Linnean Society, 50(3), pp. 149-177.

Smith, M.F. and Patton, J.L., 1999. Phylogenetic relationships and the radiation of sigmodontine rodents in South America: evidence from cytochrome b. Journal of Mammalian Evolution, 6(2), pp. 89-128.

Steppan, S.J. and Schenk, J.J., 2017. Muroid rodent phylogenetics: 900-species tree reveals increasing diversification rates. PLoS One, 12(8), p. e0183070.

Swanson, M.T., Oliveros, C.H. and Esselstyn, J.A., 2019. A phylogenomic rodent tree reveals the repeated evolution of masseter architectures. Proceedings of the Royal Society B: Biological Sciences, 286(1902), p. 20190672.

Tate, G.H.H., 1932. The taxonomic history of the South and Central American akodont rodent genera: Thalpomys, Deltamys, Thaptomys, Hypsimys, Bolomys, Chroeomys, Abrothrix, Scotinomys, Akodon (Chalcomys and Akodon), Microxus, Podoxymys, Lenoxus, Oxymycterus, Notiomys, and Blarinomys. American Museum Novitates, 582, pp. 1-32.

Teta, P., Cañón, C., Patterson, B.D. and Pardiñas, U.F., 2017. Phylogeny of the tribe Abrotrichini(Cricetidae, Sigmodontinae): integrating morphological and molecular evidence into a new classification. Cladistics, 33(2), pp. 153-182.

Turnbull, W.D., 1970. Mammalian masticatory apparatus. Fieldiana Geology, 18, pp. 147–356. Verde Arregoitia, L.D., 2016. Rethinking omnivory in rodents. doi:10.20944/preprints201609.0017.v1

Vorontsov, N.N., 1959. The system of the hamster (Cricetinae) in the sphere of the world fauna and their phylogenetic relations. Biuletin Moskovskogo Obshtschestva Ispitately Prirody, Otdel Biologia, 64, pp. 134-137.

Weksler, M., 2006. Phylogenetic relationships of oryzomine rodents (Muroidea: Sigmodontinae): separate and combined analyses of morphological and molecular data. Bulletin of the American Museum of Natural History, 69(8), pp. 1-150.

Wiens, J.J., 2004. The role of morphological data in phylogeny reconstruction. Systematic Biology, 53(4), pp.653-661.

Wilson, D.E. and Reeder, D.M., 2005. Mammal species of the world: a taxonomic and geographic reference (Vol. 1). Baltimore: Johns Hopkins University Press.

Wood, A.E., 1965. Grades and clades among rodents. Evolution, 19, pp. 115-130.

CHAPTER 1: SKULL MORPHOLOGY OF THE BRAZILIAN SHREW MOUSE *BLARINOMYS BREVICEPS* (AKODONTINI, SIGMODONTINAE), WITH COMPARATIVE NOTES ON AKODONTINI RODENTS*

* Article published in the journal Zoologischer Anzeiger, 2018, vol. 277, pp. 148-161(https://doi.org/10.1016/j.jcz.2018.09.005)

Drawing of *Blarinomys breviceps* by Fernando Perini

SKULL MORPHOLOGY OF THE BRAZILIAN SHREW MOUSE *BLARINOMYS BREVICEPS* (AKODONTINI, SIGMODONTINAE), WITH COMPARATIVE NOTESON AKODONTINI RODENTS

Rafaela Velloso Missagia[1] and Fernando Araujo Perini[1]

[1] *PPG - Zoologia/Departamento de Zoologia - Instituto de Ciências Biológicas, Universidade Federal de Minas Gerais – Av. Antônio Carlos, 6627, Pampulha, Belo Horizonte, MG, Brazil.*

Abstract

Blarinomys breviceps is a shrew-like mouse, morphologically divergent from the remaining Akodontini (Cricetidae), and best known in the literature for its apparent fossorial adaptations. However, no detailed morphological description concerning its morphology and burrowing habits is available. Through a detailed osteological description and geometric morphometrics approach, we show the distinctiveness of the skull of *Blarinomys* when compared with other Akodontini. Its unique skull morphology shows some features that can be associated with its underground lifestyle. Many aspects of the peculiar morphology of *Blarinomys* may be attributedto selective pressures of the underground environment, and are convergent with the morphology of other fossorial rodents. However, in the Neotropics, *Blarinomys* represents one of the few instances of specialized fossorial habits among members of the Sigmodontinae.

Keywords: comparative morphology, fossorial adaptations, geometric morphometrics, skull morphology.Introduction

1.1. Introduction

Blarinomys breviceps (Winge 1887) is one of the most divergent South American cricetids. Its external appearance, with short ears and tail, short velvety fur, and reduced eyes, resembles some lipotyphlan insectivores, such as shrews of the genus *Blarina*, hence its generic name, *Blarinomys*, or the "shrew mouse" (Thomas 1896, Matson and Abravaya 1977) (Fig. 1.1). *Blarinomys* is included in the tribe Akodontini Vorontsov 1959 (Sigmodontinae, Cricetidae), a well-supported monophyletic group occurring mostly south of the Amazon Basin, which also includes a diverse array of species such as grass mice (genus *Akodon*) and hocicudos (genus *Oxymycterus*) (D'Elía 2003, Leite et al. 2014, Leite et al. 2015, D'Elía and Pardiñas 2015, Steppan and Schenk 2017). *Blarinomys* is recorded mainly from the Atlantic forest of southeastern Brazil, but it also occurs in adjacent Argentina (Silva et al. 2003, Paglia et al. 2005, Ventura et al. 2012). It is recognized as the sole species of the genus *Blarinomys* (Thomas 1896, Matson and Abravaya 1977), although some studies suggest high levels of genetic divergence within the species (Ventura et al. 2012).

The species is poorly represented in collections, and previous descriptions of the skull (Thomas 1896, Goeldi 1901, Gyldenstolpe 1932, Ellerman 1941, Moojen 1952, Matson and Abravaya 1977, Reig 1987) were superficial and did not added detailed morphological information, mostly highlighting the absence of the interparietal bone, the zygomatic arches not exceeding the posterior cranial breadth, the broad interorbital region, and narrow zygomatic plate. Unlike its cranial morphology, the shrew-like external morphology of *Blarinomys* (Fig. 1.1), as well as its inferred fossorial habits, figure prominently in the literature (Thomas 1896, Davis 1944, Moojen 1952, Abravaya and Matson 1975, Matson and Abravaya 1977, Geise et al. 2008, Teta and Pardiñas 2015). Davis (1944) pointed out that "the structure of the animal obviously indicates subterranean habits," but didn't elaborate on the morphological adaptations that might indicate that. The revision of Abravaya and Matson (1975) considers the species fossorial, adding natural history observations, such as the presence of burrows where the species was collected and the capture of five individuals with "half their bodies still in the burrows." A more recent and detailed work (Geise et al. 2008) did not consider its fossoriality or lack thereof.

The conditions of the underground environment constraint the morphology of its inhabitants and give rise to a specialized body plan that is found convergently among several

rodent groups. *Blarinomys* shows several characteristics on its external morphology that can be related to a fossorial habit, as shortening of ears and tail, and reduction of eyes (Agrawal 1967, Hildebrand 1985, Stein 2000) (Fig. 1.1). The relatively broad forefeet and strong and developed claws are also thought to be used to loosen soil (Hildebrand 1985, Stein 2000), and *Blarinomys* exhibits these traits. Additional locomotory specializations are reflected on the species postcranial morphology, like "short and slightly horizontal" transversal processes of the lumbar vertebrae (Carrizo et al. 2014), which decreases the ventral flexion of the vertebral column (Shapiro 1995, Argot 2003, Flores and Diaz 2009) and its overall mobility (Sargis 2001, Argot 2003, Carrizo et al. 2014), and a medially curved olecranon process of the ulna (Carrizo et al. 2014), increasing the surface of attachment and origin of muscles of the forefeet involved in digging (Vassallo 1998, Fernandez et al. 2000). Additional functional locomotory studies of postcranial elements of sigmodontine rodents (Coutinho et al. 2013, Coutinho and Oliveira 2017) show that fossorial forms, like *Blarinomys*, have a relatively large humeral diameter that increases resistance to injury during excavation. In addition, *Blarinomys*, along with other fossorial forms, presents humeri with large articular surfaces with the ulna and radius (Coutinho et al. 2013, Carrizo et al. 2014) which is related to an increased strength on the distal limb elements (Hildebrand 1985, Stein 2000, Elissamburu and Vizcaíno 2004, Samuels and Van Valkenburgh 2008, Hopkins and Davis 2009). These features are usually associated to its scratch-digging mode of burrowing, and led Hershkovitz (1966), when discussing fossorial adaptations in South American cricetids, to classify *Blarinomys* as an insectivorous shrew- or mole-like rodent, in contrast with gopher-like herbivorous/granivorous rodents, like *Kunsia tomentosus* (Lichtenstein 1830), with its robust teeth and jaws. However, besides the obvious external and postcranial modifications, scratch-digging is also reflected in many characteristicsof the skull (Stein 2000). Therefore, the skull osteology of *Blarinomys* should be divergent from other Akodontini, reflecting its habits.

Blarinomys is usually omitted from studies of fossorial adaptations in rodents (Nevo 1979, 1995, Hildebrand 1985, Stein 2000). The lack of detailed descriptions of its cranial anatomy compromises an adequate evaluation of these characteristics. In this work, we present 1) a detailed comparative anatomical description of the skull of *Blarinomys*, comparing it with other Akodontini, especially in relation to its fossorial habit, and 2) its relative position in skull shape among Akodontini species using a geometrical morphometrics approach.

1.2. Material and Methods

1.2.1. Morphological description

Specimens used in skull descriptions and in the geometric morphometrics analysis are housed in the mammal collections of the Centro de Coleções Taxonômicas of the Universidade Federal de Minas Gerais (UFMG), Museu de Ciências Naturais of the Pontifícia Universidade Católica de Minas Gerais (MCN-M), Museu Nacional (MN), and Field Museum of Natural History (FMNH) (Supplementary Material 1.S1). Descriptions are focused on qualitative differences between Blarinomys and other genera, with comments on the differences that can be related to fossorial habits in the former. Morphological bone-by-bone descriptions of the cranial structures of Blarinomys were made in comparisons with the Akodontini species *Akodon montensis* Thomas 1913, *Brucepattersonius griserufescens* Hershkovitz 1998, *Bibimys labiosus* (Winge 1887), *Castoria angustidens* (Winge 1887), *Juscelinomys candango* Moojen 1965, *Lenoxus apicalis* (Allen 1900), *Necromys lasiurus* (Lund 1840), *Oxymycterus delator* Thomas 1903, *Thalpomys lasiotis* Thomas 1916, and *Thaptomys nigrita* (Lichtenstein 1830). The comparisons were made using the generic attribution, since most of the genera here compared comprises only one (*Blarinomys*, *Castoria*, *Lenoxus*, *Thaptomys*) or two (*Juscelinomys*, *Thalpomys*) species. For the most speciose genera, like *Akodon*, *Oxymycterus*, and *Necromys*, we expect that some morphological aspects can differ when considering more morphologically divergent species.

Further comparisons were made with other Akodontini and some fossorial Sigmodontinae (e.g. Abrothrichini), using both available specimens and descriptions from the literature (Patterson 1992, Bezerra et al. 2007, Pardiñas et al. 2008). Discussions involving muscle attachments, veins, arteries and nerve passages were based on previous anatomical workswhere dissections were performed (Greene 1935, Hill 1935, Wahlert 1985, Voss 1988).

Anatomical terms follow Hill (1935), Wahlert (1985), Voss (1988), Carleton and Musser (1989),and Voss and Carleton (1993). We used the abbreviations M1, M2 and M3 for the first, second and third upper molars, respectively.

Specimens were separated into age classes according to the eruption and wear of molar tooth crowns (Myers 1989, Myers and Patton 1989). Even considering that all specimens showed substantial degree of worn on their teeth, we were able to identify three age groups in specimens

of *Blarinomys*: age class 3, with individuals showing moderate wear in all the teeth with an obliterated posteroloph on M3 (UFMG 2087, MCN-M 1472, MCN-M 2196, MCN-M 2533, MCN-M 2747); age 4, with the four major cusps still distinct, but all major lophs obliterated (UFMG 2016, UFMG 4033, UFMG 4062, MCN-M 2834, MCN-M 2837, MCN-M 2983); and

age class 5 (UFMG 2199), with molar surfaces completely worn, with flat surfaces and without discernible enamel elements.

1.2.2. Phylomorphospace analysis

In order to complement the anatomical descriptions and assess the morphological diversification through projection of the phylogeny in a multivariate morphospace, we analyzed the morphological variation of the skull of *Blarinomys* and other Akodontini using a geometrical morphometrics approach. We digitized 93 skulls of 10 genera (see Supplementary Material 1.S1 for detailed information). The two-dimensional landmarks were digitized on the skulls in dorsal, lateral and ventral views, always on the left side, using tpsDig 2.12 software (Rohlf 2007). We defined a set of 24 landmarks in dorsal view, 34 in lateral view and 30 in ventral view (Fig. 1.2; see Supplementary Material 1.S2 for detailed description of landmarks) based on previous morphometric studies of Sigmodontinae rodents (Astúa et al. 2015, Maestri et al. 2015, Maestri et al. 2016, Quintela et al. 2016) (Fig. 1.2). When landmarks of a particular view could not be marked in damaged skulls, the skull was excluded from the dataset, resulting in a different number of skulls in each view (Supplementary Material 1.S1). The resulting coordinates from the Generalized Procrustes Analysis were analyzed by Principal Components Analysis (PCA), and a Bayesian phylogeny (Steppan and Schenk 2017) was pruned and mapped into the two-dimensional plot of the first two PC axes using the "Map onto phylogeny" function of the software MorphoJ (Klingenberg 2011).

1.3. Results and Discussion

1.3.1. Comparative DescriptionGeneral Skull Anatomy

In overall morphology, the skull of *Blarinomys* shares many similarities with the generalized Akodontini skull, with relatively inflated frontal sinuses between the orbits, long rostrum, rounded braincase and an amphora-shaped interorbital region (D'Elía and Pardiñas 2015).

The braincase of *Blarinomys* is broad with thin walls, and the skull presents an overall squarish shape in dorsal and ventral views (Figs. 1.3 and 1.4). *Blarinomys* differs from other species of the tribe mainly because of the shortening of the skull in the braincase region, which affects the morphology of a number of bones and structures (see below).

Nasals

The nasals of *Blarinomys* are projected over the nasal cavity, premaxillae and incisors, and therefore none of these can be seen dorsally (Fig. 1.3). In lateral view, its dorsal edge is straight, following the overall straight profile of the skull (Fig. 1.5). The nasals of *Blarinomys* resemble *Akodon* and *Bibimys*, but in *Blarinomys* the nasals are more anteriorly projected. Despite having procumbent nasals, the rostral region of *Blarinomys* differentiates from the elongate rostra of *Brucepattersonius*, *Lenoxus*, and *Oxymycterus*, which present a tubular shape (Fig. 1.6). The tubular-shaped rostra of these taxa may serve as support for a long and mobile snout, which is useful for searching insects in the litter (Hershkovitz 1994). This feature is cited as a morphological characteristic of insectivorous rodents, related to the ability of closing the mouth quickly (Samuels 2009), and is also found in the Sulawesi and Philippine shrew-rats (e.g. *Tateomys*, *Melasmothrix*, and *Sommeromys*, with the later presenting a developed bony rostral tube) (Musser and Durden 2002). This difference may indicate that *Blarinomys* explores the substrate in an alternative way, as it may move within or below the leaf litter (Geise et al. 2008), rather than probing through it. *Castoria*, *Juscelinomys*, and *Thalpomys* have slightly projected nasal bones, with the former lacking the trumped-shaped nasal projections of the insectivorous taxa. *Thaptomys* and *Necromys* are the only taxa examined where the short nasals do not surpass the premaxillary bones and the incisors (Fig. 1.6); in *Thaptomys*, the nasal cavity can even be seen in dorsal view. The anterior tip of the nasal bones is rounded in *Akodon*, *Blarinomys*, *Castoria*, *Lenoxus*, *Necromys*, and *Brucepattersonius*, whereas in *Oxymycterus*, *Thaptomys*, and *Juscelinomys* it is more squared (Fig. 1.7) where the suture between the nasals ends slightly before the anterior portion of these bones, leaving a notch between the paired nasals on the most distal part of the rostrum.

Premaxillae

Ventrally, the premaxillae form the anterior portion of the palate via the palatal process of

the premaxilla, where the narrowest, anterior part of the incisive foramina are located (Figs. 1.4 and 1.8). In lateral view, the premaxillae are anteriorly protruded in *Akodon*, *Bibimys*, *Blarinomys Brucepattersonius*, *Castoria*, *Juscelinomys*, *Lenoxus*, and *Oxymycterus* through some irregular projections that are continuous with and end in the gnathic process (when present). In *Brucepattersonius* and *Oxymycterus*, the premaxillae contribute to the rostral tube (Fig. 1.6). In *Necromys*, *Thalpomys*, and *Thaptomys* these projections, as well as the gnathic process, are incipient (Fig. 1.6). Agrawal (1967) argued that protruded premaxillae could have the same function of proodont incisors in fossorial forms with orthodont incisors. Because these projections are present in nonfossorial forms such as *Akodon*, they cannot be attributed to the fossorial habit of *Blarinomys*. However, Stein (2000) mentioned that a massive rostrum with anteriorly projected premaxillae may serve as support for the nose pad, which is conspicuous in *Blarinomys* (Fig. 1.1) and may have a function in burrowing.

Maxillae

The incisive foramina appear on the ventral portion of the rostrum, just behind the incisors, and are divided between the premaxillary and maxillary processes. They are long openings that transmit palatine arteries and ducts of the Jacobson organ (Hill 1935). These foramina are tear-shaped in *Blarinomys* and *Lenoxus*, while in the other species, less flaring foramina are separated by a narrower premaxillary process (Fig. 1.8).

The anterior part of the orbit is formed by the zygomatic process of the maxilla. As observed by Voss (1988), the depth of the zygomatic notch, an excavated portion on the anterodorsal margin of each maxilla, is related to the width of the zygomatic plate. In *Blarinomys*, the zygomatic plate is narrower and less anteriorly projecting than in the other analyzed species, which makes its zygomatic notch shallower (Fig. 1.7). In the insectivorous *Brucepattersonius*, *Lenoxus*, *Juscelinomys*, and *Oxymycterus* the zygomatic plate, where the anterior deep masseter originates (Voss 1988), is narrower than in the herbivorous *Bibimys* and *Necromys* (Fig. 1.6). This may be related to the increased surface area for attachment of masticatory muscles on the zygomatic plates of herbivorous species. Additionally, the zygomatic plate is slanted posteriorly in lateral view in these species, and not vertically inserted on therostrum as in *Akodon*, *Bibimys*, *Castoria*, *Necromys*, *Thalpomys*, and *Thaptomys* (Fig. 1.6).

There is also a difference between *Blarinomys* and the other species concerning the angle

of the inferior root of the zygomatic plate relative to the axis of the skull wall, which approximates a right angle in *Blarinomys* (Fig. 1.8). This configuration gives a more or less squared-off appearance to the zygomatic plate in dorsal view (Carleton and Musser 1989) and may contribute to the oval shaped and wide lumen of the infraorbital foramen observed in *Blarinomys* (see below). On the other species, the zygomatic process of the maxilla reaches the wall of the skullin a more convergent way, giving a more elongated shape to the zygoma (Fig. 1.8).

On the ventral side of the zygomatic plate, the masseteric tubercle, a rounded bone projection or rugosity marking the origin of the superficial masseter (Voss 1988), can be distinguished (Figs. 1.6 and 1.8). In comparison with the other species, the masseteric tubercle is more pronounced in *Blarinomys*, *Brucepattersonius*, *Oxymycterus*, and *Lenoxus* (Figs. 1.6 and 1.8). According to Voss (1988) and Fabre et al. (2017), more prominent masseteric tubercles are found in animalivorous rodents, and may be related to this diet. Additionally, the masseteric tubercle is located on the ventral side of the zygomatic plate, closer to the tooth row, on *Blarinomys*, *Oxymycterus* and *Lenoxus*. On the other taxa, the masseteric tubercle, found as elongated rugosity, is located on the ventral part of the rostrum (Fig. 1.8).

The infraorbital foramen is located on the rostral part of the maxilla. In anterior view, it has an oval/semicircular shape, and it is limited by the lateral side of the rostrum and the inferior zygomatic root. In all species except *Blarinomys*, the lumen is wider in the dorsal part, but constricted ventrally. In *Blarinomys*, the lumen is wide both above and below (Fig. 1.9), resulting in an ovoid shape, which was also highlighted by Ellerman (1941). According to Voss (1988), the dorsal part of the foramen transmits the infraorbital beam of M. zygomaticomandibularis and, near the rostrum, the nasolacrimal membranous duct. This portion is similar between *Blarinomys*and the other species. According to Greene (1955), the ventral part of the infraorbital foramen transmits sensorial nerves of the second division of the fifth cranial nerve (=trigeminal nerve) – which innervates the mystacial vibrissae and surrounding integumentary structures – and is muchwider in *Blarinomys*. In his dissections of semiaquatic ichthyomyines, Voss (1988) found that the ventral portion of the infraorbital foramina, which were also as wide as the dorsal part as in *Blarinomys*, transmitted a thick tract/band of fibers, instead of a flat sheet of nerves passing through the narrower ventral part of the infraorbital foramina typical of non-aquatic muroids. Fossorial rodents use their vibrissae for close-range orientation on the substrate (Stein, 2000), as do semiaquatic rodents (Voss 1988). If the wide ventral portion of the infraorbital foramen in *Blarinomys* implies

an increased innervation of the mystacial vibrissae, it seems reasonable to infer that the mystacial vibrissae are specially developed and may also be used for orientation and locomotion underground.

The sphenopalatine foramen is located above the molar rows, on the ventromedial portion of each orbit, and transmits the sphenopalatine nerve and blood vessels, and a branch of the maxillary (Hill 1935). In *Blarinomys*, *Lenoxus*, and *Necromys*, this foramen is antero-posteriorly elongated and positioned above the M2 and M3. In other akodontines, it is less conspicuous and more circular.

Lacrimals

In *Blarinomys*, the paired lacrimal bones are located anterodorsally on the orbit (Figs. 1.3 and 1.7), contacting mainly the maxillary bone. In *Akodon* and *Necromys* no projection is observed, and the lacrimals are entirely incorporated into the superior root of the zygomatic plate. In *Bibimys*, a conspicuous projection can be seen. In *Brucepattersonius*, *Lenoxus*, *Thaptomys*, and *Oxymycterus*, the lacrimal bone equally contacts the frontomaxillary suture. These species, as *Bibimys*, present a more conspicuous lacrimal projection than *Blarinomys*.

Frontals

The frontals form the skull roof and are located between the two orbits. The frontals contact the parietals through the coronal suture, which surrounds the posterior part of the skull, behind the orbits (Fig. 1.3). The coronal suture has a semicircular/rounded shape in mostakodontines, except in *Blarinomys* and *Bibimys*, in which the suture has a more open angle, probably because of the broadening of the posterior region of the skull.

The frontals cover most of the interorbital region of the skull. The frontal sinuses, located on the anterior margin of the orbits near the zygomatic processes, are more inflated in *Blarinomys* (Fig. 1.7) and *Thaptomys*, compared to other akodontines. The frontal sinuses arepart of the paranasal sinuses, along with the maxillary and sphenoidal sinuses, that can be described as “spaces between the necessary bony struts and pillars” that are associated with the nasal cavities (Novacek 1993); its functional significance needs to be analyzed in each particular case.

The sinuses may reduce the weight of the skull (Novacek 1993) or may represent an expansion of the ethmoturbinals, resulting in an increased olfactory capacity (Moore 1981). They

also may have a role in heat loss and sound resonation (Moore 1981), or be only structurally incidental and have no function at all (Weidenreich 1941). In this work, we didn't observe the interior of the sinuses to check the degree of pneumatization or size of ethmoturbinals; however, we can infer that, considering the small size of the eyes in *Blarinomys* (Fig. 1.1; see below), the species may rely chiefly on other senses, like touch and olfaction, for orientation and foraging in the substrate.

The interorbital region of *Blarinomys* is smoothly rounded without supraorbital ridgesand, probably due to the inflated frontal sinuses, the interorbital constriction is not well-defined(Fig. 1.7). *Brucepattersonius*, *Lenoxus*, *Oxymycterus*, and *Thaptomys* present a similar condition,but the interorbital region is more marked. In the remaining species, the interorbital region iswell defined, with *Thalpomys* and *Necromys* presenting a constricted interorbital region with supraorbital ridges (Fig. 1.7). *Akodon*, *Bibimys*, *Brucepattersonius*, *Castoria*, *Juscelinomys*, *Lenoxus*, *Oxymycterus*, and *Thaptomys* present a supraorbital region without supraorbital ridges, as *Blarinomys*. In lateral view, the nasals and frontals form a straight dorsal profile in *Blarinomys*, *Brucepattersonius*, *Lenoxus*, and *Oxymycterus*, whereas in *Akodon*, *Bibimys*, *Castoria*, *Necromys*, *Thalpomys*, and *Thaptomys*, a more convex profile is observed.*Juscelinomys* also presents a convex profile of the rostrum, with a swollen region on the frontals.

The paired supraorbital foramina are located on the edges of the dorsal part of each orbit (Fig. 1.10) and transmit small blood vessels of the dorsal region of the orbital fossae to the venous system that surrounds the olfactory lobes of the brain (Greene 1955, Voss 1988). The ethmoid foramen is located on each side of the frontal, on the medial portion of the orbits. The ethmoid foramen lies anterodorsally to the optic foramen (Fig. 1.10), above the M2 in *Bibimys*, *Castoria*, and *Thaptomys*; and in *Oxymycterus* it lies behind the molar series. In all the other taxa, the foramen is dorsal to the M3. According to Hill (1935), it transmits the anterior ethmoid nerve into the cranial cavity.

Jugals

The jugals fill the small gap between the zygomatic processes of the maxilla and squamosal, completing the zygomatic arch, which surrounds the orbital portion of the skull. In all species observed, the zygomatic arch is delicate and the jugal is just a small component of it. However, in *Blarinomys*, *Bibimys*, and *Lenoxus*, the jugal is relatively large and robust, occupying

a larger part of the zygomatic arch, and the zygomatic process of the maxilla and squamosal are more separated from each other. The two zygomatic processes are closer in *Castoria*, *Necromys*, *Oxymycterus* and *Thaptomys*, and actually overlap in *Akodon*, *Brucepattersonius*, and *Juscelinomys*, but are never in contact. As highlighted by Thomas (1896), the zygomatic arch of *Blarinomys* "barely exceeds the posterior cranial breadth," creatingthe subconical conformation of the skull (Fig. 1.3). Shimer (1903) considered the "zygomatic arches not extending outside the greatest width of the skull" as a morphological adaptation of fossorial mammals, reducing its projections. However, the fact that the zygomatic arch barely exceeds the breadth of the braincase in *Blarinomys* (Fig. 1.7) may be due to the enlargement of the latter (see below).

Interparietal

Contrary to what has been described in other works (Matson and Abravaya 1977, Geise et al. 2008), the unpaired interparietal bone is present in some individuals of *Blarinomys* but, according to Gudinho and Iack Ximenes (2015), its size tends to suffer an ontogenetic decrease.

In our sample, the interparietal can be seen in some individuals between the parietal and occipital (UFMG 2087, MCN-M 2196) but, in other specimens, it is observed only through the foramen magnum (UFMG 2016, UFMG 2199), or may be completely absent (UFMG 4033, UFMG 4062, MCN-M 1472, MCN-M 2747, MCN-M 2834, MCN-M 2837, MCN-M 2533, MCN-M 2983). We did not observe an ontogenetic pattern of decrease in our sample, where the presence or absence of the interparietal may represent an intraspecific variation, because in the older individuals (age class 5, UFMG 2199), the interparietal can still be observed through the foramen magnum. The interparietal is present in the other species (Fig. 1.7), where it is short anteroposteriorly and its transversal length does not surpass the parietal length. In *Thaptomys* it reaches only a diminutive size (Moojen 1952, Teta et al. 2015), and it is absent in one specimen (UFMG 1850).

Despite the interparietal being relatively small in all akodontines, its reduction was used as one of the justifications by Thomas (1896) for reassigning *Blarinomys*, previously allocated in *Oxymycterus*, to its own genus. According to Agrawal (1967) the ontogenetic reduction of the interparietal is common in fossorial species and is due to the pressure from the occiput posteriorly and from the squamosals laterally (Agrawal 1967: 11). In *Blarinomys*, its reduction seems to be related to an expansion of the parietal bones (Gudinho and Iack Ximenes 2015) and the occiput

(see below), because the squamosals do not seem particularly larger in *Blarinomys* than in the other Akodontini species.

Parietal

In *Blarinomys*, the parietals are dorsally flattened, giving a more or less straight profile to the braincase in lateral view (Fig. 1.5). *Brucepattersonius*, *Lenoxus*, *Juscelinomys*, and *Oxymycterus* show a similar condition, while *Akodon*, *Bibimys*, *Castoria*, *Necromys*, *Thaptomys*, and *Thalpomys* have a more convex profile. The dorsal flattening of the skull, together with a forward-leaning occiput (Figs. 1.3 and 1.7), are mentioned by Agrawal (1967) as a way to "give momentum to the animal using the head as a shovel during digging," and is cited by Stein (2000) as responsible for an increase of the surface area of attachment of neck muscles (see above).

On each side of the braincase, on the suture between the parietal, squamosal and supraoccipital, there are the lambdoidal ridges. In *Blarinomys*, the lambdoidal ridges are slightly more pronounced than in some of the other species, forming a crest that extends laterally untilthe subsquamosal fenestra (Fig. 1.5). In some of the other taxa (e.g. *Oxymycterus*), the lambdoidal ridge is less conspicuous and extends posteriorly to the subsquamosal fenestra, near the mastoid.

According to Stein (2000), in fossorial forms the lambdoidal ridge increases in size, which increases the surface for the insertion of neck muscles. Besides its greater development, the lambdoidal ridges suffer an anteriorly directed displacement in *Blarinomys*, reaching a more anterior position on the skull when compared to the other species (Fig. 1.7), apparently because of an expansion of the occipitals. This displacement may be associated with more developed neck muscles inserting in larger areas on the skull (Agrawal 1967), for moving the head when excavating (see below).

Squamosal

Blarinomys and *Akodon* present rectangular shaped squamosals, with the squamosalparietal suture forming a straight line until it reaches the lambdoidal ridge on each side of the braincase. In the other species this suture does not form a straight line and the squamosal have a more irregular shape, with a rectangular process invading the parietals. In the ventral region of the squamosal there are two foramina. The postglenoid foramen, bounded by the squamosal dorsally and by the tympanic bulla ventrally, transmits the transverse sinus (Greene 1955).

Posterior to the postglenoid foramen lies the subsquamosal fenestra, which is also bordered by the squamosal dorsally, but ventrally it is in contact with the mastoid. The two foramina are separated by the hamular process of the squamosal, and the proportion of each one varies in the species analyzed. These two foramina are equal in size in *Akodon*, *Castoria*, and *Thalpomys*, while in the other species the subsquamosal fenestra is smaller than the postglenoid foramen. Despite some attempt to find homologous relations between the subsquamosal fenestra and other structures that transmits vessels or nerves (Musser 1982), we follow Hill (1935) and Voss (1988) in the assumption that this fenestra does not transmits any nerve or vein. Its reduction in some of the taxa analyzed may be related to the shortening of the skull and, therefore, not indicative of any circulatory change.

Palatine

The palatine bones form the rear part of the hard palate (Figs. 1.4 and 1.8). According to the classification of Hershkovitz (1962), the bony palate of *Blarinomys* is classified as short ("with median posterior borders of palatines not extending behind posterior plane of third molars") and wide ("with distance between inner borders of first molars greater than length of either molar") and appears to be more robust in *Blarinomys* and *Thaptomys*, and wider in *Blarinomys* and *Bibimys*.

The palatine bones extend, anteriorly, to the protocone of the second upper molars and, posteriorly, to the mesopterygoid fossa. The mesopterygoid fossa of *Blarinomys* is broad and square shaped (Fig. 1.8). A more or less square shaped mesopterygoid fossa is also found in *Bibimys*, *Brucepattersonius*, *Lenoxus*, and *Thaptomys*, whereas this fossa is more rounded in other species (Fig. 1.8). The mesopterygoid fossa is wider in *Juscelinomys* and narrower in *Bibimys*.

Pterygoid

In lateral view, the pterygoids of *Blarinomys* have a more or less straight profile, at the same height of the molar series. The hamular process of the pterygoid is higher and more delicate in *Blarinomys* than in the other Akodontini species analyzed, with its most posterior partfollowing the shape of the closely located auditory bullae. The parapterygoid fossa is shorter and wider in *Blarinomys*, particularly anteriorly (Fig. 1.8), when compared with other species, particularly *Juscelinomys*, where the parapterygoid fossa is longer.

Sphenoid complex

The presphenoid, a rod-shaped bone bounded on the sides by sphenopalatine vacuities, when present, and by the pterygoid, is more robust in *Blarinomys* compared to the slender and delicate bone of *Akodon* and *Necromys*. The sphenopalatine vacuities are long fenestrae that are located on the sides of the presphenoid, on the dorsolateral walls of the mesopterygoid fossa (Fig. 1.4). These vacuities are absent in *Thaptomys*, *Oxymycterus*, *Lenoxus*, and *Juscelinomys*. In *Blarinomys* and *Brucepattersonius*, they are present as narrow openings that reach the basisphenoid. *Akodon*, *Bibimys*, *Castoria*, and *Necromys* present broad vacuities which, as in *Blarinomys* and *Brucepattersonius*, exceed the basisphenoid-presphenoid suture. The basisphenoid can be seen between the presphenoid and the basioccipital and is a slightly concave bone with a trapezoidal shape in all specimens examined (Fig. 1.8). In all species, the alisphenoids have a small exposure on the lateral view of each orbit and can also be seen in the ventral side of the skull, where they are located near the auditory bullae, bearing some of the foramina related to the carotid circulation of the skull (see below).

The paired orbitosphenoids consist of small components of the lateral walls of the orbits, located just above the pterygoid, between the alisphenoid and the posterior part of the frontal. They contain the optic foramen, which is small and inconspicuous in *Blarinomys* compared to the large optic foramen of *Akodon*, *Castoria*, *Necromys*, and *Thalpomys*. (Fig. 1.10). In *Brucepattersonius*, *Bibimys*, *Juscelinomys*, *Lenoxus*, and *Thaptomys*, this foramen is small, but it does not reach the tiny size seen in *Blarinomys*. Occasionally, in some specimens of *Blarinomys*, the optic foramen is doubled, with a small accessory foramen located anterodorsally to it. The optic foramen transmits the optic nerve and the ophthalmic artery, and its small size (along with the small size of the eyes) allows us to infer that it transmits a correspondingly small optic nerve, and that *Blarinomys* relies on other senses for its orientation underground.

Occipital complex

The occipitals form the posterior wall of the skull, behind the parietals and the squamosals, and delimit the foramen magnum. All akodontines observed have a foramen magnum with a hexagonal shape, limited by the basioccipital ventrally, and by the supraoccipitaland exoccipitals dorsolaterally. On both sides of the foramen magnum are the paroccipital processes, which are longer and straighter in *Blarinomys* than in the other species, where these processes are shorter

and curved. In dorsal view, the medial portion of the occipitals is flattened in *Blarinomys* and *Thaptomys*, contributing to the overall squarish shape of the skull (Figs. 1.3 and 1.7). In the other species, this portion is posteriorly projected, especially in *Thalpomys*. In *Juscelinomys*, a relatively developed occipital crest can be observed. The occipital complex occupies a larger portion of the lateral wall of the braincase in *Blarinomys* (Fig. 1.5) than in the other species. As mentioned above, this anterior projection, together with the flattening of the

occipital plate, increases the insertion area of the neck muscles that moves the head when digging (Agrawal 1967).

Probably owing to the overall shortening of the skull, the basioccipital is wider and shorter in *Blarinomys* and *Thaptomys*, so this bone does not reach the bony eustachian tubes of the auditory bullae, as it does in the other species. Its posterior portion bears the hypoglossal foramina, one on each side, near the occipital condyles, from which the hypoglossal nerve emerges (Hill 1935).

Middle Ear Ossicles and Auditory Bullae

Blarinomys appears to have relatively large, globular and inflated auditory bullae (Davis 1944). The bulla is wider on its posterolateral portion and becomes tapered until ending anteromedially in the bony eustachian tube. The petrosal can only be seen through a small gap between the ectotympanic and the basioccipital. On its posterior extremity, the external auditory meatus exposes the middle ear ossicles. Anterior to the tympanic bullae and next to the foramen ovale is an unossified region, the middle lacerate foramen. The overall morphology of the bullae is similar to the other Akodontini species, but more globular and rounded in shape in *Blarinomys*. The modifications of the auditory apparatus, particularly the enlarged bullae, may relate to increased sensitivity of hearing at lower frequencies in subterranean rodents (Agrawal 1967, Burda et al. 1992, Stein 2000), because high frequencies are quickly dissipated or attenuated over short distances in the underground environment (Schleich and Vassalo 2003). Allthe species analyzed here present the microtype ossicles (Mason 2015), where the malleus exhibits an orbicular apophysis, a bony projection located at the base of the manubrium, and a wide transversal lamina that can be seen between the anterior process and the neck and head of the malleus. The manubrium is located at a relatively acute angle relative to the anatomical axis. The incus is small compared to the malleus, and it is articulated medially with the oval head of the stapes through the lenticular apophysis. The stapes of the species analyzed are very similar and have a stirrup shape,

with two divergent crura that meet at the two opposite edges of the footplate. The stapedial artery passes through the intercrural foramen. In all akodontines observed, the portion of the malleus that is next to the crus longum of the incus presents a more abrupt curvature, except for *Blarinomys*, where this curvature is more rounded. Low-frequency specialists are characterized by a looser articulation of the middle ear, with more "freely mobile ossicles", which can reduce impedance and improve the transmission of low-frequency sounds through the auditory apparatus (Ravicz and Rosowski 1997, Mason 2015). This kind of bone articulation is more common in the freely mobile and transitional types (Mason 2015), where the malleus articulates with the skull in a more flexible way and the manubrium lacks an orbicular apophysis. Even though we have observed a smaller and more delicate orbicular apophysis in *Blarinomys* than in other Akodontini (Fig. 1.11), the morphology of the middle ear ossicles does not differ substantially in a way that would enhance low-frequency hearing sensitivity. Despiteits inflated auditory bullae, the auditory apparatus of *Blarinomys* appears to reflect the above- ground hearing sensitivity of this species.

The mastoid portion of the petrosal bone is exposed on the lateral side of the braincase, between the bulla and the occipital complex. In all species examined, the mastoid is moderately inflated and, except in *Oxymycterus* and *Juscelinomys*, presents a conspicuous fenestra on its contact with the occipital bones, on its posterodorsal side.

Carotid arterial supply

As no dissection of any Akodontini is available, the circulatory pattern was inferred by the presence and relative size of some foramina and grooves on the braincase, following Bugge (1970), Voss (1988) and Carleton and Musser (1989). According to Voss (1988), the pattern of vascular supply appears in three major conformations. Due to the "large stapedial foramen," the "inconspicuous posterior opening of the alisphenoid canal," and the "conspicuous anteroposterior groove on the alisphenoid and squamosal bones" (Voss 1988), we infer that *Blarinomys* presents the circulatory pattern 1 of Voss (1988), or the basic pattern of Bugge (1970). Most other Akodontini species exhibit the same pattern. Among the species of Akodontini analyzed, the only exception being *Bibimys labiosus*, which exhibits circulatory pattern 2 of Voss (1988). In this basic pattern, an anteroposterior groove is observed on the squamosal and alisphenoid bones, with a fenestra where the groove meets the depression for the buccinator and masticatory nerves, marking the passage of the supraorbital branch of the stapedial artery. The carotid artery gives rise, behind

the auditory bulla, to the internal and external carotid arteries. The former gives rise to the stapedial artery and goes into the braincase through the carotid canal. The stapedial artery then enters the bullae through the stapedial foramen and exits it via a fenestra on the anterolateral side of the bullae, where it is divided into the infraorbital and supraorbital branches. The supraorbital branch, responsible for the ophthalmic circulation (Voss 1988), passes through the squamosal and alisphenoid bones and enters the orbit by the sphenofrontal foramen, located in the suture between the alisphenoid, orbitosphenoid, and frontal bones (Hill 1935). The infraorbital branch, which covers the internal maxillary circulation (Voss 1988), enters the braincase through the posterior opening of the alisphenoid canal, next to the foramen ovale, and passes along the alisphenoid until it exits the braincase through the anterior alar fissure.

Mandible

Blarinomys has a thin and elongated mandibular ramus, with a well-developed coronoid process that is higher than the condylar process (Fig. 1.12). The capsular projection is inconspicuous, unlike *Thaptomys* and *Necromys*, where it is easily visualized. The angular process is narrow. The mandibular ramus of Blarinomys resembles the overall bauplan of insectivorous sigmodontinae rodents, like *Brucepattersonius*, *Juscelinomys*, *Lenoxus*, and *Oxymycterus*. Insectivorous species exhibits a narrower and more elongated mandible, which is associated with lower relative bite forces than the robust mandibles with wider processes of herbivores and granivores (e.g. *Necromys*), with stronger mastication (Maestri et al. 2016).

1.3.2. Phylomorphospace analysis

The skull shape variation on lateral view of the species analyzed is represented in the morphospace of the first two components of a Principal Components Analysis (PCA) of the Procrustes coordinates in Fig. 1.13. The first two principal components accounted for 48.39% of the variation. Along the first principal component (PC1) (32.86% of the variation), the main changes relate to the shape of the rostrum, with less elongated nasals, less projected premaxillary bones and a broader zygomatic plate toward more positive values. The second principal component (PC2) (15.53% of the variation) reflects changes in the height of the braincase, with shorter braincases toward positive values. Five main groupings of taxa can be seen in the PCA: *Oxymycterus* species with *Brucepattersonius* and *Lenoxus*, with negative PC1 values and high and

positive PC2 values; *Akodon* and *Castoria* with high PC2 but intermediate PC1 values; *Thaptomys* and *Necromys*, with high PC1 scores and intermediate PC2 values; *Bibimys* and *Thalpomys*, with the high PC1 scores and low PC2 values; and *Blarinomys*, with the most negative PC1 and PC2 values, occupying a distinct point on the morphospace and not grouping with any of the other species.

For the dorsal view, the two first principal component axes accounted for 54.31% of the variation (Supplementary Material 1.S3). In PC1 (39.7% of the variation), the main changes relate to a more pronounced and anteriorly displaced lambdoidal ridge (in the suture between the squamosal and occipital), besides overall longer rostra toward positive values. PC2 (14.61% of the variation) depicts narrower skulls toward positive values. *Blarinomys*, *Thaptomys*, and *Bibimys*, with relatively broader skulls, are located toward the more negative values of this axis, while *Oxymycterus*, *Brucepattersonius*, and *Lenoxus*, with narrower skulls, are positioned along the higher positive values of PC2.

In ventral view, the first two principal component axes accounted for 44.59% of the variation (Supplementary Material 1.S4). PC1 (25.70% of the variation) reflects a change in the angle in which the zygomatic arch meets the skull wall, with an angle closer to 90° towards positive values and an enlargement and anterior displacement of the lambdoidal ridge. Like in the dorsal view, *Blarinomys* is positioned in the extreme positive value of this axis, while *Necromys* and *Thalpomys* are toward more negative values. PC2 (18.89% of the variation) is related to changes in the breadth of the skull and premaxillary bones, with narrower skulls and longer premaxillae, forming the nasal tube, toward positive values. *Oxymycterus*, *Brucepattersonius*, and *Lenoxus* present high and positive PC2 values, while *Bibimys*, *Blarinomys*, and *Thalpomys* are positioned toward the more negative values. The PCA plot of dorsal, lateral and ventral views can be seen in the Supporting Information (Supplementary Material Figs. 1.S5, 1.S6 and 1.S7).

Compared with other species of the tribe, the skull of Blarinomys is unique because of its inflated and shortened braincase with anteriorly expanded occipital plate. Its isolated position in the morphospace is particularly driven by the combination of some features of its skull that are thought to be related to fossorial habits or to an insectivorous diet, like the relatively elongated rostrum, anteriorly expanded occipitals and narrow zygomatic plate. This unique combination of insectivore and fossorial trends differentiates the species from its closest relatives (e.g. *Brucepattersonius* and *Lenoxus*) which, although sharing with *Blarinomys* several morphological

features related to insectivory, have an epigeal lifestyle, lacking the fossorial features observed only in *Blarinomys*.

1.3.3. Fossorial adaptations in Sigmodontinae rodents

Morphological convergence of fossorial rodents is well documented and discussed in the literature (Lehman 1963, Agrawal 1967, Nevo 1979, 1999, Pearson 1984, Stein 2000, Lange et al. 2004) and occurs due to the similar selective pressures for the underground environment. Considering previous studies (Leite et al. 2014, Leite et al. 2015, Steppan and Schenk 2017), fossorial habits probably emerged convergently more than once in Akodontini, with non proximally related species like *Blarinomys breviceps*, *Thaptomys nigrita* and *Kunsia tomentosus* all presenting different degrees and types of fossoriality.

Kunsia has a very different morphology from *Blarinomys* and may represent an herbivorous-granivorous chisel-tooth digger or a gopher-like burrower (Hershkovitz 1966). Compared to *Blarinomys*, the species shows a heavier built skull, with a short rostrum, due to abbreviated nasal and premaxillary bones. Additionally, *Kunsia* presents a more angled skull, with large areas for muscular insertion on the broad zygomatic arch and plate, contrasting with

the delicate zygomatic region of *Blarinomys*. These anatomical differences may reflect both the distinct excavation modes and diets of the two species.

Thaptomys shows characteristics that suggests a less specialized fossorial rodent (Thomas 1916, Davis 1947, Moojen 1952, Moreira and Oliveira 2009). An overall morphological resemblance between the species and *Blarinomys* was mentioned by Thomas (1896), and the similarity of several of their features could be confirmed in our comparative description. The shortening of the skull is a feature easily noticed on both species and, although it does not reach the diminutive size as in *Blarinomys*, the optical foramen of *Thaptomys* is also relatively small. Both species have inflated nasal sinuses, leading to a weak constriction of the interorbital region, and a diminutive or even absent interparietal. Despite these similarities, *Thaptomys* presents several characteristics in the skull that more closely resemble the generalized Akodontini skull, which led to its previous allocation on the genus *Akodon* (Reig 1987). The external morphology of *Thaptomys* is also characterized by small eyes, short tail and well developed claws, which led to its recognition as a “semi-fossorial rodent” (Thomas 1916, Davis 1947, Moojen 1952, Naxara et al. 2009, Moreira and Oliveira 2009), but it still differs from the highly modified *Blarinomys*.

Some of these similarities listed above may be related to the semifossorial habit of *Thaptomys* but, apparently, the species shows several generalized features and does not reach the level of specialization observed in *Blarinomys*, as can also be seen in the morphospace analysis, where the species groups with *Akodon*, *Necromys*, *Castoria*, and *Bibimys*.

Blarinomys was traditionally considered to share special affinities with the genus *Oxymycterus*, mainly because of its relatively elongated rostrum (although not to the degree observed in species of *Oxymycterus*), molar morphology, and claws (Thomas 1896, Gyldenstolpe 1932). When he described the genus *Blarinomys*, Thomas (1896) highlighted its peculiar external morphology and inconspicuous rostral projections, compared to the nasal tube observed in *Oxymycterus* (Hershkovitz 1994). However, some of the similarities with *Oxymycterus* may be due to a shared insectivorous diet, which can be related to some morphological features of the skull, such as the narrow zygomatic plate, inconspicuous zygomatic notch, and a narrow and elongated mandible (Maestri et al. 2016). Skulls of species of *Oxymycterus* also closely resemble that of *Brucepattersonius* in general morphology, to the degree that the genus *Brucepattersonius* was originally considered part of *Oxymycterus*, sharing similar features as the elongated rostra and narrow zygomatic plates (Thomas 1896, Hershkovitz 1998). However, recent studies clearly establish that *Brucepattersonius* and *Oxymycterus* are not closely related (Leite et al. 2014, Leite et al. 2015, Steppan and Schenk 2017), indicating that features indicative of an insectivorous diet appeared convergently different times within Akodontini.

Among other sigmodontines, fossorial habits also appear in some species of the Abrotrichini tribe (e.g. the "long-clawed mice" *Chelemys*, *Notiomys,* and *Geoxus*) (Pearson 1984, Teta et al. 2017). Among this lineage, two genera (*Notiomys* and *Geoxus*) share with *Blarinomys* several cranial characteristics that may reflect their similar insectivorous diet and fossorial habits. Like *Blarinomys*, *Notiomys* and *Geoxus* present "lightly built skulls with inflated sinus strongly inclined and flared zygomatic plate, elongated and trumpeted nasals, rounded interorbital region, very weak and low-crowned molars" (Patterson 1992). In addition, these genera present developed claws which, as stated by Patterson (1992), may represent analogous characters that have an excavation function. However, *Blarinomys* does not have claws as well developed as in *Geoxus*, perhaps reflecting its habit of moving through the litter (Geise et al. 2008).

The other Abrothrichini genus, *Chelemys*, shows greater similarity to the supposed chisel-tooth digger *Kunsia*, with a more heavily built skull, a broad rostrum (Patterson

1992), a more well-defined interorbital region and high-crowned hypsodont teeth, reflecting the herbivorous diet of both genera (Patterson 1992, Bezerra et al. 2007). However, the lack of detailed ecological and functional information for most South American fossorial rodent species precludes further evolutionary discussions about the diversification paths that led to emergence of highly specialized sigmodontines, including *Blarinomys*.

1.4. Conclusion

The tribe Akodontini is a morphologically diverse group, with many species occupying many different niches and habitats, including fossorial, semi-aquatic and cursorial species. Although *Blarinomys* has been frequently mentioned in the literature as a fossorial-adapted akodontine, previous descriptions did not focus on its unique morphology. Although it exhibits several postcranial and external modifications suggesting it is a scratch-digger, *Blarinomys* presents a somewhat specialized cranial morphology for the underground life, combined with modifications related to an insectivorous diet. However, despite the singularity of its skull, reflected both in terms of qualitative comparative description and in the morphometric analysis, physiological and functional morphology studies are still needed to validate theses inferences.

Acknowledgements

We would like to thank the curators of the mammal collections of the Pontifícia Universidade Católica de Minas Gerais, Universidade Federal de Minas Gerais, Museu Nacional and Field Museum of Natural History for granting access to the specimens under their care. We also thank Bárbara T. Faleiro and Adalberto J. Santos for providing the stereomicroscope for the pictures of the auditory apparatus; Rodolfo A. Stumpp for the picture of the living *Blarinomys breviceps*; and Bárbara Rossi for most of the illustrations. We kindly thank Daniel Casali, Noe de la Sancha, and specially Bruce Patterson, for their enriching comments and suggestions. Lastly, we thank Pierre-Henri Fabre and an anonymous reviewer for their valuable comments that greatly improved the manuscript. This work was made possible with financial support of Coordenação de Aperfeiçoamento de Pessoal de Nível Superior (CAPES).

1.5. References

Abravaya, J.P. and Matson, J.O., 1975. Notes on a Brazilian mouse, Blarinomys breviceps (Winge). Contributions in Science of the Natural History Museum of Los Angeles County, 270, pp. 1-8.

Agrawal, V.C., 1967. Skull adaptations in fossorial rodents. Mammalia, 31, pp. 300-312.

Allen, J.A., 1900. On mammals collected in southeastern Peru, by H. H. Keays, with descriptions of new species. Bulletin of the American Museum of Natural History, 13, pp. 219-27.

Argot, C., 2003. Functional-adaptative anatomy of the axial skeleton of some extant marsupials and the paleobiology of the Paleocene marsupials Mayulestes ferox and Pucadelphys andinus. Journal of Morphology, 255, pp. 279-300.

Astúa, D., Bandeira, I. and Geise, L., 2015. Cranial morphometric analyses of the cryptic rodent species Akodon cursor and Akodon montensis (Rodentia, Sigmodontinae). Oecologia Australis, 19, pp. 143-157.

Bezerra, A.M.R., Carmignotto, A.P., Nunes, A.P. and Rodrigues, F.H.G., 2007. New data on the distribution, natural history and morphology of Kunsia tomentosus (Lichtenstein, 1830) (Rodentia: Cricetidae: Sigmodontinae). Zootaxa, 1505, pp. 1-18.

Bugge, J., 1970. The contribution of the stapedial artery to the cephalic arterial supply in muroid rodents. Cells Tissues Organs, 76, pp. 313-336.

Burda, H., Bruns, V. and Hickman, G.C., 1992. The ear in subterranean Insectivora and Rodentia in comparison with ground- dwelling representatives. I. Sound conducting system of the middle ear. Journal of Morphology, 214, pp. 49-61.

Carleton, M.D. and Musser, G.G., 1989. Systematic studies of oryzomyine rodents (Muridae, Sigmodontinae): a synopsis of Microryzomys. Bulletin of the American Museum of Natural History, 191, pp. 1-83.

Carrizo, L.V., Tulli, M.J., dos Santos, D.S. and Abdala, V., 2014. Interplay between postcranial morphology and locomotor types in Neotropical sigmodontine rodents. Jornal of Anatomy, 224, pp. 469-481.

Coutinho, L.C., Oliveira, J.A. and Pessoa, L.M., 2013. Morphological variation in the appendicular skeleton of Atlantic forest sigmodontine rodents. Journal of Morphology, 274, pp. 779-792.

Coutinho, L.C. and Oliveira, J.A., 2017. Relating appendicular skeletal variation of

sigmodontine rodents to locomotion modes in a phylogenetic context. Journal of Anatomy, 231(4), pp. 543-567.

D'Elía, G., 2003. Phylogenetics of Sigmodontinae (Rodentia, Muroidea, Cricetidae), with special reference to the akodont group, and with additional comments on historical biogeography. Cladistics, 19, pp. 307-323.

D'Elía, G. and Pardiñas, U.F.J., 2015. Tribe Akodontini Vorontsov 1959. Mammals of South America, Volume 2: Rodents, pp. 140-279. Chicago: University of Chicago Press.

Davis, D.E., 1944. The capture of the Brazilian mouse Blarinomys breviceps. Journal of Mammalogy, 25, pp. 367-369.

Davis, D.E., 1947. Notes on the life histories of some Brazilian mammals. Boletim do Museu Nacional, 76, pp. 1-8.

Ellerman, J.R., 1941. The families and genera of living rodents, Vol. 2: Family Muridae. London: Trustees of the British Museum (Natural History).

Elissamburu, A. and Vizcaíno, S.F., 2004. Limb proportions and adaptations in caviomorph rodents (Rodentia: Caviomorpha). Journal of Zoology, 262, pp. 145-159.

Fernandez, M.E., Vassallo, A.I. and Zarate, M., 2000. Functional morphology and palaeobiology of the Pliocene rodent Actenomys (Caviomorpha: Octodontidae): the evolution to a subterranean mode of life. Biological Journal of the Linnean Society, 71, pp. 71-90.

Flores, D.A. and Diaz, M.M., 2009. Postcranial skeleton of Glironia venusta (Didelphimorphia, Didelphidae, Caluromyinae): description and functional morphology. Zoosystematics and Evolution, 5, pp. 311-339.

Geise, L., Bergallo, H.G., Esberárd, C.E.L., Rocha, C.F.D. and Van Sluys, M., 2008. The karyotype of Blarinomys breviceps (Mammalia: Rodentia: Cricetidae) with comments on its morphology and some ecological notes. Zootaxa, 1907, pp. 47-60.

Goeldi, E.A., 1901. Dois roedores notaveis da familia dos ratos do Brazil. Boletim do Museu Paraense de Historia Natural e Ethnographia (Museu Goeldi), 3, pp. 166-180.

Greene, E.C., 1955. Anatomy of the rat. Transactions of the American Philosophical Society, 27, pp. 1-370.

Gudinho, F. and Iack Ximenes, G.E., 2015. The presence of the interparietal and its ontogeny in Blarinomys breviceps (Rodentia: Sigmodontinae). Livro de Resumos do XIII Congresso Brasileiro de Mastozoologia, p. 26.

Gyldenstolpe, N.C.G.F., 1932. A manual of Neotropical sigmodont rodents. Kunglinga Svenska Vetenskapsakademiens Handlingar, 11, pp. 1–164

Hershkovitz, P., 1962. Evolution of Neotropical cricetine rodents (Muridae) with special reference to the phyllotine group. Fieldiana Zoology, 46, pp. 1-524.

Hershkovitz, P., 1966. South American swamp and fossorial rats of the scapteromyine group (Cricetinae, Muridae) with comments on the glans penis in murid taxonomy. Zeitschrift für Säugetierkunde, 31, pp. 81-149.

Hershkovitz, P., 1994. The description of a new species of South American hocicudo or longnose mouse, genus Oxymycterus (Sigmodontinae, Muroidea), with critical review of the generic content. Fieldiana Zoology, 79, pp. 1-43.

Hershkovitz, P., 1998. Report on some sigmodontine rodents collected in southeastern Brasil with descriptions of a new genus and six species. Bonner Zoologische Beitrage, 47(3), pp. 193-256.

Hildebrand, M., 1985. Digging in quadrupeds. Functional Vertebrate Morphology, pp. 89-109. Cambridge: Belknap Press.

Hill, J.E., 1935. The cranial foramina in rodents. Journal of Mammalogy, 16, pp. 121-129.

Hopkins, S.S.B. and Davis, E.B. 2009 Quantitative morphological proxies for fossoriality in small mammals. Journal of Mammalogy, 90, pp. 1449-1460.

Klingenberg, C.P., 2011. MorphoJ: an integrated software package for geometric morphometrics. Molecular Ecology Resources, 11, pp. 353-357.

Lange, S., Stalleicken, J. and Burda, H., 2004. Functional morphology of the ear in fossorial rodents, Microtus arvalis and Arvicola terrestris. Journal of Morphology, 262, pp. 770-779.

Lehman, W.H., 1963. The forelimb architecture of some fossorial rodents. Journal of Morphology, 113, pp. 59-76.

Leite, R.N., Kolokotronis, S.O., Almeida, F.C., Werneck, F., Rogers, D.S. and Weksler, M., 2014. In the wake of invasion: tracing the historical biogeography of the South American cricetid radiation (Rodentia, Sigmodontinae). PLos One, 9, p. e100687.

Leite, Y.L., Kok, P.J. and Weksler, M., 2015. Evolutionary affinities of the ‘Lost World’ mouse suggest a late Pliocene connection between the Guiana and Brazilian shields. Journal of Biogeography, 42, pp. 706-715.

Lichtenstein, H., 1830. Darstellungen neuer oder wenig bekannte Säugethiere Abbildungen und Beschreibungen von fünf und sechzig Arten und füntzig colorirten Steindrucktafeln nach den Originalen des Zoologischen Museum der Universität zu Berlin. Berlin: C. G. Luderitz, unpaginated text belonging to 50 plates.

Lund, P.W., 1840. Tillaeg til de to sidste Afhandlinger over Brasiliens Dyreverden för sidste Jorgomvaeltning. Lagoa Santa, den 4de April 1839. Kongelige Danske Videnskabernes Selskabs Naturvidenskabelige og Mathematiske Afhandling 3 pp. 1-24.

Maestri, R., Fornel, R., Galiano, D. and Freitas, T.R.O., 2015. Niche suitability affects development: skull asymmetry increases in less suitable areas. PLos One, 10, p. e0122412.

Maestri, R., Patterson, B.D., Fornel, R., Monteiro, L.R. and Freitas, T.R.O., 2016. Diet, bite force and skull morphology in the generalist rodent morphotype. Journal of Evolutionay Biology, 29, pp. 2191-2204.

Mason, M.J., 2015. Functional morphology of rodent middle ears. Evolution of the Rodents: Advances in Phylogeny, Functional Morphology and Development, pp. 373-404. Cambridge: Cambridge University Press.

Matson, J.O., Abravaya, J.P., 1977. Blarinomys breviceps. Mammalian Species, 74, pp. 1-3. Moojen, J., 1952. Os Roedores do Brasil. Rio de Janeiro: Instituto Nacional do Livro.

Moojen, J., 1965. Nôvo gênero de Cricetidae do Brasil Central (Glires, Mammalia). Revista Brasileira de Biologia, 25, pp. 281-285.

Moore, W.J., 1981. The Mammalian Skull. Cambridge: Cambridge University Press.

Moreira, J.C. and Oliveira, J.A., 2011. Evaluating diversification hypotheses in the South American cricetid Thaptomys nigrita (Lichtenstein, 1829) (Rodentia: Sigmodontinae): an appraisal of geographical variation based on different character systems. Journal of Mammalian Evolution, 18, pp. 201-214.

Musser, G.G., 1982. Crunomys and the small-bodied shrew rats native to the Philippine Islands and Sulawesi (Celebes). Bulletin of the American Museum of Natural History, 174, pp. 1-95.

Musser, G.G. and Durden, L.A., 2002. Sulawesi Rodents: Description of a New Genus and Species of Murinae (Muridae, Rodentia) and Its Parasitic New Species of Sucking Louse (Insecta, Anoplura). American Museum Novitates, 3368, pp. 1-50.

Myers, P., 1989. A preliminary revision of the varius group of Akodon (A. dayi, dolores,

molinae, neocenus, simulator, toba and varius). Advances in Neotropical Mammalogy, pp. 5-54. Gainesville: Sandhill Crane Press.

Myers, P. and Patton, J.L., 1989. A new species of Akodon from the cloud forests of eastern Cochabamba Department, Bolivia (Rodentia: Sigmodontinae). Occasional Papers of the Museum of Zoology, The University of Michigan, 720, pp. 1-28.

Naxara, L., Pinotti, B.T. and Pardini, R., 2009. Seasonal microhabitat selection by terrestrial rodents in an old-growth Atlantic Forest. Journal of Mammalogy, 90, pp. 404–415.

Nevo, E., 1979. Adaptive convergence and divergence of subterranean mammals. Annual Review of Ecology and Systematics, 10, pp. 269-308.

Nevo, E., 1995. Mammalian evolution underground. The ecological-genetic-phenetic interfaces. Acta Theriologica, 3, pp. 9-31.

Nevo, E., 1999. Mosaic Evolution of Subterranean Mammals: Regression, Progression and Global Convergence. New York: Oxford University Press.

Novacek, M.J., 1993. Patterns of diversity in the mammalian skull. The Skull 2: Patterns of Structural and Systematic Diversity, pp. 438-545. Chicago: The University of Chicago Press.

Paglia, A.P., Perini, F.A., Lopes, M.O.G. and Palmuti, C.F.S., 2005. Novo registro de Blarinomys breviceps (Winge, 1888) (Rodentia, Sigmodontinae) no estado de Minas Gerais, Brasil. Lundiana, 6, pp. 155-157.

Pardiñas, U.F.J., D'Elía, G. and Ortiz, P.E., 2002. Sigmodontinos fósiles (Rodentia, Muroidea, Sigmodontinae) de América del Sur: estado actual de su conocimiento y prospectiva. Mastozoología Neotropical, 9, pp. 209-252.

Pardiñas, U.F.J., D'Elía, G. and Teta, P., 2008. Una introducción a los mayores sigmodontinos vivientes: revisión de Kunsia Hershkovitz, 1966 y descripción de un nuevo género (Rodentia: Cricetidae). Arquivos do Museu Nacional do Rio de Janeiro, 66, pp. 509-594.

Patterson, B.D., 1992. A new genus and species of long-clawed mouse (Rodentia: Muridae) from temperate rainforest of Chile. Zoological Journal of the Linnean Society, 106, pp. 127– 145.

Pearson, O.P., 1984. Taxonomy and natural history of some fossorial rodents of Patagonia, southern Argentina. Journal of Zoology, 202, pp. 225-237.

Quintela, F.M., Fornel, R. and Freitas, T.R., 2016. Geographic variation in skull shape of the water rat Scapteromys tumidus (Cricetidae, Sigmodontinae): isolation-by-distance plus environmental and geographic barrier effects. Anais da Academia Brasileira de Ciências, 88, pp.

451-466.

Ravicz, M.E. and Rosowski, J.J., 1997. Sound-power collection by the auditory periphery of the Mongolian gerbil Meriones unguiculatus: III. Effect of variations in middle-ear volume. The Journal of the Acoustical Society of America, 101, pp. 2135-2147.

Reig, O.A., 1987. An assessment of the systematics and evolution of the Akodontini, with the description of new fossil species of Akodon (Cricetidae, Sigmodontinae). Fieldiana Zoology, 39, pp. 347-400.

Rohlf, F.J., 2007. tps serie softwares. http//life.bio.sunysb.edu/ morph/

Samuels, J.X., 2009. Cranial morphology and dietary habits of rodents. Zoological Journal of the Linnean Society, 156, pp. 864-888.

Samuels, J.X. and Van Valkenburgh, B., 2008. Skeleton indicators and locomotor adaptations n living and extinct rodents. Journal of Morphology, 269, pp. 1387-1411.

Sargis, E.J., 2001. A preliminary qualitative analysis of the axial skeleton of tupaiids (Mammalia, Scandentia): functional morphology and phylogenetic implications. Journal of Zoology, 253, pp. 473–483.

Schleich, C.E. and Vassallo, A.I., 2003. Bullar volume in subterranean and surface-dwelling caviomorph rodents. Journal of Mammalogy, 84, pp. 185-189.

Shapiro, L.J., 1995. Functional morphology of indrid lumbar vertebrae. American Journal of Physical Anthropology, 98, pp. 323-342.

Shimer, H.W., 1903. Adaptations to aquatic, arboreal, fossorial and cursorial habits in mammals. III. Fossorial adaptations. American Naturalist, 37, pp. 819-825.

Silva, C.R., Percequillo, A.R., Iack Ximenes, G. and de Vivo, M., 2003. New distributional records of Blarinomys breviceps (Winge, 1888) (Sigmodontinae, Rodentia). Mammalia, 67, pp. 147-152.

Stein, B.R., 2000. Morphology of subterranean rodents. Life Underground: The Biology of Subterranean Rodents, pp. 19-61. Chicago: University of Chicago Press.

Steppan, S.J. and Schenk, J.J., 2017. Muroid rodent phylogenetics: 900-species tree reveals increasing diversification rates. PLos One, 12, pp. e0183070.

Teta, P. and Pardiñas, U.F.J., 2015. Genus Blarinomys Thomas, 1986. Mammals of South America, Volume 2: Rodents, pp. 208-211. Chicago: University of Chicago Press.

Teta, P., Pardiñas, U.F.J. and D'Elía, G., 2015. Genus Thaptomys Thomas, 1916.

Mammals of South America, Volume 2: Rodents, pp. 277-279. Chicago: University of Chicago Press.

Teta, P., Cañon, C., Patterson, B. and Pardiñas, U.F.J., 2017. Phylogeny of the tribe Abrotrichini (Cricetidae, Sigmodontinae): integrating morphological and molecular evidence into a new classification. Cladistics, 33, pp. 153-182.

Thomas, O., 1896. On the genera of rodents: an attempt to bring up to date the current arrangement of the order. Proceedings of the Zoological Society of London, 64, pp. 1012- 1028.

Thomas, O., 1903. New forms of Sciurus, Oxymycterus, Kannabateomys, Proechimys, Dasyprocta, and Caluromys from South America. Journal of Natural History, 11, pp. 487-493.

Thomas, O., 1913. New forms of Akodon and Phyllotis, and a new genus for "Akodon" teguina. Journal of Natural History, 11, pp. 404-409.

Thomas, O., 1916. The grouping of the South-American Muridae commonly referred to Akodon. Journal of Natural History, 8, pp. 336–340.

Vassallo, A.I., 1998. Functional morphology, comparative behaviour, and adaptation in two sympatric subterranean rodent genus Ctenomys (Rodentia: Octodontidae). Journal of Zoology, 244, pp. 415–427.

Ventura, K., Sato-Kuwabara, Y., Fagundes, V., Geise, L., Leite, Y.L.R., Costa, L.P., Silva, M.J.J., Yonenaga-Yassuda, Y. and Rodrigues, M.T., 2012. Phylogeographic structure and karyotypic diversity of the Brazilian shrew mouse (Blarinomys breviceps, Sigmodontinae) in the Atlantic Forest. Cytogenetic and Genome Research, 138, pp. 19- 30.

Voss, R.S., 1988. Systematics and ecology of ichthyomyine rodents (Muroidea). Bulletin of the American Museum of Natural History, 188, pp. 259-493.

Voss, R.S. and Carleton, M.D., 1993. A new genus for Hesperomys molitor Winge and Holochilus magnus Hershkovitz (Mammalia, Muridae) with an analysis of its phylogenetic relationship. American Museum Novitates, 3085, pp. 1-39.

Wahlert, J.H., 1985. Cranial foramina of rodents. Evolutionary Relationships Among Rodents, pp. 311-332. Boston: Springer.

Weidenreich, F., 1941. The brain and its role in the phylogenetic transformation of the human skull. Transactions of the American Philosophical Society, 31, pp. 321-442.

Winge, H., 1887. Jordfundne og nulevende Gnavere (Rodentia) fra Lagoa Santa, Minas Geraes, Brasilien: med udsigt over gnavernes indbyrdes slagtskab. E Museo Lunii, 1, pp. 1-178.

1.6. Figures

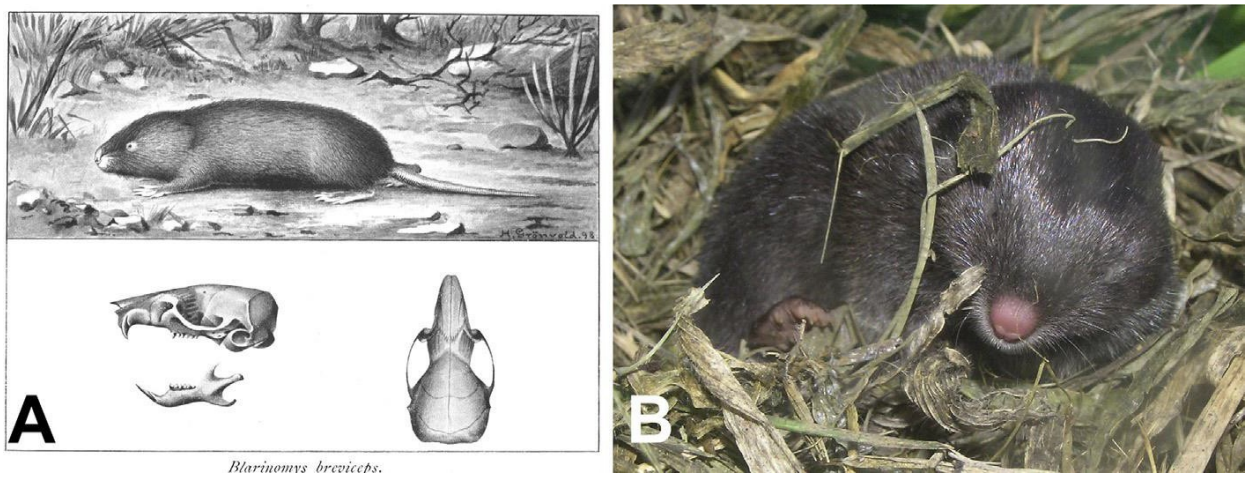

Blarinomys breviceps.

Figure 1.1. External morphology of *Blarinomys breviceps*. At left (A), the original plate from Goeldi (1901), showing the skull and external morphology of a living specimen. At right (B), a living *Blarinomys* from Viçosa, Minas Gerais, Brazil. Note the small eyes and ears, hidden under the fur, and the conspicuous nose pad. Photo by Rodolfo A. Stumpp.

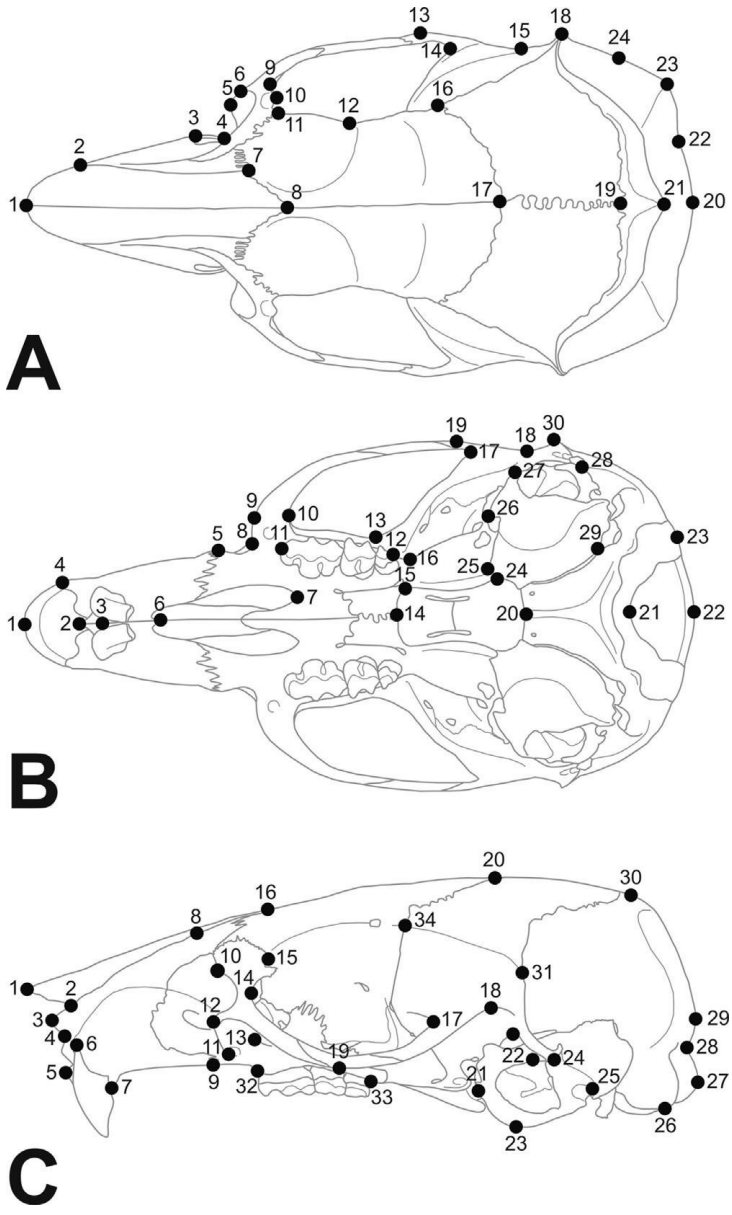

Figure 1.2. Landmark locations used in this work in dorsal (A), ventral (B) and lateral (C) views. Detailed descriptions of each landmark appear in Supplementary Material 1.S2.

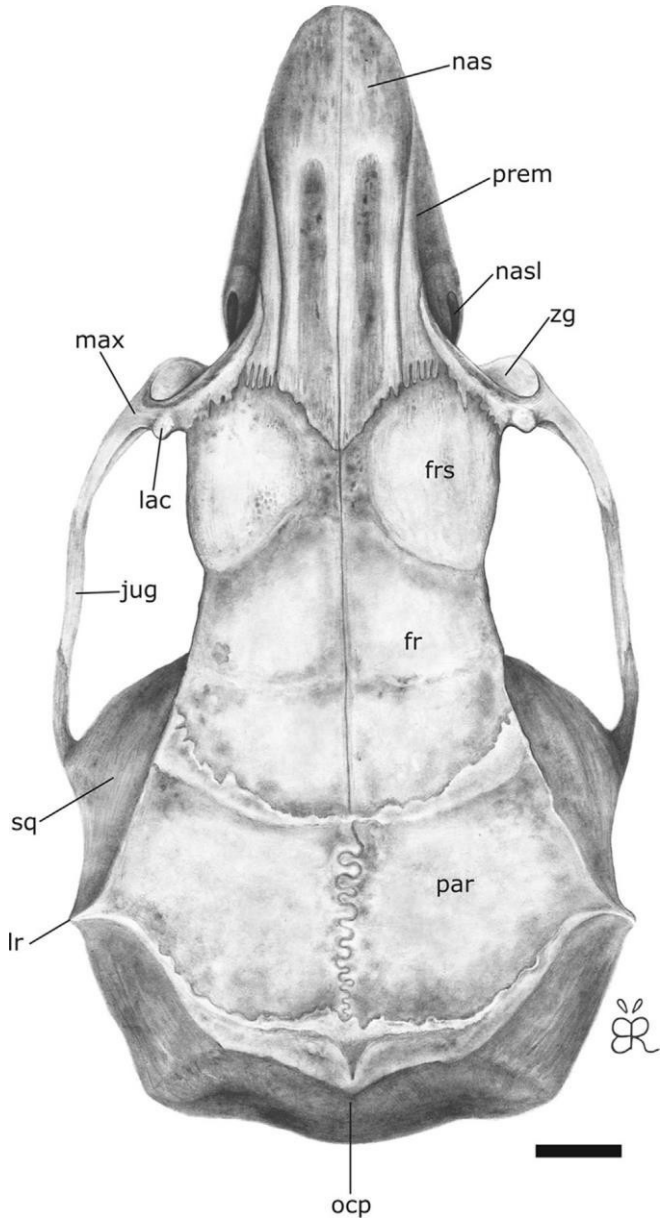

Figure 1.3. Dorsal view of the skull of *Blarinomys breviceps*. fr: frontal; frs: frontal sinus; jug: jugal; lac: lacrimal; lr: lambdoidal ridge; max: maxillary; nas: nasal; nasl: nasolacrimal foramen; ocp: occipital plate; par: parietal; prem: premaxilla; sq: squamosal; zg: zygomatic notch. Scale bar: 25mm.

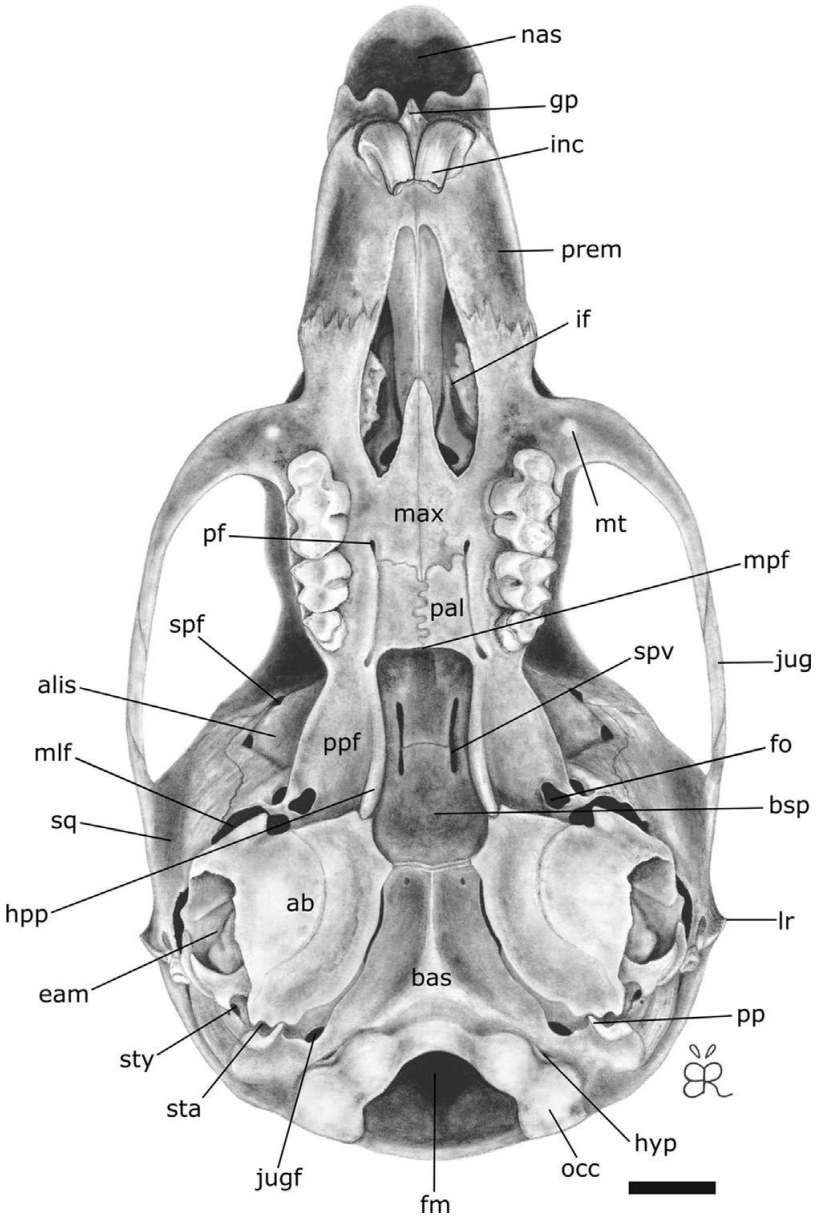

Figure 1.4. Ventral view of the skull of *Blarinomys breviceps*. ab: auditory bulla; alis: alisphenoid; bas: basioccipital; bsp: basisphenoid; eam: external auditory meatus; fm: foramen magnum; fo: foramen ovale; gp: gnathic process; hpp: hamular process of the pterygoid; hyp: hypoglossal foramen; if: incisive foramina; inc: incisive tooth; jug: jugal; jugf: jugular foramen; lr: lambdoidal ridge; nas: nasal; max: maxillary; mlf: middle lacerate foramen; mpf: mesopterygoid fossa; mt: masseteric tubercle; occ: occipital condyle; pal: palatine; par: parieta; ppf: parapterygoid fossa; prem: premaxilla; psp: presphenoid; spf: sphenofrontal foramen; sq: squamosal; spv: sphenopalatine vacuities; sta: stapedial foramen; sty: stylomastoid foramen.
Scale bar: 25mm.

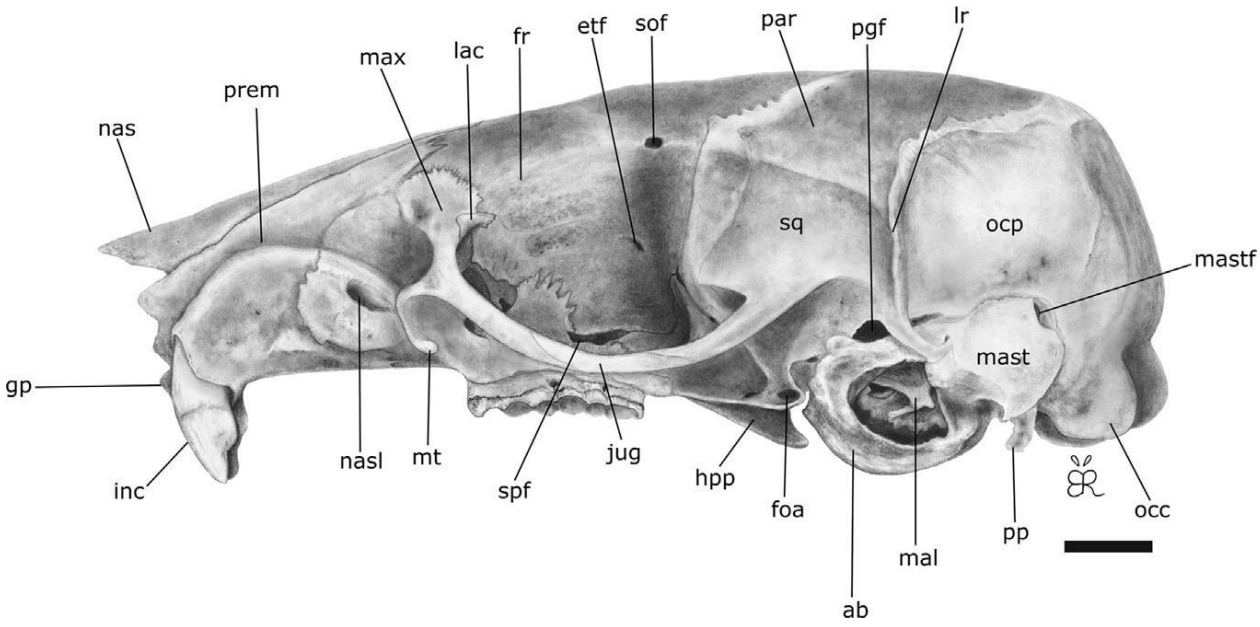

Figure 1.5. Lateral view of the skull of *Blarinomys breviceps*. ab: auditory bulla; etf: ethmoid foramen; foa: foramen ovale accessorius; fr: frontal; gp: gnathic process; hpp: hamular process of the pterygoid; inc: incisive tooth; jug: jugal; lac: lacrimal; lr: lambdoidal ridge; nas: nasal;nasl: nasolacrimal foramen; mal: malleolus; mast: mastoid; mastf: mastoid fenestra; max: maxillary; mt: masseteric tubercle; occ: occipital condyle; ocp: occipital plate; par: parietal; pgf: postglenoid foramen; pp: paraoccipital process; prem: premaxilla; sof: supraorbital foramen; spf: sphenopalatine foramen; sq: squamosal. Scale bar: 25mm.

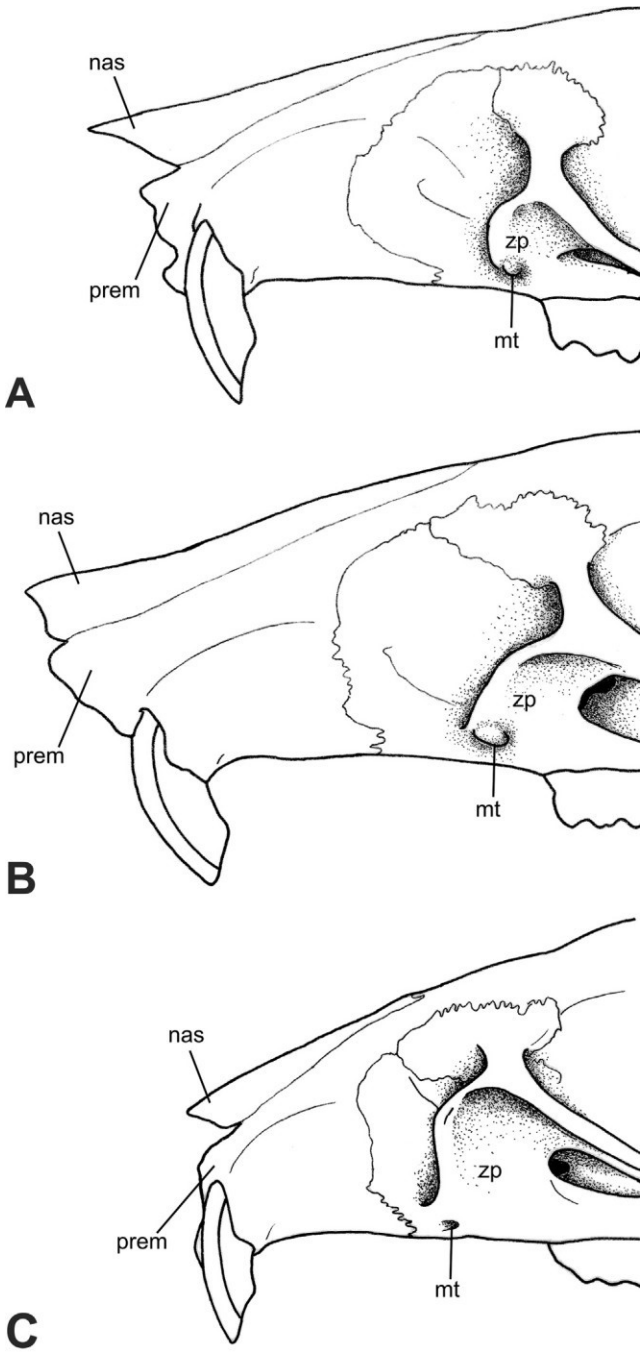

Figure 1.6. Rostral region of the skull of (A) *Blarinomys breviceps* (MCN-M 1472) (B) *Oxymycterus delator* (MCN-M 2482) and (C) *Necromys lasiurus* (MCN-M 497). nas: nasal; mt: masseteric tubercle; prem: premaxilla; zp: zygomatic plate.

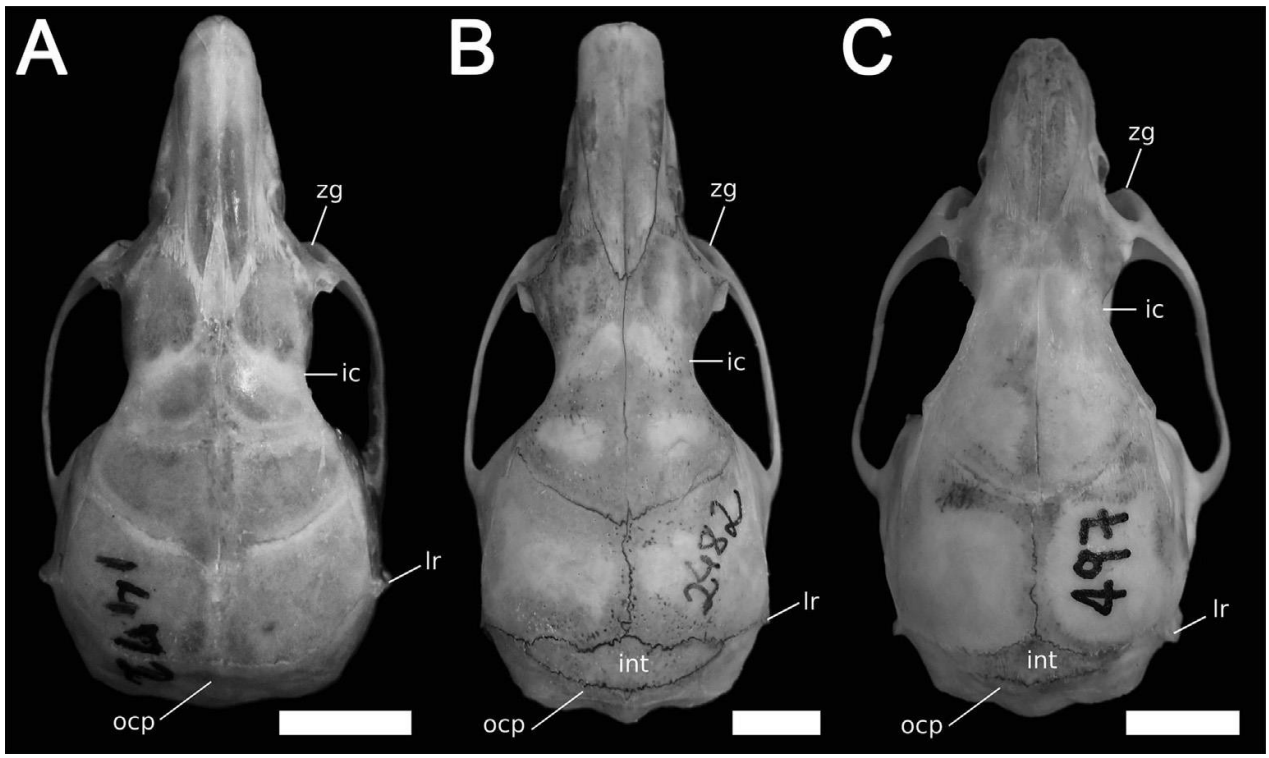

Figure 1.7. Dorsal view of the skull of (A) *Blarinomys breviceps* (MCN-M 1472); (B) *Oxymycterus delator* (MCN-M 2482); and (C) *Necromys lasiurus* (MCN-M 497). See text for morphological differences. ic: interorbital constriction; int: interparietal; lr: lambdoidal ridge; ocp: occipital plate; zg: zygomatic notch. Scale bar: 5mm.

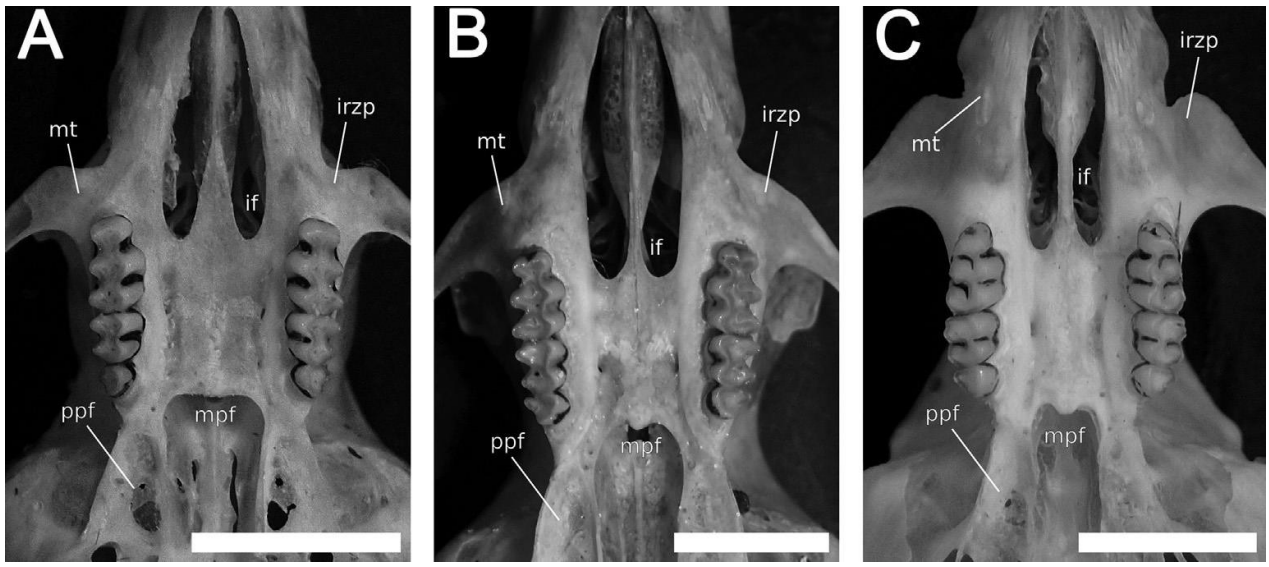

Figure 1.8. Ventral view of the skull of (A) *Blarinomys breviceps* (MCN-M 1472); (B) *Oxymycterus delator* (MCN-M 2482); and (C) *Necromys lasiurus* (MCN-M 497). See text for morphological differences. if: incisive foramina; irzp: inferior root of the zygomatic plate; mpf: mesopterygoid fossa; mt: masseteric tubercle; ppf: parapterygoid fossa. Scale bar: 5mm.

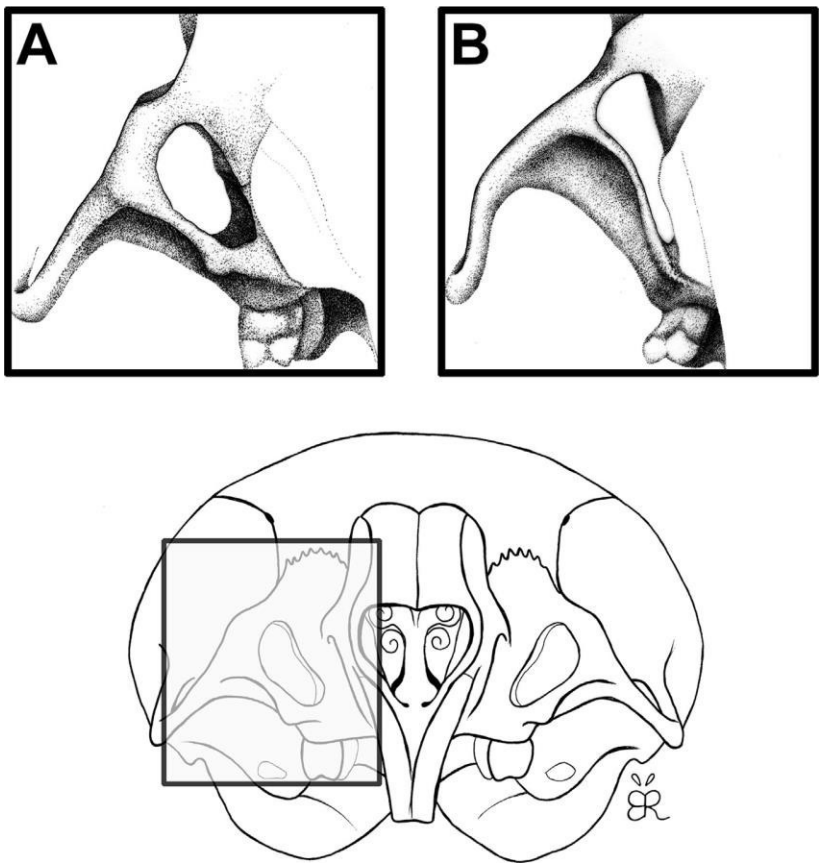

Figure 1.9. Infraorbital foramen of (A) *Blarinomys breviceps* (MCN-M 1472) and (B) *Akodon montensis* (UFMG 2705).

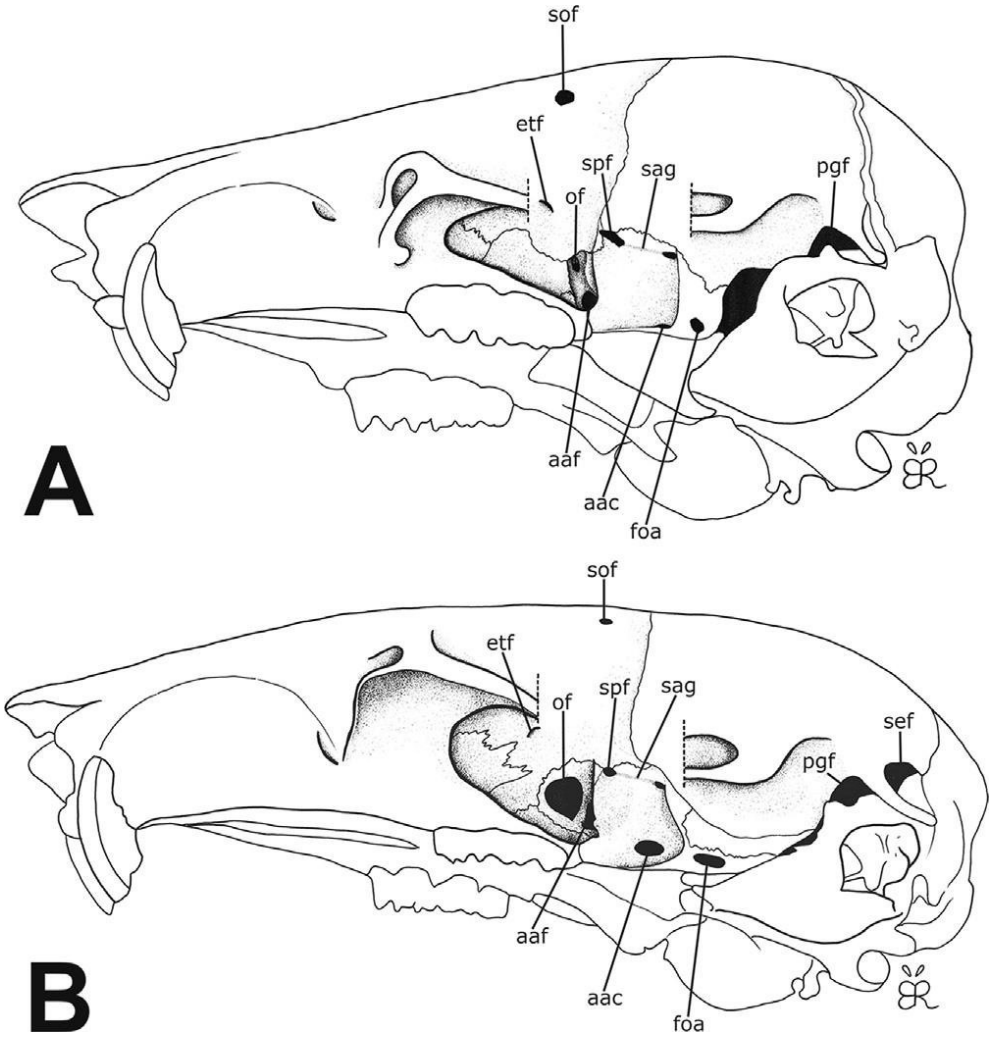

Figure 1.10. Optic region of (A) *Blarinomys breviceps* (UFMG 4062) and (B) *Akodon montensis* (UFMG 2700). Notice the small size of the optic foramen of *Blarinomys* compared with the same structure in *Akodon*. aac: anterior opening of the alisphenoid canal; aaf: anterior alar fissure; etf: ethmoid foramen; foa: foramen ovale accessorius; of: optic foramen; pgf: postglenoid foramen; sag: squamosal-alisphenoid groove; sef: subsquamosal fenestra; sof: supraorbital foramen; spf: sphenofrontal foramen.

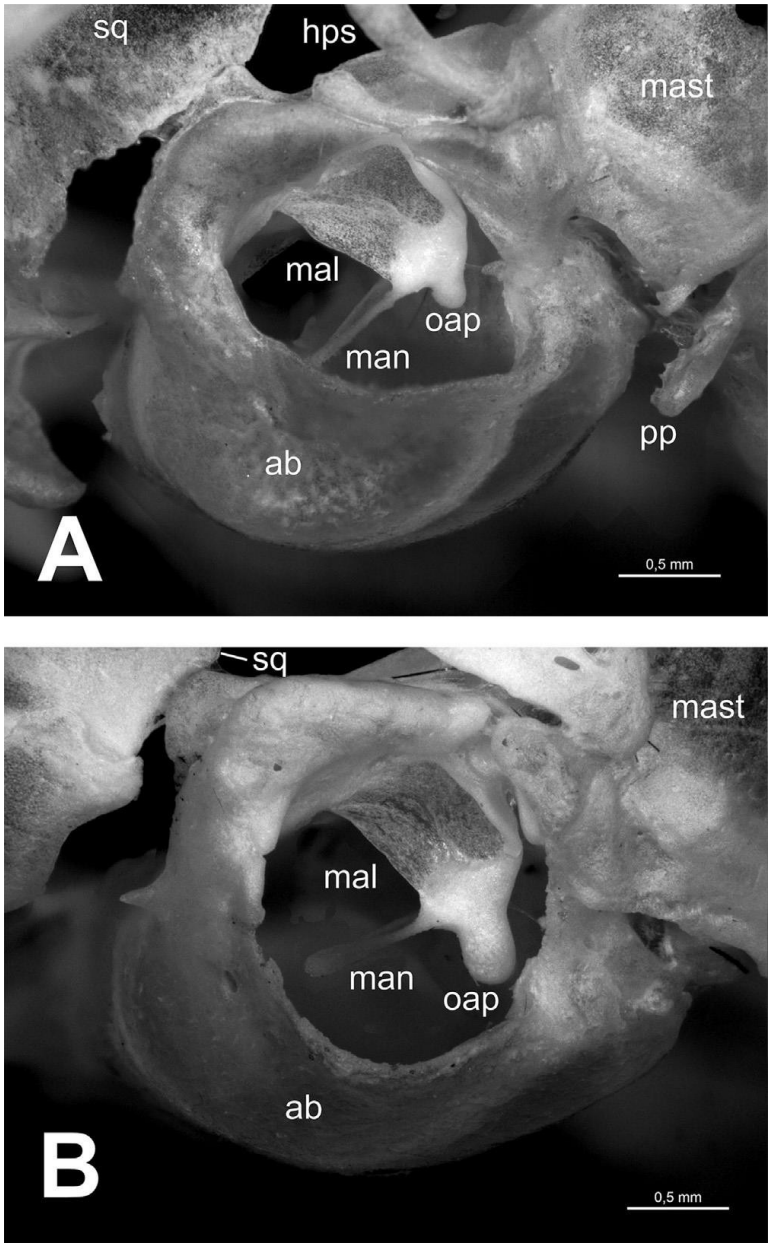

Figure 1.11. Lateral view of bullar and middle ear region on (A) *Blarinomys breviceps* (MCN-M 2837) and (B) *Akodon montensis* (UFMG 2687). Note the inconspicuous orbicular apophysis (oap) of *Blarinomys*, when compared with the same structure of *Akodon*. ab: auditory bulla; hps: hamular process of the squamosal mal: malleolus; man: manubrium; mast: mastoid; oap: orbicular apophysis; pp: paraoccipital process; sq: squamosal. Scale bar: 0.05mm.

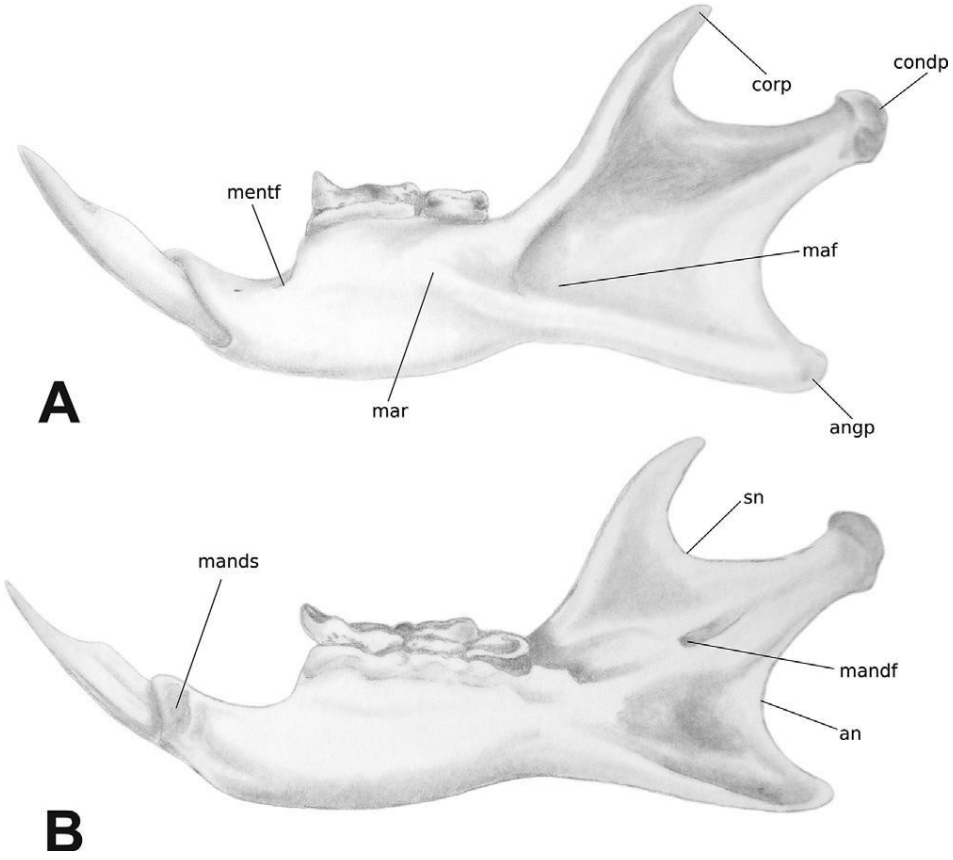

Figure 1.12: Mandible of *Blarinomys breviceps* on lateral (A) and medial (B) views. an: angular notch; angp: angular process; condp: condylar process; corp: coronoid process; mandf: mandibular foramen; mands: mandibular symphysis; maf: masseteric fossa; mar: masseteric ridge; mentf: mental foramen; sn: sigmoid notch.

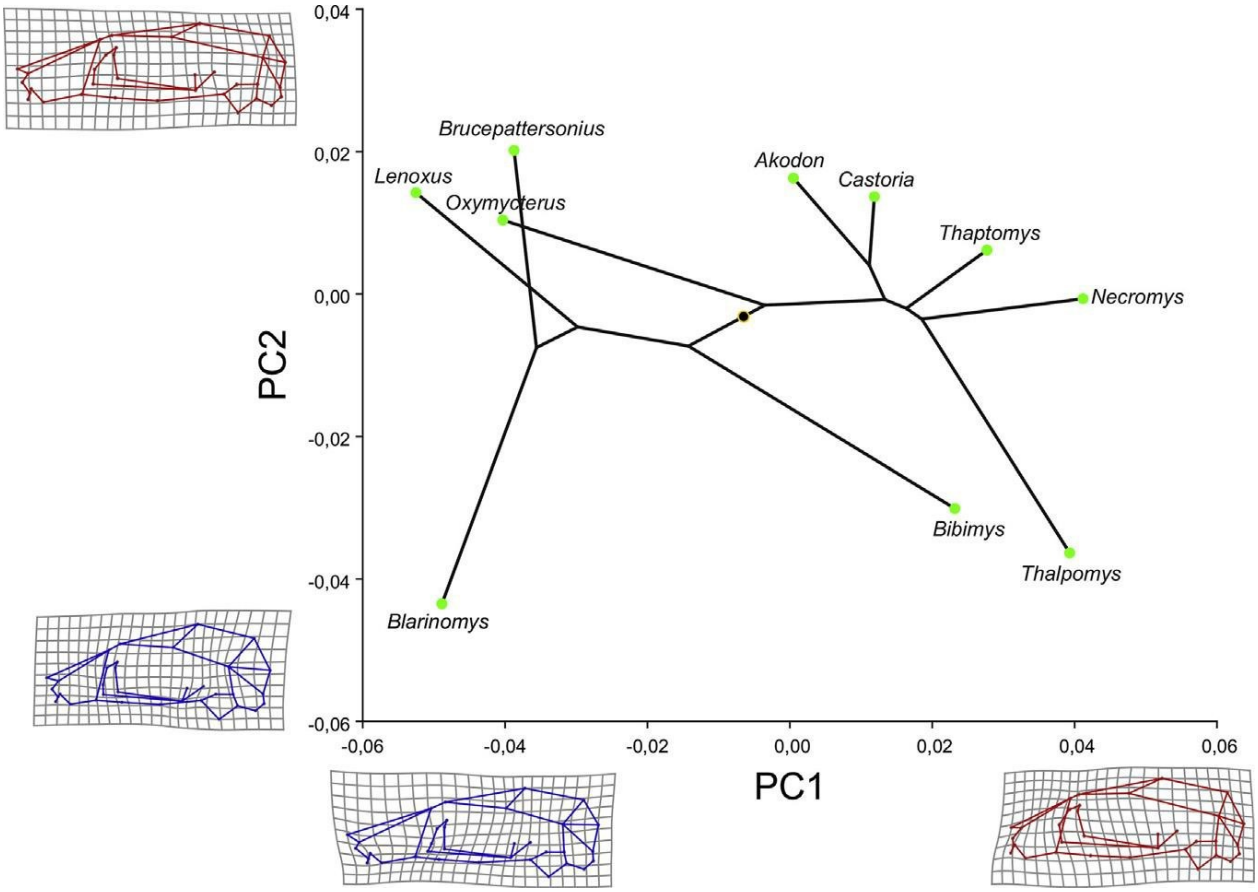

Figure 1.13. Phylomorphospace projections of the phylogeny on the first two principal components of the PCA analysis of the lateral view of the skull.

1.7. Supplementary Material

Supplementary Material 1.S1. List of specimens used in the comparative description and morphometric analyses, with respective age class.

Species	Collection number	Age class	Lateral view	Dorsal view	Ventral view
Akodon cursor	UFMG 2293	4	x	x	x
	UFMG 2310	5	x	x	x
	UFMG 2672	5	x	x	x
	UFMG 2674	5	x	x	x
	UFMG 2676	5	x	x	x
	UFMG 2677	3	x	x	x
	UFMG 2678	4	x	x	x
Akodon montensis	UFMG 2684	4	x	x	x
	UFMG 2686	5	x	x	x
	UFMG 2687	4	x	x	x
	UFMG 2699	4	x	x	x
	UFMG 2700	5	x	x	x
	UFMG 2702	4	x	x	x
	UFMG 2703	4	x	x	x
	UFMG 2704	5	x	x	x
	UFMG 2705	5	x	x	x
Bibimys labiosus	MCN-M 2162	2	-	-	x
	MCN-M 2198	2	-	-	x
	MCN-M 2833	2	x	-	x
	MCN-M 2838	2	x	x	x
	MCN-M 2839	3	x	x	x
Blarinomys breviceps	UFMG 2016	4	-	-	x
	UFMG 2087	3	-	x	-
	UFMG 2199	5	x	x	x
	UFMG 4033	4	x	-	x
	MCN-M 1472	3	x	x	x
	MCN-M 2196	3	x	-	x
	MCN-M 2533	3	x	x	x
	MCN-M 2747	3	x	x	x
	MCN-M 2834	4	-	x	x
	MCN-M 2837	4	x	x	x
	MCN-M 2983	4	x	x	x
Brucepattersonius griserufescens	UFMG 1891	4	x	x	x
	UFMG 1892	5	x	x	x
Castoria angustidens	UFMG 1852	5	x	x	x
	UFMG 1853	4	x	x	x
	UFMG 1854	4	x	-	x
	UFMG 1856	4	x	x	x
	UFMG 1857	4	x	x	x
	UFMG 1858	4	x	x	x
	UFMG 1860	3	x	x	x
	UFMG 1861	4	x	x	x
	UFMG 1862	3	x	x	x

(continued)

Kunsia tomentosus	MN 62569	4	-	-	-
	MN 62570	4	-	-	-
Juscelinomys candango	MN 23870	4	-	-	-
	MN 23871	4	-	-	-
	MN 30026	5	-	-	-
	MN 30027	5	-	-	-
	MN 30028	3	-	-	-
	MN 30030	3	-	-	-
	MN 30031	4	-	-	-
	MN 30032	5	-	-	-
Lenoxus apicalis	FMNH 20106	5	x	x	-
	FMNH 52612	4	x	x	x
	FMNH 52613	5	x	x	x
Necromys lasiurus	UFMG 219	4	x	x	x
	UFMG 221	3	x	-	x
	UFMG 2294	5	x	x	x
	UFMG 2300	3	x	x	x
	UFMG 2303	3	x	x	x
	UFMG 2304	3	x	x	x
	UFMG 2308	3	x	x	x
	UFMG 2422	5	x	-	x
	UFMG 2735	3	x	x	x
	UFMG 3835	3	x	x	x
	UFMG 3874	3	x	x	x
Oxymycterus dasytrichus	UFMG 85	4	x	x	x
	UFMG 2138	5	x	-	x
	UFMG 2140	2	x	x	x
	UFMG 3057	3	x	x	x
	UFMG 3949	5	x	x	x
	UFMG 4090	3	x	x	x
	UFMG 4150	3	x	x	x
	UFMG 4520	3	x	x	x
	UFMG 6159	3	x	x	x
Oxymycterus delator	UFMG 4005	3	x	x	x
	UFMG 4221	3	x	x	x
	UFMG 4297	3	x	x	x
Oxymycterus rufus	UFMG 4157	4	x	x	x
Thalpomys lasiotis	MN 60185	3	x	x	-
	MN 60199	3	x	-	-
	MN 60200	3	x	-	-
	MN 61652	4	x	-	-
	MN 62654	3	-	-	-
	MN 62655	4	x	-	-
	MN 62656	3	x	-	-
	MN 62657	3	x	-	-
	MN 75104	3	-	x	x
	MN 75105	3	x	-	-

(continued)

	MN 75106	3	x	x	x
	MN 75108	2	-	x	x
	MN 82159	4	-	x	x
Thaptomys nigrita	UFMG 05	4	x	x	x
	UFMG 171	5	x	x	x
	UFMG 189	4	x	x	-
	UFMG 1839	5	x	x	x
	UFMG 1841	3	x	x	x
	UFMG 1845	3	x	x	x
	UFMG 1846	4	x	x	x
	UFMG 1848	5	x	x	x
	UFMG 1850	5	x	x	x
	UFMG 1851	4	x	x	x
	UFMG 2238	4	-	x	-
Total	-	-	84	77	81

Supplementary Material 1.S2. Landmark descriptions for each view:

Dorsal view: (1) Anteriormost point of suture between nasals; (2) Anteriormost point of suture between nasal and premaxilla; (3) Superiormost point of nasolacrimal foramen; (4) Anteriormost point of zygomatic plate, proximally; (5) Anteriormost point of zygomatic notch; (6) Anteriormost point of zygomatic plate, distally; (7) Suture between nasal, frontal and premaxilla; (8) Posteriormost point of suture between nasal and frontal; (9) Posteriormost point of maximum constriction of anterorbital bridge; (10) Posteriormost point of suture between maxilla, lacrimal and frontal bones; (11) Posteriormost pointof lacrimal bone; (12) Margin of maximum constriction of interorbital region; (13) Superiormost margin of zygomatic arch; (14) Anteriormost margin of squamosal root of zygomatic arch; (15) Posteriormost margin of squamosal root of zygomatic arch; (16) Suture between frontal, squamosal and parietal; (17) Suture between frontals and parietals; (18) Superiormost point of suture between parietal and occipital plate (lambdoidal ridge); (19) Posteriormost point of parietal bones; (20) Posteriormost point of occipital plate; (21) Anteriormost point of occipital plate; (22) Deepest point between landmarks 20 and 23; (23) Posteriormost point between landmarks 22 and 24; (24) Deepest point between landmarks 18 and 23.

Lateral view: (1) Anteriormost point of nasal; (2) Anteriormost point of suture between nasal and premaxilla; (3) Anteriormost point of premaxilla; (4) Point of premaxilla most close to the incisive tooth; (5) Anteriormost point of gnathic process; (6) Anteriormost point of incisive alveolus; (7) Posteriormost point of incisive alveolus; (8) Posteriormost point of suture between nasal and premaxilla; (9) Inferiormost point of suture between premaxilla and maxilla; (10) Point of origin of superior root of zygomatic plate; (11) Point of origin of inferior root of zygomatic plate; (12) Anteriormost point of zygomatic plate; (13) Point of maximum posterior constriction of maxillary root of zygomatic plate; (14) Point of maximum posterior constriction of anterorbital bridge; (15) Suture between frontal, maxillary and lacrimal; (16) Posteriormost point of suture between nasals and frontals; (17) Point of maximal anterior constriction of squamosal root of zygomatic arch; (18) Point of maximum posterior constrictionof squamosal root of zygomatic arch; (19) Inferiormost point of zygomatic arch; (20) Superiormost point of suture between frontals and parietals; (21) Suture between squamosal, alisphenoid and auditory bulla; (22) Superiormost point of auditory bulla;

(23) Inferiormost point of auditory bulla; (24) Posteriormost point of hamular process of the squamosal; (25) Suture between auditory bulla and mastoid; (26) Inferiormost point of occipital condyle; (27) Posteriormost point of occipital condyle; (28) Point of maximum constriction of occipital plate; (29) Posteriormost point of occipital plate; (30) Superiormost point of occipital plate; (31) Suture between parietal, squamosal and occipital; (32) Anteriormost point of the first molar alveolus; (33) Posteriormost point of the third molar alveolus; (34) Point of suture between frontal, parietal and squamosal.

Ventral view: (1) Anteriormost point of suture between nasals; (2) Anteriormost point of contact between incisors; (3) Superiormost point of nasals; (4) Gnathic process; (5) Anteriormost margin of incisive foramina; (6) Posteriormost margin of incisive foramina; (7) Superiormost point of nasolacrimal foramen; (8) Anteriormost point of the maximum constriction of anterorbital bridge; (9) Anteriormost point of zygomatic plate; (10) Posteriormost point of maximum constriction of anterorbital bridge; (11) Anteriormost margin of first molar alveolus; (12) Posteriormost margin of third molar alveolus; (13) Maximum constriction of interorbital region in ventral view; (14) Posteriormost point of suture between palatine bones; (15) Lateral margin of mesopterygoid fossa; (16) Lateral margin of parapterygoid fossa; (17) Anteriormost margin of squamosal root of zygomatic arch; (18) Posteriormost margin of squamosal root of zygomatic arch; (19) Superiormost margin of zygomatic arch; (20) Midpoint suture between basisphenoid and basioccipital; (21) Anteriormost point of inferior margin of foramen magnum; (22) Posteriormost point of superior margin of foramen magnum; (23) Posteriormost margin of occipital condyle; (24) Inferiormost margin of the bony eustachian tube; (25) Superiormost margin of the bony eustachian tube; (26) Midpoint of superior margin of auditory bulla; (27) Superiormost point of external auditory meatus; (28) Inferiormost point of external auditory meatus; (29) Inferiormost point of auditory bulla; (30) Superiormost point of suture between parietal and occipital bones (lambdoidal ridge).

Supplementary Material 1.S3. Phylomorphospace projections of the phylogeny on the first two principal components of the PCA analysis of the dorsal view of the skull.

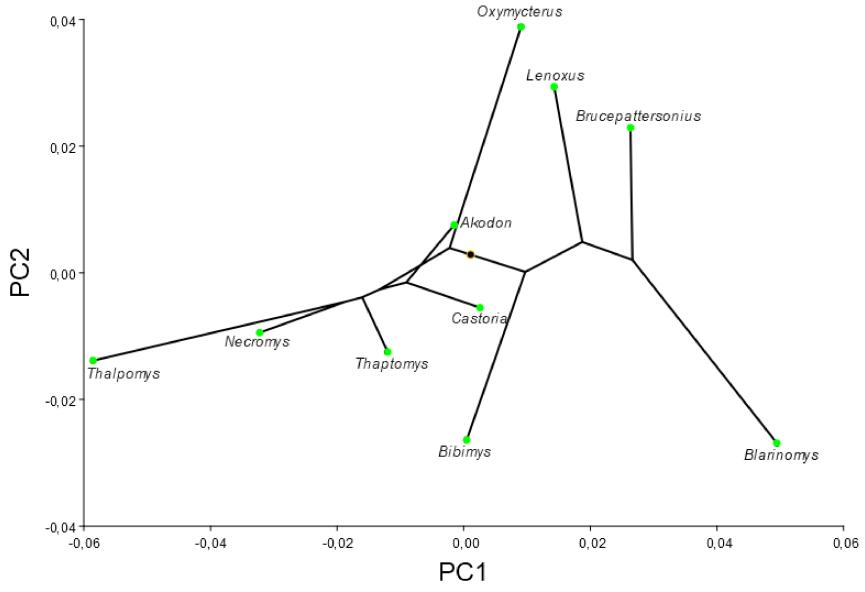

Supplementary Material 1.S4. Phylomorphospace projections of the phylogeny on the first two principal components of the PCA analysis of the ventral view of the skull.

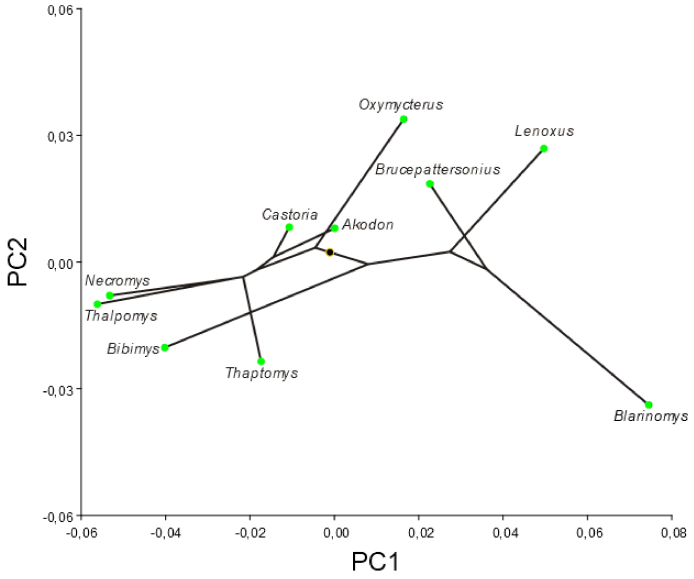

Supplementary Material 1.S5: First two principal components of the PCA analysis of the lateral view of the skull.

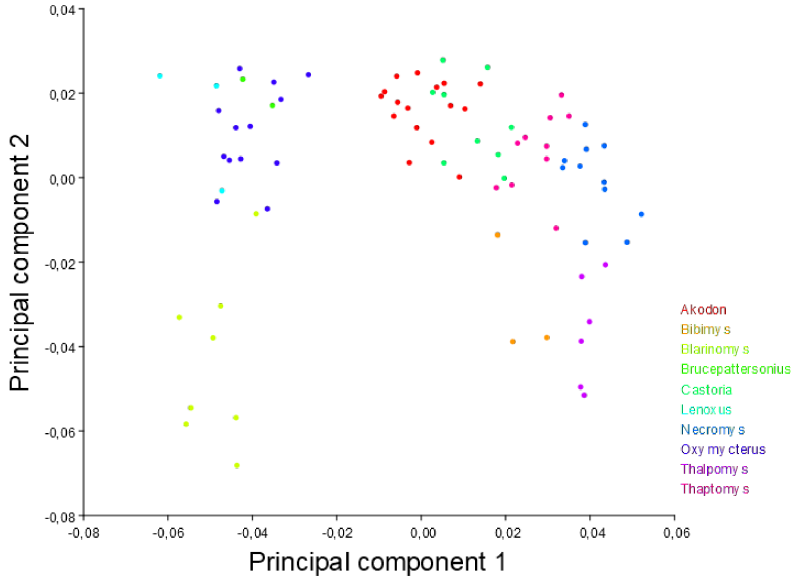

Supplementary Material 1.S6: First two principal components of the PCA analysis of the dorsalview of the skull.

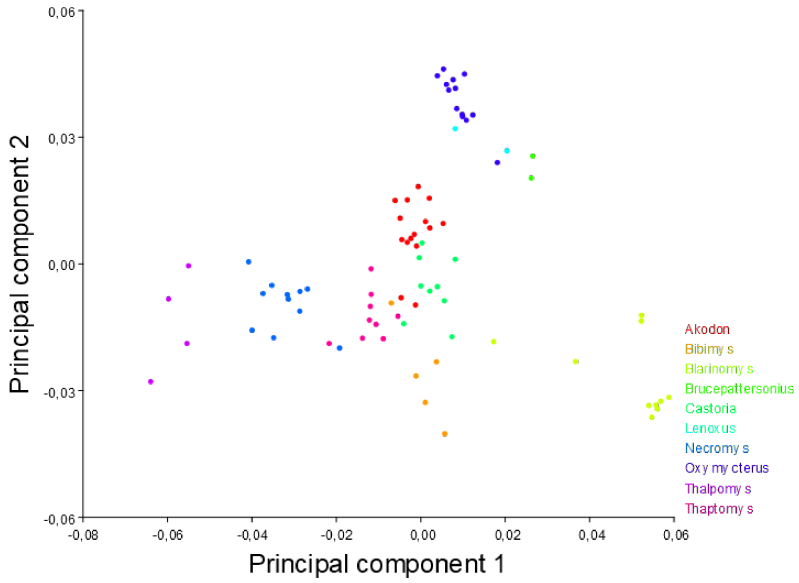

Supplementary Material 1.S7: First two principal components of the PCA analysis of the ventral view of the skull.

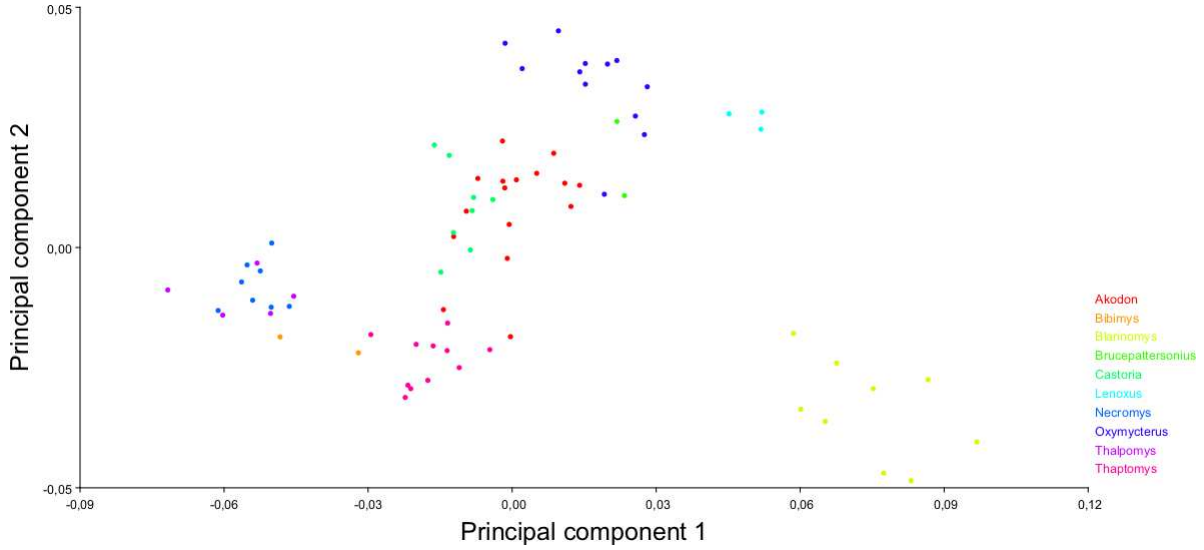

CHAPTER 2: STABLE ISOTOPIC SIGNATURES AND THE TROPHIC DIVERSIFICATION OF AKODONTINE RODENTS*

*Article published in the journal Evolutionary Ecology, 2019, vol. 33, pp. 855-872. (https://doi.org/10.1007/s10682-019-10009-0)

Drawing of *Bibimys labiosus* by Fernando Perini

STABLE ISOTOPIC SIGNATURES AND THE TROPHIC DIVERSIFICATION OF AKODONTINE RODENTS

Rafaela Missagia[1,2], Bruce Patterson[2] and Fernando A. Perini[1]

[1]*PPG - Zoologia/Departamento de Zoologia - Instituto de Ciências Biológicas, Universidade Federal de Minas Gerais – Av. Antônio Carlos, 6627, Pampulha, Belo Horizonte, MG, 31270-901, Brazil*

[2]*Integrative Research Center, Field Museum of Natural History, Chicago, IL 60605, USA*

Abstract

Stable isotope analyses are frequently used to study trophic interactions, diet, and community processes, but they have seldom been applied to investigate the trophic niche structure of entire clades. In this paper, we assess stable isotopes information in a phylogenetic context to evaluate trophic evolution across the phylogeny of a diversified group of Neotropical cricetid rodents. A total of 139 hair samples of 47 species of Akodontini rodents were collected in five museum mammal collections and submitted to stable isotope analyses for δ13C and δ15N values. The resulting isotopic niche space values were compared among species as well among the four main clades within the tribe. The phylogenetic signal of isotope values was estimated using a phylogenetic tree of Akodontini. Some of our results corroborate previous impressions that, in general, akodontines include more animal matter in their diet than other Neotropical rodents, but the lack of information for some species precludes more specific inferences. Some species appear to have relatively restricted niches, but the large variance observed in other species maybe related to dietary and habitat differences related to ecological factors throughout the distribution of wide-ranging species. We found low phylogenetic signal for δ13C and δ15N values, suggesting that the isotopic niche space was occupied independently many times throughout the akodontine evolutionary history. The δ13C/δ15N bi-plot indicates that the different lineages occupy the trophic niche space in similar ways, although differing in trophic diversity. Our results represent new ecological information and an approach that can be useful in studying the evolution of trophic

niches; they highlight the importance of museum specimen-based research for evolutionary ecology studies.

Key-words: stable isotopes, Akodontini, trophic niche, diet.

2.1. Introduction

The analysis of stable isotopes has emerged as one of the most widely used methods of diet estimation (Kelly 2000; Fry 2006; Boecklen et al. 2011; Ben-David and Flaherty 2012; Nielsen et al. 2017). Distinct ratios of light to heavy isotopes in organic compounds results from several factors affecting resource assimilation and excretion (Fry 2006; Sulzman 2007; Ben- David and Flaherty 2012). Stable isotope analyses uncover records of natural processes, measuring assimilated components that leave intrinsic signatures on organic tissues. In this way, they can help identify the resources consumed by an organism (Gannes et al. 1998; Fry 2006; Sulzman 2007; Ben-David and Flaherty 2012; Nielsen et al. 2017).

Stable isotopes have been widely used in diverse ecological investigations, including community ecology studies (e.g. Becker et al. 2013; Ofukany et al. 2014), diet tracing (e.g. Hilderbrand et al. 1996; Chiaradia et al. 2016), resource partitioning (e.g. Feranec et al. 2009; Baltensperger et al. 2015), and migration (e.g. Hobson and Koehler 2015; Vander Zanden et al. 2015). In mammals generally, and for rodents in particular, stable isotopes have been mainly used for trophic studies of communities (e.g. Dammhahn et al. 2012; Galetti et al. 2016) and paleobiology (e.g. Bocherens et al. 1994; Merceron et al. 2006), helping to elucidate feeding interactions and clarify ecosystem processes (e.g. Miller et al. 2005; Fox-Dobbs et al. 2006; Crowley et al. 2011). However, few studies incorporate isotopic data in phylogenetic analyses or draw inferences at macroecological scales (but see van Bergen et al. 2016 and MacLaren et al. 2018), and little focus has been given to variation of isotopic composition within a given species throughout its distribution, although it is known that isotopes vary according to the resources present in each region (Smiley et al. 2015).

Akodontini, the second most speciose tribe of Neotropical sigmodontine rodents, is a morphologically diverse group, exploiting many different habitats (D'Elía and Pardiñas 2015). The most recent phylogenies (Steppan and Schenk 2017, Maestri et al. 2017) show four principal lineages within the tribe. The first one comprises the genera *Akodon*, *Castoria,* and *Deltamys*, and represent the majority of Akodontini described species. The second group includes *Necromys*, *Podoxymys*, *Thalpomys*, and *Thaptomys*, and is sister-group of the latter. A third lineage, including the genera *Oxymycterus* and *Juscelinomys*, is sister-group of the *Akodon* and *Necromys* clades. Finally, a lineage comprising *Blarinomys*, *Brucepattersonius*, *Bibimys*, *Lenoxus*, *Kunsia,* and

Scapteromys, is sister to all of the previous clades (Supporting InformationFig. S1). Akodontine rodents with different dietary strategies vary widely, ranging from delicate shrew-like insectivores to robust gopher-like herbivores (Hershkovitz 1966; Reig 1980; D'Elía and Pardiñas 2015). However, direct evidence of diet is lacking for most species of Akodontini.

Many aspects of rodent ecology are difficult to study, as direct observations in nature are hampered due their small size and nocturnal and inconspicuous habits. Yet knowing the ecology of ecologically diverse groups like rodents is essential, as they are present and are important consumers in practically all terrestrial ecosystems, where they play a number of vital ecological roles such as seed dispersal (Vander Wall 2003; Dittel et al. 2015), insect consumption (Ellis et al. 1998), and as food for predators (Kotler et al. 1994; Jonsson et al. 2000).

Skull and teeth morphology can be used to infer ecological aspects like diet, providing ecological information of years of evolution (Samuels 2009; Davis and Pineda-Munoz 2016; Pineda-Munoz et al. 2017). Yet the relation between form and function is not always straightforward, and gross morphology may be informative only when considering less specific diet groupings (Davis and Pineda-Munoz 2016). Diet reconstructions of rodents have been done primarily through the analysis of feces or stomach contents (Reichman 1975; Meserve et al. 1988; Talamoni et al. 2008; Pinotti et al. 2011). However, this kind of analysis is restricted to items consumed in the last hours or days (Davis and Pineda-Munoz 2016; Nielsen et al. 2017). On the other hand, stable isotope analysis gives information of resources consumed over weeksto months, depending on the analyzed tissue (Tieszen et al. 1983; Miller 2008; Davis and Pineda-Munoz 2016), and is applicable to specimens deposited in collections over the course of decades and across a species' entire distribution. This wide applicability appears even more valuable for groups such as Akodontini, which includes species available only by their type series (e.g. *Podoxymys roraimae*), or even considered extinct (e.g. *Juscelinomys candango*).

Here, we report stable isotope results of carbon and nitrogen from hair samples of 47 species of Akodontini rodents. This study represents the first attempt to gather a large amount of isotopic data and analyze it in an explicitly phylogenetic context over a macroevolutionary scale. We use stable isotope values to: 1) evaluate differences in stable isotope signatures of 47 species of Akodontini rodents; 2) compare the results with ecological information from the literature for akodontine species; 3) compare the four main Akodontini lineages for their trophic niche; and 4) test the $\delta^{13}C$ and $\delta^{15}N$ averaged values for phylogenetic signal. To discuss our results, and based

on the available literature, we here assume that the carbon and nitrogen isotopic composition of tissues are directly related to the $\delta^{15}N$ and $\delta^{13}C$ of resources consumed, trophic level, foraging location, and to the discrimination factor of each element (Bearhop et al. 2004; Ben-David and Flaherty 2012).

2.2. Material and Methods

2.2.1. Data Collection

Stable isotope analysis can be performed on different tissues, and the tissue type can affect the interpretations of diet (Tieszen et al. 1983; Boecklen et al. 2011; Ben-David and Flaherty 2012; Davis and Pineda-Munoz 2016; Nielsen et al. 2017). Hair, like other metabolically inactive tissues, records the stable isotope composition of the resources consumed at the time that it was grown, not from the sampling date (Tieszen et al. 1983; Miller et al. 2008).Hair has a lower turnover rate, related to its semiannual replacement via moutling (Tieszen et al. 1983; Miller et al. 2008; Ben-David and Flaherty 2012), and so represent resource acquisition over a longer time span (up to about 80 days; Tieszen et al. 1983; Boecklen et al. 2011) than more metabolically active tissues, such as liver and blood, that are continuously replaced and reflect diets over a shorter amount of time (from approximately 3 to 40 days; Tieszen et al. 1983;Miller et al. 2008; Boecklen et al. 2011). We chose to sample hair because it records diets over a longer time span, especially in view of the relatively short generation times of rodents (Read and Harvey 1989; Dobson and Oli 2007). Thus, the hair of rodents reflects diet over a substantial period of a rodent's life time, and the small volumes needed for analysis are more readily available in museum collections.

The stable isotope analysis consumes small amounts of tissue and, in the case of our hair samples, we took approximately 1 mg, corresponding to approximately 0.5 cm^2 of the skin. The hair samples were preferentially taken from museum skins with visible damage, usually from the preparation process. The samples were taken as close to the hair root as possible, from the inside portion of the hindlimb, to avoid disrupting diagnostic features. In order to control for age, only adult specimens (with associated skulls and the third molar fully erupted) were sampled. Hair sampling was conducted in the mammal collections of the Field Museum of Natural History (FMNH), American Museum of Natural History (AMNH), National Museum of Natural History (NMNH), Centro de Coleções Taxonômicas of Universidade Federal de Minas Gerais (UFMG),

and Museu de História Natural of Pontifícia Universidade Católica of Minas Gerais (MCNM). In all, 139 hair samples of 47 species of Akodontini rodents were collected, with an average of three samples per species, depending on the number of specimens available (see Supporting Information Table S1 for a detailed list of samples). We sought to maximize taxonomic samplingto enhance the power of analyzing isotopic information in a phylogenetic context, so that relatively few specimens per species were sampled. However, this procedure allowed for a large sample of Akodontini species and almost all genera to be included in our analysis.

2.2.2. Stable Isotope Analysis

The collected samples were cleaned according to the procedure described by O'Connel and Hedges (1999). Each sample was submerged twice in a 2:1 v/v solution of methanol and chloroform, for 1 hour each, and then rinsed twice in distilled water, for 20 minutes each. Afterwards, they were wrapped in aluminum foil and oven-dried at 40 °C overnight to remove any excess water. The hair samples were sent to the Stable Isotope Facility of the University of Wyoming, where they were homogenized and placed in a tin capsule for processing. The samples were analyzed on the continuous flow isotope ratio mass spectrometer (Thermo Finnigan Delta Plus XP Isotope Ratio MS; Thermo Finnigan LLC, Somerset, New Jersey) by an elemental analyzer (Costech 4010 Elemental Analyzer; Costech Analytical Technologies Inc., Valencia, California) and interface (Finnigan Conflo III Universal Interface). Standard uncertainties were calculated based on 68 replicates of the standard deviations of the reference material, varying from 0.03‰ to 0.05‰ for carbon and from 0.04‰ to 0.05‰ for nitrogen. The analyses were replicated on the samples periodically throughout the sample, totaling nine replicates, and the mean standard deviation for replicates was 0.07‰ for both $\delta^{13}C$ and $\delta^{15}N$.

The isotopic ratios were reported as δ values in permil (‰) relative to the Vienna Pee Dee Belemnite (VPDB) and AIR reference scales for carbon and nitrogen, respectively, as follows:

$$\delta X = (R_{sample}/R_{standard} - 1) * 1000$$

Where δX is $\delta^{15}N$ or $\delta^{13}C$, R_{sample} is the ratio of heavy to light isotope of the sample, and $R_{standard}$ is the ratio of heavy to light isotope of the standard for each element (Fry 2006; Sulzman 2007; Ben-David and Flaherty 2012). Standard values were obtained from the International

Atomic Energy Agency and the National Institute of Standards and Technology.

From the isotopic signature of a specimen, it is possible to infer the ultimate source of its carbon based on its $\delta^{13}C$ values (Bender 1971; Peterson and Fry 1987; Sulzman 2007). In terrestrial ecosystems, the $\delta^{13}C$ value is generally used to distinguish the different photosynthetic pathways used by C3 and C4 plants, due to distinct fractionation of stable isotopes of carbon during this process (Bender 1971; Peterson and Fry 1987; O'Leary et al. 1992; Gannes et al. 1998; Post 2002; Marshall et al. 2007). Because $\delta^{13}C$ values vary according to the available resources in the ecosystem, different studies assume different ranges for each photosynthetic pathway (e.g. DeNiro and Epstein 1978; Galetti et al. 2016; O'Leary 1988). In general, $\delta^{13}C$ values between -20‰ and -37‰ are usually related to the consumption of C3 plants, while $\delta^{13}C$ values between -9‰ and -19‰ are linked to the consumption of C4 plants (Van der Merwe 1982;Vogel 1993; Cerling and Ehleringer 2000; Marshall et al. 2007). Because we sampled throughoutSouth America and various different biomes, here we will interpret the values of $\delta^{13}C$ as a gradient, with lower values of $\delta^{13}C$ as indicators of C3 plants, and higher values as indicators of C4 plants (e.g. MacLaren et al. 2018). The $\delta^{13}C$ is a dietary proxy that can also be used, when interpreted appropriately, as an environmental proxy, with more negative values indicating an animal with a browsing habit that eats mostly C3 plants, and more positive values depicting grazers feeding on C4 grasses (DeNiro 1987; Gannes et al. 1998; Marshall et al. 2007; MacLaren et al. 2018).

The discrimination factor (*i.e.* the difference in isotopic composition between a predator and its prey) is also relevant to estimating resource consumption (DeNiro and Epstein 1978, 1981). The discrimination factor of $\delta^{15}N$ is used to estimate trophic position, since the $\delta^{15}N$ of consumers is usually enriched by 3-4‰ with each trophic level, higher values indicating greater consumption of animal matter (DeNiro and Epstein 1981; Peterson and Fry 1987; Kelly 2000; Ben-David and Flaherty 2012). For $\delta^{13}C$, the discriminantion factor is lower, averaging ca. 1‰ for hair samples (DeNiro and Epstein 1978, Tieszen et al. 1983).

2.2.3. Data Analysis

The $\delta^{13}C$ and $\delta^{15}N$ values obtained in the stable isotope analyses were plotted on the $\delta^{13}C/\delta^{15}N$ bi-plot using the software PAST v.3 (Hammer et al. 2001). In order to compare the results of stable isotopes with the inferred diet for the analyzed species, we compiled ecological data from the literature (Supporting Information Table S2). Besides comparing the isotope values

among the analyzed species, we also compared the isotopic niche space occupied by the four main lineages of the tribe, here treated as the *Akodon* group (*Akodon*, *Castoria* and *Deltamys*), *Necromys* group (*Necromys*, *Podoxymys*, *Thalpomys*, and *Thaptomys*), *Oxymycterus* group (*Oxymycterus* and *Juscelinomys*) and *Scapteromys* group (*Blarinomys*, *Brucepattersonius*, *Bibimys*, *Lenoxus*, *Kunsia* and *Scapteromys*).

The six polygon dispersion metrics proposed by Layman et al. (2007) were applied to the dataset to allow comparisons between the isotopic niche space occupied by each of the four groups, here calculated as follows: 1) $\delta^{15}N$ range (NR) is the distance between the two species with the highest and lowest $\delta^{15}N$ values; 2) $\delta^{13}C$ range (CR) is the distance between the two species with the highest and lowest $\delta^{13}C$ values; 3) Total area (TA) is a measure of the total area of space occupied by each group on the bi-plot; 4) Mean distance to centroid (CD) is the average Euclidean distance of each species to the $\delta^{13}C$-$\delta^{15}N$ centroid of the group; 5) Mean nearest neighbor distance (NND) is the mean of the Euclidean distances to each species' nearest neighbor within the groups on the $\delta^{13}C$-$\delta^{15}N$ bi-plot space; 6) Standard deviation of nearest neighbor distance (SDNND) is the standard deviation of the Euclidean distances to each species' nearest neighbor on the $\delta^{13}C$-$\delta^{15}N$ bi-plot space. We also performed hypothesis-testing procedures for differences in centroid location and dispersion metrics (CD and NND) among the four main lineages, following Turner et al. (2010). These analyses were performed using the SIBER package and the script provided in Turner et al. (2010), in the R environment v3.4.3 (R Core Team 2017).

The trophic niche of each lineage was delimited through Stable Isotope Bayesian Ellipses (SIBER) (Jackson et al. 2011). SIBER uses a multivariate ellipse-based approach to generate corrected standard ellipse areas (units of $‰^2$), preventing the interference of sample sizes and outliers inherent to convex hulls (Jackson et al. 2011). The SEAc, representing the core isotopic niche area (containing 40% of the data, as opposed to the convex hull which includes 100% of the data), allows the comparison of groups with different sample sizes (Jackson et al. 2011). A SEAc estimate for each group is made by a Bayesian iterative process based on a subsample of the group's stable isotope values, considering the uncertainty in the sampled data (Jackson et al. 2011). The analysis were performed using the packages 'siar' (Parnell and Jackson 2013) and 'SIBER' (Jackson et al. 2011), in the R environment v3.4.3 (R Core Team 2017).

The $\delta^{13}C$ and $\delta^{15}N$ values were averaged for each species and mapped on a pruned Bayesian phylogeny of Sigmodontinae (Maestri et al. 2017) to show the variation across the topology. The

phylogenetic signal of the $\delta^{13}C$ and $\delta^{15}N$ values was estimated by using Blomberg's K (Blomberg et al. 2003), and p-values were estimated to test for significant difference from K=0, with the lack of significance indicating no correlation between species. Thephylogenetic signal analysis was performed using the 'philosig' function, and the averaged $\delta^{13}C$ and $\delta^{15}N$ values were mapped onto the tree using the 'contMap' function, both from the 'phytools' package (Revell 2012). Analyses were performed in the R environment v3.4.3 (R Core Team 2017).

2.3. Results

Stable isotope values of analyzed Akodontini specimens ranged from -25.9‰ to -7.9‰ for $\delta^{13}C$, and from 2.3‰ to 15.3‰ for $\delta^{15}N$. In terms of species, *Bibimys labiosus*, *Castoria angustidens* and *Akodon budini* had the lowest $\delta^{15}N$ values, whereas *Necromys obscurus*, *Akodon lutescens,* and *Deltamys kempi* had the highest values. On the $\delta^{13}C$ axis, *B. labiosus*, *Necromys lasiurus* and *Juscelinomys huanchacae* had the highest values, and *Akodon mimus, A. budini* and *C. angustidens* had the lowest (Fig. 2.1). *Akodon montensis* and *A. cursor* presented the highest standard deviations for $\delta^{13}C$ (7.01 and 6.20, respectively), whereas *N. obscurus* and *Scapteromys aquaticus* presented the highest standard deviations for $\delta^{15}N$ (3.84 and 3.04, respectively). *Akodon kofordi* and *A. iniscatus* presented the lowest standard deviation for both axes (Fig. 2.2, Supporting Information Table 2.S2). In terms of clades, the *Scapteromys* group had the highest standard deviation for both $\delta^{13}C$ and $\delta^{15}N$, while the *Akodon* and *Oxymycterus* groups had the lowest for $\delta^{13}C$ and $\delta^{15}N$, respectively. The *Oxymycterus* group had the highest average $\delta^{15}N$ value, while the *Necromys* group had the lowest. On the $\delta^{13}C$ axis, the *Necromys* and *Akodon* groups occupy the extreme positions, with the former having the higher mean value (Supporting Information Table 2.S2).

The four main clades differ in terms of their dispersion on the stable isotope bi-plot. The *Scapteromys* and *Akodon* groups had a significant difference regarding the distance of the species from the group centroid (difference = 1.47, $P<0.05$). The species of the *Scapteromys* group are widespread along the plot ($CD_{ScapteromysGroup}$= 4.83), while the *Akodon* group speciesare more densely packed ($CD_{AkodonGroup}$= 3.36), with the lowest CD and NND (Table 2.1). The centroids of the four lineages did not differ significantly in position on the bi-plot (Fig. 2.3b), except for the *Necromys* and *Akodon* groups (distance = 2.62, $P<0.05$). The mean nearest neighbor

distance (NND) did not differ significantly between lineages (Table 2.2).

The convex hulls and standard ellipses (SEAc for small sample size correction) based on maximum likelihood estimates for the four lineages are depicted in Table 1 and Figure 2.3a. The *Scapteromys* group presents the largest SEAc (SEAc=35.66), while the SEAc of the other lineages are similar in size, not varying substantially among the *Akodon, Necromys* and *Oxymycterus* groups (Supporting Information 2.S3). However, the pairwise tests indicated that the *Scapteromys* group has a high probability of being larger than the other groups (with probabilities = 0.94, 0.90 and 0.95 for *Oxymycterus*, *Necromys* and *Akodon* groups,respectively).

The isotopic values were mapped on the tree topology (Figure 2.4), and presented a low phylogenetic signal ($\delta^{15}N$: K=0.36, p=0.02; $\delta^{13}C$: K=0.36, p=0.03).

2.4. Discussion

The present work stands out as the first approach to quantify and estimate diet aspects of a clade through a comprehensive analysis with broad phylogenetic sampling. Some of these species lack any trophic information whatsoever and the diets of others are poorly documented. Some of our results substantiate reports in the literature, while others represent important new ecological information for a relatively poorly known group. The Akodontini tribe has some species that are rarely collected and are present in small numbers in collections, and, especially for those (e.g. *Podoxymys roraimae*, *Juscelinomys huanchacae,* and *Bibimys labiosus*), the stableisotopic values here reported are useful as new information about their trophic niche. Moreover, these results allowed the testing of hypothesis on trophic diversity of Akodontini rodents based on a standardized sampling and methodology, giving comparable results for a large number of Akodontini species, as opposed to the existing and relatively limited evidence for the majority of species here considered. However, it is important to point out that a direct relationship between these results and the diet of the species analyzed in this study should be avoided. Considering the limited sampling per species, the inherent issues related to sampling biases could not be fully addressed here, and require careful data interpretation as stable isotope values represent a mixture of extrinsic and intrinsic factors, reflecting not only the composition of the assimilated resources.

The ecological niche of akodontines have been previously inferred from their skull, teeth, and external morphology (Hershkovitz 1966, 1994; Reig 1972, 1980). Although most inferences

were made when the tribe had a different taxonomic conformation (it formerly included Abrothrichini and excluded *Scapteromys*, *Bibimys* and *Kunsia*), several authors saw the Akodontini as a radiation of specialized insectivores (Hershkovitz 1966; Reig 1972; Glanz 1984). Reig (1972) described them as "a group of mainly insectivorous small predators" that "play the role of small predators of arthropods and other small invertebrates". Hershkovitz (1966) considered *Oxymycterus*, *Blarinomys*, and "many akodonts" as soricine cricetids feeding mainly on insects and worms, as opposed to the more robust, though still insectivorous *Scapteromys,* and to the gopher-like, herbivorous *Kunsia.* Comparing our isotope results with those and other stable isotope values of Sigmodontinae rodents (Galetti et al. 2016), most of the analyzed akodontine species have relatively high $\delta^{15}N$ values, indicating that they occupy higher trophic levels (DeNiro and Epstein 1981; Peterson and Fry 1987; Kelly 2000; Ben-David and Flaherty 2012).

Although we have little to no diet information for some of these species (e.g. *A. toba* and *O. quaestor*), both stable isotope and stomach content analysis corroborate isotopic values for others. For instance, Teta et al. (2007) reported that the stomachs of four individuals of *Deltamys kempi* contained mainly insects and insect larvae, and high consumption of arthropods by *Necromys obscurus* is also well documented (Barlow 1969; Ellis et al. 1998). Studying a small mammal assemblage in the Atlantic Forest, Galetti et al. (2016) found that *Blarinomys breviceps* and *Brucepattersonius soricinus* represented the third and highest trophic level of consumers of the sampled site, presenting relatively higher $\delta^{15}N$ values than the other species. *A. lutescens*, in turn, was considered one of the species with a specialized diet, with most analyzed stomachs containing only insects (Pizzimenti and de Salle 1980). Stomach content analysis have also shown that *O. dasytrichus, O. delator, B. soricinus* and *B. breviceps* all feed mainly on arthropods (Geise et al. 2008; Talamoni et al. 2008; Pinotti et al. 2011). In general, stomach content analyses show that akodontines consume more animal matter compared with species belonging to other tribes, often excepting *Necromys* and *Kunsia* (Barlow 1969; Pizzimenti and deSalle 1980; Ellis et al. 1998; Solari 2007; Talamoni et al. 2008; Huiman 2008; Pinotti et al. 2011; Zevallos 2014).

On the other hand, some species presented lower $\delta^{15}N$ values (e.g. *Castoria angustidens*, *Bibimys labiosus* and *Akodon budini*). Very little is known about the diet of these species, although Thomas (1918:190) highlighted the distinctive cheek teeth of *A. budini* as "very hypsodont, high, and narrow", which is usually related to a more herbivorous diet (Williams and Kay 2001), and Pardiñas et al. (2016a) noted the disproportionate size of the molar teeth of *Castoria* in relation to

skull size. The relatively high degree of hypsodonty of *Bibimys* was related to its consumption of vegetal matter (Pardiñas et al. 2017), which was corroborated by an analysis of stomach content of two individuals (Diório 2014). However, we should highlight that low values of $\delta^{15}N$ cannot always be related to herbivory. The $\delta^{15}N$ signature of plants is determined by atmospheric fixation, denitrification, and volatilization of ammonia into the soil (Shearer and Kohl 1986; Ambrose 1991), which, in its turn, are affected by several environmental factors. High values of $\delta^{15}N$ on plants, for example, may be related to arid, warmer and/or nutrient rich environments (Bate 1981; Granhall 1981; Ambrose 1991; Amundson et al. 2003). On the other hand, $\delta^{15}N$ values decrease with increasing rainfall and decrease in soil temperature and humidity (Ambrose 1991; Swap et al. 2004; Amundson et al. 2003).

The bivariate isotopic niche space also allows inferences on the type of habitat in which the animals lived (Newsome et al. 2007), a common approach in the study of paleodiets (e.g. Merceron et al. 2006; Fox-Dobbs et al. 2008). Some species, like *B. labiosus, N. lasiurus,* and *J. huanchacae,* present high values of $\delta^{13}C$, indicating that their diet included C4 plants, which tend to grow in drier and more open environments. In contrast, *A. budini*, *A. mimus,* and *C. angustidens* occupy the most negative portion of the spectrum of $\delta^{13}C$, indicating that C3 plants comprised their carbon sources and likely live in more forested areas. This is corroborated, to some extent, by distribution records and land cover data, as *A. budini* and *A. mimus* are both found along the Yungas forests of Argentina and Bolivia (Vargas et al. 2007; Pardiñas et al. 2015), while *J. huanchacae* and *N. lasiurus* are more commonly registered on grasslands and open savannas (Geise et al. 2010; Emmons and Patton 2012). Although literature is scant, *B. labiosus* is mentioned as occurring in forested habitats (Pardiñas et al. 2016b), which is not apparent in our results for this species.

We observed a large variance in the stable isotope values of some species (e.g. *A. cursor, A. montensis* and *O. quaestor*). For example, specimens of the same species collected in nearby localities presented discrepant values of $\delta^{13}C$ and $\delta^{15}N$ (e.g. *A. montensis, A. dayi,* and *N. lenguarum*), suggesting a lability on the consumption of resources. Although some of the low variances observed are likely related to sampling problems (individuals collected in the same localities due to sampling limitations - e.g. *A. budini* - or restricted distributions - e.g. *P. roraimae*), others seem to be linked to a greater specificity in resource consumption (e.g. *A. azarae*, as discussed previously by Ellis et al. (1998)). Widespread akodontine rodents are knownto have

large differences in resource consumption related to distinct nutritional requirements associated with different habitats (Cerqueira et al. 2003). It seems well established that isotopic composition throughout the geographic range of a single species of rodent may be affected by regional differences related to vegetation, topography, and climate, sometimes producing large variation (Smiley et al. 2015). Therefore, the sampling strategy used here probably contributed tothe large isotope variation found in some taxa. Additionally, other factors can affect the isotope signatures and cloud inferences about the isotopic niche of species, like nutritional condition and metabolic rates of the specimen (Bearhop et al. 2002, 2004; Martínez del Rio et al. 2009). Nevertheless, our data suggest that some species, especially the ones affected by seasonal fluxes in resources, may present considerable variation in diet throughout their distributions.

Closely related species are probably similar in morphological, behavioral, life-history and ecological traits, but the phylogenetic signal of each trait may vary (Losos 2008). While morphological traits are expected to have higher phylogenetic signal, more labile ecological traits, like diet, usually have lower phylogenetic signals (Blomberg et al. 2003; Kamilar and Cooper 2013). The low phylogenetic signal was hence expected for the $\delta^{13}C$ and $\delta^{15}N$ values, since they record dietary information over shorter time spans than morphology does. Additionally, the low phylogenetic signal observed can be an outcome of error in the tip values, since dietary information is based on data of only a few specimens and may compound uncertainties in tree topology (Bomblerg et al. 2003).

The lack of phylogenetic clustering of the clades corroborates the low phylogenetic signal found for the $\delta^{13}C$ and $\delta^{15}N$ values. If we analyze the clustering pattern of successively more inclusive clades of Akodontini, we could evaluate if clades closer to the tips become more specialized in their dietary habits. In that case, we would expect to see a pattern in which each clade occupies a distinct region of the isotope space and convex hulls increase in size as one approach the root. However, this is not what we observed. In turn, all clades occupy the bi-plot in a similar way, suggesting that, throughout the evolution of the group, different parts of the isotopic niche space were occupied independently by each clade. The fossil record of the tribe is scant, and does not provide any insights about the evolution of dietary adaptations. However, qualitative dietary ancestral reconstruction for Akodontini indicate an omnivorous diet as plesiomorphic for the tribe (Maestri et al. 2017), and our data suggests that generalized diets maybe ancestral, with insectivorous and herbivorous dietary behaviors evolving independently withinthe tribe.

When corrected for sample size, it is clear that the *Akodon* group convex hull size is due to the number of sampled individuals, showing standard ellipses of similar size to the *Necromys* and *Oxymycterus* groups. On the other hand, there seems to be a greater trophic diversity in the *Scapteromys* group, considering that it presents a relatively larger ellipse than the other lineages and its individual points are more distant both from each other and from the centroid. The opposite happens with the *Akodon* group, which has the lowest dispersion of individual samples (between themselves and the centroid), differing significantly in these aspects when compared to the *Scapteromys* group. The trophic diversity of the *Scapteromys* group is corroborated by stomach content analyses and morphological features that suggest dietary specialization by several species of this lineage, also corroborated by their extreme positions on the isotopic niche plot (Hershkovitz 1966; Reig 1972; Geise et al. 2008; Pinotti et al. 2011; Bezerra and Pardiñas 2016).

When interpreting the results, it is important to emphasize that the stable isotope values can be affected by extrinsic factors of the environment (Post 2002; Casey and Post 2011). Previous stable isotope studies highlight the importance of estimating an isotopic baseline for theresources available on the environment where the specimen was sampled, considering that the $\delta^{13}C$ and $\delta^{15}N$ values change according to the resources on the base of the food web (Post 2002). This is related to several factors that alter the isotopic composition of terrestrial resources, suchas aridity, temperature, humidity, nutrient availability, and soil pH (Casey and Post 2011 and references therein). Although we agree on the importance of an isotopic baseline, given the geographical and temporal coverage of our sample, it would be virtually impossible to collect all the possible resources consumed by all of our samples. The same problem affects paleoecological studies (Casey and Post 2011), but this does not preclude paleoenvironmental inferences from isotopic data (e.g. Secord et al. 2008). Nevertheless, inferences should be made with caution, especially when based on small samples, as values of $\delta^{13}C$ and $\delta^{15}N$ may correlate with environmental factors like soil moisture, precipitation, temperature, humidity, and elevation (Bate 1981; Granhall 1981; Ambrose 1991; Knight et al. 1995; Sparks and Ehleringer 1997; Swap et al. 2004; Chen et al. 2005; Kohn 2010; Casey and Post 2011). To avoid the effect of these extrinsic factors, these results should be combined with a habitat independent dietary proxy.

Stable isotopes represent a powerful tool for ecological and evolutionary studies (Newsome et al. 2007), but physiological, ecological, and behavioral features may vary between specimens and cause variation in their data (e.g. Sponheimer et al. 2003). Our understanding of

stable isotope values needs to be improved, incorporating better knowledge of physiological factors affecting stable isotope signature (Bearhop et al. 2004), laboratory-based experimental studies, and development of theoretical models (Martínez del Rio et al. 2009). Despite these caveats, isotopes allow a quantitative representation of diet far more nuanced than the discrete categories typically used in broad-scale dietary studies (e.g. granivore, insectivore, etc). In addition, all of our samples were taken from specimens deposited in mammal collections, highlighting the importance of research based on tissue samples from museum collections (Schmitt et al. 2018). Moreover, the data generated in this study could be incorporated into a future isotope repository (Pauli et al. 2017), facilitating its application in upcoming studies.

Critically, no proxy can represent the true diet (Nielsen et al. 2017). In order to diminish the effect of extrinsic environmental factors that can affect stable isotope data on our ecological interpretations, these results should ideally be combined with a less habitat dependent dietary proxy. Therefore, multiple lines of evidence should be used in estimating the trophic niche of an organism (Chiaradia et al. 2016; Davis and Pineda-Munoz 2016; Nielsen et al. 2017). While skull and dental morphology can reflect dietary information over evolutionary time, proxies like stable isotopes cover a smaller temporal range (Davis and Pineda-Munoz 2016), while still integrating over a longer time interval than traditional dietary proxies, such as stomach contents or direct feeding observations (Dalerum and Angerbjörn 2005; Davis and Pineda-Munoz 2016). Nevertheless, some of our stable isotope results are corroborated by other dietary proxies with different time scales, especially for those species apparently specialized in resource consumption. Species that are recurrently mentioned as insectivorous based on skull, dental or gut morphology, like *Blarinomys breviceps*, *Brucepattersonius soricinus,* and *Oxymycterus* species, presented correspondingly high values of $\delta^{15}N$, while the most notably herbivorous species living in open areas of central Brazil, *Kunsia tomentosus*, had correspondingly high values of $\delta^{13}C$. As specified above, several akodontine species registered stable isotopic values that are corroborated by stomach content analysis.

The stable isotope data here presented represent new ecological information that can be useful in defining and studying the evolution of the trophic niche of sigmodontine rodents. More comprehensive sampling, by season, ecoregion, and with more individuals per species, is needed to clarify components of dietary variability, and to understand the differences between species. Future studies using stable isotope mixing models can better specify consumed food items by

Akodontini species, probably unveiling differences in the exploitation of resources by species belonging to the same dietary category (e.g. insectivores). Moreover, additional detailed data on the natural history of Akodontine species are desirable, which, combined with information from other dietary proxies, can improve our knowledge on the trophic niche of akodontine rodents.

Acknowledgments

We thank Robert Voss, Darrin Lunde, Louise Emmons and Claudia Costa who kindly allowed the sampling of specimens under their care for the stable isotope analysis. We gratefully acknowledge Isabel Distefano and Kevin Feldheim from the Field Museum's Pritzker Laboratory for Molecular Systematics and Evolution, and Jennifer Melo de Andrade and Teofânia Dutra Amorim from the Centro de Pesquisas Hidráulicas of Universidade Federal de Minas Gerais for the logistical assistance with the preparation of the hair samples. We thank Chandelle Macdonald and the Stable Isotope Facility staff of the University of Wyoming for performing the stable isotope analysis of the samples; and Adam Ferguson and John Phelps from the Field Museum of Natural History for help with the sampling process and shipping. Raisa Rodarte and Raul Costa provided useful information on stable isotope studies on preliminary stages of this work. We are grateful for useful comments from two anonymous reviewers and from the Associate Editor and Editor-in-Chief, that greatly improved the manuscript. The dispatch of the samples from Brazil was authorized according to registration A06DC31 of Sisgen. Coordenação de Aperfeiçoamento de Pessoal de Nível Superior (CAPES) gave R.V.M. financial support through regular (Finance Code 0001) and PDSE (88881.133833/2016-1) fellowships.

2.5. References

Ambrose, S.H., 1991. Effects of diet, climate and physiology on nitrogen isotope abundances in terrestrial foodwebs. Journal of Archaeological Science, 18(3), pp. 293-317.

Baltensperger, A.P., Huettmann, F., Hagelin, J.C. and Welker, J.M., 2015. Quantifying trophic niche spaces of small mammals using stable isotopes (δ15N and δ13C) at two scales across Alaska. Canadian Journal of Zoology, 93(7), pp. 579-588.

Barlow, J.C., 1969. Observations on the biology of rodents in Uruguay. Royal Ontario Museum Life Sciences Contributions, 75, pp. 1-59.

Bate, G.C., 1981. Nitrogen cycling in savanna ecosystems. Ecological Bulletins (Sweden),

pp. 463-475.

Bearhop, S., Adams, C.E., Waldron, S., Fuller, R.A. and MacLeod, H., 2004. Determining trophic niche width: a novel approach using stable isotope analysis. Journal of Animal Ecology, 73(5), pp. 1007-1012.

Bearhop, S., Waldron, S., Votier, S.C. and Furness, R.W., 2002. Factors that influence assimilation rates and fractionation of nitrogen and carbon stable isotopes in avian blood and feathers. Physiological and Biochemical Zoology, 75(5), pp. 451-458.

Becker, E.L., Cordes, E.E., Macko, S.A., Lee, R.W. and Fisher, C.R., 2013. Using stable isotope compositions of animal tissues to infer trophic interactions in Gulf of Mexico lower slope seep communities. PLoS ONE, 8(12), p. e74459.

Ben-David, M. and Flaherty, E.A., 2012. Stable isotopes in mammalian research: a beginner's guide. Journal of Mammalogy, 93(2), pp. 312-328.

Bezerra, A.M. and Pardiñas, U.F.J., 2016. Kunsia tomentosus (Rodentia: Cricetidae). Mammalian Species, 48, pp. 1-9.

Bocherens, H., Fizet, M. and Mariotti, A., 1994. Diet, physiology and ecology of fossil mammals as inferred from stable carbon and nitrogen isotope biogeochemistry: implications for Pleistocene bears. Palaeogeography, Palaeoclimatology, Palaeoecology, 107(3-4), pp. 213-225.

Boecklen, W.J., Yarnes, C.T., Cook, B.A. and James, A.C., 2011. On the use of stable isotopes in trophic ecology. Annual Review of Ecology, Evolution, and Systematics, 42, pp. 411-440.

Carleton, M.D., 1973. A survey of gross stomach morphology in New World Cricetinae (Rodentia, Muroidea), with comments on functional interpretations. Miscellaneous Publications, Museum of Zoology, University of Michigan, 146, pp. 1-43

Casey, M.M. and Post, D.M., 2011. The problem of isotopic baseline: reconstructing the diet and trophic position of fossil animals. Earth-Science Reviews, 106(1-2), pp. 131-148.

Cerqueira, R., Santori, R.T., Gentile, R. and Guapyassu, S.M.S., 2003. Micrographical ecological differences between two populations of Akodon cursor (Rodentia, Sigmodontinae) in a Brazilian Restinga. Journal of Advance Zoology, 24, pp. 46-52.

Chen, S., Bai, Y., Lin, G. and Han, X., 2005. Variations in life-form composition and foliar carbon isotope discrimination among eight plant communities under different soil moisture conditions in the Xilin River Basin, Inner Mongolia, China. Ecological Research, 20(2), pp. 167-

176.

Chiaradia, A., Ramírez, F., Forero, M.G. and Hobson. K.A., 2016. Stable Isotopes (δ13C, δ15N) combined with conventional dietary approaches reveal plasticity in central-place foraging behavior of little penguins Eudyptula minor. Frontiers in Ecology and Evolution, 3, p. 00154.

Crowley, B.E., Godfrey, L.R. and Irwin, M.T., 2011. A glance to the past: subfossils, stable isotopes, seed dispersal, and lemur species loss in southern Madagascar. American Journal of Primatology, 73(1), pp. 25-37.

D'Elía, G. and Pardiñas, U.F.J., 2015. Tribe Akodontini Vorontsov 1959. Mammals of South America, Volume 2: Rodents, pp. 140-144. Chicago: Chicago University Press.

Dammhahn, M., Soarimalala, V. and Goodman, S.M., 2013. Trophic niche differentiation and microhabitat utilization in a species-rich montane forest small mammal community of eastern Madagascar. Biotropica, 45(1), pp. 111-118

Davis, M. and Pineda-Munoz, S., 2016. The temporal scale of diet and dietary proxies. Ecology and Evolution, 6(6), pp. 1883-1897.

Dalerum, F. and Angerbjörn, A., 2005. Resolving temporal variation in vertebrate diets using naturally occurring stable isotopes. Oecologia, 144(4), pp. 647-658.

DeNiro, M.J., 1987. Stable isotopy and archaeology. American scientist, 75(2), pp.182-191.

DeNiro, M.J. and Epstein, S., 1978. Influence of diet on the distribution of carbon isotopes in animals. Geochimica et Cosmochimica Acta, 42(5), pp. 495-506.

Diório, D.G., 2014. Análise da espécie Bibimys labiosus (Winge 1887)(Rodentia, Sigmodontinae) ao longo da sua distribuição geográfica no Brasil. Msc. dissertation, Universidade Federal de Ouro Preto.

Dobson, F.S. and Oli, M.K., 2007. Fast and slow life histories of mammals. Ecoscience, 14(3), pp. 292-299.

Dittel, J.W., Lambert, T.D. and Adler, G.H., 2015. Seed dispersal by rodents in a lowland forest in central Panama. Journal of Tropical Ecology, 31(5), pp. 403-412.

Ellis, B.A., Mills, J.N., Glass, G.E., McKee Jr, K.T., Enria, D.A. and Childs, J.E., 1998. Dietary habits of the common rodents in an agroecosystem in Argentina. Journal of Mammalogy, 79(4), pp. 1203-1220.

Emmons, L.H. and Patton, J.L., 2012. Taxonomic revision of Bolivian Juscelinomys

(Rodentia, Cricetidae) with notes on morphology and ecology. Mammalia, 76(3), pp. 285-294.

Feranec, R.S., Hadly, E.A. and Paytan, A., 2009. Stable isotopes reveal seasonal competition for resources between late Pleistocene bison (Bison) and horse (Equus) from Rancho La Brea, southern California. Palaeogeography, Palaeoclimatology, Palaeoecology, 271(1- 2), pp. 153-160.

Fox-Dobbs, K., Stidham, T.A., Bowen, G.J., Emslie, S.D. and Koch, P.L., 2006. Dietary controls on extinction versus survival among avian megafauna in the late Pleistocene. Geology, 34(8), pp. 685-688.

Fox-Dobbs, K., Leonard, J.A. and Koch, P.L., 2008. Pleistocene megafauna from eastern Beringia: Paleoecological and paleoenvironmental interpretations of stable carbon and nitrogen isotope and radiocarbon records. Palaeogeography, Palaeoclimatology, Palaeoecology, 261(1-2), pp. 30-46.

Fry, B., 2006. Stable isotope ecology (Vol. 521). New York: Springer.

Galetti, M., Rodarte, R.R., Neves, C.L., Moreira, M. and Costa-Pereira, R., 2016. Trophic niche differentiation in rodents and marsupials revealed by stable isotopes. PLoS One, 11(4), p. e0152494.

Gannes, L.Z., Del Rio, C.M. and Koch, P., 1998. Natural abundance variations in stable isotopes and their potential uses in animal physiological ecology. Comparative Biochemistry and Physiology Part A: Molecular & Integrative Physiology, 119(3), pp. 725-737.

Geise, L., Bergallo, H.G., Esberárd, C.E.I., Rocha, C.F.D., Van Sluys, M., 2008. The karyotype of Blarinomys breviceps (Mammalia: Rodentia: Cricetidae) with comments on its morphology and some ecological notes. Zootaxa, 1907, pp. 47-60.

Geise, L., Paresque, R., Sebastião, H., Shirai, L.T., Astúa, D. and Marroig, G., 2010. Non-volant mammals, Parque Nacional do Catimbau, Vale do Catimbau, Buíque, state of Pernambuco, Brazil, with karyologic data. Check list, 6(1), pp. 180-186.

Granhall, U., 1981. Biological nitrogen fixation in relation to environmental factors and functioning of natural ecosystems. Terrestrial Nitrogen Cycles, pp. 131-144. Stockholm: Swedish Natural Science Research Council.

Hammer, Ø, Harper, D.A. and Ryan, P.D., 2001. PAST: paleontological statistics software package for education and data analysis. Palaeontologia Electronica, 4(1), p. 9.

Hershkovitz, P., 1966. South American swamp and fossorial rats of the scapteromyine

group (Cricetinae, Muridae) with comments on the glans penis in murid taxonomy. Zeitschrift für Säugetierkunde 31, pp. 81-149.

Hershkovitz, P., 1994. The description of a new species of South American hocicudo or long- nose mouse, genus Oxymycterus (Sigmodontinae, Muroidea), with critical review of the generic content. Fieldiana Zoology, 79, pp. 1-43.

Hilderbrand, G.V., Farley, S.D., Robbins, C.T., Hanley, T.A., Titus, K. and Servheen, C., 1996. Use of stable isotopes to determine diets of living and extinct bears. Canadian Journal of Zoology, 74(11), pp. 2080-2088.

Hobson, K.A., Alisauskas, R.T. and Clark, R.G., 1993. Stable-nitrogen isotope enrichment in avian tissues due to fasting and nutritional stress: implications for isotopic analyses of diet. The Condor, 95(2), pp. 388-394.

Hobson, K.A. and Koehler, G., 2015. On the use of stable oxygen isotope (δ18O) measurements for tracking avian movements in North America. Ecology and evolution, 5(3), pp. 799- 806.

Huiman, M.C.N., 2008. Dieta y morfología del estómago en roedores de los bosques montanos del departamento Huánuco, Perú. Ph.D. dissertation, Universidad Nacional Mayor de San Marcos.

Jackson, A.L., Inger, R., Parnell, A.C. and Bearhop, S., 2011. Comparing isotopic niche widths among and within communities: SIBER–Stable Isotope Bayesian Ellipses in R. Journal of Animal Ecology, 80(3), pp. 595-602.

Jonsson, P., Koskela, E. and Mappes, T., 2000. Does risk of predation by mammalian predators affect the spacing behaviour of rodents? Two large-scale experiments. Oecologia, 122(4), pp. 487-492.

Knight, J.D., Thies, J.E., Singleton, P.W. and Van Kessel, C., 1995. Carbon isotope composition of N 2-fixing and N-fertilized legumes along an elevational gradient. Plant and Soil, 177(1), pp. 101-109.

Kotler, B.P., Brown, J.S. and Mitchell, W.A., 1994. The role of predation in shaping the behavior, morphology and community organization of desert rodents. Australian Journal of Zoology, 42(4), pp. 449-466.

Layman, C.A., Araujo, M.S., Boucek, R., Hammerschlag-Peyer, C.M., Harrison, E., Jud, Z.R., Matich, P., Rosenblatt, A.E., Vaudo, J.J., Yeager, L.A. and Post, D.M., 2012. Applying stable

isotopes to examine food-web structure: an overview of analytical tools. Biological Reviews, 87(3), pp. 545-562.

Maclaren, J.A., Hulbert Jr, R.C., Wallace, S.C. and Nauwelaerts, S., 2018. A morphometric analysis of the forelimb in the genus Tapirus (Perissodactyla: Tapiridae) reveals influences of habitat, phylogeny and size through time and across geographical space. Zoological Journal of the Linnean Society, 184(2), pp. 499-515.

Maestri, R., Upham, N.S. and Patterson, B.D., 2019. Tracing the diversification history of a Neogene rodent invasion into South America. Ecography, 42(4), pp. 683-695.

Marshall, J.D., Brooks, J.R. and Lajtha, K., 2007. Sources of variation in the stable isotopic composition of plants. Stable isotopes in ecology and environmental science, 2, pp. 22- 60.

Martínez del Rio, C., Wolf, N., Carleton, S.A. and Gannes, L.Z., 2009. Isotopic ecology ten years after a call for more laboratory experiments. Biological Reviews, 84(1), pp. 91-111.

Merceron, G., Zazzo, A., Spassov, N., Geraads, D. and Kovachev, D., 2006. Bovid paleoecology and paleoenvironments from the Late Miocene of Bulgaria: evidence from dental microwear and stable isotopes. Palaeogeography, Palaeoclimatology, Palaeoecology, 241(3-4), pp. 637-654.

Meserve, P.L., Lang, B.K. and Patterson, B.D., 1988. Trophic relationships of small mammals in a Chilean temperate rainforest. Journal of Mammalogy 69(4), pp. 721-730.

Miller, G.H., Fogel, M.L., Magee, J.W., Gagan, M.K., Clarke, S.J. and Johnson, B.J., 2005. Ecosystem collapse in Pleistocene Australia and a human role in megafaunal extinction. Science, 309(5732), pp. 287-290.

Miller, J.F., Millar, J.S. and Longstaffe, F.J., 2008. Carbon-and nitrogen-isotope tissue–diet discrimination and turnover rates in deer mice, Peromyscus maniculatus. Canadian journal of Zoology, 86(7), pp. 685-691.

Newsome, S.D., Martinez del Rio, C., Bearhop, S. and Phillips, D.L., 2007. A niche for isotopic ecology. Frontiers in Ecology and the Environment, 5(8), pp. 429-436.

Nielsen, J.M., Clare, E.L., Hayden, B., Brett, M.T. and Kratina, P., 2018. Diet tracing in ecology: Method comparison and selection. Methods in Ecology and Evolution, 9(2), pp. 278-291.

O'Connell, T.C. and Hedges, R.E., 1999. Investigations into the effect of diet on modern human hair isotopic values. American Journal of Physical Anthropology: The Official Publication of the American Association of Physical Anthropologists, 108(4), pp. 409-

425.

O'Leary, M.H., 1988. Carbon isotopes in photosynthesis. Bioscience, 38(5), pp. 328-336.

O'Leary, M.H., Madhavan, S. and Paneth, P., 1992. Physical and chemical basis of carbon isotope fractionation in plants. Plant, Cell & Environment, 15(9), pp. 1099-1104.

Ofukany, A.F., Wassenaar, L.I., Bond, A.L. and Hobson, K.A., 2014. Defining fish community structure in Lake Winnipeg using stable isotopes (δ13C, δ15N, δ34S): Implications for monitoring ecological responses and trophodynamics of mercury & other trace elements. Science of the Total Environment, 497, pp. 239-249.

Pardiñas, U.F.J., Geise, L., Ventura, K. and Lessa, G., 2016. A new genus for Habrothrix angustidens and Akodon serrensis (Rodentia, Cricetidae): again paleontology meets neontology in the legacy of Lund. Mastozoología neotropical, 23(1), pp. 93-115.

Pardiñas, U.F.J., Patterson, B.D., D'Elía, G. and Teta, P., 2016b. Bibimys labiosus (errata version published in 2017). The IUCN Red List of Threatened Species 2016: e.T2802A115063837. Available from http://dx.doi.org/10.2305/IUCN.UK.2016-3.RLTS.T2802A22356418.en (accessed January 2019).

Pardiñas, U.F.J., Teta, P., Alvarado-Serrano, D., Geise, L., Jayat, J.P., Ortiz, P.E., Gonçalves, P.R. and D'Elia, G., 2015. Genus Akodon Meyen, 1833. Mammals of South America, Volume 2: Rodents, pp. 144-204. Chicago: Chicago University Press.

Pardiñas, U.F.J., Voglino, D. and Galliari, C.A., 2017. Miscellany on Bibimys (Rodentia, Sigmodontinae), a unique akodontine cricetid. Mastozoología Neotropical, 24(1), pp. 241-250.

Parnell, A. and Jackson, A., 2013. siar: Stable Isotope Analysis in R. R package version 4.2.

Pauli, J.N., Newsome, S.D., Cook, J.A., Harrod, C., Steffan, S.A., Baker, C.J., Ben-David, M., Bloom, D., Bowen, G.J., Cerling, T.E. and Cicero, C., 2017. Opinion: Why we need a centralized repository for isotopic data. Proceedings of the National Academy of Sciences, 114(12), pp. 2997-3001.

Peterson, B.J. and Fry, B., 1987. Stable isotopes in ecosystem studies. Annual Review of Ecology and Systematics, 18(1), pp. 293-320.

Pinotti, B.T., Naxara, L. and Pardini, R., 2011. Diet and food selection by small mammals in an old-growth Atlantic forest of south-eastern Brazil. Studies on Neotropical Fauna and Environment, 46(1), pp. 1-9.

Pizzimenti, J.J., and de Salle, R.O.B, 1980. Dietary and morphometric variation in some Peruvian rodent communities: the effect of feeding strategy on evolution. Biological Journal of the Linnean Society, 13(4), pp. 263-285.

Post, D.M., 2002. Using stable isotopes to estimate trophic position: models, methods, and assumptions. Ecology, 83(3), pp. 703-718.

R Core Team., 2017. R: A language and environment for statistical computing. R Foundation for Statistical Computing, Vienna, Austria. URL https://www.R-project.org/.

Read, A.F. and Harvey, P.H., 1989. Life history differences among the eutherian radiations. Journal of Zoology, 219(2), pp. 329-353.

Reichman, O.J., 1975. Relation of desert rodent diets to available resources. Journal of Mammalogy, 56(4), pp. 731-751.

Reig, O.A., 1972. The evolutionary history of the South American cricetid rodents. Ph.D. dissertation, University of London, London.

Reig, O.A., 1987. An assessment of the systematics and evolution of the Akodontini, with the description of new fossil species of Akodon (Cricetidae, Sigmodontinae). Fieldiana Zoology, 39, pp. 347-399.

Revell, L.J., 2012. phytools: An R package for phylogenetic comparative biology (and other things). Methods in Ecology and Evolution, 3, pp. 217-223.

Schmitt, C.J., Cook, J.A., Zamudio, K.R. and Edwards, S.V., 2018. Museum specimens of terrestrial vertebrates are sensitive indicators of environmental change in the Anthropocene. Philosophical Transactions of the Royal Society B, 374(1763), p. 20170387.

Secord, R., Wing, S.L. and Chew, A., 2008. Stable isotopes in early Eocene mammals as indicators of forest canopy structure and resource partitioning. Paleobiology, 34(2), pp. 282-300.

Smiley, T.M., Cotton, J.M., Badgley, C. and Cerling, T.E., 2016. Small-mammal isotope ecology tracks climate and vegetation gradients across western North America. Oikos, 125(8), pp. 1100-1109.

Solari, S., 2007. Trophic relationships within a highland rodent assemblage from Manu National Park, Cusco, Peru. The quintessential naturalist: Honoring the life and legacy of Oliver P. Pearson, pp. 225-240. California: University of California Publication Zoology.

Sparks, J.P. and Ehleringer, J.R., 1997. Leaf carbon isotope discrimination and nitrogen content for riparian trees along elevational transects. Oecologia, 109(3), pp. 362-367.

Steppan, S.J. and Schenk, J.J., 2017. Muroid rodent phylogenetics: 900-species tree reveals increasing diversification rates. PLoS One, 12(8), p. e0183070.

Sulzman, E.W., 2007. Stable isotope chemistry and measurement: a primer. Stable isotopes in ecology and environmental science, p. 1-21. London: Blackwell Scientific.

Talamoni, S., Couto, D., Junior, D and Diniz, F., 2008. Diet of some species of Neotropical small mammals. Mammalian Biology, 73, pp. 337-341.

Teta, P., Cueto, G. and Suarez, O., 2007. New data on morphology and natural history of Deltamys kempi Thomas, 1919 (Cricetidae, Sigmodontinae) from central-eastern Argentina. Zootaxa, 1665, p. 4351.

Tieszen, L.L., Boutton, T.W., Tesdahl, K.G. and Slade, N.A., 1983. Fractionation and turnover of stable carbon isotopes in animal tissues: implications for δ 13 C analysis of diet. Oecologia, 57(1-2), pp. 32-37.

Turner, T.F., Collyer, M.L. and Krabbenhoft, T.J., 2010. A general hypothesis-testing framework for stable isotope ratios in ecological studies. Ecology, 91(8), pp. 2227-2233.

van Bergen, E., Barlow, H.S., Brattström, O., Griffiths, H., Kodandaramaiah, U., Osborne, C.P. and Brakefield, P.M., 2016. The stable isotope ecology of mycalesine butterflies: implications for plant–insect co-evolution. Functional Ecology, 30(12), pp. 1936-1946.

Vander Zanden, H.B., Tucker, A.D., Hart, K.M., Lamont, M.M., Fujisaki, I., Addison, D.S., Mansfield, K.L., Phillips, K.F., Wunder, M.B., Bowen, G.J. and Pajuelo, M., 2015. Determining origin in a migratory marine vertebrate: a novel method to integrate stable isotopes and satellite tracking. Ecological Applications, 25(2), pp. 320-335.

Vander Wall, S.B., 2003. Effects of seed size of wind-dispersed pines (Pinus) on secondary seed dispersal and the caching behavior of rodents. Oikos, 100(1), pp. 25-34.

Vargas, J., Flores, P. and Martínez, J., 2007. Pequeños mamíferos en dos áreas protegidas de la vertiente oriental boliviana, considerando la variación altitudinal y la formación vegetacional. Revista Virtual Redesma. Availabe from http://revistavirtual .redesma .org

/vol2 /pdf /ambiental/mamiferos.pdf (accessed December 2018).

Williams, S.H. and Kay, R.F., 2001. A comparative test of adaptive explanations for hypsodonty in ungulates and rodents. Journal of Mammalian Evolution, 8(3), pp. 207-229.

Zevallos, C., 2014. Dieta de roedores Sigmodontinos (Rodentia: Cricetidae) en los bosques montanos del valle del Río Holpas. Bsc. thesis, Universidad Nacional Mayor de San Marcos, Lima,

Peru.

2.7. Figures

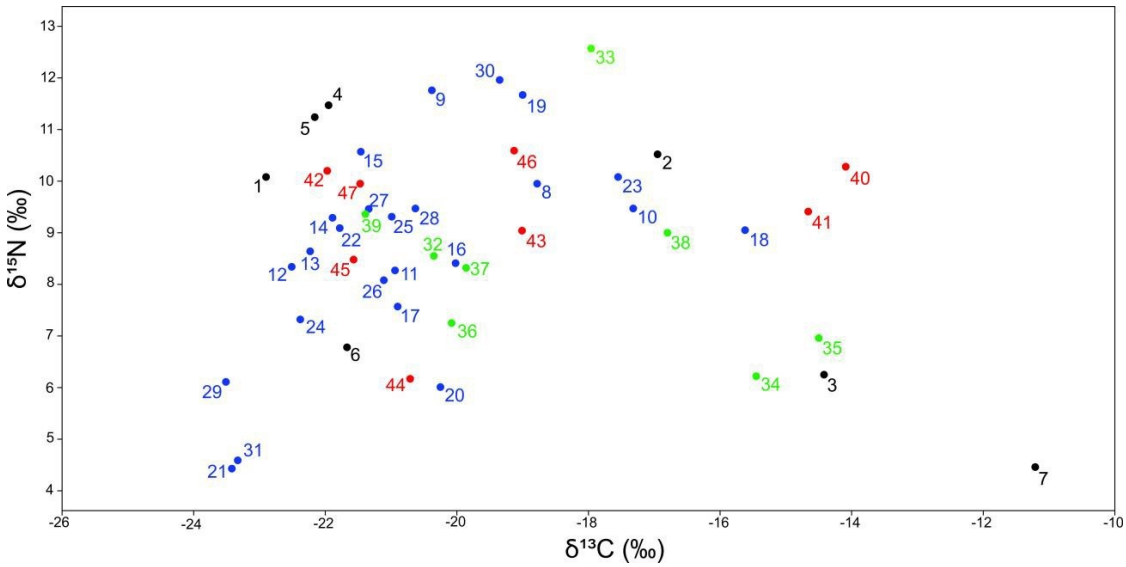

Figure 2.1. Plot with species-averaged values of $\delta^{13}C$ and $\delta^{15}N$. δ values are in permil (‰), and were calculated as the ratio of heavy to light isotope relative to the ratio of the standard for each element (VPDB and AIR reference scales for carbon and nitrogen, respectively). Species are represented by numbers, and colored according to each one of the four main lineages: **1**, *Scapteromys aquaticus*; **2**, *S. tumidus*; **3**, *Kunsia tomentosus*; **4**, *Blarinomys breviceps*; **5**, *Brucepattersonius soricinus*; **6**, *Lenoxus apicalis*; **7**, *Bibimys labiosus*; **8**, *Akodon subfuscus*; **9**, *Akodon lutescens*; **10**, *Akodon spegazzinii*; **11**, *Akodon boliviensis*; **12**, *Akodon azarae*; **13**, *Akodon kofordi*; **14**, *Akodon fumeus*; **15**, *Akodon montensis*; **16**, *Akodon cursor*; **17**, *Akodon iniscatus*; **18**, *Akodon dayi*; **19**, *Akodon toba*; **20**, *Akodon albiventer*; **21**, *Akodon budini*; **22**, *Akodon simulator*; **23**, *Akodon varius*; **24**, *Akodon torques*; **25**, *Akodon mollis*; **26**, *Akodon orophilus*; **27**, *Akodon affinis*; **28**, *Akodon aerosus*; **29**, *Akodon mimus*; **30**, *Deltamys kempi*; **31**, *Castoria angustidens*; **32**, *Necromys amoenus*; **33**, *Necromys obscurus*; **34**, *Necromyslenguarum*; **35**, *Necromys lasiurus*; **36**, *Necromys urichi*; **37**, *Podoxymys roraimae*; **38**, *Thalpomys lasiotis*; **39**, *Thaptomys nigrita*; **40**, *Juscelinomys huanchacae*; **41**, *Oxymycterusdelator*; **42**, *Oxymycterus amazonicus*; **43**, *Oxymycterus dasytrichus*; **44**, *Oxymycterus nasutus*; **45**, *Oxymycterus paramensis*; **46**, *Oxymycterus quaestor*; **47**, *Oxymycterus rufus*.

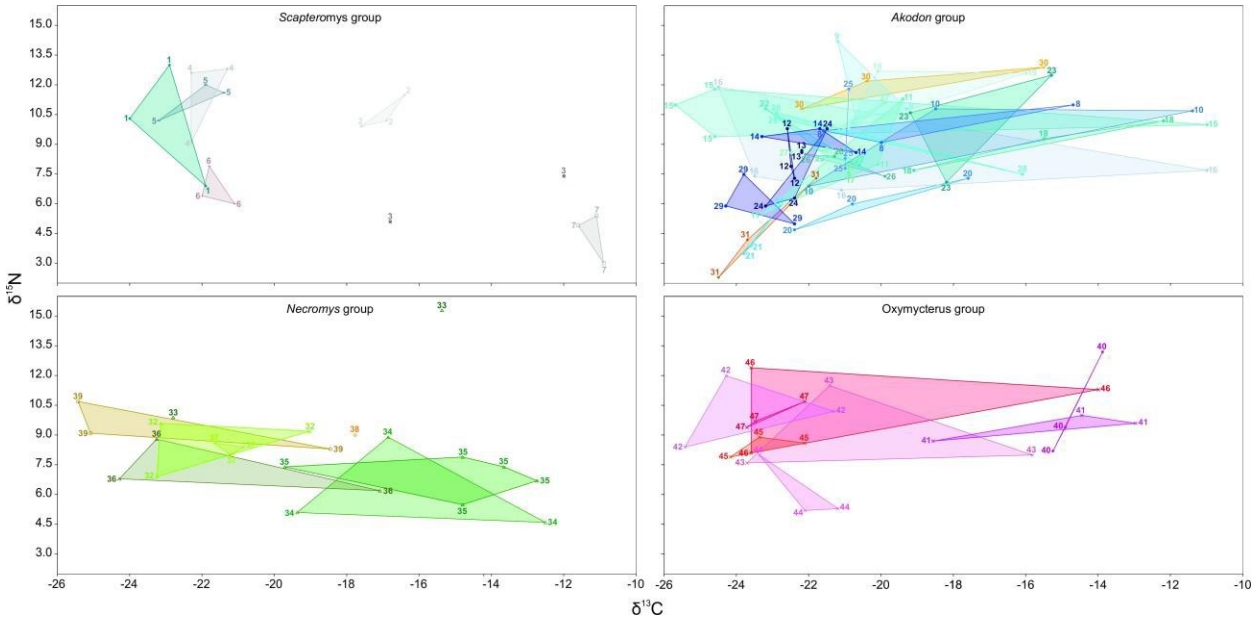

Figure 2.2. Plots with $\delta^{13}C$ and $\delta^{15}N$ values in permil (‰) for each specimen of the *Scapteromys*, *Oxymycterus*, *Necromys* and *Akodon* groups. δ values were calculated as the ratio of heavy to light isotope relative to the ratio of the standard for each element (VPDB and AIR reference scales for carbon and nitrogen, respectively). Species are represented by numbers: **1**, *Scapteromys aquaticus*; 2, *Scapteromys tumidus*; **3**, *Kunsia tomentosus*; 4, *Blarinomys breviceps*; **5**, *Brucepattersonius soricinus*; 6, *Lenoxus apicalis*; 7, *Bibimys labiosus*; **8**, *Akodon subfuscus*; 9, *Akodon lutescens*; **10**, *Akodon spegazzinii*; 11, *Akodon boliviensis*; **12**, *Akodon azarae*; **13**, *Akodon kofordi*; **14**, *Akodon fumeus*; **15**, *Akodon montensis*; 16, *Akodon cursor*; **17**, *Akodon iniscatus*; **18**, *Akodon dayi*; 19, *Akodon toba*; **20**, *Akodon albiventer*; **21**, *Akodon budini*; **22**, *Akodon simulator*; **23**, *Akodon varius*; **24**, *Akodon torques*; **25**, *Akodon mollis*; **26**, *Akodon orophilus*; 27, *Akodon affinis*; **28**, *Akodon aerosus*; **29**, *Akodon mimus*; **30**, *Deltamys kempi*; **31**, *Castoria angustidens*; **32**, *Necromys amoenus*; **33**, *Necromys obscurus*; **34**, *Necromyslenguarum*; **35**, *Necromys lasiurus*; **36**, *Necromys urichi*; **37**, *Podoxymys roraimae*; **38**, *Thalpomys lasiotis*; **39**, *Thaptomys nigrita*; **40**, *Juscelinomys huanchacae*; **41**, *Oxymycterusdelator*; **42**, *Oxymycterus amazonicus*; **43**, *Oxymycterus dasytrichus*; **44**, *Oxymycterus nasutus*; **45**, *Oxymycterus paramensis*; **46**, *Oxymycterus quaestor*; **47**, *Oxymycterus rufus*.

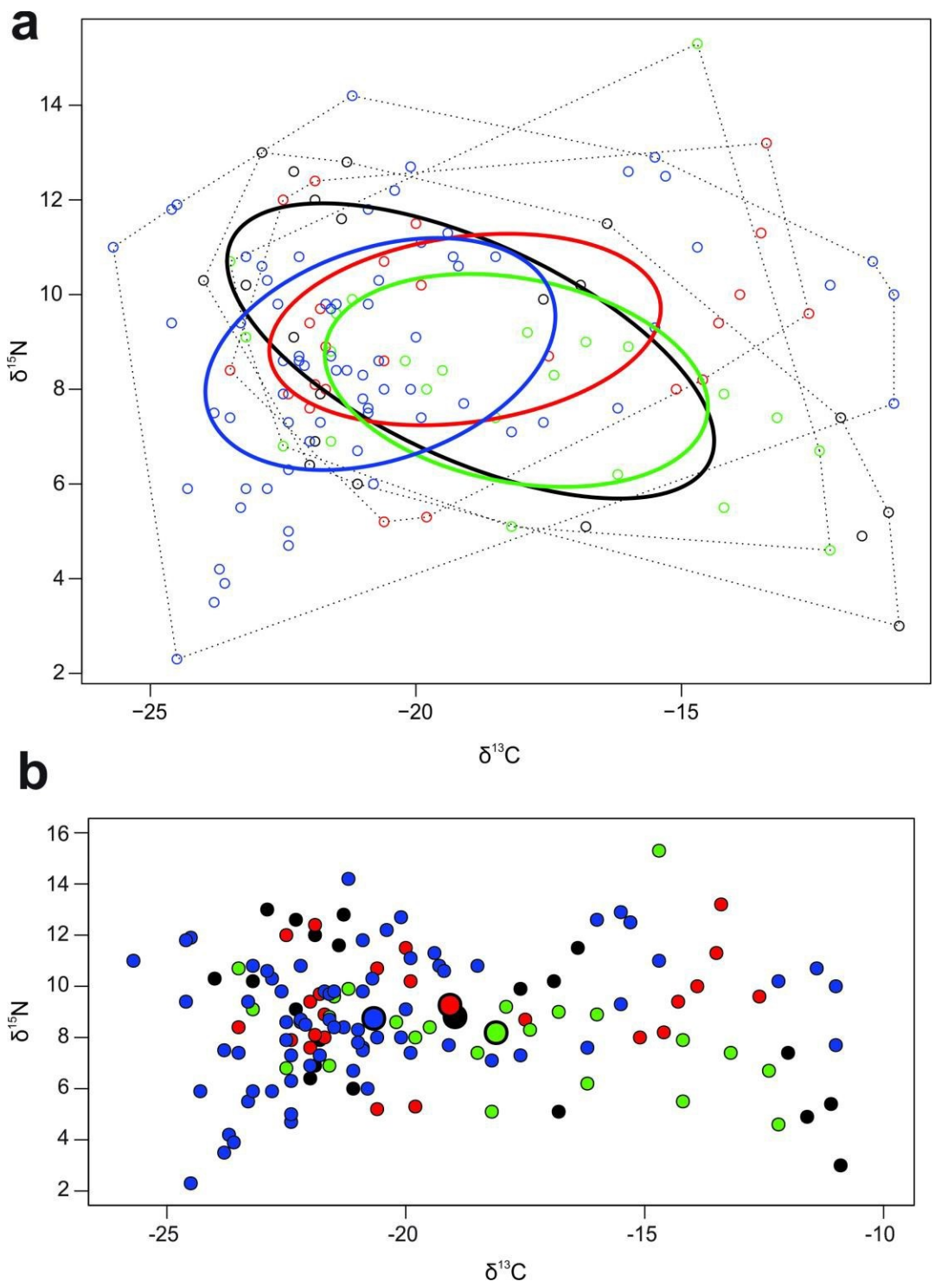

Figure 2.3. Plot with the respective SIBER ellipses (a) and centroids (b) for the *Scapteromys* (black), *Oxymycterus* (red), *Necromys* (green) and *Akodon* (blue) groups. $\delta^{13}C$ and $\delta^{15}N$ valuesare in permil (‰), and δ values were calculated as the ratio of heavy to light isotope relative tothe ratio of the standard for each element (VPDB and AIR reference scales for carbon and nitrogen, respectively).

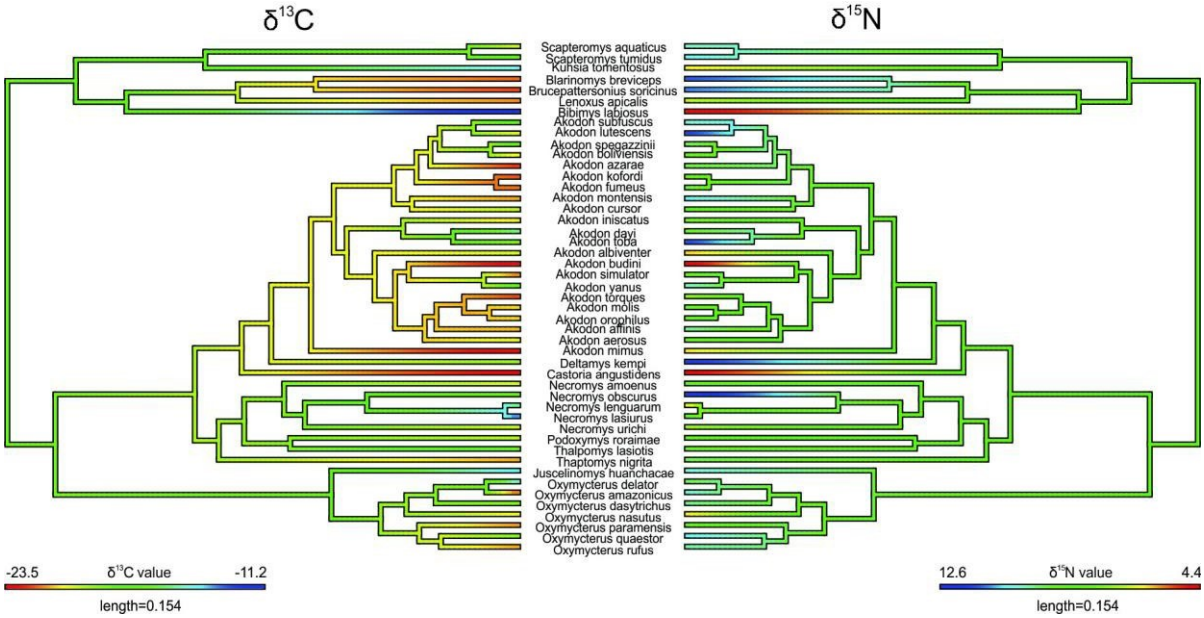

Figure 2.4. $\delta^{13}C$ and $\delta^{15}N$ values in permil (‰) mapped onto the pruned phylogeny of akodontine rodents (Maestri et al. 2017). δ values were calculated as the ratio of heavy to light isotope relative to the ratio of the standard for each element (VPDB and AIR reference scales forcarbon and nitrogen, respectively).

2.8. Tables

Table 2.1. Layman metrics and standard ellipses sizes for each group (NR: distance between the two species with the highest and lowest $\delta^{15}N$ values; CR: distance between the two species with the highest and lowest $\delta^{13}C$ values; CD: distance to the centroid; NND: nearest neighbor distance; SDNND: standard deviation of the Euclidean distances to each species' nearest neighbor; TA: total area of the convex hull; SEA: standard ellipse area; SEAc: standard ellipse area corrected for small size).

Group	NR	CR	CD	NND	SDNND	TA	SEA	SEAc
Scapteromys	10.00	13.10	4.83	1.13	0.90	72.99	33.78	35.66
Oxymycterus	8.00	10.90	3.75	0.85	0.53	58.62	21.86	22.85
Necromys	10.70	11.30	3.57	1.38	1.26	77.61	23.57	24.69
Akodon	11.90	14.70	3.36	0.58	0.45	111.08	23.64	23.98

Table 2.2. P-values for the analyzed metrics between each pair of groups (MD: centroid position; CD: distance to centroid; NND: nearest neighbor distance; * indicates significant values).

	Scapteromys - *Oxymycterus*	*Scapteromys* – *Necromys*	*Scapteromys* – *Akodon*	*Oxymycterus* – *Necromys*	*Oxymycterus* – *Akodon*	*Necromys* – *Akodon*
MD	0.874	0.513	0.097	0.253	0.07	0.001*
CD	0.139	0.085	0.017*	0.782	0.481	0.73
NND	0.382	0.45	0.655	0.053	0.886	0.117

2.9. Supplementary Material

Supplementary Material 2.S1: Isotope values for each specimen, including voucher numbers and locality.

Voucher	Species	δ13C	δ15N	Locality
FMNH 24540	*Akodon aerosus*	-16.2	7.6	Tingo Maria, Leoncio Prado, Huanuco, Peru
FMNH 43232	*Akodon aerosus*	-22.8	10.3	Pastaza, Rio Pindo Yaco, Ecuador
FMNH 78375	*Akodon aerosus*	-22.9	10.6	San Juan, Sandia, Puno, Peru
AMNH 181479	*Akodon affinis*	-21.6	8.7	Cauca, Popayan, Colombia
AMNH 33000	*Akodon affinis*	-22.5	8.6	Tolima, Ibague, Colombia
AMNH 71222	*Akodon affinis*	-19.9	11.1	Cundinamarca, San Juan de Rioseco, Colombia
FMNH 107597	*Akodon albiventer*	-17.6	7.3	Tarata, 5 km NE, Tacna, Peru
FMNH 107876	*Akodon albiventer*	-20.8	6.0	Chucuito, Ilave, 35 km S, 5 km W, Puno, Peru
FMNH 162735	*Akodon albiventer*	-22.4	4.7	Tarija, Cieneguillas, roadside 2 km SE, Bolivia
FMNH 23347	*Akodon azarae*	-22.4	7.3	Buenos Aires, Urdampilleta (=La Torrecita), Argentina
FMNH 27627	*Akodon azarae*	-22.5	7.9	Soriano, Dolores, 15 mi SW, Uruguay
FMNH 29206	*Akodon azarae*	-22.6	9.8	Dpto Minas, Polanco, Uruguay
FMNH 107834	*Akodon boliviensis*	-20.1	8.0	Chucuito, Ilave, 35 km S, 5 km W, Puno, Peru
FMNH 162753	*Akodon boliviensis*	-23.3	5.5	Oruro, Basin E of Lago Poopo, 4 km by rd N Huancane, Bolivia
FMNH 43375	*Akodon boliviensis*	-19.4	11.3	Anta, Huarocondo, Cuzco, Peru
FMNH 23355	*Akodon budini*	-23.6	3.9	Jujuy, Mountains W of Yala, Argentina
FMNH 23361	*Akodon budini*	-22.8	5.9	Jujuy, Mountains W of Yala, Argentina
FMNH 46121	*Akodon budini*	-23.8	3.5	Jujuy, Higuerilla, Argentina
UFMG 1835	*Akodon cursor*	-23.5	7.4	Passa Quatro, Minas Gerais, Brazil
UFMG 2671	*Akodon cursor*	-24.5	11.9	Marliéria, Minas Gerais, Brazil
UFMG 2676	*Akodon cursor*	-21.1	6.7	Una, Bahia, Brazil
UFMG 2718	*Akodon cursor*	-11.0	7.7	Iperó, São Paulo, Brazil
FMNH 21575	*Akodon dayi*	-12.2	10.2	Chapare, Todos Santos, Cochabamba, Bolivia
FMNH 21578	*Akodon dayi*	-19.1	7.7	Chapare, Chapare, Cochabamba, Bolivia
FMNH 46154	*Akodon dayi*	-15.5	9.3	Chapare, Todos Santos, Cochabamba, Bolivia
FMNH 46144	*Akodon fumeus*	-21.7	9.8	Chapare, Palmar, Cochabamba, Bolivia
FMNH 74881	*Akodon fumeus*	-23.3	9.4	Ayopaya, El Choro, Cochabamba, Bolivia
FMNH 79892	*Akodon fumeus*	-20.7	8.6	Sandia, Sandia, Puno, Peru
FMNH 29127	*Akodon iniscatus*	-20.9	7.6	Neuquen, Chos-Malal, Argentina
FMNH 41285	*Akodon iniscatus*	-20.9	7.5	Rio Negro, Pichi Mahuida, Argentina
FMNH 52553	*Akodon kofordi*	-22.2	8.6	Sandia, Limbani, Puno, Peru
FMNH 52555	*Akodon kofordi*	-22.2	8.7	Sandia, Limbani, Puno, Peru
FMNH 49696	*Akodon lutescens*	-20.7	10.3	Chuquibambilla, Grau, Apurimac, Peru
FMNH 50975	*Akodon lutescens*	-21.2	14.2	Cochabamba, Bolivia
FMNH 74884	*Akodon lutescens*	-19.3	10.8	El Choro, Ayopaya, Bolivia
AMNH 264920	*Akodon mimus*	-22.4	5.0	Santa Barbara, La Paz, Bolivia
AMNH 268803	*Akodon mimus*	-24.3	5.9	Cochabamba, Bolivia
AMNH 268826	*Akodon mimus*	-23.8	7.5	La Paz, Bolivia
FMNH 19286	*Akodon mollis*	-21.0	7.8	Hacienda Limon, Celendin, Cajamarca, Peru
FMNH 24446	*Akodon mollis*	-20.9	11.8	La Quinua, Pasco, Peru
FMNH 53388	*Akodon mollis*	-21.0	8.3	Volcan Pichincha, Pichincha, Ecuador
UFMG 2694	*Akodon montensis*	-11.0	10.0	Ponta Porã, Mato Grosso do Sul, Brazil
UFMG 2702	*Akodon montensis*	-24.6	9.4	Ponta Porã, Mato Grosso do Sul, Brazil
UFMG 2721	*Akodon montensis*	-24.6	11.8	Foz do Iguaçu, Paraná, Brazil

(continued)

UFMG 2725	*Akodon montensis*	-25.7	11.0	Foz do Iguaçu, Paraná, Brazil
NMNH 19752	*Akodon orophilus*	-22.1	8.5	Molinopampa, Chachapoyas, Amazonas, Peru
NMNH 24773	*Akodon orophilus*	-19.9	7.4	Hacienda Exito, Leoncio Prado, Huanuco, Peru
NMNH 35363	*Akodon orophilus*	-21.3	8.4	Puca Tambo, Rioja, San Martin, Peru
FMNH 29135	*Akodon simulator*	-20.6	8.0	Outro Cerro, Catamarca, Argentina
FMNH 30110	*Akodon simulator*	-21.5	8.4	Concepcion, Caelu Caleu, Tucuman, Argentina
FMNH 35250	*Akodon simulator*	-23.2	10.8	Rivadavia, Salta, Argentina
FMNH 29130	*Akodon spegazzinii*	-22.0	6.9	Otro Cerro, Catamarca, Argentina
FMNH 30184	*Akodon spegazzinii*	-18.5	10.8	Concepcion, Caelu Caleu, Tucuman, Argentina
FMNH 46147	*Akodon spegazzinii*	-11.4	10.7	Metan, La Represa, Salta, Argentina
FMNH 107744	*Akodon subfuscus*	-20.0	9.1	Cailloma, Arequipa, Peru
FMNH 49686	*Akodon subfuscus*	-14.7	11.0	Hacienda Urco, near Calca, Cuzco, Peru
FMNH 53137	*Akodon subfuscus*	-21.6	9.7	Limbani, Sandia, Puno, Peru
FMNH 164136	*Akodon toba*	-20.1	12.7	Chaco, Avia Terai, Argentina
FMNH 164170	*Akodon toba*	-16.0	12.6	Presidente Hayes Trans-Chaco Hwy, km 412; Experimental Farm, 2 km W Cruze Pioneros--Pioneros, Paraguay
FMNH 46142	*Akodon toba*	-20.9	9.8	Boqueron, Filadelfia, 35 km W, Toledo, Paraguay
FMNH 170524	*Akodon torques*	-23.2	5.9	Paucartambo, Puesto de Vigilancia Acjanaco, Cuzco, Peru
FMNH 43369	*Akodon torques*	-21.5	9.8	Urubamba, Torontoy, Cuzco, Peru
FMNH 78705	*Akodon torques*	-22.4	6.3	Marcapata, Cuzco, Peru
FMNH 21560	*Akodon varius*	-18.2	7.1	Tarata, Parotani, Cochabamba, Bolivia
FMNH 50160	*Akodon varius*	-15.3	12.5	Cercado, Cochabamba, Bolivia
FMNH 50977	*Akodon varius*	-19.2	10.6	Colomi, Cochabamba, Bolivia
MCNM 2162	*Bibimys labiosus*	-11.1	5.4	Divino, Minas Gerais, Brazil
MCNM 2838	*Bibimys labiosus*	-10.9	3.0	Barão de Cocais, Minas Gerais, Brazil
MCNM 2839	*Bibimys labiosus*	-11.6	4.9	Barão de Cocais, Minas Gerais, Brazil
UFMG 2016	*Blarinomys breviceps*	-22.3	12.6	Una, Bahia, Brazil
UFMG 2087	*Blarinomys breviceps*	-21.3	12.8	Jussari, Bahia, Brazil
UFMG 4062	*Blarinomys breviceps*	-22.3	9.1	Mariana, Minas Gerais, Brazil
FMNH 94409	*Brucepattersonius soricinus*	-21.9	12.0	Morretinho, São Paulo, Brazil
FMNH 94448	*Brucepattersonius soricinus*	-21.4	11.6	Primeiro Morro, São Paulo, Brazil
FMNH 94505	*Brucepattersonius soricinus*	-23.2	10.2	Primeiro Morro, São Paulo, Brazil
UFMG 1855	*Castoria angustidens*	-21.8	7.3	Itanhandu, Minas Gerais, Brazil
UFMG 1856	*Castoria angustidens*	-23.7	4.2	Delfim Moreira, Minas Gerais, Brazil
UFMG 2198	*Castoria angustidens*	-24.5	2.3	Una, Bahia, Brazil
AMNH 206100	*Deltamys kempi*	-20.4	12.2	Melo, Cerro Largo, Uruguay
AMNH 206119	*Deltamys kempi*	-15.5	12.9	Santiago Vazquez, Montevideo, Uruguay
AMNH 206147	*Deltamys kempi*	-22.2	10.8	Lascano, Rocha, Uruguay
NMNH 584508	*Juscelinomys huanchacae*	-14.6	8.2	Velasco Province, Santa Cruz, Bolivia
NMNH 584509	*Juscelinomys huanchacae*	-14.3	9.4	Velasco Province, Santa Cruz, Bolivia
NMNH 584510	*Juscelinomys huanchacae*	-13.4	13.2	Velasco Province, Santa Cruz, Bolivia
FMNH 122710	*Kunsia tomentosus*	-12.0	7.4	San Joaquin, Mamore, El Beni, Bolivia
FMNH 122711	*Kunsia tomentosus*	-16.8	5.1	San Bartolo, 15 km N, Mamore, El Beni, Bolivia
AMNH 16065	*Lenoxus apicalis*	-21.1	6.0	Sandia, Puno, Peru
AMNH 72605	*Lenoxus apicalis*	-21.8	7.9	Larecaja, La Paz, Bolivia
AMNH 72611	*Lenoxus apicalis*	-22.0	6.4	Larecaja, La Paz, Bolivia
FMNH 107680	*Necromys amoenus*	-21.5	9.6	Chivay, 5 km NNE, Caylloma, Arequipa, Peru
FMNH 107875	*Necromys amoenus*	-21.6	6.9	Ilave, 35 km S, 5 km W, Chucuito, Puno, Peru
FMNH 49671	*Necromys amoenus*	-17.9	9.2	Hacienda Collacachi, Puno, Peru
UFMG 3871	*Necromys lasiurus*	-13.2	7.4	Sabará, Minas Gerais, Brazil

(continued)

UFMG 3916	*Necromys lasiurus*	-14.2	5.5	Nova Lima, Minas Gerais, Brazil
UFMG 4214	*Necromys lasiurus*	-12.4	6.7	Felixlandia, Minas Gerais, Brazil
FMNH 117152	*Necromys lasiurus*	-18.5	7.4	Exaltacion, Yacuma, El Beni, Bolivia
FMNH 164235	*Necromys lasiurus*	-14.2	7.9	Trans-Chaco Hwy, km 412; Experimental Farm, 2 km W Cruze Pioneros--Pioneros, Presidente Hayes, Paraguay
NMNH 584523	*Necromys lenguarum*	-12.2	4.6	Velasco Province, Santa Cruz, Bolivia
NMNH 584525	*Necromys lenguarum*	-18.2	5.1	Velasco Province, Santa Cruz, Bolivia
NMNH 584529	*Necromys lenguarum*	-16.0	8.9	Velasco Province, Santa Cruz, Bolivia
FMNH 122687	*Necromys obscurus*	-21.2	9.9	Pergamino, Buenos Aires, Argentina
FMNH 35357	*Necromys obscurus*	-14.7	15.3	Colon, Montevideo, Uruguay
NMNH 280767	*Necromys urichi*	-16.2	6.2	Valledupar District, Cesar, Colombia
NMNH 540711	*Necromys urichi*	-22.5	6.8	Saint John Parish, Tobago, Trinidad and Tobago
NMNH 560659	*Necromys urichi*	-21.6	8.8	Cerro Neblina, Amazonas, Venezuela
NMNH 521496	*Oxymycterus amazonicus*	-23.5	8.4	Agrovila Da Uniao, 18 Km S, 19 Km W, Altamira, Pará, Brazil
NMNH 546023	*Oxymycterus amazonicus*	-22.5	12.0	Mojui dos Campos, Santarem, Para, Brazil
NMNH 546030	*Oxymycterus amazonicus*	-19.9	10.2	Aripuanã, Mato Grosso, Brazil
FMNH 145437	*Oxymycterus dasytrichus*	-22.0	7.6	Estação Boracéia, São Paulo, Brazil
FMNH 53874	*Oxymycterus dasytrichus*	-15.1	8.0	Fazenda da Lapa, Rio de Janeiro, Brazil
FMNH 94529	*Oxymycterus dasytrichus*	-20.0	11.5	Primeiro Morro, São Paulo, Brazil
UFMG 3832	*Oxymycterus delator*	-17.5	8.7	Augusto de Lima, Minas Gerais, Brazil
UFMG 3922	*Oxymycterus delator*	-13.9	10.0	Itabirito, Minas Gerais, Brazil
UFMG 4202	*Oxymycterus delator*	-12.6	9.6	São Roque de Minas, Minas Gerais, Brazil
FMNH 27652	*Oxymycterus nasutus*	-21.7	8.0	San Jose, Uruguay
FMNH 29252	*Oxymycterus nasutus*	-19.8	5.3	Treinta Y Tres, Uruguay
FMNH 29253	*Oxymycterus nasutus*	-20.6	5.2	Treinta Y Tres, Uruguay
FMNH 162845	*Oxymycterus paramensis*	-22.4	7.9	Ayopaya, El Choro, Cochabamba, Bolivia
FMNH 23320	*Oxymycterus paramensis*	-21.7	8.9	Mountains W of Yala, Jujuy, Argentina
FMNH 74894	*Oxymycterus paramensis*	-20.6	8.6	Narvaez, ca 10 km by rd W, Tarija, Bolivia
FMNH 26595	*Oxymycterus quaestor*	-21.9	12.4	Arroyo Paranay-Guazu, Misiones, Argentina
FMNH 26757	*Oxymycterus quaestor*	-13.5	11.3	Joinvile, Santa Catarina, Brazil
FMNH 34380	*Oxymycterus quaestor*	-21.9	8.1	Teresopolis, Rio de Janeiro, Brazil
FMNH 122697	*Oxymycterus rufus*	-22.0	9.4	General Lavalle, Mar del Tuyu, Buenos Aires, Argentina
FMNH 95138	*Oxymycterus rufus*	-20.6	10.7	Pereyra, Buenos Aires, Argentina
FMNH 98285	*Oxymycterus rufus*	-21.8	9.7	Punta Lara, Buenos Aires, Argentina
AMNH 75582	*Podoxymys roraimae*	-19.5	8.4	Gran Sabana, Bolivar, Venezuela
AMNH 75583	*Podoxymys roraimae*	-19.8	8.0	Gran Sabana, Bolivar, Venezuela
AMNH 75585	*Podoxymys roraimae*	-20.2	8.6	Gran Sabana, Bolivar, Venezuela
FMNH 29160	*Scapteromys aquaticus*	-21.9	6.9	Delta del Paraná, Isla Ella, Argentina
FMNH 98286	*Scapteromys aquaticus*	-24.0	10.3	Punta Lara, Buenos Aires, Argentina
FMNH 98287	*Scapteromys aquaticus*	-22.9	13.0	Punta Lara, Buenos Aires, Argentina
AMNH 206247	*Scapteromys tumidus*	-16.9	10.2	Punta del Este, Maldonado, Uruguay
AMNH 206267	*Scapteromys tumidus*	-17.6	9.9	Lascano, Rocha, Uruguay
AMNH 206280	*Scapteromys tumidus*	-16.4	11.5	Cardona, Soriano, Uruguay
FMNH 128326	*Thalpomys lasiotis*	-16.8	9.0	nearby Fundacion Zoo-Botanica, Distrito Federal, Brazil
FMNH 230387	*Thaptomys nigrita*	-23.2	9.1	2.7Km N-3.9KmW Pico da Bandeira, Cachoeira Bonita, Minas Gerais, Brazil
FMNH 26820	*Thaptomys nigrita*	-23.5	10.7	Rio Rarana, Caraguatay, 100 mi S Rio Iguassu, Missiones, Argentina
FMNH 35353	*Thaptomys nigrita*	-17.4	8.3	Santa Catarina, Brazil

Supplementary Material 2.S2: $\delta^{13}C$ and $\delta^{15}N$ average values for 47 species of Akodontini rodents and for the groups representing the four main lineages, with respective standard deviations.

Species	$\delta^{13}C$		$\delta^{15}N$	
	Average	SD	Average	SD
Akodon aerosus	-20.634403	3.85422763	9.4724778	1.65731464
Akodon affinis	-21.3376944	1.31424107	9.46427373	1.38626325
Akodon albiventer	-20.2491633	2.43712335	6.0063257	1.26830658
Akodon azarae	-22.5113067	0.09029214	8.3441897	1.26691029
Akodon boliviensis	-20.9443504	2.05809574	8.2739866	2.9011907
Akodon budini	-23.4154887	0.56365799	4.4306188	1.31913588
Akodon cursor	-20.0216418	6.19583569	8.41230188	2.32911106
Akodon dayi	-15.6225738	3.4411289	9.051931	1.27325278
Akodon fumeus	-21.8934377	1.28231393	9.2914277	0.6136722
Akodon iniscatus	-20.9036656	0.02793291	7.5665812	0.06983005
Akodon kofordi	-22.2295517	0.02220308	8.6438125	0.07838067
Akodon lutescens	-20.3842167	0.98224634	11.7569337	2.11717298
Akodon mimus	-23.5110648	0.96445684	6.11276687	1.24816836
Akodon mollis	-20.9906061	0.08027725	9.3115817	2.13867686
Akodon montensis	-21.4575179	7.01279905	10.5674482	1.03795907
Akodon orophilus	-21.1118165	1.11855167	8.0791646	0.62284855
Akodon simulator	-21.7786423	1.33776535	9.0902236	1.52950172
Akodon spegazzinii	-17.3161426	5.39257366	9.471806	2.18658834
Akodon subfuscus	-18.7797831	3.61010268	9.9450891	0.98527933
Akodon toba	-19.0022884	2.65255525	11.6748708	1.61851588
Akodon torques	-22.3806426	0.82592436	7.3196947	2.17479871
Akodon varius	-17.5494472	2.01081366	10.076426	2.75729303
Bibimys labiosus	-11.2067255	0.35382764	4.46220053	1.26694435
Blarinomys breviceps	-21.9518525	0.60661425	11.469302	2.08818209
Brucepattersonius soricinus	-22.1594927	0.90707292	11.2440144	0.95104478
Castoria angustidens	-23.3346043	1.40233551	4.59223953	2.50133017
Deltamys kempi	-19.3536056	3.49783966	11.9648555	1.06976046
Juscelinomys huanchacae	-14.0862414	0.6386025	10.2751827	2.58450304
Kunsia tomentosus	-14.4205991	3.36627376	6.24699805	1.64528142
Lenoxus apicalis	-21.668432	0.46020291	6.77916213	1.01242067
Necromys amoenus	-20.3464017	2.11126761	8.5507682	1.48041739
Necromys lasiurus	-14.4983879	2.36601121	6.95915628	0.95108557
Necromys lenguarum	-15.4508972	3.05055425	6.22225997	2.3738906
Necromys obscurus	-17.9606846	4.54805071	12.5683002	3.83566474
Necromys urichi	-20.0834512	3.41006517	7.25126227	1.34840031
Oxymycterus amazonicus	-21.9691938	1.88500419	10.2015134	1.81681468

(continued)

Oxymycterus dasytrichus	-19.012764	3.53754171	9.044704	2.10273367
Oxymycterus delator	-14.6607335	2.52017	9.41068463	0.65654615
Oxymycterus nasutus	-20.7134092	0.97171079	6.1739398	1.56578422
Oxymycterus paramensis	-21.5688416	0.90196453	8.47824893	0.55333027
Oxymycterus quaestor	-19.129998	4.85163395	10.5922572	2.21881873
Oxymycterus rufus	-21.4696104	0.73761796	9.94669787	0.65937949
Podoxymys roraimae	-19.8612966	0.33464281	8.324358	0.30470754
Scapteromys aquaticus	-22.8957312	1.05409275	10.0821794	3.0362337
Scapteromys tumidus	-16.949864	0.61224932	10.5206062	0.82172738
Thalpomys lasiotis	-16.8	0	9	0
Thaptomys nigrita	-21.3929296	3.43750752	9.36022313	1.22153121
Scapteromys group	-18.7503853	4.59104243	8.68635182	2.79971864
Oxymycterus group	-19.076349	3.10286715	9.26540356	1.43264159
Necromys group	-18.2992561	2.51586653	8.529541	1.95262245
Akodon group	-20.6964023	1.98791575	8.70504279	1.99545462

Supplementary Material 2.S3: Plot with SEAc sizes for each group (1: "*Scapteromys"* group; 2: "*Oxymycterus"* group; 3: "*Necromys"* group; 4: "*Akodon"* group). The boxes represent the 95, 75 and 50% credible intervals in ascending order of size. The black circles and the red squares represent the modes and the maximum likelihood estimate for the corresponding SEAc, respectively.

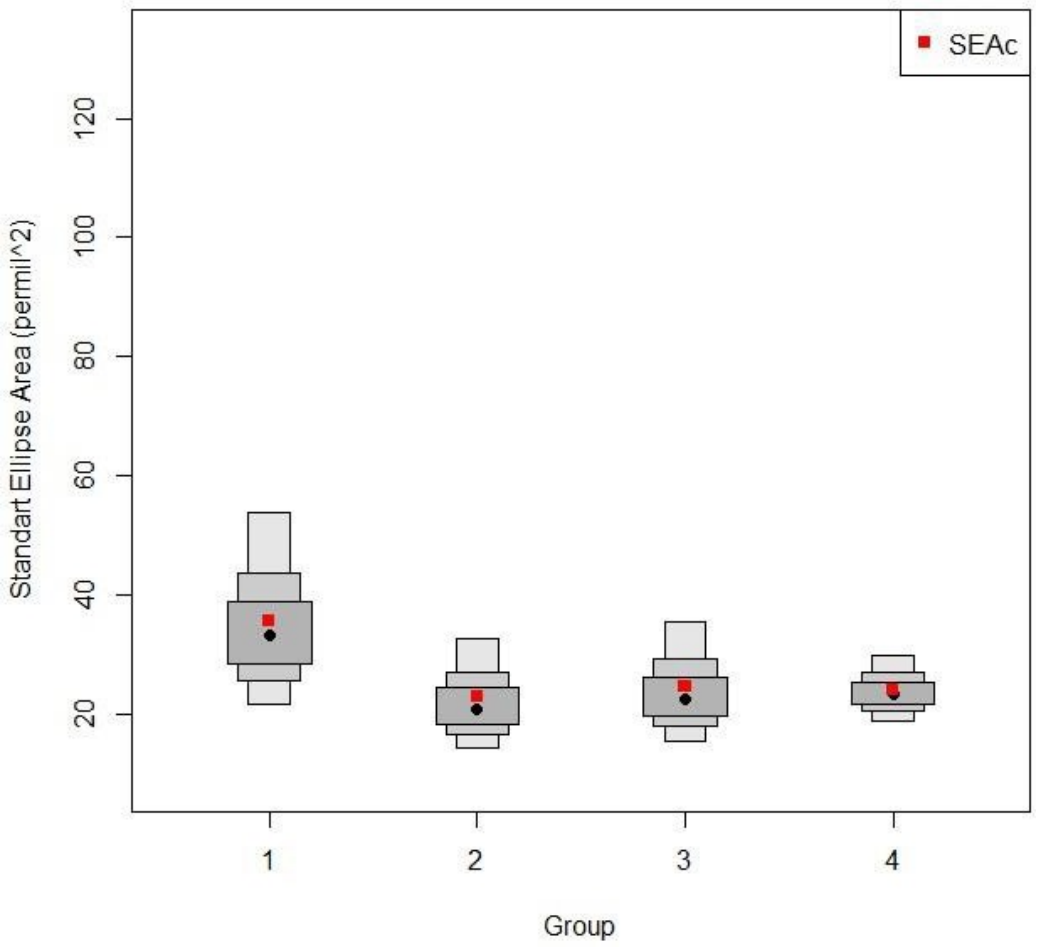

CHAPTER 3: JAW FUNCTIONAL MORPHOLOGY REFLECTS DIET IN AKODONTINE RODENTS

Drawing of *Necromys lasiurus* by Fernando Perini

JAW FUNCTIONAL MORPHOLOGY REFLECTS DIET IN AKODONTINE RODENTS

Rafaela V. Missagia[1,2], Bruce D. Patterson[2] and Fernando A. Perini[1]

[1]PPG - Zoologia/Departamento de Zoologia - Instituto de Ciências Biológicas, Universidade Federal de Minas Gerais – Av. Antônio Carlos, 6627, Pampulha, Belo Horizonte, MG, Brazil

[2]Integrative Research Center, Field Museum of Natural History, Chicago, IL 60605, USA

Abstract

Changes on masticatory muscles can occur due to dietary pressures, and are often reflected on the morphology of the cranial complex of vertebrates. Among cricetid rodents, the Akodontini tribe presents a diverse array of feeding ecologies, particularly of insectivorous species, but the possible effect of diet on the group's cranial morphology have never been tested. In the present work we quantify functional measurements of mechanical advantage and bite forceon the jaw of akodontine rodents to assess their relationship between each other and to two different diet proxies; and test whether it is possible to recognize morphological convergence on the morphospace in response to feeding ecology in the tribe. Functional measurements of muscle in- and out-levers and bite force from mandibles of Akodontini rodents were computed. The analysis of variance for mechanical advantage values suggest significant differences between the dietary categories, with insectivores presenting the lowest mechanical advantages. Mechanical advantage is positively correlated with bite force, and both generally increases from insectivores to herbivores. Only δ13C values are significantly correlated with both functional measurements, with higher values associated with C4 consumers. Higher bite force and mechanical advantage seems determinant for consuming C4 plants, but not invertebrates.

Keywords: functional morphology, bite force, mechanical advantage, PGLS.

3.1. Introduction

The influence of feeding ecology on the masticatory apparatus of vertebrates has been studied extensively (Satoh and Iwaku 2006, Christiansen and Wroe 2007, Santana et al. 2010, Hampton et al. 2011, Muschick et al. 2012). Dietary pressures are often reflected in masticatory muscles, and their sizes and lines of action relate to cranial shape in many groups (Herrel et al. 1998, Satoh 1999, Huber et al. 2008, Fabre et al. 2018). Therefore, differences in feeding ecology between species are usually connected to and may be governed by functional properties of the skull (Anderson et al. 2008).

The mammalian mandible is especially relevant in ecomorphological studies due to its high functional demands (Crompton 1995). The jaw serves mainly as an insertion area for the masticatory muscles that originate on the skull (Crompton 1995, Greaves 2012), and its mechanics can be thought of as a two-dimensional structure where the jaw works as a lever that rotates around its joint and is subject to forces applied to it by the masticatory muscles (Hiiemäe and Ardran 1968, Turnbull 1970, Greaves 2012). Mechanical advantage is a functional trait that represents a trade-off between force and speed on a system of levers (Uicker et al. 2011), and hasbeen widely applied to the skull complex of vertebrates (Westneat 1994, Sakamoto 2010, Hampton 2011, Becerra et al. 2014, Fabre et al. 2017). The jaw is, therefore, subject to selective forces (Schwenk and Rubega 2005), and several studies have documented a strong correlation between the dietary habits and jaw morphology in mammals (Ross et al. 2012, Grossnickle and Polly 2013, Verde Arregoitia et al. 2017).

Rodents can be considered the most successful group of living mammals, representing almost half of its extant diversity (Wilson and Reeder 2005). The rodent skull has a distinctive morphology when compared to other mammals, mainly due to a long diastema separating the ever-growing incisors from a reduced cheek teeth row, giving rise to two distinct functional regions in the skull (Wood 1965, Landry 1970, Turnbull 1970). The incisors and molars are in occlusion alternately (i.e., when incisors are in occlusion, the cheek teeth are not, and vice versa). This dual occlusal pattern creates a potential trade-off, allowing some rodents to strengthen incisor bite force and others to optimize bite force at molars (Cox et al. 2012). In some rodents, the infraorbital foramen is enlarged and crossed by masseter bundles which attach to the rostrum, increasing muscle's strength (Satoh 1997, Satoh and Iwaku 2004a). The glenoid fossa of rodents is oriented

longitudinally, restricting mediolateral movements of the condylar process of the jaw and enabling forward and oblique chewing movements (Satoh and Iwaku 2004a). In addition, the masseter muscle is well developed and subdivided, whereas the temporal muscle occupies a smaller percentage of the total musculature of the skull (Wood 1965, Turnbull1970, Satoh and Iwaku 2004a). Although this morphological conformation is commonly associated to herbivory (Turnbull 1970, but see Landry 1970), different morphologies and diets are found within this basic pattern, generally related to distinct ecological pressures (Landry 1970, Satoh and Iwaku 2004, Samuels 2009).

In rodents, the development of the masseter and its rostral displacement led to high masticatory efficiency at both incisors and molars (Wood 1965, Turnbull 1970). The rostral displacement occurred independently in different portions of the masseter throughout the evolutionary history of rodents: in the so-called sciuromorph condition, the deep masseter moved dorsally, originating along the zygomatic plate and improving bite force at the incisors; in the hystricomorph condition, the medial masseter originates on the rostrum, improving chewing efficiency at the molars; and in the myomorph condition, the medial portion of the masseter originates on the rostrum and its deep portion extends to the zygomatic plate (Wood 1965, Turnbull 1970, Satoh and Iwaku 2004a, Cox et al. 2012, Swanson et al. 2019). The myomorph morphology, which combines aspects of sciuromorph and hystricomorph types (Cox et al. 2012, Maestri et al. 2016, Swanson et al. 2019), offers improved performance at both gnawing and chewing when compared with the others (Maestri et al. 2016). Rodents with this type of muscular arrangement are considered "high-performance generalists" (Cox et al. 2012, Maestriet al. 2016), and this functional versatility probably contributed to an ecological release that triggered the exploration of different types of resources (Maestri et al. 2016), and to the subsequent spread of myomorph rodents in the form of various ecotypes around the world, from specialist herbivores (e.g. *Chiropodomys* and *Holochilus*; Hershkovitz 1955, Musser and Durden 2002) to fish-eating carnivores (e.g. *Ichthyomys* and *Hydromys*; Voss 1988, Fabre et al. 2017) and shrew-like insectivores (e.g. *Rhynchomys*, *Sommeromys* and *Oxymycterus*; Hershkovitz 1994, Musser and Durden 2002).

Insectivorous species are found almost exclusively among myomorph rodents (Maestri et al. 2016, but see the sciuromorph *Rhinosciurus laticaudatus*), and present a peculiar phenotype associated with the demands of this diet (Vorontzov 1979, Samuels 2009, Rowe et al. 2016,

Martinez et al. 2018). Herbivorous and granivorous rodents usually have strong bites, commonly related to skull shape changes like short and robust rostra, wide incisors, and broad zygomatic arches (Samuels 2009). Insectivorous species, on the other hand, are "weaker biters" (Maestri et al. 2016), and can be recognized by their long and narrow rostra, delicate zygomatic arches, and small temporal fossae, associated with the reduction of masticatory muscle origins and changes in the mechanics of mastication (Samuels 2009, Maestri et al. 2016).

Sigmodontinae rodents are a group of Neotropical cricetids, and part of the highly diverse myomorphous clade Muroidea (Patton et al. 2015). Studies have shown that, among sigmodontines, insectivorous species are morphologically specialized when compared to other groups (Maestri et al. 2016). Akodontini, the second most diverse tribe of Sigmodontinae, is apparently rich in insectivorous species (D'Elía and Pardiñas, 2015, Reig 1972, 1987). Stomach content and stable isotopes analyses point to a marked consumption of invertebrates by various akodontine rodents (Pizzimenti and DeSalle 1980, Ellis et al. 1998, Galetti et al. 2016, Missagia et al. in press), and several authors have highlighted their apparent morphological specializations towards insectivory, which seem to have evolved repeatedly and convergently (Reig 1972, 1987, Hershkovitz 1966, Missagia and Perini 2018).

There have been numerous comparative studies focused on the functional significance of masticatory muscles in murid rodents (Satoh 1998, 1999, Fabre et al. 2017, Ginot et al. 2018a, 2018b), but these are less common in cricetid rodents (e.g. Satoh and Iwaku 2004b, 2006). According to Samuels (2009) and Maestri et al. (2016), rodents with similar dietary specializations can be recognized by their convergent skull morphology. If feeding ecology has influenced skull evolution through selection on aspects related to mechanical advantage, then thecorresponding functional measures should vary according to different diets. We also expect mechanical advantage to be correlated with bite force, with greater mechanical advantage in species with a stronger bite, and lower mechanical advantages in insectivorous species that are "weaker biters" (Maestri et al. 2016). In the present work we quantify functional measurements on the jaws of akodontine rodents to assess their relationship to bite force and diet. We also tested whether it is possible to recognize morphological convergence in response to feeding ecology on different lineages of Akodontini.

3.2. Material and Methods

3.2.1. Data collection

Rodent's jaw can be divided into two functional portions: one formed by the pair of ever-growing incisors and other formed by the cheek-teeth (Landry 1970). The mechanical advantage (MA) can be calculated as the ratio between in- and out-lever arms of each masticatory muscle (Uicker et al. 2011). The distance from the jaw joint is an important factor to be considered when analyzing mechanical advantage, because it influences the resulting force produced by this system (Greaves 2012). Mechanical advantages of each muscle are increased by longer distancesbetween the muscle insertion and the jaw joint (in-lever), and decreased in muscles that insert closer to the joint (Greaves 2012). The out-lever arms are the distance from the bite point to the jaw joint, negatively related to the resulting mechanical advantage. Therefore, smaller out-levers are related to greater mechanical advantages (Uicker et al. 2011). We calculated two out-levers, one considering the tip of the incisors and other considering the molars as the bite point (Fig. 3.1). For the in-levers, we considered the linear distance of the point of insertion of each muscle to the jaw joint (Fig. 3.1), based on previous muscular dissections (Voss 1988, Satoh and Iwaku 2006, Fabre et al. 2017), CTscan images (Cox et al. 2012, Baverstock et al. 2013, Ginot et al. 2018a), and biomechanical models (Herring and Herring 1974) of muroid rodents. We chose to compare the mechanical advantage of the deep masseter, superficial masseter, and temporal muscles since they belong to the main adductors muscular groups of the jaw and are the most active during mastication on rodents (Hiiemae 1971, Weijs and Dantuma 1975, Satoh and Iwaku 2004a). The masseter was divided in two portions, deep and superficial, based on functional interpretations (Hiimae 1971).

We calculated bite force (BF) as an index proposed by Freeman and Lemen (2008), which compared five bending forces indexes to *in vivo* bite force of cricetid rodents. The authors recommend the use of the index $Z_{i,}$ a measure of rigidity to bending of the incisors, since it was highly correlated with the *in vivo* bite force ($R^2 = 0.96$). The index Z was originally proposed by Popov (1999), and is here calculated for the incisors as $Z=wh^2/6$, where w is the medial-lateral width and h is the ventral-dorsal length of the lower incisor near its alveolus (Freeman and Lemen 2008). This value is then transformed to Newtons (N) according to the regressionequation of Freeman and Lemen (2008), as $\log 10(\text{bite force}) = 0.559 \times \log 10(Z_i) + 1.432$.

Functional measurements of muscle in- and out-levers were computed from lateral digital

images of 858 mandibles, belonging to 63 species of Akodontini rodents (Supplementary Material 3.S1), using the software ImageJ (Rasband 1997). We sampled an average of 14 individuals per species, with at least 1 and at most 27 specimens per species. Additionally, incisor measurements were taken from 987 specimens of 61 species of Akodontini rodents, following Freemen and Leman (2008), to calculate bite force. Sampling was restricted to adult specimens (i.e., with the third molar fully erupted), to control for possible allometric age effects (Greaves 2000, Zelditch et al. 2004, Hernandez et al. 2017). An average of 16 individuals per species were sampled for bite force, with at least 1 and at most 34 specimens per species. The analyzed specimens are deposited in the mammal collections of the Field Museum of Natural History (FMNH), American Museum of Natural History (AMNH), National Museum of Natural History (UMNH), Museu de História Natural of Pontifícia Universidade Católica of Minas Gerais (MCNM), and Museu Nacional of Universidade Federal do Rio de Janeiro (MN) (see Supplementary Material 3.S1 for voucher numbers).

3.2.2. Data analysis

We compared functional morphology with two different dietary proxies. First, we categorized analyzed species based on diet data found in the literature. Where possible, we used quantitative information on the proportion of items from stomach content analysis, as suggested by Pineda-Munoz and Alroy (2014), but such data are available for only one third of akodontine species included in this study (see Supplementary Material 3.S2 and 3.S3 for details). Otherwise, we used non-quantitative data from the literature (Supplementary Material 3.S3) based on their primary food resources (Samuels 2009, Pineda-Munoz and Alroy 2014). Thus, we classified the species into three dietary categories: 1) omnivores: generalist species without clear food preferences or with balanced proportions of items on their stomach; 2) herbivores: species that preferentially consume vegetal matter, including seeds, fruits, and fibrous parts of plants; or with plant matter representing more than 70% of their stomach content; 3) insectivores: species that consume mainly invertebrates, like chitinous insects, soft-bodied larvae, and earthworms; or with animal matter representing more than 70% of their stomach content. Some species included in this latter category may eventually consume small vertebrates (e.g. *Oxymycterus rufus*; Perera 2002), but they are not their primary source of resource. When more than one source of stomach content analysis was available, we took the mean value. The species with conflicting qualitative

information were allocated in the most comprehensive category (omnivore).

The differences between the mechanical advantage of each muscle and the dietary categories were assessed by Kruskall-Wallis tests due to the lack of normality and heteroscedasticity of these variables, even after transformations (Supplementary Material 3.S4). Species without dietary data (11.1% of analyzed species) could not be allocated to any category and were excluded from the analyses. Finally, we performed paired Dunn's post-hoc comparisons between each dietary category, recommended when sample sizes of each group are unequal (Zar 2010), with adjusted p-values (Holm, 1979). The analysis of variance, normality and homoscedasticity tests, and post-hoc comparisons were performed using the "stats", "car", "lawstat", and "PMCMR" packages (Fox and Weisberg 2011, Pohlert 2014, R Core Team 2017, Gastwirth et al. 2019).

For the second proxy, we used stable isotope values from Missagia et al. (in press). $\delta^{15}N$ values can be used to estimate trophic position, because the $\delta^{15}N$ is usually enriched by 3-4‰ with each trophic level on the food chain (DeNiro and Epstein 1981, Peterson and Fry 1987). Higher values of $\delta^{15}N$ indicate higher trophic levels (DeNiro and Epstein 1981, Minagawa and Wada 1984, Peterson and Fry 1987), and were here used as an indicative of consumption of animal matter. The carbon isotope can be used to differentiate plants with different photosynthetic pathways, allowing to differentiate browsers (C_3 consumers) from grazers (C_4 consumers). Thus, $\delta^{13}C$ values allow us to access the hardness of the resource to be processed by the masticatory apparatus, with plants C_4 being more associated with greater bite forces due to itsfibrous nature when compared to C_3 plants. Considering this, it is expected that (1) species that consume more animal material (i.e. with higher $\delta^{15}N$ values) have lower MAs and BF; and (2) higher MA and BF values are associated with consumption of C_4 plants (i.e. higher $\delta^{13}C$ values), because of the mechanical requirements of processing this type of food (e.g. grasses).

We performed a Principal Components Analysis (PCA) on species' averages for the calculated MA of the deep masseter, superficial masseter and temporal muscles, to assess clustering of the dietary groups. Species without dietary data were included and assigned to the "unknown" category.

The most recent phylogenetic hypotheses for Akodontini (Maestri et al. 2017, 2019) were

used to divide the tribe into four main lineages to assess their pattern of occupation of the functional morphospace: the *"Scapteromys"* lineage, which includes *Scapteromys*, *Kunsia*, *Bibimys*, *Blarinomys*, *Brucepattersonius,* and *Lenoxus*; the *"Oxymycterus"* lineage, comprising *Oxymycterus* and *Juscelinomys*; the *"Necromys"* lineage, including *Necromys, Podoxymys, Thalpomys,* and *Thaptomys*; and the *"Akodon"* lineage, comprising the highly diverse *Akodon* genus, together with *Deltamys* and *Castoria*. In order to visualize how the lineages are distributed in the morphospace defined by their MA, we plotted the pruned Sigmodontinae phylogeny of Maestri et al. (2017, 2019) onto the first two principal components of the PCA of the averaged mechanical advantages values by Akodontini genera. The PCA and phylomorphospace analyses were performed using the packages "FactoMineR", "factoextra" and"phytools" (Lê et al. 2008, Revell 2012, Kassambara and Mundt 2017).

Additionally, we performed phylogenetically informative regressions (phylogenetic generalized least squares - PGLS) (Martins and Hansen 1997) to test for potential correlations between BF and MA. Considering the differences in body size found among akodontines (D'Elía and Pardiñas 2015), the BF was regressed against body mass values before being compared with MA (a self-corrected measure) to exclude the influence of size on bite force that could possibly hide diet related differences (Freeman and Lemen 2008). Body mass information was taken from Maestri et al. (2016b) and Pardiñas et al. (2017), and phylogenetic information from Maestri etal. (2017, 2019). Additionally, we performed PGLS analysis of stable isotope data on MA and BF values. Species sampling on PGLS analyses changed according to data availability, that is, species not sampled in the available tree (Maestri et al. 2017) and with no available body mass information were excluded from these analyses, as were species with no isotope information in the corresponding analyses. The PGLS analyses were performed using the R package "caper" (Orme et al. 2018). This and all previously described analyses were performed on the R environment (R Core Team 2017).

3.3. Results

The analysis of variance for MA values suggest significant differences between the dietary categories (Table 3.1, Fig. 3.2). According to the post-hoc paired comparisons, insectivores have a significant lower MA (lower in-lever/out-lever ratios) at both bite points, compared with

herbivores and omnivores, in almost all scenarios (Table 3.1, Fig. 3.2). Herbivores and omnivores differ significantly when considering the MAs, with herbivores having significant larger MAs than omnivores (Table 3.1, Fig. 3.2).

The first two axes of the PCA plot account for 89.9% of the total variance (Figs. 3.3 and 3.4). An overall increase of the MA, influenced mainly by the superficial masseter, seems to be ruling the distribution of points along the first axis (Supplementary Material 3.S5), with insectivore and herbivore species on the two opposite extremes (Fig. 3.3). While *Kunsia tomentosus* and *Gyldenstolpia planaltensis* occupy the extreme positive values of the first component, *Oxymycterus* species, next to *Blarinomys*, *Lenoxus*, *Brucepattersonius*, *Podoxymys*, and *Akodon mimus,* are concentrated in the negative end. The remaining species are concentratedin the central region of the plot. The mechanical advantage of the deep masseter at incisors and temporal at both bite points exerts a greater influence on the second component (Supplementary Material 3.S5). When depicting the gradient of bite force on the MA plot, we can see that larger BFs tend to be located on the right upper quadrant, while lower BFs can be found on the lower left quadrant (Fig. 3.4).

When plotting the phylogeny by genus in the morphospace, we can see that the more ancient lineage have a greater dispersion, occupying both extremes of the first axis (*"Scapteromys"* lineage, Fig. 3.5). The *"Oxymycterus"* lineage seems to occupy a very restricted and specialized space, corresponding to lower mechanical advantages (Fig. 3.5), while the "*Akodon*" lineage is concentrated on the central region (Fig. 3.5). The "*Necromys*" lineage have a greater dispersion on the plot when compared with the latter two, with *Podoxymys* closer to the insectivore species (Fig. 3.5).

We found a significant correlation between body mass and bite force (R^2 = 0.29, F =21.9, p = 2.894e-05). Most Akodontini species are below the predictor line, having weaker bite forces for their size (Fig. 3.6). The PGLS regression of the first component of MA and BF residuals shows a significant correlation between the two variables (R^2=0.32, F = 23.47, p = 1.224e-05). Higher values of MA are associated with stronger BFs, while low MA values are associated with weaker BFs (Figs. 3.4 and 3.6). The $\delta^{13}C$ values are significantly correlated with both MA (R^2 = 0.18, F =9.69, p = 0.003216) and BF values (R^2 = 0.12, F =6.37, p = 0.01538), with higher MA

and BF values associated with C_4 consumers (Fig. 3.7). No correlation was found for $\delta^{15}N$ (Table3.2).

3.4. Discussion

According to Samuels (2009), insectivorous rodents can be recognized by their elongated rostrum, narrow zygomatic arches, small temporal fossae, and degenerated incisors. When analyzing the influence of diet and bite force on the skull shape of sigmodontine rodents, Maestri et al. (2016) found that insectivorous species, or "weaker biters", have the most distinctive shape among the dietary categories, being associated with more elongated mandible and skulls. All these morphological differences reflect morphofunctional aspects of this diet, especially the reduction of muscle insertion areas. The elongation of the rostrum and jaw represent a trade-off between bite force and jaw closing speed, favoring the capture of prey over force (Samuels 2009). The narrowing of both the zygomatic plate and temporal fossa reduces the area of insertion for the deep masseter and temporal muscles, respectively (Samuels 2009). All these morphological modifications are associated with the mechanical demands of consuming less resistant food items. Greater mechanical advantage, and hence bite forces, are necessary and emphasized in herbivorous and omnivorous species. Since the mechanical advantage equation is relatively simple, it is easy to see how each morphological component contributes to its magnitude and, therefore, to the observed differences between diet categories.

The distances from the bite points to the jaw joint (out-levers) are inversely proportional to their mechanical advantages. Therefore, the more elongate jaws of insectivorous akodontines contribute to their reduced mechanical advantages, while herbivores, with shorter jaws, have a generally greater mechanical advantage. The deep masseter is the largest and most powerful masseter component on muroid rodents, responsible mainly for adducting the jaw (Turnbull 1970, Hiiemäe 1971, Satoh and Iwaku 2004a, 2004b, Baverstock et al. 2013). In insectivorous species, the masseteric ridge, the insertion of the deep masseter on the jaw, is posteriorly displaced. Its distance to the jaw joint (the deep masseter in-lever) is therefore shorter. The mechanical advantage of the deep masseter in insectivore akodontines is smaller because the shorter in-lever is combined with longer out-levers. The decrease in the muscle's size, as shown by its reduced origin areas on the zygomatic plate, is added to these features, collectively explaining the smaller bite forces of insectivore rodents (Maestri et al. 2016).

The superficial masseter forms the most superficial layer of the masseter (Cox and Jeffrey 2015). It originates at the masseteric tubercle, located ventral to the zygomatic plate, and attaches

at the angular process of the jaw (Turnbull 1970, Herring and Herring 1974, Cox et al. 2011, Baverstock et al. 2013). This layer of the masseter has a nearly horizontal line-of-action, almost perpendicular to the skull, and mainly protracts the jaw. It also affects the jaw closing power stroke, both in gnawing and chewing (Cox and Jeffrey 2015). Several studies have observed a strong correlation between the distance of the superficial masseter from the jaw joint and higher consumption of vegetal matter (Verde Arregoitia et al. 2017), with insectivore speciessacrificing bite force in order to increase speed, favoring prey capture (Samuels 2009). The relationship between the distance of coronoid and condylar processes and the bite point to the jaw joint is also smaller in insectivorous species, reflecting lower temporal mechanical advantages in relation to omnivores and herbivores. The temporal muscle may be useful in stabilizing the jaw joint during mastication, mainly controlling the forward forces generated by the masseter (Satoh 1997). It has also been argued that it may work as a jaw retractor (Hiiemäe 1970, Gorniak 1977) or in restricting lateral movements during mastication (Byrd 1981).

In any case, it seems that crushing arthropod exoskeletons offers less resistance to cheek teeth chewing than does vegetal matter. This is evident in the differences between dietary categories in the MA of masticatory muscles. Additionally, the longer jaw of insectivorous species is characteristic of species that feed on live prey, favoring speed at the expense of bite force (Fabre et al. 2017). Mechanical advantage generally increases from insectivores to herbivores, but the difference in the contribution of each muscle indicates that insectivore species may exploit resources in different ways, judging from their greater dispersion along the second axis. Species of *Oxymycterus* have greater mechanical advantages of the deep masseter compared to other species that also consume animal resources (e.g. *Akodon mimus, Blarinomys breviceps, Brucepattersonius soricinus*). This probably reflects their consumption of larger prey which, in turn, may require greater bite forces. However, muscle dissections are essential to refine these conclusions, offering more specific information (e.g. direction and size of the fibers) which directly affect morphofunctional interpretations.

The dispersion of lineages in the morphospace reflects their functional diversity and, at least in part, their time of diversification, showing independent evolutionary transitions into insectivory. The "*Scapteromys*" lineage appears to be the most diversified in terms of its dietary morphology, since it occupies a larger area of the plot, including both extremes of the first axis. Its morphological diversity may be related to its age, since it diversified earlier than the others

clades (approximately 5.8 mya, Maestri et al. 2019), giving rise to specialized forms such as the herbivores *Kunsia* and *Bibimys,* as well as the insectivores *Blarinomys* and *Brucepattersonius*. *Scapteromys*, although still morphologically similar, seem to be moving away from *Kunsia* toward smaller mechanical advantages, reflecting its more insectivorous diet (Hershkovitz 1966, Barlow 1969, Pardiñas et al. 2008).

On the other hand, the *Akodon* group, one of the youngest and least diversified in termsof dietary morphology, is concentrated in the central region of the plot, not reaching extreme positions as some other more specialized species. *Akodon* is often described as a generalist genus (Emmons and Feer 1997, Talamoni 2008). However, data from stomach contents show that some species (e.g. *A. torques* and *A. orophilus*) feed mainly on invertebrates and, according to our analyses, have corresponding smaller mechanical advantages than species considered omnivorous or herbivorous. The dispersion of *Akodon* species in the PCA plot shows variation in their mechanical advantages, which may be related to dietary diversification inside the genus. Yet, the apparent diversity of resources consumed by *Akodon* species is surpassed by more extreme levels of morphological specialization shown by other genera in the tribe.

The *Necromys* group seems to span both functional extremes, with *Podoxymys* closer to the insectivorous lineages and *Necromys* and *Thaptomys* displaced towards herbivory. *Necromys* species apparently consume seeds frequently (Linares 1998, Cuélar and Noss 2003, Talamoni et al. 2008), but do not reach the herbivorous specializations found in *Kunsia*. *Kunsia*, the largest living species of Sigmodontinae (Hershkovitz 1966, Bezerra and Pardiñas 2016), has all the characteristic features of species with a strong bite: relatively robust rostrum and jaw with a broad zygomatic plate (Samuels 2009, Maestri et al. 2016), that are probably due to their consumption of C4 plants. Although showing some of these characteristics, *Necromys* species seem to be more opportunistic in resource consumption (Talamoni et al. 2008).

Species of the *Oxymycterus* lineage, on the other hand, represent a more specialized insectivore lineage, which has been recognized in several studies and confirmed by stomach content and morphological analysis of their digestive tract (Vorontzov 1979, Hinojosa et al. 1987, Hershkovitz 1998). However, ours is the first work to analyse their morphology in functional terms, confirming the suitability of the functionality of the jaw for insectivory. The same relationship holds true for *Blarinomys* and *Brucepattersonius*, of the *Scapteromys* clade, both also known to be strongly insectivorous (dos Reis et al. 1996, Pinotti et al. 2010, Galetti et al. 2016).

The majority of akodontini species presented weaker bite forces than expected for its size, and the positive correlation between MA and BF allows us to conclude that mechanical advantage is an informative functional characteristic when studying the feeding ecology of rodents. However, these variables are not perfectly correlated and most species of the tribe are concentrated well below the regression line, suggesting that they have lower bite forces than expected for their mechanical advantage, even after size corrections. Mechanical advantages are two-dimensional models of complex, three-dimensional muscle systems (Ginot et al. 2019), and greater deviations from the regression line imply that bite performance is influenced by factors not considered in this study, like jaw shape, length and cross-sectional areas of muscles, molar tooth features (e.g. crown height, molar area in occlusal view), and even ecological factors, like competition (Freeman and Lemen 2008, Becerra et al. 2014, Ginot et al. 2018a, Ginot et al. 2019). Still, measures of mechanical advantage, unlike direct muscle proxies, are easier to acquire for a large number of individuals, making them useful as morphological indicators of diet.

The significant correlation between MA and BF and $\delta^{13}C$ values indicates that there seems to be a differentiation in functional attributes according to the type of vegetal resources onsumed. Consumption of C_4 plants is associated with higher values of MA and BF, probably due to the fibrous and lignified tissues that require larger bite forces to be processed (Heckathornet al. 1999). C_4 plants are generally difficult to digest and have lower nutritional quality, being more commonly consumed by larger animals (e.g. *Kunsia tomentosus*), which require a greater amount of available resources and usually have greater bite forces (Clauss et al. 2013).

The lack of significant correlation between functional measures and $\delta^{15}N$ values may be reflecting the fact that, while having higher BF and MA is determinant for consuming C_4 plants, these factors, although correlated with different diet categories, are not restrictive for consumption of invertebrates. That is, individuals with higher BF to MA can consume, in addition to C_4 plants, seeds and invertebrates, while individuals with intermediate or lower BF and MA are restricted to the consumption of C_3 plants and invertebrates. The lack of correlation between $\delta^{15}N$ values and the functional traits can reflect the opportunistic consumption of invertebrates by species with wider trophic niches, which may be due to seasonal and geographic variation in the supply of this kind of resource (Meserve et al. 1988, Vieira 2003, Talamoni et al. 2008). However, conclusions should be drawn with caution, since stable isotopes are highly subject to interspecific variations and the sample size of stable isotopes per species used as reference may not be representative of

the species' entire distribution (Missagia et al. in press).

Generalist rodents can be labile in their feeding habits, consuming seeds, leaves, invertebrates, and fungi in different proportions (Landry 1970, Samuels 2009). The choice of resource often varies with season and locality (Glanz 1982, Borchet and Hansen 1983, Meserve et al. 1988), and many authors have suggested that resource choice may depend more on availability in the environment than on evolutionary constraints (Meserve et al. 1988). Various proposals for a standard classification of mammal diets have been suggested (Gagnon and Chew 2000, Mendoza et al. 2005), but, although necessary to draw general conclusions, categorizing species according to diet is not always a simple task: for most species, information is inadequate to describe the variation in resource consumption (Pineda-Munoz and Alroy 2014). Even within the categories, the variation is large: herbivory species can consume seeds, leaves and fruits of C_3 or C_4 plants, with direct implications for BF and MA requirements. Similarly, the consumption of invertebrates varies between insectivorous species. For example, the consumption of chitinous shelled invertebrates and non-chitinous worms and larvae (Verde Arregoitia 2016), and even small vertebrates (Perera 2002), obviously requires different BF and MA. It is possible that these categories are very simplistic, and should be disaggregated, when possible, according to the mechanical challenges proportioned by the most consumed resources (Santana et al. 2010, Verde Arregoitia 2016).

Rodents are cryptic and opportunistic, making it difficult to collect ecological information. As a result, dietary data for rodents are sometimes limited to stomach and feces content (Barlow 1969, Meserve et al. 1990, Talamoni et al. 2008). More recently, stable isotopes and metabarcoding of feces have been used in trophic niche studies (Galetti et al. 2016, Hawlitschek et al. 2018, Robeson et al. 2018, Missagia et al. in press), thus allowing the access of this information in a broader scale. Additionally, muscle dissections and CTscanning offers more detailed information on how muscles affect feeding efficiency (Cox et al. 2011, 2012). Considering this, studying feeding ecology, including its morphofunctional basis, is a work in progress.

Acknowledgments

We thank the curators from other mammal collections (AMNH, Robert Voss; USNM, Darrin Lunde; MCNM, Claudia Costa; MN, João Oliveira) who allowed access of specimens

under their care. Dallas Krentzel and Fernando Sicuro provided useful insights on mechanical advantage that greatly improved this manuscript. This work was made possible with financial support of Coordenação de Aperfeiçoamento de Pessoal de Nível Superior (CAPES - Finance Code 0001) which granted R.V.M. with regular and sandwich fellowships (88881.133833/2016-1).

3.5. References

Anderson, R.A., McBrayer, L.D. and Herrel, A., 2008. Bite force in vertebrates: opportunities and caveats for use of a nonpareil whole-animal performance measure. Biological Journal of the Linnean Society, 93, pp. 709-720.

Baverstock, H., Jeffery, N.S. and Cobb, S.N., 2013. The morphology of the mouse masticatory musculature. Journal of Anatomy, 223(1), pp. 46-60.

Becerra, F., Echeverría, A.I., Casinos, A. and Vassallo, A.I., 2014. Another one bites the dust: bite force and ecology in three caviomorph rodents (Rodentia, Hystricognathi). Journal

of Experimental Zoology Part A: Ecological Genetics and Physiology, 321(4), pp. 220-232.

Borchert, M. and Hansen, R., 1983. Effects of flooding and wildfire on valley side wet campo rodents in Central Brazil. Revista Brasileira de Biologia, 43, pp. 229-240.

Byrd, K.E., 1981. Mandibular movement and muscle activity during mastication in the guinea pig (Cavia porcellus). Journal of Morphology, 170(2), pp. 47-169.

Christiansen, P. and Wroe, S., 2007. Bite forces and evolutionary adaptations to feeding ecology in carnivores. Ecology, 88(2), pp. 347-358.

Clauss, M., Steuer, P., Müller, D.W., Codron, D. and Hummel, J., 2013. Herbivory and body size: allometries of diet quality and gastrointestinal physiology, and implications for herbivore ecology and dinosaur gigantism. PLoS One, 8(10), p. e68714.

Crompton, A.W. 1995. Masticatory function in nonmammalian cynodonts and early mammals. Functional morphology in vertebrate paleontology, pp. 55-75. Cambridge: Cambridge University Press.

D'Elía, G. and Pardiñas, U.F.J., 2015. Tribe Akodontini Vorontsov 1959. Mammals of South America, Volume 2: Rodents, pp. 140-144. Chicago: University of Chicago Press.

Ellis, B.A., Mills, J.N., Glass, G.E., McKee Jr, K.T., Enria, D.A. and Childs, J.E., 1998.

Dietary habits of the common rodents in an agroecosystem in Argentina. Journal of Mammalogy, 79(4), pp. 1203-1220.

Fabre, P.H., Herrel, A., Fitriana, Y., Meslin, L. and Hautier, L., 2017. Masticatory muscle architecture in a water-rat from Australasia (Murinae, Hydromys) and its implication for the evolution of carnivory in rodents. Journal of Anatomy, 231(3), pp. 380-397.

Fabre, A.C., Perry, J.M., Hartstone-Rose, A., Lowie, A., Boens, A. and Dumont, M., 2018. Do muscles constrain skull shape evolution in strepsirrhines? The Anatomical Record, 301(2), pp.291-310.

Fox, J. and Weisberg, S., 2011. An {R} companion to applied regression. Thousand Oaks CA: Sage. URL: http://socserv.socsci.mcmaster.ca/jfox/Books/Companion

Freeman, P.W., and Lemen, C.A., 2008. A simple morphological predictor of bite force in rodents. Journal of Zoology, 275(4), pp. 418-422.

Gagnon, M. and Chew, A.E., 2000 Dietary preferences in extant African Bovidae. Journal of Mammalogy, 81, pp. 490–511.

Galetti, M., Rodarte, R.R., Neves, C.L., Moreira, M. and Costa-Pereira, R., 2016. Trophic niche differentiation in rodents and marsupials revealed by stable isotopes. PLoS One, 11(4), p. e0152494.

Gastwirth, J.L., Yulia, R.G., Wallace, H.W.L., Lyubchich, V., Miao, W. and Noguchi, K., 2019. lawstat: Tools for Biostatistics, Public Policy, and Law. R package version 3.3 https://CRAN.R-project.org/package=lawstat

Ginot, S., Herrel, A., Claude, J. and Hautier, L., 2018a. Skull size and biomechanics are good estimators of in vivo bite force in murid rodents. The Anatomical Record, 301(2), pp. 256-266.

Ginot, S., Claude, J. and Hautier, L., 2018b. One skull to rule them all? Descriptive and comparative anatomy of the masticatory apparatus in five mouse species. Journal of Morphology, 279(9), pp. 1234-1255.

Ginot, S., Herrel, A., Claude, J., and Hautier, L., 2019. Morphometric models for estimating bite force in Mus and Rattus: mandible shape and size do better than lever-arm ratios. Journal of Experimental Biology, 222(12), p. jeb-204867.

Gorniak, G.C., 1977. Feeding in golden hamsters, Mesocricetus auratus. Journal of Morphology, 154(3), pp. 427-458.

Greaves, W.S., 2000. Location of the vector of jaw muscle force in mammals. Journal of Morphology, 243(3), pp. 93-299.

Greaves, W.S., 2012. The mammalian jaw: a mechanical analysis. Cambridge: Cambridge University Press.

Grossnickle, D.M. and Polly, P.D., 2013. Mammal disparity decreases during the Cretaceous angiosperm radiation. Proceedings of the Royal Society B: Biological Sciences, 280(1771), p. 20132110.

Hampton, P.M., 2011. Comparison of cranial form and function in association with diet in natricine snakes. Journal of Morphology, 272(12), pp. 1435-1443.

Hawlitschek, O., Fernández-González, A., Balmori-de la Puente, A. and Castresana, J., 2018. A pipeline for metabarcoding and diet analysis from fecal samples developed for a small semi-aquatic mammal. PLoS one, 13(8), p. e0201763.

Heckathorn, S.A., McNaughton, S.J. and Coleman, J.S., 1999. C4 plants and herbivory. C4 plant biology, pp.285-312. London: Academic Press.

Herrel, A., Aerts, P., and De Vree, F., 1998. Ecomorphology of the lizard feeding apparatus: a modelling approach. Netherlands Journal of Zoology, 48, pp. 1-25.

Hernandez, G., Garcia, S., Vilela, J.F. and de la Sancha, N.U., 2017. Ontogenetic variation of an omnivorous generalist rodent: the case of the montane akodont (Akodon montensis). Journal of Mammalogy, 98(6), 1741-1752.

Herring, S.W. and Herring, S.E., 1974. The superficial masseter and gape in mammals. The American Naturalist, 108(962), 561-576.

Hershkovitz, P., 1955. South American marsh rats, genus Holochilus, with a summary of sigmodont rodents. Fieldiana: Zoology, 37, pp. 639-673, plates 617-629.

Hershkovitz, P., 1966. South American swamp and fossorial rats of the scapteromyine group (Cricetinae, Muridae) with comments on the glans penis in murid taxonomy. Zeitschrift für Säugetierkunde 31, pp. 81-149.

Hershkovitz, P., 1994. The description of a new species of South American hocicudo or long- nose mouse, genus Oxymycterus (Sigmodontinae, Muroidea), with critical review of the generic content. Fieldiana Zoology, 79, pp. 1-43.

Hershkovitz, P., 1998. Report of some sigmodontinae rodents collected in southeastern Brazil with description of a new genus and six new species. Bonner Zoologische Beitrage, 47, pp.

193-256.

Hiiemäe, K.M. and Ardran, G.M., 1968. A cinefluorographic study of mandibular movement during feeding in the rat (Rattus norvegicus). Journal of Zoology, 154, pp. 139-154.

Hiiemäe K.M., 1971. The structure and function of the jaw muscles in the rat (Rattus norvegicus L.) III. The mechanics of the muscles. Zoological Journal of the Linnean Society, 50, pp. 111-132.

Holm, S., 1979. A simple sequentially rejective multiple test procedure. Scandinavian Journal of Statistics, pp. 65-70.

Huber, D.R., Claes, J.M., Mallefet, J. and Herrel, A., 2008. Is extreme bite performance associated with extreme morphologies in sharks? Physiological and Biochemical Zoology, 82, pp. 20-28.

Kassambara, A. and Mundt, F., 2017. factoextra: extract and visualize the results of multivariate data analyses. R package version 1.0.5. https://CRAN.R-project.org/package=factoextra

Landry Jr, S.O., 1970. The Rodentia as omnivores. The Quarterly Review of Biology, 45(4), pp. 351-372.

Lê, S., Josse, J. and Husson, F., 2008. FactoMineR: an R package for multivariate analysis. Journal of Statistical Software, 25(1), pp. 1-18.

Maestri, R., Patterson, B.D., Fornel, R., Monteiro, L.R. and de Freitas, T.R.O., 2016. Diet, bite force and skull morphology in the generalist rodent morphotype. Journal of Evolutionary Biology, 29(11), pp. 2191-2204.

Maestri, R., Monteiro, L.R., Fornel, R., Upham, N.S., Patterson, B.D. and de Freitas, T.R.O., 2017. The ecology of a continental evolutionary radiation: Is the radiation of sigmodontine rodents adaptive? Evolution, 71(3), pp. 610-632.

Maestri, R., Upham, N.S. and Patterson, B.D., 2019. Tracing the diversification history of a Neogene rodent invasion into South America. Ecography, 42(4), pp. 683-695.

Martins, E.P. and Hansen, T.F., 1997. Phylogenies and the comparative method: a general approach to incorporating phylogenetic information into the analysis of interspecific data. The American Naturalist, 149(4), pp. 646-667.

Martinez, Q., Lebrun, R., Achmadi, A.S., Esselstyn, J.A., Evans, A.R., Heaney, L.R., Miguez, R.P., Rowe, K.C. and Fabre, P.H., 2018. Convergent evolution of an extreme dietary

specialisation, the olfactory system of worm-eating rodents. Scientific Reports, 8(1), p.17806.

Mendoza, M., Janis, C.M. and Palmqvist, P., 2005. Ecological patterns in the trophic-size structure of large mammal communities: a 'taxon-free' characterization. Evolutionary Ecology Research, 7(4), pp. 505–530.

Meserve, P.L., Lang, B.K. and Patterson, B.D., 1988. Trophic relationships of small mammals in a Chilean temperate rainforest. Journal of Mammalogy 69(4), pp. 721-730.

Missagia, R.V. and Perini, F.A., 2018. Skull morphology of the Brazilian shrew mouse Blarinomys breviceps (Akodontini; Sigmodontinae), with comparative notes on Akodontini rodents. Zoologischer Anzeiger, 277, pp. 148-161.

Muschick, M., Indermaur, A. and Salzburger, W., 2012. Convergent evolution within an adaptive radiation of cichlid fishes. Current Biology, 22(24), pp. 2362-2368.

Musser, G.G. and Durden, L.A., 2002. Sulawesi rodents: description of a new genus and species of Murinae (Muridae, Rodentia) and its parasitic new species of sucking louse (Insecta, Anoplura). American Museum Novitates, 3368, pp. 1-50.

Orme, D., Freckleton, R., Thomas, G., Petzoldt, T., Fritz, S., Isaac, N. and Pearse, W., 2018. caper: comparative analyses of phylogenetics and evolution in R. R package version

1.0.1. https://CRAN.R-project.org/package=caper

Patton, J.L., Pardiñas, U.F. and D'Elía, G. (eds), 2015. Mammals of South America, Volume 2: Rodents. Chicago: University of Chicago Press.

Pardiñas, U.F.J., Myers, P., León-Paniagua, L., Ordóñez-Garza, N., Cook, J., Kryštufek, B., Haslauer, R., Bradley, R., Shenbrot, G., Patton, J., 2017. Family Cricetidae. Handbook of the Mammals of the World, Volume 7: Rodents II, pp. 204-279. Barcelona: Lynx Edicions.

Perera, A., 2002. Los mamíferos de la Argentina y la región austral de Sudamérica. Buenos Aires: Editorial El Ateneo.

Pineda-Munoz, S. and Alroy, J., 2014. Dietary characterization of terrestrial mammals. Proceedings of the Royal Society B: Biological Sciences, 281(1789), p. 20141173.

Pizzimenti, J.J., and de Salle, R.O.B, 1980. Dietary and morphometric variation in some Peruvian rodent communities: the effect of feeding strategy on evolution. Biological Journal of the Linnean Society, 13(4), pp. 263-285.

Pohlert, T., 2014. The pairwise multiple comparison of mean ranks package (PMCMR). R package https://CRAN.R-project.org/package=PMCMR.

Popov, E.P., 1999. Engineering mechanics of solids. New Jersey: Prentice-Hall.

R Core Team., 2017. R: A language and environment for statistical computing. R Foundation for Statistical Computing, Vienna, Austria. URL https://www.R-project.org/.

Rasband, W., 1997. ImageJ. US National Institutes of Health, Bethesda, MD. https://imagej.nih.gov/ij/

Reig, O.A., 1972. The evolutionary history of the South American cricetid rodents. Ph.D. dissertation, University of London, London.

Reig, O.A., 1987. An assessment of the systematics and evolution of the Akodontini, with the description of new fossil species of Akodon (Cricetidae, Sigmodontinae). Fieldiana Zoology, 39, pp. 347-399.

Revell, L.J., 2012. phytools: An R package for phylogenetic comparative biology (and other things). Methods in Ecology and Evolution, 3, pp. 217-223.

Robeson, M.S., Khanipov, K., Golovko, G., Wisely, S.M., White, M.D., Bodenchuck, M., Smyser, T.J., Fofanov, Y., Fierer, N. and Piaggio, A.J., 2018. Assessing the utility of metabarcoding for diet analyses of the omnivorous wild pig (Sus scrofa). Ecology and Evolution, 8(1), pp. 185-196.

Ross, C.F., Iriarte-Diaz, J. and Nunn, C.L., 2012. Innovative approaches to the relationship between diet and mandibular morphology in primates. International Journal of Primatology, 33(3), pp. 632-660.

Rowe, K.C., Achmadi, A.S. and Esselstyn, J.A., 2016. Repeated evolution of carnivory among Indo-Australian rodents. Evolution, 70(3), pp. 653-665.

Sakamoto, M., 2010. Jaw biomechanics and the evolution of biting performance in theropod dinosaurs. Proceedings of the Royal Society B: Biological Sciences, 277, pp. 3327-3333.

Samuels, J.X., 2009. Cranial morphology and dietary habits of rodents. Zoological Journal of the Linnean Society, 156(4), pp. 864-888.

Santana, S.E., Dumont, E.R. and Davis, J.L., 2010. Mechanics of bite force production and its relationship to diet in bats. Functional Ecology, 24(4), pp. 776-784.

Satoh, K., 1997. Comparative functional morphology of mandibular forward movement during mastication of two murid rodents, Apodemus speciosus (Murinae) and Clethrionomys rufocanus (Arvicolinae). Journal of Morphology, 231, pp. 131-142.

Satoh, K., 1998. Balancing function of the masticatory muscles during incisal biting in two

murid rodents, Apodemus speciosus and Clethrionomys rufocanus. Journal of Morphology, 236, pp. 49-56.

Satoh, K., 1999. Mechanical advantage of area of origin for the external pterygoid muscle in two murid rodents, Apodemus speciosus and Clethrionomys rufocanus. Journal of Morphology, 240(1), pp. 1-14.

Satoh K. and Iwaku F., 2004a. Functional anatomy of masticatory muscles in rodents. Journal of Gifu Dental Society, 30, pp. 21-28.

Satoh, K. and Iwaku, F., 2004b. Internal architecture, origin-insertion site, and mass of jaw muscles in Old World hamsters. Journal of Morphology, 260(1), pp. 101-116.

Satoh, K. and Iwaku, F., 2006. Jaw muscle functional anatomy in northern grasshopper mouse, Onychomys leucogaster, a carnivorous murid. Journal of Morphology, 267, pp. 987-999.

Swanson, M.T., Oliveros, C.H. and Esselstyn, J.A., 2019. A phylogenomic rodent tree reveals the repeated evolution of masseter architectures. Proceedings of the Royal Society B: Biological Sciences, 286(1902), p. 20190672.

Talamoni, S.A., Couto, D., Júnior, D.A.C. and Diniz, F.M., 2008. Diet of some species of Neotropical small mammals. Mammalian Biology, 73(5), pp. 337-341.

Turnbull, W.D., 1970. Mammalian masticatory apparatus. Fieldiana Geology, 18, pp. 147–356. Uicker, J.J., Pennock, G.R. and Shigley, J.E., 2011. Theory of machines and mechanisms. Vol. 1. New York: Oxford University Press.

Verde Arregoitia, L.D., 2016. Rethinking omnivory in rodents. doi:10.20944/preprints201609.0017.v1

Verde Arregoitia, L.D., Fisher, D.O. and Schweizer, M., 2017. Morphology captures diet and locomotor types in rodents. Royal Society Open Science, 4(1), p. 160957.

Vieira, M.V., 2003. Seasonal niche dynamics in coexisting rodents of the Brazilian Cerrado. Studies on Neotropical Fauna and Environment, 38(1), pp. 7-15.

Vorontsov, N.N., 1979. Evolution of the alimentary system in myomorph rodents. Washington: Smithsonian Institution and the National Science Foundation.

Voss, R.S., 1988. Systematics and ecology of ichthyomyine rodents (Muroidea): patterns of morphological evolution in a small adaptive radiation. Bulletin of the American Museum of Natural History, 188, pp. 259-493.

Weijs, W.A. and Dantuma, R., 1975. Electromyography and mechanics of mastication in

the albino rat. Journal of Morphology, 146(1), pp. 1-33.

Westneat, M.W., 1994. Transmission of force and velocity in the feeding mechanisms of labrid fishes (Teleostei, Perciformes). Zoomorphology, 114, pp. 103-118.

Wilson, D.E. and Reeder, D.M., 2005. Mammal species of the world: a taxonomic and geographic reference (Vol. 1). Baltimore: Johns Hopkins University Press.

Wood, A.E., 1965. Grades and clades among rodents. Evolution, 19, pp. 115-130.

Zar, J.H., 2010. Biostatistical Analysis, 5th ed. New Jersey: Pearson Prentice Hall, Upper Saddle River.

Zelditch, M.L., Lundrigan, B.L. and Garland Jr, T., 2004. Developmental regulation of skull morphology. I. Ontogenetic dynamics of variance. Evolution & Development, 6(3), pp. 194-206.

3.6. Figures

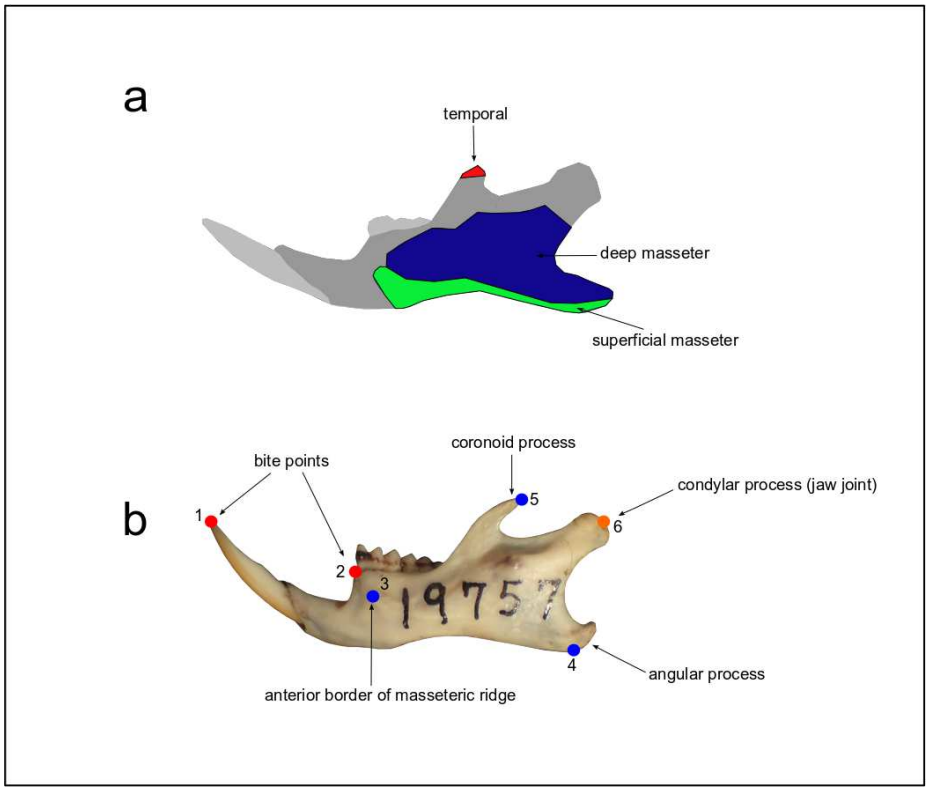

Figure 3.1. Jaw of muroid rodents representing (a) muscle insertion areas of *Mus musculus* modified from on Baverstock et al. 2013 used as basis for this study; (b) points used for mechanical advantages calculations represented on an Akodontini rodent (*Akodon aerosus* FMNH 19757). Red circles represent both bite points (1: incisor bite point. 2: molars bite point); blue circles represent insertion points of analyzed muscle masses (3: deep masseter; 4: superficial masseter; 5: temporal); orange circle represent the jaw joint. Out-levers were calculated as 1-6: incisor out-lever and 2-6: molars out-lever; In-levers were calculated as 3-6: deep masseter in-lever; 4-6: superficial masseter in-lever and; 5-6: temporal in-lever.

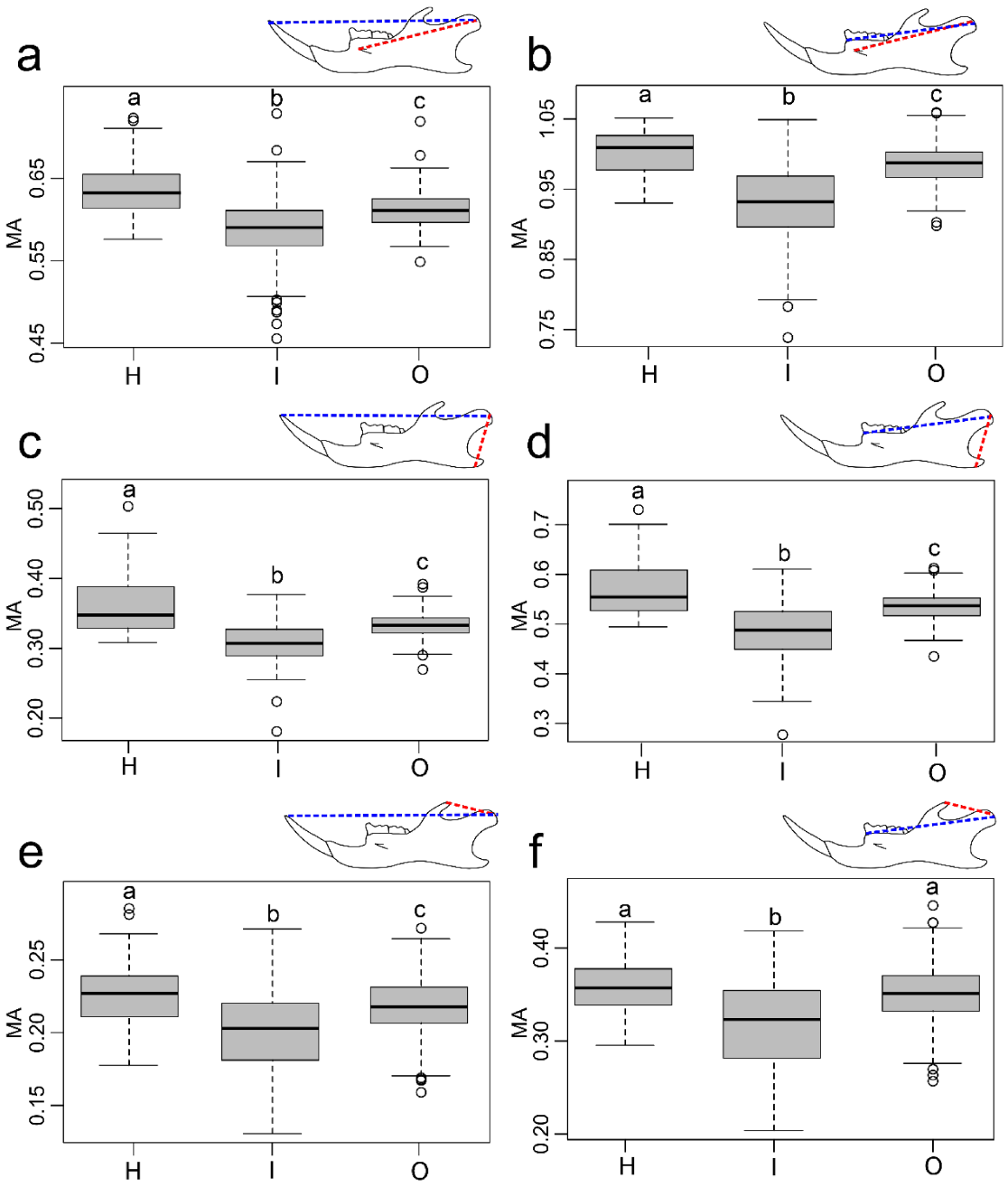

Figure 3.2. Mechanical advantage of each muscle mass (deep masseter, a, b; superficial masseter, c, d; temporal, e, f) at the incisors and molars. Diet categories are indicated by the letters at the x axis (H: herbivores; I: insectivores, O: omnivores). Muscle in-lever shown as red dotted lines, and jaw out-levers shown as blue dotted lines. Boxes represent 50% of each sample, and the whiskers present each one 25%. The median is represented by the bold line. Outliers are shown as open circles. Letters above plots indicate statistical significance (at $P < 0.05$) in Dunn's pairwise comparisons between groups, with different letters representing significant differences.

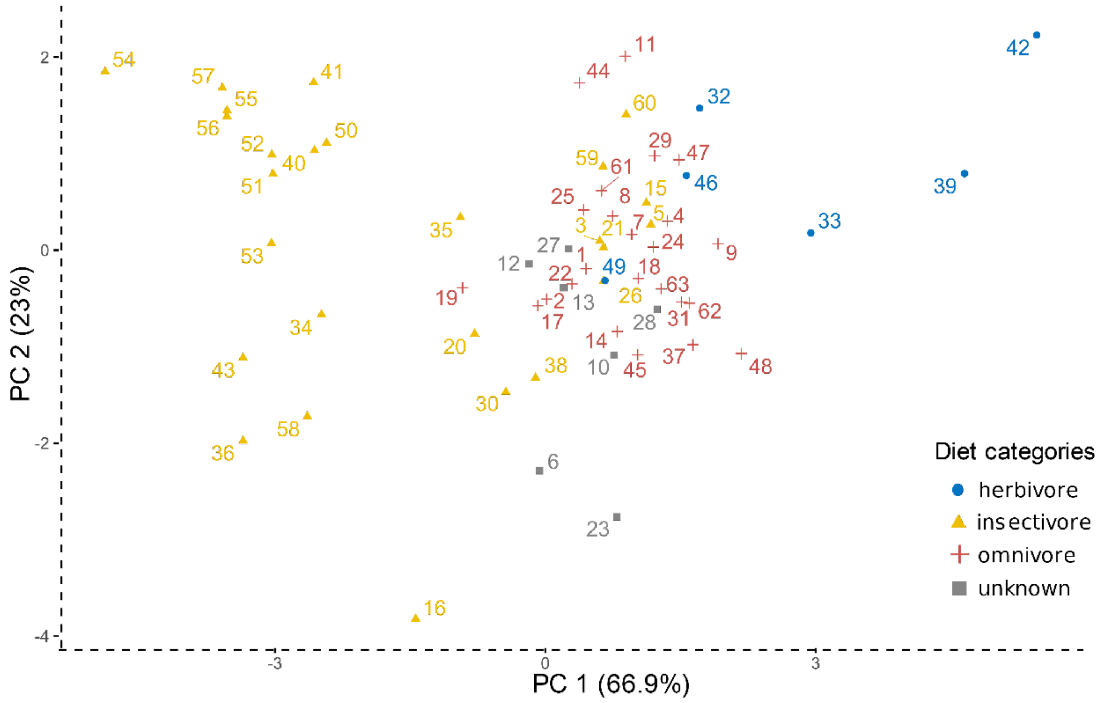

Figure 3.3. Principal component analysis of mechanical advantage values for each muscle at the two bite points, with species categorizes by diet group. 1: *A. aerosus*, 2: *A. affinis*, 3: *A. albiventer*, 4: *A. azarae*, 5: *A. boliviensis*, 6: *A. budini*, 7: *A. cursor*, 8: *A. dayi*, 9: *A. dolores*, 10: *A. fumeus*, 11: *A. iniscatus*, 12: *A. juninensis*, 13: *A. kofordi*, 14: *A. juninensis*, 15: *A. lutescens*, 16: *A. mimus*, 17: *A. mollis*, 18: *A. montensis*, 19: *A. mystax*, 20: *A. orophilus*, 21: *A. paranaensis*, 22: *A. reigi*, 23: *A. siberiae*, 24: *A. simulator*, 25: *A. spegazzinii*, 26: *A. subfuscus*, 27: *A. surdus*, 28: *A. sylvanus*, 29: *A. toba*, 30: *A. torques*, 31: *A. varius*, 32: *B. chacoensis*, 33: *B.labiosus*, 34: *B. breviceps*, 35: *B. griserufescens*, 36: *B. soricinus*, 37: *C. angustidens*, 38: *D. kempi*, 39: *G. planaltensis*, 40: *J. candango*, 41: *J. huanchacae*, 42: *K. tomentosus*, 43: *L. apicalis*, 44: *N. amoenus*, 45: *N. lactens*, 46: *N. lasiurus*, 47: *N. lenguarum*, 48: *N. obscurus*, 49: *N. urichi*, 50: *O. amazonicus*, 51: *O. dasytrichus*, 52: *O. delator*, 53: *O. hiska*, 54: *O. nasutus*, 55: *O. paramensis*, 56: *O. quaestor*, 57: *O. rufus*, 58: *P. roraimae*, 59: *S. aquaticus*, 60: *S. tumidus*, 61: *T. cerradensis*, 62: *T. lasiotis*, 63: *T. nigrita*.

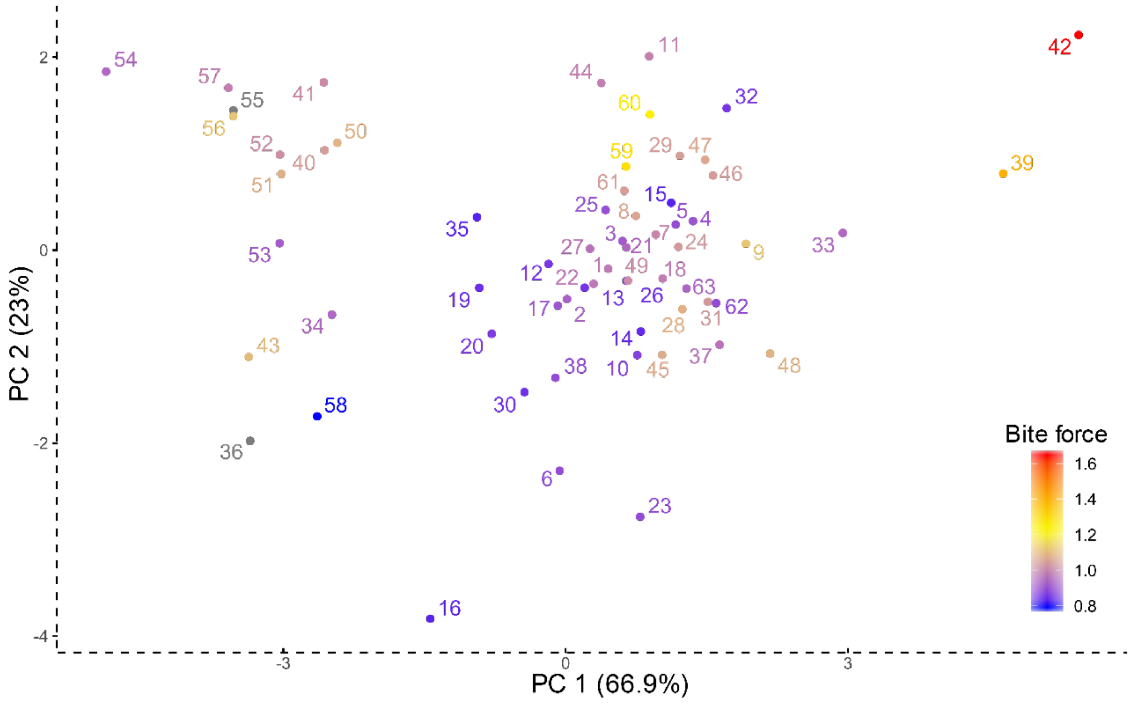

Figure 3.4. Principal component analysis of mechanical advantage values for each muscle at the two bite points, with the gradient of bite force depicted from weakest (blue) to strongest (red). 1: *A. aerosus*, 2: *A. affinis*, 3: *A. albiventer*, 4: *A. azarae*, 5: *A. boliviensis*, 6: *A. budini*, 7: *A. cursor*, 8: *A. dayi*, 9: *A. dolores*, 10: *A. fumeus*, 11: *A. iniscatus*, 12: *A. juninensis*, 13: *A. kofordi*, 14: *A. juninensis*, 15: *A. lutescens*, 16: *A. mimus*, 17: *A. mollis*, 18: *A. montensis*, 19: *A. mystax*, 20: *A. orophilus*, 21: *A. paranaensis*, 22: *A. reigi*, 23: *A. siberiae*, 24: *A. simulator*, 25: *A. spegazzinii*, 26: *A. subfuscus*, 27: *A. surdus*, 28: *A. sylvanus*, 29: *A. toba*, 30: *A. torques*, 31: *A. varius*, 32: *B. chacoensis*, 33: *B. labiosus*, 34: *B. breviceps*, 35: *B. griserufescens*, 36: *B. soricinus*, 37: *C. angustidens*, 38: *D. kempi*, 39: *G. planaltensis*, 40: *J. candango*, 41: *J. huanchacae*, 42: *K. tomentosus*, 43: *L. apicalis*, 44: *N. amoenus*, 45: *N. lactens*, 46: *N. lasiurus*, 47: *N. lenguarum*, 48: *N. obscurus*, 49: *N. urichi*, 50: *O. amazonicus*, 51: *O. dasytrichus*, 52: *O. delator*, 53: *O. hiska*, 54: *O. nasutus*, 55: *O. paramensis*, 56: *O. quaestor*, 57: *O. rufus*, 58: *P. roraimae*, 59: *S. aquaticus*, 60: *S. tumidus*, 61: *T. cerradensis*, 62: *T. lasiotis*, 63: *T. nigrita*.

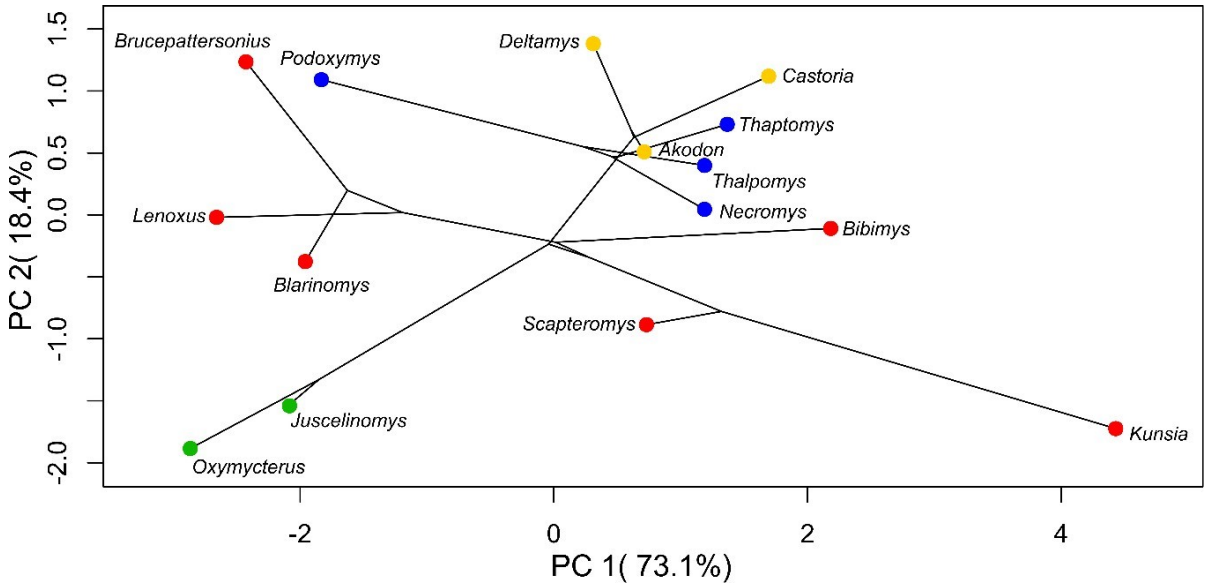

Figure 3.5. Phylomorphospace plot depicting Akodontini genera on mechanical advantage morphospace. Colors represent different lineages: red: "*Scapteromys*", green: "*Oxymycterus*", blue: "*Necromys*", and yellow: "*Akodon*".

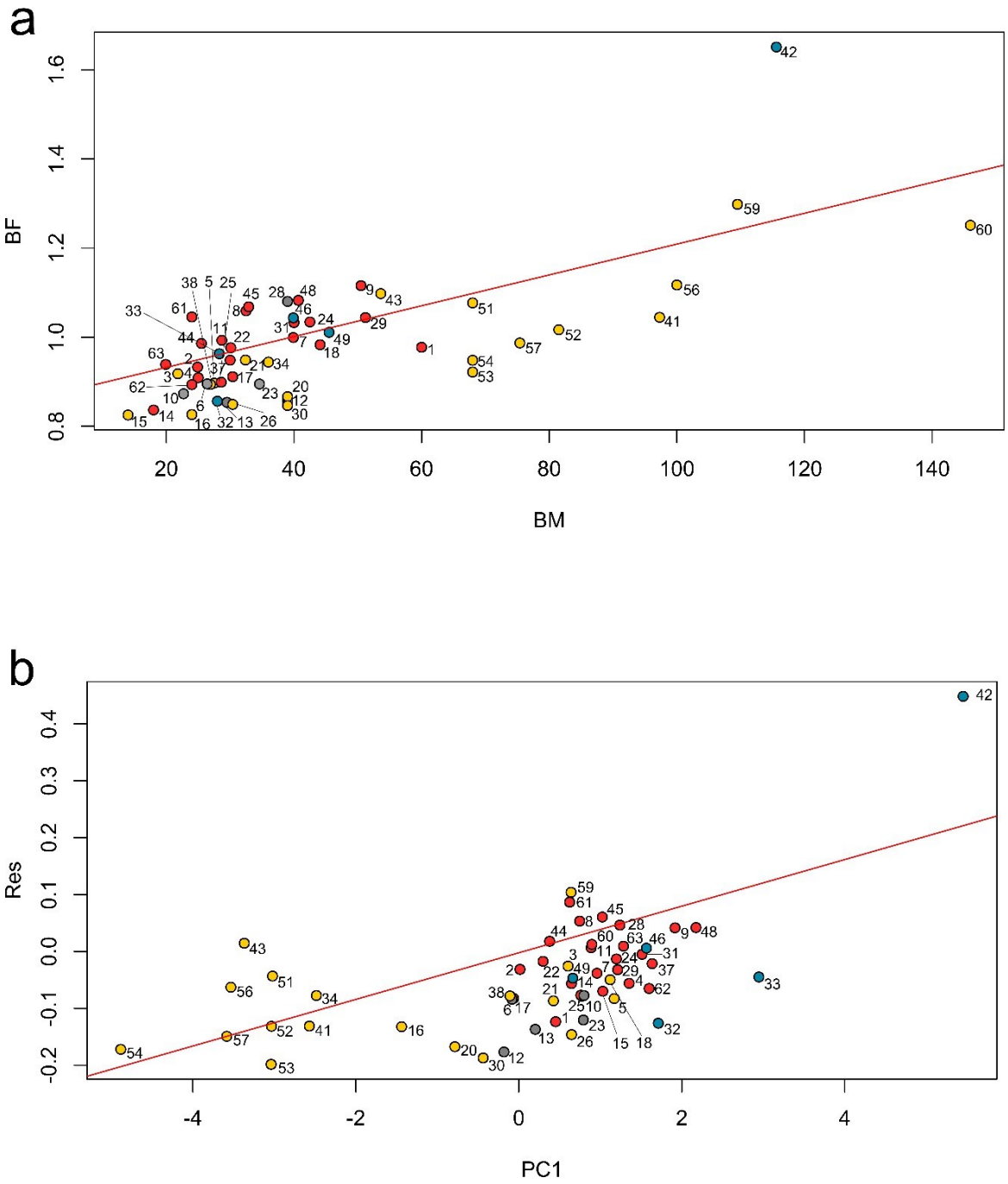

Figure 3.6. Phylogenetic regression (PGLS) of the (a) logarithm of bite force on body mass and (b) the residuals of the regression between logarithm of bite force on body mass and first component of mechanical advantage of Akodontini rodents, colored by diet group (yellow: insectivores; red: omnivores; blue: herbivores; gray: unknown). Red line represents the PGLS predicted line.

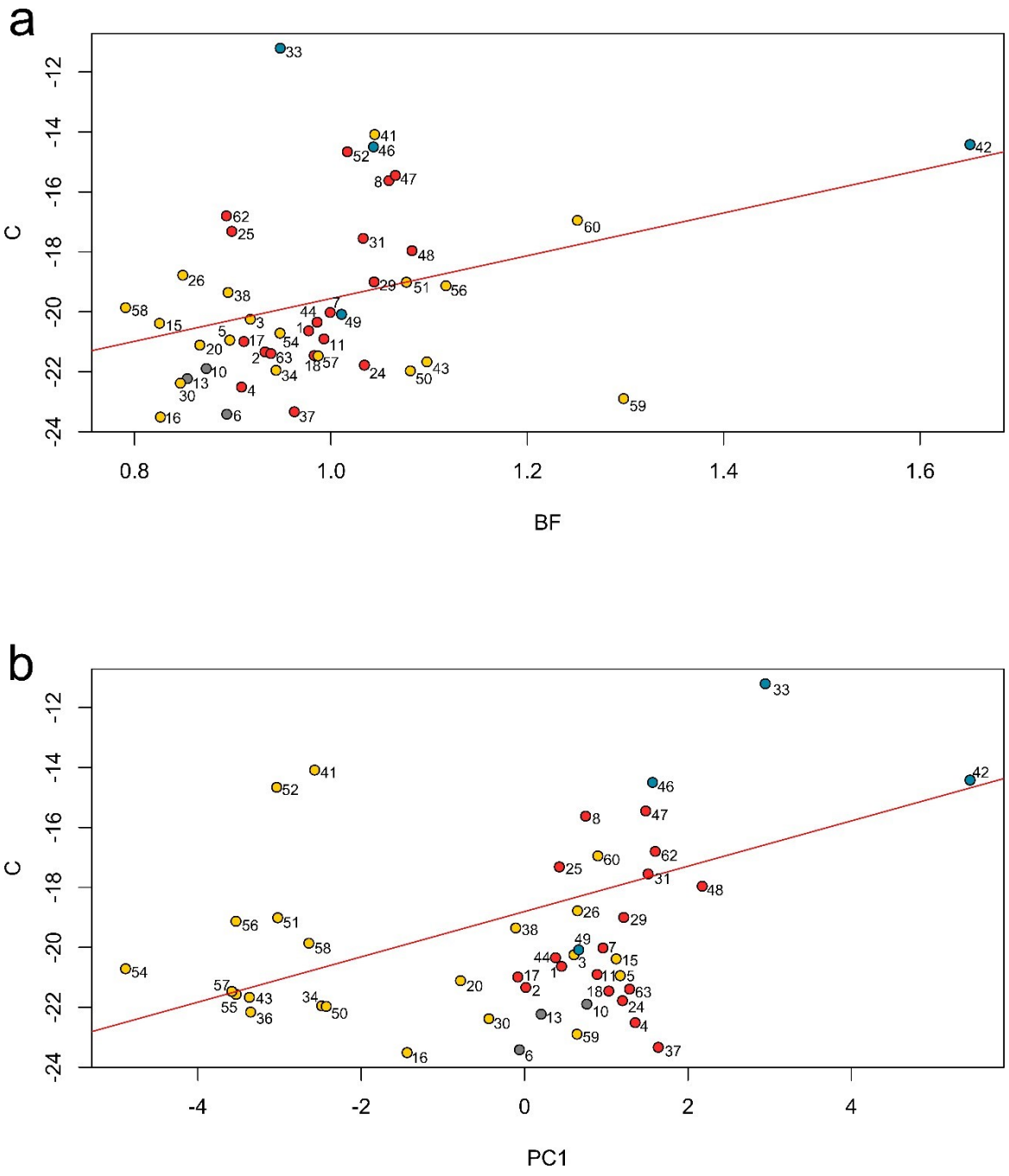

Figure 3.7. Phylogenetic regression (PGLS) of the $\delta^{13}C$ on (a) logarithm of bite force, and (b) first component of mechanical advantage of Akodontini rodents, colored by diet group (yellow: insectivores; red: omnivores; blue: herbivores; gray: unknown). Red line represents the PGLS predicted line.

3.7. Tables

Table 3.1. Kruskal Wallis and Dunn's post hoc pairwise comparisons results for differences on mechanical advantage (MA) of each muscle (DM: deep masseter; SM: superficial masseter; ™: temporal masseter) at the two bite points (inc: incisive; mol: molars) between the dietary categories. P-values in bold indicate statistical significance (P < 0.05*, P<0.01**, P<0.001***).

MA	Kruskal Wallis			Dunn's post hoc significance test		
	X^2	P	df	herbivore x insectivore	omnivore x insectivore	herbivore x omnivore
DM(inc)	193.55	**< 2e-16*** **	2	**< 2e-16*** **	**< 2e-16*** **	**1e-06*** **
DM(mol)	294.75	**< 2e-16*** **	2	**<2e-16*** **	**<2e-16*** **	**0.003****
SM(inc)	233.41	**< 2e-16*** **	2	**< 2e-16*** **	**< 2e-16*** **	**0.00015*** **
SM(mol)	258.3	**< 2e-16*** **	2	**<2e-16*** **	**<2e-16*** **	**0.0019****
TM(inc)	113.85	**< 2e-16*** **	2	**1.5e-14*** **	**< 2e-16*** **	**0.016***
TM(mol)	116.61	**< 2e-16*** **	2	**8.9e-12*** **	**<2e-16*** **	0.27

Table 3.2. Summary of the PGLS linear models for bite force and first component of MA values as function of log of body mass (log BM), residuals of bite force regressed against body mass (Res), and stable isotope values. P values in bold indicate statistical significance (P < 0.05*, P<0.01**, P<0.001***).

Statistic	Bite Force			PC1(MA)		
	log BM	$\delta^{13}C$	$\delta^{15}N$	Res	$\delta^{13}C$	$\delta^{15}N$
R^2	0.2926	0.129	0.0005464	0.3152	0.1772	0.02401
F	21.09	6.37	0.02351	23.47	9.69	1.107
P	**2.89e-05*** **	**0.01538***	0.878857	**1.22e-05*** **	**0.003216****	0.2984

3.8. Supplementary Material

Supplementary Material 3.S1: Specimens used for functional measurements.

Mechanical advantage
Akodon aerosus: FMNH 170360, FMNH 170362 FMNH 170366, FMNH 170371, FMNH 170379, FMNH 170383, FMNH 170384, FMNH 170396, FMNH 170397, FMNH 170399, FMNH 19265, FMNH 19266, FMNH 19268, FMNH 19757, FMNH 24502, FMNH 24506, FMNH 24512, FMNH 24540, FMNH 75480, FMNH 78375
Akodon affinis: AMNH 181479, AMNH 32991, AMNH 32992, AMNH 32994, AMNH 33005, AMNH 33007, AMNH 33018, AMNH 71208, AMNH 71212, AMNH 71213, AMNH 71215, AMNH 71217, AMNH 71218, AMNH 71222, AMNH 71223, AMNH 71226, AMNH 71227, AMNH 71230
Akodon albiventer: FMNH 107470, FMNH 107475, FMNH 107478, FMNH 107488, FMNH 107619, FMNH 107634, FMNH 107643, FMNH 107644, FMNH 107646, FMNH 129981, FMNH 129992, FMNH 129993, FMNH 129995, FMNH 129996, FMNH 162647, FMNH 162681, FMNH 162683, FMNH 162685, FMNH 162707, FMNH 52575
Akodon azarae: FMNH 22233, FMNH 23333, FMNH 23335, FMNH 23337, FMNH 3338, FMNH 23344, FMNH 27614, FMNH 27617, FMNH 27624, FMNH 27632, FMNH 27636, FMNH 27662, FMNH 29189, FMNH 29200, FMNH 29205, FMNH 29207, FMNH 9214, FMNH 29222, FMNH 98282, FMNH 98283
Akodon boliviensis: FMNH 107641, FMNH 107830, FMNH 107834, FMNH 107923, FMNH 107928, FMNH 107940, FMNH 162749, FMNH 162751, FMNH 162753, FMNH 167969, FMNH 43376, FMNH 43377, FMNH 49699, FMNH 49702, FMNH 51293, FMNH 52544, FMNH 52545, FMNH 52549, FMNH 52551, FMNH 64339
Akodon budini: FMNH 23351, FMNH 23352, FMNH 23355, FMNH 23356, FMNH 23357, FMNH 23359, FMNH 23360, FMNH 23361, FMNH 23362, FMNH 23363, FMNH 23364, FMNH 23365, FMNH 23369, FMNH 23370, FMNH 23371, USNM 259611, USNM 259612
Akodon cursor: FMNH 123060, FMNH 123061, FMNH 123062, FMNH 123063, FMNH 141602, FMNH 141603, FMNH 141604, FMNH 145329, FMNH 145330, FMNH 145332, FMNH 230328, FMNH 230329, FMNH 230332, FMNH 26578, FMNH 26581, FMNH 26584, FMNH 94449, FMNH 94450, FMNH 94452, FMNH 94468
Akodon dayi: FMNH 140809, FMNH 140810, FMNH 21575, FMNH 21578, FMNH 21588, FMNH 46145, USNM 276608, USNM 276609, USNM 390141, USNM 584503, USNM 584504, USNM 584505, USNM 584506
Akodon dolores: FMNH 35243, USNM 364531
Akodon fumeus: FMNH 46143, FMNH 74874, FMNH 74875, FMNH 74876, FMNH 74877, FMNH 74878, FMNH 74879, FMNH 74881, FMNH 74882, FMNH 74883, USNM 290907, USNM 290927
Akodon iniscatus: FMNH 29127, FMNH 29128, FMNH 35248, FMNH 41284, FMNH 41285, USNM 236314
Akodon juninensis: AMNH 231329, AMNH 231334, AMNH 231337, AMNH 231338, AMNH 231340, FMNH 23671, FMNH 23673, FMNH 75561
Akodon kofordi: FMNH 18181, FMNH 52553, FMNH 52554, FMNH 52555, FMNH 52556,

USNM 172966

Akodon lindberghi: FMNH 128293, FMNH 128295, FMNH 12829, FMNH 128297, MN 33681, MN 33682, MN 33683, MN 33684, MN 33685, MN 33686, MN 33687, MN 33703, MN 48026, MN 67123

Akodon lutescens: FMNH 21559, FMNH 49696, FMNH 49697, FMNH 50975, FMNH 74884, FMNH 74886, FMNH 74887, FMNH 74890, FMNH 74891

Akodon mimus: AMNH 264910, AMNH 264911, AMNH 264913, AMNH 264914, AMNH 264915, AMNH 264918, AMNH 264919, AMNH 264920, AMNH 268803, AMNH 268823, AMNH 268826, AMNH 268828, AMNH 268829, AMNH 268831, AMNH 268832

Akodon mollis: FMNH 129213, FMNH 129215, FMNH 129219, FMNH 129224, FMNH 19272, FMNH 19280, FMNH 19281, FMNH 19282, FMNH 19284, FMNH 20902, FMNH 20905, FMNH 20909, FMNH 20910, FMNH 23658, FMNH 23660, FMNH 23662, FMNH 81348, FMNH 81367, FMNH 81370, FMNH 81375

Akodon mystax: FMNH 230333, FMNH 230334, FMNH 230335, MN 69602, MN 69605, MN 69606, MN 69609, MN 69613, MN 69623, MN 69627, MN 69628, MN 69629, MN 69644

Akodon montensis: FMNH 18185, FMNH 23844, FMNH 26817, FMNH 26834, FMNH 26838, FMNH 26845, FMNH 26846, FMNH 26847, FMNH 29438, FMNH 34038, FMNH 47956

Akodon orophilus: FMNH 19719, FMNH 19721, FMNH 19722, FMNH 19725, FMNH 19729, FMNH 19731, FMNH 19732, FMNH 19733, FMNH 19734, FMNH 19737, FMNH 19738, FMNH 19739, FMNH 19740, FMNH 19741, FMNH 23669, FMNH 24495, FMNH 24500, FMNH 24535, FMNH 24773, FMNH 24774

Akodon paranaensis: FMNH 232547, FMNH 232563, FMNH 23257, FMNH 232578, FMNH 232579, FMNH 232624, FMNH 232651, FMNH 232652, MN 48041, MN 48067, MN 69675, MN 69676, MN 69677, MN 69679

Akodon reigi: MN 62119, MN 62120

Akodon siberiae: AMNH 260423, AMNH 260424, AMNH 260425, AMNH 260426, AMNH 260427, AMNH 260428, AMNH 260430, AMNH 260431, AMNH 260434, AMNH 260578, AMNH 260579, AMNH 260594

Akodon simulator: FMNH 29134, FMNH 29137, FMNH 30109, FMNH 30110, FMNH 30112, FMNH 30115, FMNH 30117, FMNH 30119, FMNH 30120, FMNH 30122, FMNH 30123, FMNH 30128, FMNH 30131, FMNH 30132, FMNH 35249

Akodon spegazzinii: FMNH 29122, FMNH 29123, FMNH 30181, FMNH 30182, FMNH 30184, FMNH 30185, FMNH 30189, FMNH 34997, USNM 259279, USNM 259280, USNM 259282, USNM 259632, USNM 259633

Akodon subfuscus: FMNH 107744, FMNH 107754, FMNH 107760, FMNH 107766, FMNH 107771, FMNH 107772, FMNH 107777, FMNH 107794, FMNH 107810, FMNH 107814, FMNH 107817, FMNH 75523, FMNH 75524, FMNH 75525, FMNH 75527, FMNH 75529, FMNH 75531, FMNH 75532, FMNH 75533, FMNH 75535, FMNH 75550

Akodon surdus: FMNH 43371, FMNH 43372, FMNH 83476, AMNH 264272

Akodon sylvanus: AMNH 264274

Akodon toba: FMNH 157165, FMNH 157179, FMNH 157182, FMNH 157187, FMNH 157188, FMNH 157195, FMNH 157201, FMNH 157209, FMNH 164101, FMNH 164136, FMNH 164159, FMNH 164161, FMNH 164164, FMNH 164168, FMNH 164170, FMNH 164173, FMNH 164178,

FMNH 164179, FMNH 164180, FMNH 164182, FMNH 164183, FMNH 46161
Akodon torques: FMNH 170501, FMNH 170503, FMNH 170506, FMNH170508, FMNH 170509, FMNH 170510, FMNH 170511, FMNH 170517, FMNH 170519, FMNH170523, FMNH 170524, FMNH 171861, FMNH 171862, FMNH 172221, FMNH 172225, FMNH172227, FMNH 172229, FMNH 172231, FMNH 172233, FMNH 43366, FMNH 43367, FMNH 43368, FMNH 43369, FMNH 43370, FMNH 78707, FMNH 78708
Akodon varius: AMNH 38667, AMNH 38670, AMNH 38674, AMNH 38675, FMNH 50160, FMNH 50980, FMNH 50981
Bibimys chacoensis: USNM 236239
Bibimys labiosus: MN 62395, MN 62601, MZUFV 753, PGR 210, PRG 1034, MCNM 2162, MCNM 2198, MCNM 2827, MCNM 2829, MCNM 2833, MCNM 2838, MCNM 2839
Blarinomys breviceps: MN 13353, MN 29445, MN 29446, MN 29447, MN 29453, MN 29454, MN 29456, MN 29457, MN 29458, MN 29461, MN 29464, MN 29466, MN 37029, MN 37030, MN 68873, MN 68882, MN 70223, MN 70224, MN 70225, MN 70226, MN 71774, MN 71837, MN 77786
Brucepattersonius griserufescens: MN 70232, MN 71755, MN 71764, MN 71771
Brucepattersonius soricinus: FMNH 230356, FMNH 94480
Castoria angustidens: FMNH 230337, FMNH 230338, FMNH 230339, FMNH 230340, FMNH 230345, FMNH 230346, FMNH 230348, FMNH 230349, FMNH 230350, FMNH 230351, FMNH 230352, FMNH 230353
Deltamys kempi: AMNH 206097, AMNH 206102, AMNH 206115, AMNH 206117, AMNH 206118, AMNH 206119, AMNH 206120, AMNH 206121, AMNH 206139, AMNH 206140, AMNH 206142, AMNH 206157, AMNH 206158, AMNH 206159, AMNH 206161, AMNH 206163, AMNH 206164, AMNH 206165, MN 42090, MN 42091, MN 42092, MN 42097, MN 42098, MN 42099, MN 42100
Gyldenstolpia planaltensis: MN 21835, MN 21836, MN 21837, MN 21838, MN 21839, MN 21840, MN 21841, MN 21842, MN 21843, MN 21845, MN 21846, MN 21847, MN 21848, MN 21849, MN 21850, MN 34299
Juscelinomys candango: MN 23870, MN 23871, MN 30026, MN 30027, MN 30028, MN 30031, MN 30032
Juscelinomys huanchacae: USNM 584508, USNM 584509, USNM 584510, USNM 584511, USNM 584512, USNM 584513, USNM 584514
Kunsia tomentosus: MN 2054, MN 2055, MN 53969, MN 62567, MN 62569
Lenoxus apicalis: AMNH 15815, AMNH 16064, AMNH 16065, AMNH 16067, AMNH 16553, AMNH 16555, AMNH 16556, AMNH 16557, AMNH 16558, AMNH 16559, AMNH 264854, AMNH 264855, AMNH 264856, AMNH 264857, AMNH 72604, AMNH 72605, AMNH 72607, AMNH 72609, AMNH 72610, AMNH 72611, AMNH 72615, AMNH 72618, AMNH 72620, AMNH 72624, FMNH 20106, FMNH 52612, FMNH 52613
Necromys amoenus: FMNH 107665, FMNH 107680, FMNH 107699, FMNH 107702, FMNH 107728, FMNH 107838, FMNH 107861, FMNH 107862, FMNH 107864, FMNH 107875, FMNH 49671, FMNH 49672, FMNH 49676, FMNH 49677, FMNH 49750, USNM 194725
Necromys lasiurus: FMNH 117120, FMNH 117124, FMNH 128331, FMNH 128334, FMNH 128335, FMNH 128337, FMNH 128338, FMNH 164214, FMNH 164226, FMNH 164227, FMNH

164235, FMNH 164320, FMNH 25196, FMNH 25197, FMNH 25198, FMNH 25200, FMNH 25201, FMNH 96114, FMNH 96115
Necromys lactens: FMNH 162771, FMNH 23366
Necromys lenguarum: FMNH 157220, FMNH 164229, FMNH 164244, FMNH 164324, FMNH 164325
Oxymycterus amazonicus: FMNH 94524, USNM 519783, USNM 519784, USNM 519785, USNM 546025, USNM 546028, USNM 546029, USNM 546030, USNM 546031
Oxymycterus dasytrichus: FMNH 145437, FMNH 145438, FMNH 145441, FMNH 145443, FMNH 53874, FMNH 53875, FMNH 94525, FMNH 94526, FMNH 94529, USNM 545060, MCNM 1300, MCNM 1477, MCNM 3072, MCNM 3074, MCNM 3158
Oxymycterus delator: MCNM 2482, MCNM 3073, MCNM 3075, MCNM 3076, MCNM 3126, MCNM 3256, MCNM 3259, MCNM 3260, MCNM 3333, MCNM 3512, FMNH 128320, FMNH 128321, FMNH 128322, FMNH 128323
Oxymycterus hiska: AMNH 72889, AMNH 91303, AMNH 91601, AMNH 91602
Oxymycterus nasutus: CAZ 100, CAZ 106, CAZ 108, CAZ 118, CAZ 122, CAZ 125, CAZ 129, CAZ 133, CAZ 138, CAZ 63, FMNH 27652, MN 42435, MN 42436
Oxymycterus paramensis: FMNH 162837, FMNH 162839, FMNH 162841, FMNH 162845, FMNH 162851, FMNH 22234, FMNH 23316, FMNH 23319, FMNH 23320, FMNH 23322, FMNH 23324, FMNH 23325, FMNH 35251, FMNH 41280, FMNH 46151, FMNH 50985, FMNH 50986, FMNH 50987, FMNH 74892, FMNH 74893, FMNH 74894, FMNH 74895, FMNH 74896, FMNH 74898, FMNH 74899, FMNH 74900, FMNH 74901
Oxymycterus quaestor: FMNH 23843, FMNH 26586, FMNH 26587, FMNH 26595, FMNH 26754, FMNH 26756, FMNH 26757, FMNH 34377, FMNH 34380, FMNH 35354, USNM 259577, USNM 462120, USNM 462121, USNM 462123, USNM 484400, USNM 484401, USNM 484402, USNM 484404, USNM 484405
Oxymycterus rufus: FMNH 122696, FMNH 122697, FMNH 136923, FMNH 136927, FMNH 136928, FMNH 136929, FMNH 230386, FMNH 26754, FMNH 26757, FMNH 95138, FMNH 98285, MN 65522, MN 65523, MN 65525, MN 65526, MN 65531, MN 66193, USNM 236328, USNM 282159, USNM 309164
Podoxymys roraimae: AMNH 75583, AMNH 75584, AMNH 75585, AMNH 75586
Scapteromys aquaticus: FMNH 29160, FMNH 98286, FMNH 98289, MN 62304, MN 62305, MN 62308, MN 62309, MN 62310, MN 62312
Scapteromys tumidus: AMNH 206209, AMNH 206220, AMNH 206221, AMNH 206222, AMNH 206230, AMNH 206231, AMNH 206240, AMNH 206247, AMNH 206248, AMNH 206261, AMNH 206267, AMNH 206272, AMNH 206278, AMNH 206280, AMNH 235431, AMNH 235432, AMNH 235433, MN 32855
Thalpomys cerradensis: FMNH 128328, MN 33502 type
Thalpomys lasiotis: FMNH 128326, FMNH 128327, MN 24361, MN 60198, MN 60199, MN 60200, MN 60201, MN 61652, MN 61653, MN 62654, MN 62655, MN 62656, MN 62657, MN 62658, MN 62659, MN 66008, MN 75104, MN 75105, MN 82159
Thaptomys nigrita: FMNH 220012, FMNH 230387, FMNH 230388, FMNH 230389, FMNH 230390, FMNH 26820, FMNH 47952, USNM 460539, USNM 460541, USNM 484233, USNM 484235, USNM 484236, USNM 484237, USNM 484239, USNM 484240, USNM 484241, USNM

484243, USNM 484244, USNM 484245

Bite force

Akodon aerosus: FMNH 172190, FMNH 172192, FMNH 172193, FMNH 172195, FMNH 172197, FMNH 19265, FMNH 19266, FMNH 19268. FMNH 19757, FMNH 24502, FMNH 24506, FMNH 24510, FMNH 24512, FMNH 41474, FMNH 43232, FMNH 65705, FMNH 66402, FMNH 68614, FMNH 75475, FMNH 75476, FMNH 75479, FMNH 75480, FMNH 78709

Akodon affinis: AMNH 181479, AMNH 181479, AMNH 32991, AMNH 32992, AMNH 32994, AMNH 32995, AMNH 32999, AMNH 33000, AMNH 33005, AMNH 33007, AMNH 33018, AMNH 71208, AMNH 71212, AMNH 71213, AMNH 71215, AMNH 71217, AMNH 71218, AMNH 71222, AMNH 71223, AMNH 71226, AMNH 71227, AMNH 71230

Akodon albiventer: FMNH 107479, FMNH 107488, FMNH 107491, FMNH 107497, FMNH 107554, FMNH 107568, FMNH 107578, FMNH 107579, FMNH 107592, FMNH 129981, FMNH 129982, FMNH 129983, FMNH 129992, FMNH 162679, FMNH 162685, FMNH 162707, FMNH 162725, FMNH 53621, FMNH 53622, FMNH 53623, FMNH 53624

Akodon azarae: FMNH 23328, FMNH 23331, FMNH 23333, FMNH 23334, FMNH 23337, FMNH 23340, FMNH 23341, FMNH 27613, FMNH 27614, FMNH 27615, FMNH 27624, FMNH 27627, FMNH 27632, FMNH 27633, FMNH 27635, FMNH 27636, FMNH 29189, FMNH 29191, FMNH 29205, FMNH 29211, FMNH 29213, FMNH 29222, FMNH 29223

Akodon boliviensis: FMNH 107641, FMNH 107868, FMNH 107869, FMNH 107882, FMNH 107883, FMNH 107886, FMNH 107917, FMNH 107928, FMNH 107969, FMNH 162747, FMNH 162749, FMNH 162751, FMNH 162753, FMNH 52542, FMNH 52543, FMNH 52545, FMNH 52547, FMNH 52548, FMNH 52549, FMNH 64339

Akodon budini: FMNH 23351, FMNH 23352, FMNH 23355, FMNH 23356, FMNH 23357, FMNH 23358, FMNH 23359, FMNH 23360, FMNH 23361, FMNH 23362, FMNH 23363, FMNH 23364, FMNH 23365, FMNH 23369, FMNH 23370, FMNH 23371, FMNH 35345, FMNH 39467, USNM 259611, USNM 259612

Akodon cursor: FMNH 123060, FMNH 123061, FMNH 123062, FMNH 145329, FMNH 145332, FMNH 145348, FMNH 145354, FMNH 145355, FMNH 230321, FMNH 230323, FMNH 230326, FMNH 230328, FMNH 26578, FMNH 26580, FMNH 26581, FMNH 26583, FMNH 26584, FMNH 26627, FMNH 94441, FMNH 94445, FMNH 94446, FMNH 94449, FMNH 94452

Akodon dayi: FMNH 140810, FMNH 21574, FMNH 21575, FMNH 21577, FMNH 21578, FMNH 21579, FMNH 21581, FMNH 21582, FMNH 21584, FMNH 21587, FMNH 21588, FMNH 21590, USNM 276608, USNM 276609, USNM 390141, USNM 390160, USNM 390161, USNM 390162, USNM 390252, USNM 390699, USNM 390727, USNM 584503, USNM 584504, USNM 584505, USNM 584506

Akodon dolores: FMNH 35243, USNM 364531

Akodon fumeus: FMNH 162755, FMNH 46143, FMNH 46144, FMNH 74874, FMNH 74875, FMNH 74876, FMNH 74877, FMNH 74878, FMNH 74879, FMNH 74880, FMNH 74881, FMNH 74882, FMNH 74883, FMNH 79891, FMNH 79892, FMNH 79893, USNM 271433, USNM 290907, USNM 290927

Akodon iniscatus: FMNH 29127, FMNH 29128, FMNH 35248, FMNH 35347, FMNH 35348, FMNH 41284, FMNH 41285, USNM 236314

Akodon juninensis: FMNH 23671, FMNH 23673, FMNH 75561, AMNH 231234, AMNH 231235, AMNH 231236, AMNH 231237, AMNH 231238, AMNH 231240, AMNH 231241, AMNH 231243
Akodon kofordi: FMNH 18181, FMNH 52553, FMNH 52554, FMNH 52555, FMNH 52556, FMNH 75483, USNM 172966
Akodon lindberghi: FMNH 128293, FMNH 128295, FMNH 128296, FMNH 128297, FMNH 128298, MN 33681, MN 33682, MN 33683, MN 33684, MN 33685, MN 33686, MN 33687, MN 33703, MN 48026, MN 67123
Akodon lutescens: FMNH 21559, FMNH 49696, FMNH 49697, FMNH 50974, FMNH 50975, FMNH 50976, FMNH 51928, FMNH 74884, FMNH 74885, FMNH 74886, FMNH 74887, FMNH 74888, FMNH 74889, FMNH 74890, FMNH 74891
Akodon mimus: AMNH 264910, AMNH 264911, AMNH 264913, AMNH 264914, AMNH 264915, AMNH 264918, AMNH 264919, AMNH 264920, AMNH 264921, AMNH 268803, AMNH 268823, AMNH 268826, AMNH 268828, AMNH 268829, AMNH 268831, AMNH 268832, AMNH 275471
Akodon mollis: FMNH 129219, FMNH 129224, FMNH 129225, FMNH 129228, FMNH 19280, FMNH 19281, FMNH 19284, FMNH 19285, FMNH 19307, FMNH 19316, FMNH 2366, FMNH 23662, FMNH 23663, FMNH 23664, FMNH 81349, FMNH 81363, FMNH 81366, FMNH 81367, FMNH 81375, FMNH 81376, FMNH 81378, FMNH 92014, FMNH 92016, FMNH 92018
Akodon montensis: FMNH 18183, FMNH 18184, FMNH 18185, FMNH 23844, FMNH 6848, FMNH 26849, FMNH 26850, FMNH 26851, FMNH 26853, FMNH 26855, FMNH 26858, FMNH 26863, FMNH 29145, FMNH 29146, FMNH 29437, FMNH 29438, FMNH 34037, FMNH 34038, FMNH 47956
Akodon mystax: FMNH 230333, FMNH 230334, FMNH 230335, MN 69602, MN 69605, MN 69606, MN 69609, MN 69613, MN 69623, MN 69627, MN 69628, MN 69629, MN 69644, MN 69645, MN 69664, MN 69665
Akodon orophilus: FMNH 19704, FMNH 19707, FMNH 19710, FMNH 19717, FMNH 19718, FMNH 19719, FMNH 19721, FMNH 19722, FMNH 19725, FMNH 19726, FMNH 19747, FMNH 19748, FMNH 19749, FMNH 19750, FMNH 19754, FMNH 23657, FMNH 23669, FMNH 23674, FMNH 24495, FMNH 24496, FMNH 24498, FMNH 24500, FMNH 24535, FMNH 24773, FMNH 24774
Akodon paranaensis: FMNH 232547, FMNH 232554, FMNH 232563, FMNH 232578, FMNH 232579, FMNH 232624, FMNH 232651, FMNH 232652, MN 48041, MN 48067, MN 69675, MN 69676, MN 69677, MN 69679
Akodon reigi: MN 62119, MN 62120
Akodon siberiae: AMNH 260423, AMNH 260424, AMNH 260425, AMNH 260426, AMNH 260427, AMNH 260428, AMNH 260430, AMNH 260431, AMNH 260434, AMNH 260578, AMNH 260580, AMNH 260594
Akodon simulator: FMNH 29120, FMNH 29134, FMNH 29135, FMNH 29137, FMNH 29138, FMNH 29139, FMNH 29140, FMNH 29141, FMNH 29142, FMNH 29144, FMNH 30109, FMNH 30110, FMNH 30112, FMNH 30115, FMNH 30117, FMNH 30123, FMNH 30127, FMNH 30128, FMNH 30131, FMNH 35249
Akodon spegazzinii: USNM 259279, USNM 259280, USNM 259282, USNM 259632, USNM

259633, FMNH 29122, FMNH 29123, FMNH 30181, FMNH 30182, FMNH 30184, FMNH 30185, FMNH 30189, FMNH 30190, FMNH 30191, FMNH 30196, FMNH 34997, FMNH 46147
Akodon subfuscus: FMNH 107744, FMNH 107755, FMNH 107765, FMNH 107766, FMNH 107768, FMNH 107776, FMNH 52570, FMNH 52665, FMNH 75512, FMNH 75513, FMNH 75516, FMNH 75518, FMNH 75519, FMNH 75525, FMNH 75528, FMNH 75530, FMNH 75531, FMNH 75535, FMNH 75536, FMNH 75550, FMNH 75551, FMNH 75560, FMNH 84422, FMNH 84423
Akodon surdus: FMNH 43371, FMNH 43372, FMNH 83476, USNM 194639, USNM 194641, USNM 194642, USNM 194643, USNM 194644, USNM 194645, USNM 194650, USNM 194651, USNM 194652, USNM 194653, USNM 194655, USNM 194656, USNM 194657, USNM 194660, USNM 194694
Akodon sylvanus: AMNH 264272, AMNH 264274
164178, FMNH 164179, FMNH 164180, FMNH 164182, FMNH 164183, FMNH 46142, FMNH 46161
Akodon torques: FMNH 170501, FMNH 170503, FMNH 170506, FMNH 170508, FMNH 170509, FMNH 170510, FMNH 170519, FMNH 170523, FMNH 170524, FMNH 170526, FMNH 172225, FMNH 172227, FMNH 172229, FMNH 43366, FMNH 43367, FMNH 43368, FMNH 43369, FMNH 43370, FMNH 78704, FMNH 78705, FMNH 78706, FMNH 78707, FMNH 78708
Akodon varius: FMNH 21560, FMNH 50160, FMNH 50977, FMNH 50978, FMNH 50979, FMNH 50980, FMNH 50981, FMNH 50982, FMNH 50983, FMNH 51929, AMNH 38667, AMNH 38670, AMNH 38674, AMNH 38675
Bibimys chacoensis: USNM 236239
Bibimys labiosus: MCNM 2162, MCNM 2198, MCNM 2436, MCNM 2827, MCNM 2829, MCNM 2833, MCNM 2838, MCNM 2839, MN 62061, MN 62395, PGR 201, PGR 210, PRG 1034
Blarinomys breviceps: MCNM 1377, MCNM 1472, MCNM 2196, MCNM 2197, MCNM 2534, MCNM 2836, MCNM 2837, MCNM 2846, MCNM 2983, MCNM 3332, MN 13353, MN 29446, MN 29447, MN 29453, MN 29454, MN 29456, MN 29457, MN 29458, MN 29461, MN 29464, MN 29466, MN 29945, MN 31193, MN 37029, MN 37030, MN 68873, MN 68882, MN 70223, MN 70224, MN 70225, MN 70226, MN 71774, MN 71837, MN 77786
Brucepattersonius griserufescens: MN 70232, MN 71755, MN 71764, MN 71771
Castoria angustidens: FMNH 230337, FMNH 230338, FMNH 230339, FMNH 230340, FMNH 230341, FMNH 230342, FMNH 230344, FMNH 230345, FMNH 230346, FMNH 230347, FMNH 230348, FMNH 230349, FMNH 230350, FMNH 230351, FMNH 230352, FMNH 230353
Deltamys kempi: AMNH 206097, AMNH 206098, AMNH 206102, AMNH 206115, AMNH 206116, AMNH 206117, AMNH 206118, AMNH 206119, AMNH 206120, AMNH 206121, AMNH 206139, AMNH 206140, AMNH 206142, AMNH 206147, AMNH 206157, AMNH 206158, AMNH 206159, AMNH 206161, AMNH 206163, AMNH 206164, AMNH 206165, MN 42068, MN 42084, MN 42088, MN 42090, MN 42090, MN 42091, MN 42092, MN 42096, MN 42097, MN 42098, MN 42099, MN42100
Gyldenstolpia planaltensis: MN 21835, MN 21836, MN 21837, MN 21838, MN 21839, MN 21840, MN 21841, MN 21842, MN 21843, MN 21844, MN 21845, MN 21846, MN 21847, MN 21848, MN 21849, MN 21850, MN 34299

Juscelinomys huanchacae: USNM 584508, USNM 584509, USNM 584510, USNM 584511, USNM 584512, USNM 584513, USNM 584514
Juscelinomys candango: MN 23870, MN 23871, MN 30026, MN 30027, MN 30028, MN 30030, MN 30031, MN 30032
Kunsia tomentosus: MN 2054, MN 2055, FMNH 122711, MN 53969, MN 62569, MN 62657, USNM 364760, USNM 584516
Lenoxus apicalis: FMNH 20106, FMNH 52612, FMNH 52613, AMNH 15815, AMNH 16065, AMNH 16067, AMNH 16553, AMNH 16555, AMNH 16556, AMNH 16557, AMNH 16558, AMNH 16559, AMNH 264854, AMNH 264855, AMNH 264856, AMNH 264857, AMNH 72604, AMNH 72605, AMNH 72607, AMNH 72609, AMNH 72610, AMNH 72611, AMNH 72615, AMNH 72618, AMNH 72620, AMNH 72624
Necromys amoenus: FMNH 107608, FMNH 107665, FMNH 107665, FMNH 107680, FMNH 107699, FMNH 107702, FMNH 107728, FMNH 107838, FMNH 107861, FMNH 107862, FMNH 107864, FMNH 107864, FMNH 107875, FMNH 107875, FMNH 49671, FMNH 49672, FMNH 49676, FMNH 49676, FMNH 49677, FMNH 49750, FMNH 49750, USNM 194725
Necromys lactens: FMNH 162771, FMNH 23366
Necromys lasiurus: FMNH 128331, FMNH 128334, FMNH 128335, FMNH 128337, FMNH 128338, FMNH 164214, FMNH 164226, FMNH 164227, FMNH 164235, FMNH 164320, FMNH 171120, FMNH 171122, FMNH 171124, FMNH 25196, FMNH 25197, FMNH 25198, FMNH 25200, FMNH 25201, FMNH 96114, FMNH 96115
Necromys lenguarum: FMNH 157220, FMNH 164324, FMNH 164325, FMNH 164329, FMNH 164344, USNM 584523, USNM 584525, USNM 584529, USNM 584531, USNM 584533, USNM 584534, USNM 584538, USNM 584539, USNM 584540, USNM 584541
Necromys obscurus: FMNH 122687, FMNH 35357
USNM 442343, USNM 442350, USNM 540711, USNM 560659, USNM 85567
Oxymycterus amazonicus: USNM 519783, USNM 519784, USNM 519785m USNM 519786, USNM 546026, USNM 546028, USNM 546029, USNM 546030, USNM 546031
Oxymycterus dasytrichus: FMNH 145437, FMNH 145438, FMNH 145441, FMNH 145442, FMNH 145443, FMNH 145444, FMNH 145445, FMNH 53874, FMNH 53875, FMNH 94525, FMNH 94526, FMNH 94529, MCNM 1300, MCNM 1477, MCNM 3072, MCNM 3074, MCNM 3158, USNM 545060
Oxymycterus delator: FMNH 128320, FMNH 128321, FMNH 128322, FMNH 128323, FMNH 128324, MCNM 2482, MCNM 3073, MCNM 3075, MCNM 3076, MCNM 3126, MCNM 3256, MCNM 3260, MCNM 3260, MCNM 3333, MCNM 3512
Oxymycterus hiska: AMNH 72889, AMNH 91601, AMNH 91602, AMNH 91603
Oxymycterus nasutus: CAZ 100, CAZ 106, CAZ 108, CAZ 118, CAZ 122, CAZ 125, CAZ 129, CAZ 133, CAZ 138, CAZ 63, MN 42435, MN 42436, USNM 259578, USNM 282160, USNM 460550, USNM 460551, USNM 461881, USNM 484394, USNM 484395, USNM 484396, USNM 484397, USNM 543121
Oxymycterus quaestor: FMNH 23843, FMNH 26754, FMNH 26757, FMNH 34375, FMNH 34377, FMNH 34380, FMNH 35354, USNM 122696, USNM 259577, USNM 462120, USNM 462121, USNM 462123, USNM 484400, USNM 484401, USNM 484402, USNM 484404, USNM 484405

Oxymycterus rufus: MN 65522, MN 65523, MN 65525, MN 65526, MN 65529, MN 65531, MN 66193, USNM 236296, USNM 236328, USNM 309164
Podoxymys roraimae: AMNH 75583, AMNH 75584, AMNH 75585
Scapteromys aquaticus: FMNH 29160, FMNH 98288, FMNH 98289, MN 62304, MN 62305, MN 62307, MN 62308, MN 62309, MN 62310, MN 62311, MN 62312, MN 62312, FMNH 122713, FMNH 122714
Scapteromys tumidus: AMNH 206209, AMNH 206220, AMNH 206221, AMNH 206222, AMNH 206230, AMNH 206231, AMNH 206240, AMNH 206245, AMNH 206247, AMNH 206248, AMNH 206261, AMNH 206267, AMNH 206272, AMNH 206278, AMNH 206280, AMNH 235431, AMNH 235432, AMNH 235433, MN 32855
Thalpomys cerradensis: MN 34241, MN 75105, MN 33502
Thalpomys lasiotis: FMNH 128326, FMNH 128327, MN 24361, MN 60197, MN 60198, MN 60199, MN 60200, MN 60201, MN 61652, MN 61653, MN 62654, MN 62655, MN 62656, MN 62657, MN 62658, MN 62659, MN 66008, MN 75104, MN 81597, MN 82159
Thaptomys nigrita: FMNH 220012, FMNH 230387, FMNH 230388, FMNH 230389, FMNH 230390, FMNH 26819, FMNH 26820, FMNH 35353, FMNH 47952, FMNH 63786, FMNH 63787, FMNH 93083, USNM 460539, USNM 460541, USNM 484233, USNM 484234, USNM 484235, USNM 484236, USNM 484237, USNM 484239, USNM 484240, USNM 484241, USNM 484243, USNM 484244, USNM 484245

Supplementary Material 3.S2: Stomach content data used in this study as basis for diet categorization of akodontine rodents.

Species	Proportion					N	Reference
	invertebrates	plant material			fungi		
		total	leaves	seeds			
Akodon albiventer	70.83%						Huayta 2016
	86%		14%			6	Pizzimenti and DeSalle 1980
Akodon azarae	52.60%		12.60%	31.80%		85	Ellis et al. 1998
	54.2-70.2%		23.4-38.3%	6.4-7.5%		18	Suarez and Bonaventura 2001
	70%	20%				11	Barlow 1969
	34.3%%	64.2%	28.5%	35.7%		60	Bilenca et al. 1992
Akodon boliviensis	61.86%					-	Huayta 2016
	78%	22%				26	Pizzimenti and DeSalle 1980
Akodon lutescens	91%	9%				4	Pizzimenti and DeSalle 1980
Akodon montensis	34.30%	65.7%	11%	12.9%	4.4%	37	Talamoni et al. 2008
Akodon orophilus	90.1%	3.31%				37	Huiman 2008
Akodon paranaensis	75%	25%				17	Casella and Cáceres 2006
Akodon subfuscus	91.15%					-	Huayta 2016
	59.3%	17%				-	Solari 2007
Akodon torques	87.93%	4.98%			0.57%	162	Zevallos 2014
	65.47%	21.02%				18	Solari 2007
Blarinomys breviceps	100%					2	dos Reis 1996
Brucepattersonius soricinus	80-100%					9	Pinotti et al. 2010
Necromys amoenus	72%	28%				6	Pizzimenti and DeSalle 1980
		62.53%				-	Huayta 2016
Necromys lasiurus	27.30%	72.6%	9.6%	20.2%		27	Talamoni et al. 2008

(continued)

Necromys obscurus			15.70%			7	Barlow 1969
	<20%		<20%	50%		9	Ellis et al. 1994
	33.40%			40.20%		43	Ellis et al. 1998
Oxymycterus dasytrichus	100%					1	Pinotti et al. 2010
Oxymycterus delator	70%					-	Suarez 1994
	62%	37%	9.2%	5.8%	2.9%	16	Talamoni et al. 2008
	100%					4	Talamoni et al. 1999
Oxymycterus paramensis	72.96%	13.27%				31	Solari 2007
Oxymycterus hiska	100%					2	Hinojosa et al. 1987
Oxymycterus rufus	76.7-80%		10.5-12.5%	6.9-9.35%		93	Suarez and Bonaventura 2001
Scapteromys tumidus	87.5-87.8%			0-1.6%		16	Suarez and Bonaventura 2001
	85%					11	Barlow 1969
Thaptomys nigrita	0-60%					8	Pinotti et al. 2010

Supplementary Material 3.S3: Diet categorizations for akodontine rodents used in this study based on stomach content and qualitative data from literature.

Species	Diet	Reference
Akodon aerosus	O	Bernal et al. 2016
Akodon albiventer	I	Pizzimenti and DeSalle 1980, Díaz and Barquez 2007, Iriarte 2008, Dunnum et al.2016
Akodon affinis	O	Quiceno 1993
Akodon azarae	O	Barlow 1969, Ellis et al. 1998, Suarez and Bonaventura 2001, Ellis et al. 1994,Dalby 1975, Perera 2002
Akodon boliviensis	I	Pizzimenti and DeSalle 1980, Eisenberg and Redford 2000
Akodon budini	-	-
Akodon cursor	O	Carvalho et al. 1999, Talamoni et al. 1999
Akodon dayi	O	Cuéllar and Noss 2003
Akodon dolores	O	Martinez et al. 1990, Giannoni et al. 2005
Akodon fumeus	-	-
Akodon iniscatus	O	Ojeda 2000
Akodon lutescens	I	Pizzimenti and DeSalle 1980
Akodon lindberghi	O	Paglia et al. 2012
Akodon mimus	I	Dunnum et al. 2016
Akodon mollis	O	Pardiñas et al. 2017
Akodon montensis	O	Talamoni et al. 2008, Vieira et al. 2006
Akodon mystax	O	Paglia et al. 2012
Akodon orophilus	I	Huiman 2008, Noblecita and Pacheco 2012
Akodon reigi	O	Paglia et al. 2012
Akodon siberiae	-	-
Akodon simulator	O	Ojeda 2000
Akodon spegazzinii	O	Barquez et al. 1991
Akodon paranaensis	I	Casella e Cáceres 2006
Akodon subfuscus	I	Solari 2007, Huayta 2016
Akodon toba	O	Cuéllar and Noss 2003
Akodon torques	I	Kelt et al. 2007, Solari 2007, Zevallos 2014, Sahley et al. 2015
Akodon varius	O	Cuéllar and Noss 2003
Bibimys chacoensis	H	Pardiñas et al. 2017
Bibimys labiosus	H	Diório 2014, Pardiñas et al. 2017
Blarinomys breviceps	I	Davis 1944, Abravaya e Matson 1975, dos Reis et al. 1996, Geise et al. 2008, Galetti et al. 2016
Brucepattersonius griserufescens	I	Hershkovitz 1998
Brucepattersonius soricinus	I	Pinotti et al. 2010, Galetti et al. 2016
Castoria angustidens	O	Paglia et al. 2012

(continued)

Deltamys kempi	I	Massoia 1964, Bianchini and Delupi 1994, Teta et al. 2007, Teta et al. 2016
Gyldenstolpia planaltensis	H	Paglia et al. 2012
Juscelinomys candango	I	Moojen 1965, Emmons 2015
Juscelinomys huanchacae	I	Emmons and Patton 2012, Emmons 2015
Lenoxus apicalis	I	Vorontzov 1979
Kunsia tomentosus	H	Miranda Ribeiro 1914, Kay and Madden 1997, Eisenberg and Redford 2000, Williams and Kay 2001, Bezerra et al. 2007, Bezerra & Pardinas 2016
Necromys amoenus	O	Pizzimenti and DeSalle 1980
Necromys lactens	O	Ojeda 2000
Necromys lasiurus	H	Alho 1982, Alho et al. 1986, Talamoni et al. 1999
Necromys lenguarum	O	Cuéllar and Noss 2003
Necromys obscurus	O	Barlow 1969, Ellis et al. 1994
Necromys urichi	H	Linares 1998, Eisenberg e Redford 2000
Oxymycterus amazonicus	I	Hershkovitz 1994
Oxymycterus dasytrichus	I	Pinotti et al. 2010
Oxymycterus delator	I	Talamoni et al. 2008, Borchert & Hansen 1983; Talamoni et al. 1999, Redford 1984
Oxymycterus hiska	I	Hinojosa et al. 1987
Oxymycterus nasutus	I	Barlow 1969, D'Elía and Teta 2016
Oxymycterus paramensis	I	Solari 2007, Dunnum et al. 2017
Oxymycterus quaestor	I	Hershkovitz 1994
Oxymycterus rufus	I	Kravetz 1972, Dalby 1975, Suarez 1994, Perera 2002
Podoxymys roraimae	I	Linares 1998
Scapteromys aquaticus	I	Massoia 1961, Hershkovitz 1966, Pardiñas et al. 2008
Scapteromys tumidus	I	Massoia and Fornes 1964, Hershkovitz 1966, Barlow 1969, Pardiñas et al. 2008, Eisenberg and Redford 1999
Thalpomys cerradensis	O	Marinho Filho et al. 2002
Thalpomys lasiotis	O	Marinho Filho et al. 2002
Thaptomys nigrita	O	Pinotti et al. 2010

References used as basis for diet categorization

Abravaya, J.P. and Matson, J.O., 1975. Notes on a Brazilian mouse, Blarinomys breviceps (Winge). Contributions in Science of the Natural History Museum of Los Angeles County, 270, pp. 1-8

Alho, C.J.R., 1982. Brazilian Rodents: Their Habitats and Habits. Mamalian Biology in South America, pp. 143-166. Special Publications Series, Pymatuning Laboratory of Ecology, University of Pittsburgh, Linesville, Pennsylvania.

Alho, C.J.R., Pereira, L.A. and Paula, A.D., 1986. Patterns of habitat utilization by small mammal populations in cerrado biome of central Brazil. Mammalia, 50(4), pp. 447-460.

Barlow, J.C., 1969. Observations on the biology of rodents in Uruguay. Royal Ontario Museum Life Sciences Contributions, 75, pp. 1-59.

Barquez, R.M., Mares, M.A. and Ojeda, R.A., 1991. The Mammals of Tucuman. Los Mamíferos de Tucumán. Special Publication, Oklahoma Museum of Natural History, Norman, Oklahoma.

Bernal, N., Dunnum, J. and Vivar, E., 2016. Akodon aerosus. The IUCN Red List of Threatened Species 2016: e.T723A22380418. http://dx.doi.org/10.2305/IUCN.UK.2016-2.RLTS.T723A22380418.en. Downloaded on 27 January 2019.

Bezerra, A.M., Carmignotto, A.P., Nunes, A.P. and Rodrigues, F.H., 2007. New data on the distribution, natural history and morphology of Kunsia tomentosus (Lichtenstein, 1830) (Rodentia: Cricetidae: Sigmodontinae). Zootaxa, 1505, pp. 1-18.

Bezerra, A.M. and Pardiñas, U.F.J., 2016. Kunsia tomentosus (Rodentia: Cricetidae). Mammalian Species, 48(930), pp. 1-9.

Bianchini, J. and Delupi, L., 1994. Consideraciones sobre el estado sistemático de Deltamys kempi Thomas, 1917 (Cricetidae, Sigmodontinae). Physis 49, pp. 27-35.

Bilenca, D.N., Kravetz, F.O. and Zuleta, G.A., 1992. Food habits of Akodon azarae and Calomys laucha (Cricetidae, Rodentia) in agroecosystems of central Argentina. Mammalia, 56(3), pp. 371-384.

Borchert, M. and Hansen, R.L., 1983. Effects of flooding and wildfire on valley side wet campo rodents in central Brazil. Revista Brasileira de Biologia 43, pp. 229– 40.

Carvalho, F.M.V., Pinheiro, P.S., dos Santos Fernandez, F.A. and Nessimian, J.L., 1999. Diet of small mammals in Atlantic Forest fragments in southeastern Brazil. Revista Brasileira de Zoociências, 1(1), pp. 91-101.

Casella, J. and Cáceres, N.C., 2006. Diet of four small mammal species from Atlantic forest patches in South Brazil. Neotropical Biology and Conservation, 1(1), pp. 5-11.

Cuéllar, E. and Noss, A., 2003. Mamíferos del Chaco y de la Chiquitania de Santa Cruz, Bolivia. Santa Cruz: Wildlife Conservation Society & Editorial Fan.

D'Elía, G. and Teta, P., 2016. Oxymycterus nasutus (errata version published in 2017). The IUCN Red List of Threatened Species 2016: e.T15789A115129860. http://dx.doi.org/10.2305/IUCN.UK.2016-3.RLTS.T15789A22377924.en. Downloaded on 27 January 2019.

Dalby, P.L., 1975. Biology of pampa rodents (Balcarce Area, Argentina). Publications of the Museum of Michigan State University, Biological Series 5, pp. 149-271.

Davis, D.E., 1944. The capture of the Brazilian mouse Blarinomys breviceps. Journal of Mammalogy, 25(4), pp. 367-369.

Díaz, M.M. and Barquez, R.M., 2007. The wild mammals of Jujuy Province, Argentina: systematics and Distribution. In The quintessential naturalist: Honoring the life and legacy of Oliver P. Pearson, pp. 417– 578. California: University of California Publication Zoology.

Diório, D.G., 2014. Análise da espécie Bibimys labiosus (Winge 1887) (Rodentia, Sigmodontinae) ao longo da sua distribuição geográfica no Brasil. Msc Thesis, Universidade Federal de Ouro Preto.

dos Reis, S.F., Pombal, J.P., Nessimian, J.L. and Pessoa, L.M., 1996. Altitudinal distribution and feeding habits of Blarinomys breviceps (Winge, 1888) (Rodentia: Muridae). Zeitschrift Fur Saugetierkunde - International Journal of Mammalian Biology, 61, pp. 253-255.

Dunnum, J., Vargas, J., Bernal, N., Zeballos, H., Vivar, E., Patterson, B., Pardinas, U. and Jayat, J.P., 2016. Akodon albiventer (errata version published in 2017). The IUCN Red List of Threatened Species 2016 e.T725A115051226. http://dx.doi.org/10.2305/IUCN.UK.2016-3.RLTS.T725A22380752.en. Downloaded on 27 January 2019.

Dunnum, J., Vargas, J., Bernal, N., Pacheco, V., Zeballos, H. and Vivar, E., 2016. Akodon mimus (errata version published in 2017). The IUCN Red List of Threatened Species 2016: e.T746A115052068. http://dx.doi.org/10.2305/IUCN.UK.2016- 3.RLTS.T746A22383254.en. Downloaded on 27 January 2019.

Dunnum, J., Vargas, J., Bernal, N., Patterson, B., Zeballos, H. and Vivar, E., 2017. Oxymycterus paramensis (errata version published in 2018). The IUCN Red List of Threatened Species 2017: e.T115590985A123797242. http://dx.doi.org/10.2305/IUCN.UK.2017-3.RLTS.T115590985A115591155.en. Downloaded on 27 January 2019.

Eisenberg, J.F. and Redford, K.H., 1999. Mammals of the Neotropics. The Central Neotropics. Chicago: The University of Chicago Press.

Eisenberg J.F. and Redford K.H., 2000. Mammals of the Neotropics: Volume 3 (The Central Neotropics: Ecuador, Peru, Bolivia, Brazil). Chicago: The University of Chicago Press.

Ellis, B.A., Mills, J.N., Kennedy, E.J., Maiztegui, J.I. and Childs, J.E., 1994. The relationship among diet, alimentary tract morphology, and life history for five species of rodents from the central Argentine pampa. Acta Theriologica, 39(4), pp. 345-355.

Ellis, B.A., Mills, J.N., Glass, G.E., McKee Jr, K.T., Enria, D.A. and Childs, J.E., 1998. Dietary habits of the common rodents in an agroecosystem in Argentina. Journal of Mammalogy, 79(4), pp. 1203-1220.

Emmons, L.H., 2015. Genus Juscelinomys Moojen, 1965. Mammals of South America, volume 2: Rodents, pp. 225-228. Chicago: The University of Chicago Press.

Emmons, L.H. and Patton, J.L., 2012. Taxonomic revision of Bolivian Juscelinomys (Rodentia, Cricetidae) with notes on morphology and ecology. Mammalia, 76(3), pp. 285-294.

Galetti, M., Rodarte, R.R., Neves, C.L., Moreira, M. and Costa-Pereira, R., 2016. Trophic niche differentiation in rodents and marsupials revealed by stable isotopes. PLoS one, 11(4), p. e0152494.

Geise, L., Bergallo, H.G., Esberárd, C.E.I., Rocha, C.F.D. and Van Sluys, M., 2008. The karyotype of Blarinomys breviceps (Mammalia: Rodentia: Cricetidae) with comments on its morphology and some ecological notes. Zootaxa, 47(60), pp. 47-60.

Giannoni, S.M., Borghi, C.E., Dacar, M. and Campos, C.M., 2005. Main food categories in diets of sigmodontine rodents in the Monte (Argentina). Mastozoología Neotropical, 12(2), pp. 181-187.

Hershkovitz, P., 1966. South American swamp and fossorial rats of the scapteromyine group (Cricetinae, Muridae) with comments on the glans penis in murid taxonomy. Zeitschrift für Säugetierkunde 31, pp. 81-149.

Hershkovitz, P., 1994. Description of a new species of South American hocicudo, or long-nose mouse, genus Oxymycterus (Sigmodontinae, Muroidea), with a critical review of the generic content. Fieldiana Zoology 79, pp. 1-43.

Hershkovitz, P., 1998. Report on some sigmodontine rodents collected in southeastern Brazil with descriptions of a new genus and six new species. Bonner Zoologische Beiträge, 47, pp. 193–256.

Hinojosa, P.F., Anderson, S. and Patton, J.L., 1987. Two new species of Oxymycterus (Rodentia) from Peru and Bolivia. American Museum Novitates, 2898, pp. 1-17.

Huayta, A.J.D., 2016. Aspectos evolutivos de la dieta de roedores Filotinos y Akodontinos (Rodentia: Cricetidae) de los andes del sur del Perú. Bsc. thesis, Universidad Nacional Mayor de San Marcos, Lima, Peru.

Huiman, M.C.N., 2008. Dieta y morfología del estómago en roedores de los bosques montanos del departamento Huánuco, Perú. Bsc. thesis, Universidad Nacional Mayor de San Marcos, Lima, Peru.

Iriarte, A., 2008. Mamíferos de Chile. Barcelona: Lynx Edicions.

Kay R.F., and Madden R.H., 1997. Mammals and rainfall: paleoecology of the middle Miocene at La Venta (Colombia, South America). Journal of Human Evolution, 32, pp. 161–199.

Kravetz, F.O., 1972. Estudio del regimen alimentario, períodos de actividad y otros rasgos ecológicos en uma población de “Ratón Hocicudo” (Oxymycterus rufus platensis Thomas) de Punta Lara. Acta Zoologica Lilloana, 29, pp. 201-12.

Linares, O.J., 1998. Mamíferos de Venezuela. Caracas: Sociedad Conservacionista Audubon de Venezuela.

Marinho-Filho, J., Rodrigues, F.H. and Juarez, K.M., 2002. The Cerrado mammals: diversity, ecology, and natural history. The Cerrados of Brazil: Ecology and natural history of a neotropical savanna, pp. 266-284. New York: Columbia University Press.

Martinez, R.L., Bocco, M.E., Mónaco, N. and Polop, J., 1990. Winter diet in Akodon Dolores Thomas, 1916. Mammalia, 54(2), pp. 197-206.

Massoia, E., 1961. Notas sobre los cricétidos de la selva marginal de Punta Lara (Mammalia, Rodentia). Publicaciones del Museo Municipal de Mar del Plata, 1(4), pp. 115-134.

Massoia, E., 1964. Sistemática, distribución geográfica y rasgos etoecológicos de Akodon (Deltamys) kempi (Rodentia, Cricetidae). Physis, 24, pp. 299-305.

Massoia. E. and Fornes, A., 1964. Notas sobre el género Scapteromys (Rodentia-Cricetidae). I. Sistemática, distribución geográfica y rasgos etoecológicos de Scapteromys tumidus (Water house). Physis, 24, pp. 279-97.

Miranda Ribeiro, A., 1914. História Natural, Zoologia, Mamíferos. Comissão de linhas telegráficas estratégicas de Mato Grosso ao Amazonas, 13, Anexo 5.

Moojen, J., 1965. Nôvo gênero de Cricetidae do Brasil Central (Glires, Mammalia). Revista Brasileira de Biologia, 25(3), pp. 281-285.

Noblecilla, M.C., and Pacheco, V., 2012. Dieta de roedores sigmodontinos (Cricetidae) en los bosques montanos tropicales de Huánuco, Perú. Revista Peruana de Biología, 19(3), pp. 317-322.

Ojeda, R.A., Blendinger, P.G. and Brandl, R., 2000. Mammals in South American drylands: faunal similarity and trophic structure. Global Ecology and Biogeography, 9(2), pp. 115-123.

Paglia, A.P., Fonseca, G.A.B., Rylands, A.B., Herrmann, G., Aguiar, L.M.S., Chiarello, A.G. Leite, Y.L.R., Costa, L.P., Siciliano, S., Kierulff, M.C.M., Mendes, S.L., Tavares, V.C., Mittermeier, R.A. and Patton, J.L., 2012. Annotated Checklist of Brazilian Mammals, 2nd edition. Arlington: Conservation International.

Pardiñas, U.F.J., D’Elía, G. and Teta, P., 2008. Una introducción a los mayores sigmodontinos vivientes: revisión de Kunsia Hershkovitz, 1966 y descripción de un nuevo género

(Rodentia: Cricetidae). Arquivos do Museu Nacional, 66(3-4), pp. 509-594.

Pardiñas, U.F.J., Voglino, D. and Galliari, C.A., 2017. Miscellany on Bibimys (Rodentia, Sigmodontinae), a unique akodontine cricetid. Mastozoología Neotropical, 24(1), pp. 241-250.

Pardiñas, U.F.J., Myers, P., León-Paniagua, L., Ordóñez-Garza, N., Cook, J., Kryštufek, B., Haslauer, R., Bradley, R., Shenbrot, G. and Patton, J., 2017. Family Cricetidae. Handbook of the Mammals of the World, Volume 7: Rodents II. Barcelona: Lynx Edicions.

Perera, A., 2002. Los mamíferos de la Argentina y la región austral de Sudamérica. Buenos Aires: Editorial El Ateneo.

Pinotti, B.T., Naxara, L. and Pardini, R., 2011. Diet and food selection by small mammals in an old-growth Atlantic forest of south-eastern Brazil. Studies on Neotropical Fauna and Environment, 46(1), pp. 1-9.

Pizzimenti, J.J. and De Salle, R.O.B., 1980. Dietary and morphometric variation in some Peruvian rodent communities: the effect of feeding strategy on evolution. Biological Journal of the Linnean Society, 13(4), pp. 263-285.

Quiceno, C.A., 1993. Sistematica y distribución del género Akodon (Rodentia: Cricetidae) en el Valle del Cauca. Undergraduate thesis, Universidad del Valle, Cali, Colombia.

Redford, K.H., 1984. Mammalian predation on termites: tests with the burrowing mouse (Oxymycterus roberti) and its prey. Oecologia, 65, pp. 145-52.

Sahley, C.T., Cervantes, K., Pacheco, V., Salas, E., Paredes, D. and Alonso, A., 2015. Diet of a sigmodontine rodent assemblage in a Peruvian montane forest. Journal of Mammalogy, 96(5), pp. 1071-1080.

Solari, S., 2007. Trophic relationships within a highland rodent assemblage from Manu National Park, Cusco, Peru. The quintessential naturalist: Honoring the life and legacy of Oliver P. Pearson, pp. 225-240. California: University of California Publication Zoology. Suarez, O.V., 1994. Diet and habitat selection of Oxymycterus rutilans (Rodentia, Cricetidae). Mammalia, 58, pp. 225– 34.

Suarez, O. and Bonaventura S., 2001. Habitat use and diet in sympatric species of rodents of the low Parana delta, Argentina. Mammalia, 65(2), pp. 161-176.

Talamoni, S.A., Couto, D., Lopes, M.O.G. and Cordeiro-Júnior, D.A., 1999. Dieta de algumas espécies de pequenos mamíferos do sudeste brasileiro. Bios, 7(7), pp. 51-56.

Talamoni, S., Couto, D., Junior, D. and Diniz, F., 2008. Diet of some species of Neotropical small mammals. Mammalian Biology, 73, pp. 337-341.

Teta, P., Cueto, G. and Suárez, O., 2007. New data on morphology and natural history of

Deltamys kempi Thomas, 1919 (Cricetidae, Sigmodontinae) from central-eastern Argentina. Zootaxa, 1665, pp. 43-51.

Teta, P., D'elia, G., Christoff, A. and Gonzalez, E., 2016. Deltamys kempi. The IUCN Red List of Threatened Species 2016: e.T738A22338967. http://dx.doi.org/10.2305/IUCN.UK.2016-2.RLTS.T738A22338967.en. Downloaded on 27 January 2019.

Vieira, E., Paise, G., and Machado, P., 2006. Feeding of small rodents on seeds and fruits: a comparative analysis of three species of rodents of the Araucaria forest, southern Brazil. Acta Theriologica, 51, pp. 311-318.

Williams, S. and Kay, R., 2001. A Comparative Test of Adaptive Explanations for Hypsodonty in Ungulates and Rodents. Journal of Mammalian Evolution, 8, pp. 207–229.

Zevallos, C., 2014. Dieta de roedores Sigmodontinos (Rodentia: Cricetidae) en los bosques montanos del valle del Río Holpas. Bsc. thesis, Universidad Nacional Mayor de San Marcos, Lima, Peru.

Supplementary Material 3.S4: Normality and homoscedasticity tests for mechanical advantage data.

MA	Shapiro Wilk			Levene's test
	herbivore	insectivore	omnivore	
DM(inc)	0.05545	0.0001834	6.918e-05	3.058e-15
DM(mol)	0.02048	7.653e-05	0.2485	< 2.2e-16
SM(inc)	3.085e-06	9.737e-05	0.309	< 2.2e-16
SM(mol)	1.94e-05	5.827e-06	0.4963	< 2.2e-16
TM(inc)	0.7843	0.03018	0.2574	2.85e-08
TM(mol)	0.9252	0.0007288	0.5929	< 2.2e-16

Supplementary Material 3.S5: Contribution of each variable for the distribution of species on the first two principal components.

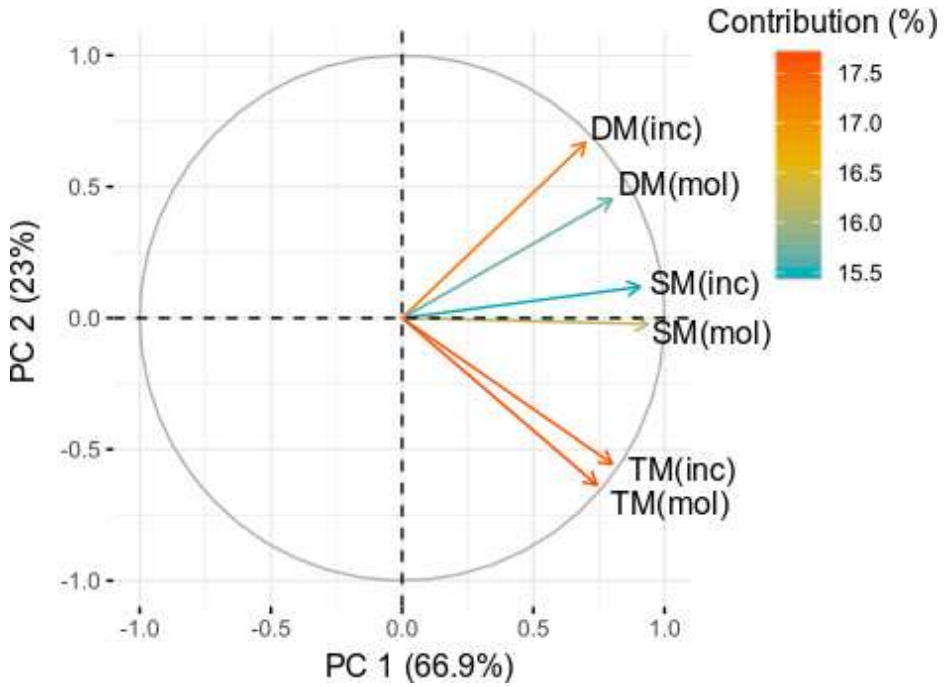

CHAPTER 4: TEMPO AND MODE OF EVOLUTION OF CRANIAL MORPHOLOGY IN AKODONTINE RODENTS

Drawing of *Akodon cursor* by Fernando Perini

TEMPO AND MODE OF EVOLUTION OF CRANIAL MORPHOLOGY IN AKODONTINE RODENTS

Rafaela V. Missagia[1,2], Daniel M. Casali[1], Bruce D. Patterson[2] and Fernando A. Perini[1]

[1]PPG - Zoologia/Departamento de Zoologia - Instituto de Ciências Biológicas, UniversidadeFederal de Minas Gerais – Av. Antônio Carlos, 6627, Pampulha, Belo Horizonte, MG, Brazil

[2]Integrative Research Center, Field Museum of Natural History, Chicago, IL 60605, USA

Abstract

The tribe Akodontini is a highly diverse group of Cricetidae rodents, and appears to be a good model for morphological evolution studies due to its diverse adaptive types and skull morphologies. Here, we test the importance of dietary adaptations and historical contingency on the evolution of the cranial complex of akodontine rodents, as well as the tribe's phylogenetic patterns of morphological disparity and convergence. Shape changes in Akodontini cranialcomplex appears to be mainly associated to rostral and mandible length, braincase height, and width of the zygomatic plate. Our model test results indicate that the evolution of Akodontini skull and mandible is strongly influenced by historical contingencies, which is corroborated by the phylogenetic signal values and the concentration of disparity towards the root. The strength of convergence was significant for some taxa that share an insectivorous diet. Despite the prevalence of historical contingencies in shaping the morphological patterns of the cranial complex of akodontines, with size and shape presenting different modes of evolution, diet appears to have a role in shaping skull and mandible morphology of akodontine rodents.

Keywords: trait evolution, Sigmodontinae, morphological disparity, convergence.

4.1. Introduction

Morphological diversity is a comparative measure that seeks out to describe the variation of form within groups at different biological levels (Wills 2001, Erwin 2007). Morphological diversity, or disparity, is often studied under an adaptational context linked to ecological and functional aspects of an organism (Wainwright 2007, Hopkins and Gerber 2018). However, the so-called constraints of morphological diversification can generally be either contingent (historical) or deterministic (ecological/adaptive), and a combination of both is what probably underlies evolutionary patterns of morphology (Erwin 2007).

The evolution of morphological diversity have been extensively explored (Foote 1997, Erwin 2007), and disparity itself have been quantified in different ways (Erwin 2007, Hopkins and Gerber 2018). In the last three decades, the availability of molecular data has increased the use of phylogenetic information in comparative studies (Felsenstein 1985, Harvey and Pagel 1991, Blomberg and Garland 2002, Garamszegi 2014), allowing the inclusion of historical factors when assessing morphological diversity, which began to be described by trait evolutionary models (Harvey and Rambaut 2000, Harmon 2010, Adams 2014) and phylogenetic patterns of morphological evolution (Harmon et al. 2003, Glor 2010).

Rodents present a distinctive skull when compared to other mammals, mainly due to the highly developed ever-grown incisors and the diastema separating them from the rest of the cheek teeth (Wood 1965, Landry 1970, Turnbull 1970). However, they manage to encompass an impressive morphological skull diversity, while maintaining their inherent morphological constraints (Samuels 2009). Part of these differences are often linked to feeding ecology (Satoh 1999, Samuels 2009, Fabre et al. 2017), and the functional influence of masticatory muscles may have led to a pattern of evolution of convergent morphologies driven by dietary preferences (Vorontzov 1979, Samuels 2009, Rowe et al. 2016). Morphological patterns of the skull on rodents, and their relation to diet, are often subject of investigation (Vorontzov 1979, Satoh et al. 2006, Samuels 2009, Cano et al. 2013, Fabre et al. 2017, Ginot et al. 2018), but only recently evolutionary patterns behind the evolution of skull shape began to be taken into consideration (e.g. Renaud et al. 2007, Álvarez et al. 2013, Casanovas-Vilar and van Dam 2013).

The tribe Akodontini is the second most diverse clade within Sigmodontinae, the most diverse subfamily of cricetid rodents. They are endemic to South America, sharing a long

evolutionary history in this continent (Maestri et al. 2019), and are highly variable in life history and ecology. The tribe includes fossorial species such as *Blarinomys* and the woolly giant rat *Kunsia*, swamp rats of the *Scapteromys* genus, and cursorial generalists belonging to the genus *Akodon* and *Necromys* (D'Elía and Pardiñas 2015). Several authors have also pointed out the occurrence of insectivorous shrew-like rats that appears to have arisen convergently within the tribe, and are mainly recognized by external and cranial characteristics (Hershkovitz 1966, Reig 1978, Missagia and Perini 2018). In addition, discontinuity in size patterns within Akodontini may also be associated to feeding ecology, since bite force is known to be related to size in vertebrates (Freeman and Lemen 2008).

The Akodontini seems to be a good model for studies of morphological evolution, due to its diversity in adaptive types and skull morphologies (Reig 1987, D'Elía and Pardiñas 2015, Missagia et al. in prep). However, macroevolutionary patterns remain, for the most part, unexplored in the group. Moreover, several studies which explore the tempo and mode of evolution of morphology in varied taxa tend to focus mostly on ecological factors as the single possible causal explanation, neglecting the possible contribution of historical contingency for theevolved forms being studied, or only accounting for evolutionary history indirectly, avoiding modeling historical factors as an explicit alternative hypothesis (Slater et al. 2010, Monteiro and Nogueira 2011, Maestri et al. 2017, Rossoni et al. 2019). Here, we aim to evaluate the evolution of the cranial complex (skull + mandible) of akodontine rodents, accessing the importance of dietary adaptations and historical contingency in a model test framework. The relative influence of phylogeny and diet on skull morphology is investigated, as well as the tribe's phylogenetic patterns of morphological disparity and convergence.

4.2. Materials and methods

4.2.1. Data collection and landmark definition

We digitized 607 skulls and 651 mandibles of 59 Akodontini species, corresponding to 71% of the tribe's recognized diversity according to Pardiñas et al. (2017). We sampled only adult specimens, determined by the presence of the third molar fully erupted, to avoid possible ontogenetic effects on morphology (Zelditch et al. 2004). A list of voucher numbers of the analyzed specimens, including housing collections, can be found in Supplementary Material 4.S1.

The 26 landmarks of the lateral view of the skull and 16 of the mandible were digitizedon tpsDig2 software (Rohlf 2007), and were treated separately in our analyses (Figure 4.1, Supplementary Material 4.S2). The landmarks were selected seeking to cover as much of the morphological variation as possible, including structures with functional significance and muscle attaching points, such as zygomatic plates and the masseteric ridge. Some landmarks could not be marked in some skulls due to breakage, and they were estimated with the function *estimate.missing* using the "TPS" method of the *geomorph* package. The landmarks were then superimposed with a Generalized Procrustes Analysis (GPA) to remove the effects of scale, position, and orientation. The resulting GPA coordinates were submitted to a principal component analysis using the *plotTangentspace* function, to extract the scores for each principal component. The mean shape (PC scores) and logarithmized centroid size of skull and mandible was calculated for each species using the *aggregate* function. For the shape data (both skull and mandible), we used the first three principal components, selected by a Broken Stick model (MacArthur 1957), using the *evplot* function of *ggplot2* package (Wickham 2016). All subsequent analyses used those datasets as inputs, unless stated otherwise. Landmark superimposition, principal component analysis and average values calculations were performed on the *geomorph* and *stats* packages (R Core Team 2017, Adams et al. 2019). This and all subsequent analyzes were conducted in the R environment (R Core Team 2017), using the phylogenetic hypothesis of Maestri et al. (2107, 2019).

4.2.2. Diet data categories

In order to compare skull shape and size with diet, we used the defined dietary categories for Akodontini species from Missagia et al. (in prep). Quantitative information of proportion of items from stomach content analysis was used as the basis for allocating species in the different diet categories (Pineda-Munoz and Alroy 2014). When not available, species were categorized according to qualitative data from the literature based on their primary consumed resources (Samuels 2009, Pineda-Munoz and Alroy 2014). Species were classified into three dietary categories: 1) omnivores: generalist species without clear food preferences or with balanced proportions of items on their stomachs; 2) herbivores: species that consume vegetal matter preferentially, or with vegetal matter representing more than 70% of their stomach content; 3) insectivores: species that consume animal matter preferentially, or with animal matter representing more than 70% of their stomach content. Species for which we could not find more

detailed information (10.17% of analyzed species) were here treated as omnivores, following Maestri et al. (2017).

4.2.3. General patterns of disparity and convergence

For exploratory visualization of the morphological disparity associated to shape, we plotted the values of the three PCs, pairwise, in morphospace with the function *phylomorphospace* in the package *phytools* (Revell 2012). To visualize this variation in time, we also plotted traitgrams for each PC and size data with function *phenogram* in package *phytools* (Revell 2012). The trees depicted on the traitgrams and morphospaces were colored according to the three dietary categories, as defined above, and to the four Akodontini major lineages: the "*Scapteromys"* lineage, comprising *Scapteromys, Kunsia, Blarinomys, Brucepattersonius, Lenoxus* and *Bibimys* genera; the "*Oxymycterus*" lineage, comprising *Oxymycterus* and *Juscelinomys*; the "*Necromys*" lineage, including *Necromys, Podoxymys, Thalpomys,* and *Thaptomys*; and the "*Akodon*" lineage, comprising the *Akodon* genus, together with *Deltamys* and *Castoria* (Maestri et al. 2019) (Supplementary Material 4.S3 depicts lineages and diet categories in the Akodontini tree).

4.2.4. Phylogenetic signal

The phylogenetic signal of skull size and shape was evaluated using K-mult (Adams 2014), the multivariate generalization of K statistic, with the function *physignal* in package *geomorph*. For size data, which is univariate, this analysis is reduced to the standard K statistic (Blomberg et al. 2003). Values of K statistic equal to 1 indicates a perfect expectation of phylogenetic signal given a Brownian Motion (BM) model of evolution (Felsenstein 1985). Values above 1 indicates a stronger signal than expected by BM, with closely related taxa more similar (and distantly related taxa more dissimilar) than expected, suggesting some phylogenetic conservatism at the tips relative to the base of the tree. Values below 1 indicate that closely related taxa are more divergent (and distantly related taxa more similar) than BM would suggest, which can be interpreted as a liability toward the tips relative to the base (Blomberg et al. 2003). To access significance, p-values were calculated comparing our estimates to a null distribution (no signal) obtained after 999 random permutations of the tip values (Blomberg et al. 2003, Adams 2014).

4.2.5. Disparity through time

The multivariate disparity through time, measured by the mean disparity within clades at each node on a phylogeny (Harmon et al. 2003), was evaluated using function *dtt* of *geiger* package (Harmon 2008). The function also creates a distribution of 1000 simulated curves, generated with a Brownian Motion model. The empirical and simulated curves were compared with Morphological Disparity Index (MDI) (Slater 2010) to evaluate its significance with a two- tailed test. MDI measures the area delimited by the empirical curve and the median of the simulated curves. Positive values of MDI indicates that within-clade disparity exceeds BM expectations, relative to between-clade disparity, suggesting a Late Burst (Edwards et al. 2015)or OU model (Hansen 1997, Butler and King 2004), while negative MDI values are suggestive of an Early Burst model (Harmon et al. 2003), where within-clade disparities are below of BM expectations, relative to between-clade disparity (Machado et al. 2018, Rossoni et al. 2019).

4.2.6. Node decomposition of trait-based diversity

To evaluate how the morphological disparity in the Akodontini cranial complex is distributed among the nodes of the phylogeny, we applied the diversity decomposition method developed by Pavoine et al. (2010), using the function *decdiv* in *adiv* package (Pavoine 2018). We generated euclidean distance matrices for size and shape with function *dist* in package *stats*. The function *decdiv* offers different ways to decompose disparity among nodes. The first option (O1), uses the original algorithm described by Pavoine (2010) in which the beta trait diversity measure at each node is weighted by the relative number of descending species of the given node. So, as the number of descending species increases, the node disparity values also increase, which is useful to explore disparity in communities as a density-dependent measure. Two other options (O2 and O3) were implemented in *decdiv*, which avoid weighing nodes by diversity, and apply a penalization for the number of descending lineages, so as the number of the descending lineages increases, the node disparity slightly decreases. There are also two other options (O4 and O5) which simply decompose O1 into a disparity measure independent of the weights relative to the number of descending lineages (O4), and just these weights (O5). Since exploratory results of O2, O3 and O4 returned effectively identical results, we applied O2 to our datasets, as it is more adequated than O1 for assessing the morphological disparity *per se*, since option O1 can attribute great disparity to a node as a function of its lineage density, despite lowor moderate morphological

disparity. The function *rtestdecdiv* was used to conduct the three testsdeveloped by Pavoine et al. (2010) over the distribution of the disparity in the nodes of the Akodontini tree. These tests evaluate if the observed distribution can be explained by a single node (1), a few nodes (2) and if there is a root skewed concentration in disparity (3). Root skewness reflects phylogenetic signal, with closely related species more similar to each other than expected by chance, while changes skewed to the tips are indicative of greater trait dissimilarity among closely related taxa (Pavoine et al. 2010, Rossoni et al. 2019). The significance was accessed with 1000 permutations of the tip values, being the first two tests one- tailed (greater), and the third, two-tailed. All analyses with *decdiv/rtestdecdiv* used Euclidean Diversity Index (EDI) as a measure of quadratic entropy to estimate the trait-based diversity, andnodes were ranked according to the complexity criterion.

4.2.7. Model fit and model selection

In order to evaluate the influence of both historical contingency and ecology in the evolutionary rates and regimes of shape and size of the skull and mandible of Akodontini, we defined 17 models considering divisions of the tree structure (major clades) and diet, and applied them to each dataset, mapping them with function *make.simmap* of package *phytools*. We incorporated the error associated with the estimated mean values of each species in all analyses. Model fitting and comparinson was performed in *mvMORPH* (Clavel et al. 2015). We used three models of continuous trait evolution: Brownian Motion (BM), Ornstein-Uhlenbeck (OU), and Early-Burst (EB). While the first two models are available as single or multi-rate versions, EB is a single rate model. The models were fitted using the functions *mvBM*, *mvOU* and *mvEB*, setting "sparse" as the method to calculate the log-likelihood during the model fitting process. The historical factor was accounted for by dividing the tree into the four main lineages, and testing if the rates and regimes are independent of any particular division of the tree structure (BM1, OU1, EB), or if multiple regimes are associated with two (BMM2, OUM2), three (BMM3, OUM3) or all four (BMM4, OUM4) major lineages in our tree. The ecological hypotheses were defined using the dietary categories defined above. We tested each category against all other taxa in a pairwise comparison: omnivores x specialists (D_BMM2_1, D_OUM2_1), insectivores x non- insectivores (D_BMM2_2, D_OUM2_2) and herbivores x non-herbivores (D_BMM2_3, D_OUM2_3); and each of the three diets as a distinct category: omnivores x insectivores x herbivores (D_BMM3_4, D_OUM3_4) (Supplementary Material 4.S3). The single rate models (BM1/OU1/EB) also

function as controls in the case of no effect of diet in the rates and number of evolutionary regimes. The support for each model was evaluated with the Akaike Information Criterion corrected for small sample size (AICc), and models were ranked by ΔAICc (models with ΔAICc values above four are poorly supported by the data) (Harmon 2018) and Akaike weights (Burnham and Anderson 2002). To account for the stochastic reconstruction of the ancestral states while mapping the categories in tree, we performed 100 replications, summarizing the mean and median values of ΔAICc and Akaike weights and their respective standard errors.

4.2.8. Exploring morphological convergence

In order to evaluate a putative convergent pattern of evolution in the cranial shape of one set of taxa, given their distribution in phylomorphospace and in the first axis depicted on the traitgram, we verify the derived nature of values of PC1 for these taxa with Ancestral States Reconstruction (ASR). The taxa suspected of converge were: *Oxymycterus amazonicus, O. dasytrichus, O. delator, O. hiska, O. nasutus, O. paramensis, O. quaestor, O. rufus, Akodon mimus, Podoxymys roraimae, Blarinomys breviceps, Brucepattersonius soricinus,* and *Lenoxus apicalis*. We reconstructed the ancestral states of PC1 using ASR with function *estim* in package *mvMORPH*, using the best-fitting model obtained in our model selection analyses. We used the function *contMap* of the package *phytools* to plot the ASRs. Additionally, we performed the ASR for diet categories with *ace* function of the *phytools* package in order to evaluate the most likely ancestral diet for Akodontini. We evaluated the Mk models "Equal Rates" (ER) and "Symmetric" (SYM), and chose the best using Akaike weights and ΔAICc.

Given the results of the previous analysis, we used the approach advised by Stayton (2015), available on *convevol* package (Stayton 2018), to test the frequency and strength of convergence in the skull shape of akodontine rodents. Since *convevol* requires a previous hypothesis of convergence, we applied the set of taxas defined based on visual inspection of phylomorphospace and traitgram plot for PC1. For the frequency (C5), we estimated the number of independent entrances in the defined convergent area (the area of phylomorphospace occupiedby taxa listed above) with function *convnum* and access significance, after 100 simulations, with function *convnumsig*.

We also estimated the strength of convergence using four metrics (C1, C2, C3 and C4)

available in *convevol*, checking the significance after 100 simulations and an estimated cutoff value, with function *convratsig*. C1 measures the distance in morphospace "closed" by convergent evolution for pairs of tip lineages in the convergent space (*D*tip), compared to the maximum distance between these taxa (*D*max; tip or ancestral) in those lineages (C1 = 1 - (*D*tip -*D*max)). It ranges from 0 to 1, being 0 a case of no convergence at all, and 1 that the lineages are effectively indistinguishable, given the traits under analysis. Since many tips can be involved in convergence, the mean of all pairwise comparisons is calculated. C1 gives a measure of relative convergence and do not differentiate cases where the clustering in the morphospace resulting from convergence is from different absolute magnitudes, but it is possible to estimate the degree of convergence in absolute terms using C2 (C2 = *D*max - *D*tip). Stayton (2015) also proposed two measures that allows C2 to be standardised as a proportion (like is C1), and hence comparable between datasets. C3 standardize C2 relative to the total morphological branch length leading to the ancestors of all convergent lineages (C3 = C2/tot.*lineage*), while C4 does it relative to the total morphological branch length in the clade subsuming all convergent lineages (C4 = C2/tot.*clade*).

4.3. Results

4.3.1. General patterns of disparity and convergence

In the PCA results for the skull, PC1 accounts for 40.6% of total variation, while PC2 was responsible for 11.5%, and PC3, 8.8% (Supplementary Material 4.S4). When analysing the mandible, PC1 accounted for 32.9%, PC2 for 14.2%, and PC3 for 13.3% (Supplementary Material 4.S4). The general distribution of species on the morphospace is depicted in Figures 4.2 and 4.3. For the skull, the first PC is mainly related to shape differences of the rostrum and zygomatic plate, with shorter rostra and wider zygomatic plates towards more negative values and longer rostra and narrow zygomatic plates towards more positive values (Figure 4.2). PC2 is related to differences on the height of the braincase, with lower braincases towards more positivevalues and higher braincases towards negative values (Figure 4.2). PC3 represents a pattern of shape change reflecting the relative position of some elements, such as auditory bulla and zygomatic plate, which are displaced ventrally towards higher values, and dorsally towards lowervalues (Figure 4.2).

In the PCA results for the mandible, PC1 shows its general shortening towards more negative values (Figure 4.3), while PC2 is related to changes of the masseteric ridge, which is

closer to the first molar alveolus towards more negative values, and of the angular process, which is more posteriorly displaced towards positive values (Figure 4.3). PC3 depicts changes in the posterior part of the mandibular ramus, including the position of the distal end of the coronoid process, displaced posteriorly towards lower values, and a general shortening of this region, with the angular and condylar processes anteriorly displaced toward lower values (Figure4.3).

When plotting the phylogeny on trait space, we can observe a greater phylogenetic structuring in the traitgram that represents the mandible when compared to the skull (Figures 4.4, 4.5, 4.6 and 4.7). The skull traitgram shows that the first lineages to diverge occupy both extremes along PC1 axis. For the mandible, we see that the lineages are less overlapped, with the *"Oxymycterus"* lineage occupying the upper portion of the traitgram (Figure 4.4). The two sets of data (skull and mandible) show a greater disparity towards the root. Both skull and mandible datasets show a greater dispersion of the *"Scapteromys"* lineage along PC2 axis, occupying both ends (Figure 4.4). On the traitgram depicting the PC3 of skull shape, the *"Oxymycterus"* lineage occupies the upper portion, and the *"Akodon"* lineage, the lower, with the other two lineages overlapping in the middle (Figure 4.5). When considering mandible shape, the *"Oxymycterus"* and *"Necromys"* lineages are concentrated in the middle of the traitgram, while the upper and lower extremes are occupied by the *"Akodon"* and *"Scapteromys"* lineages, respectively (Figure4.5).

For diet, it is possible to see a greater overlap of insectivorous species on the traitgram depicting PC1 of the skull, which converge towards one end. The same is not true when considering PC2, in which both insectivorous and herbivorous species are widespread along the axis (Figure 4.6). For the mandible, species of *Oxymycterus* appear isolated and more concentrated towards higher values of the PC1 traitgram (Figure 4.6). There is no separation among the different diet categories in PC3 of the two datasets (Figure 4.7). When plotting the size for both skull and mandible, the traitgram shows a separation between *Kunsia, Scapteromys*, and the "*Oxymycterus*" lineage towards more positive values in relation to the other species, with the "*Scapteromys"* lineage occupying both size extremes (Figures 4.5 and 4.7).

4.3.2. Phylogenetic signal

All four datasets (size and shape, for skull and mandible) showed a significant phylogenetic signal ($p < 0.05$) in K-mult analyses. For all of them, but skull shape, K statistic wasabove one, while skull shape K statistic returned a value slightly below the BM expectations. K statistic for

size was higher than to shape in both cases, and values for mandible were higher thanfor skull for size and shape (skull shape = 0.9825, skull size = 1.1562, mandible shape = 1.0509, mandible size = 1.2282).

4.3.3. Disparity through time

General patterns of within-clade disparity through time were very similar for the size and shape of both skull and mandible in Akodontini. The DTT plots show an initial peak of within-clade disparity, followed by a general decrease of these values through time, with the empirical curve being below the median of the simulated for most of the time. Around 3.0 myrs, the within-clade disparity of shape had a small peak with a plateau that lasted until approximately

3.7 myrs, in which the line of the empirical curve overlapped (skull shape) or crossed above (mandible shape) the simulated median, although keeping within the variation of the null curves. All MDI values were positive, but in all cases they were non-significant, failing to reject the null hypothesis that BM describes the observed temporal trends in disparity better than alternative models (Figure 4.8). Values of MDI were higher for size datasets, both for skull and mandible.

4.3.4. Node decomposition of trait-based diversity

When applying *decdiv* to skull size and shape datasets, all three tests were significant, suggesting a tendency of disparity to be concentrated close to the root in a few or even in a single node, what also constitutes a strong indicative of phylogenetic signal (Table 4.1, Figures 4.9 and 4.10). For mandible shape, there is a root skewed pattern with disparity concentrated in a few,but not a single node, while for mandible size, the only significant test was to root-skewness, with the disparity more dispersed across the nodes of the tree (Table 4.1, Figures 4.9 and 4.10). Node contribution for disparity varied across datasets, and we consider here values corresponding to >10% as a substantial contribution of a node to entire clade disparity (Figures

4.9 and 4.10, Supplementary Material 4.S5). We observed a greater concentration of nodes related to major values of disparity in the "*Scapteromys"* lineage, irrespective of dataset. The "*Necromys"* lineage is also of some noticeable importance for disparity distribution relative to skull shape.

4.3.5. Model fit and model selection

For the skull size data, the best relative support was found for BMM4 model (mean Akaike weight = 0.66 +/- 0.01), which receives moderate support, followed by D_BMM2_1 (mean Akaike weight = 0.07 +/- 0.01), which receive a much lower relative support (mean ΔAICc = 5.47+/- 0.57) (Supplementary Material 4.S6). For skull shape, the best fitting model was OU1 (mean Akaike weight = 0.57 +/- 0.01), and the second best fit was OUM2 (mean Akaike weight = 0.20 +/- 0.01). It is not possible to exclude this second model as a plausible candidate (mean ΔAICc = 2.58+/- 0.26) (Supplementary Material 4.S6).

For the mandible size, BMM4 is also the most well supported model (mean Akaike weight = 0.59 +/- 0.01), and D_BMM2_1 is the second best fit (mean Akaike weight = 0.07 +/- 0.01), fitting much worse than BMM4 (mean ΔAICc = 4.96+/- 0.18) (Supplementary Material 4.S6). Mandible shape is best described by a OU1 model (mean Akaike weight = 0.57 +/- 0.02), as for skull shape, followed by D_OUM2_3 (mean Akaike weight = 0.11 +/- 0.01), also with a considerably worse fit than OU1 (mean ΔAICc = 5.48+/- 0.45). (Supplementary Material 4.S6).

4.3.6. Exploring morphological convergence

The ASR analyses indicates insectivory as the most likely ancestral state for Akodontini (Supplementary Material 4.S7), and derived values for the skull shape of the convergent taxa according to the PC1 data (Supplementary Material 4.S8). The ER model had the best fit for diet dataset (Akaike weight = 0.53) but SYM model cannot be rejected, (Akaike weight = 0.47, ΔAICc = 0.2). Despite that, both models are consistent in reconstruct the ancestral diet as insectivorous, although the best fitted model attributes higher probability to this than the second best does (Supplementary Material 4.S7).

The results of *convevol* indicated that four lineages entered the convergent area of phylomorphospace (Supplementary Material 4.S9), but the frequency test (C5) is non-significant. However, all measures of strength of selection (C1-C4) were significant ($p < 0.01$) (Table 4.2).

4.4. Discussion

4.4.1. General patterns of disparity over time and clades

Changes of shape in the tribe Akodontini seem to be mainly associated to rostral and mandible length, braincase height, and width of the zygomatic plate. Although not decisive in

shaping skull and mandible morphology according to our best fitted models, the main morphological changes seem to be related to muscle insertions (e.g. zygomatic plate) and functional traits (e.g. rostrum and mandible length), which has been demonstrated to be correlated to bite force (Maestri et al. 2016, Missagia et al. in prep). Similar results were found for sigmodontine rodents elsewhere (Maestri et al. 2017, Missagia and Perini 2018), and may indicate a pattern consistent with the influence of diet in skull and mandible shape, with herbivorous and insectivorous species occupying opposite ends of the axis.

The distribution of species in the morphospace and traitgrams shows larger disparities in the "*Scapteromys"* lineage, which is further supported by our other results. The plots of disparity through time, despite its conformance to a global pattern which does not deviate from a BM model, presents a considerably low between-clade disparity closer to the root, indicating that the lineages initially occupied a similar region in morphospace, but with considerable within-clade disparity, which decreases toward the tips. When decomposing the disparity among the nodes of the tree, it becomes clear that this within-clade disparity is strongly concentrated in the nodes closer to the origin of the "*Scapteromys"* lineage and in some of its internal nodes. The phylogenetic signal results are also in overall agreement with the concentrated disparity towards the root of tree, at least for size data, with the shape signal closer to the expectation of BM. The "*Scapteromys"* clade achieved high levels of morphological specialization that seems to accompany a corresponding ecological diversity, since it accounts for most of different dietary and locomotory habits found in the tribe (Hershkovitz 1966, Maestri et al. 2017, Missagia et al. in press and references therein).

DTT plots for skull and mandible shape show some evidence of a slight increase in within-clade disparity around 3.0-3.7 myrs, which is coincident with the greater contribution of the node in the origin of the clade comprising *Podoxymys*, *Thalpomys,* and *Thaptomys* observed in *decdiv* results. The disparity in phylomorphospace and traitgrams among *Podoxymys* and its sister taxa is also evident. This increase in disparity is probably due to a dietary shift in *Podoxymys*, which departs from the generalized skull of its sister lineage, lying instead next to other akodontine insectivorous species.

4.4.2. Ecological and historical factors

Although previous studies have observed that some changes in the skull and mandible of Akodontini can be related to feeding ecology (Samuels 2009, Maestri et al., 2016, Missagia et al.

in prep), our analyses indicated that skull and mandible variation in shape and size were better fitted to models that do not reflect a major influence of diet as a general pattern for the tribe.

Our results for size data indicate that the evolution of Akodontini skull and mandible are strongly influenced by historical contingencies, with each of the four main clades evolving with its unique random tendencies according to a multi-regime Brownian Motion. Shape data were better fitted to an OU processes with a single optima, which can be related to other ecological aspects not measured here. Ornstein-Uhlenbeck models are usually interpreted as models of adaptive evolution in which stabilizing selection pull the traits towards optimum values, or as traits following shifts in peaks in an adaptive landscape (Hansen 1997, Butler and King 2004, Cressler et al. 2015), and some unsampled ecological variables could be responsible for such adaptive processes in the evolution of skull and mandible shapes. Nevertheless, OU also reflects historical contingency or "phylogenetic inertia", represented by evolutionary constraints in trait variance due to previous evolutionary dynamics, which could have been adaptive or not (Hansen and Orzack 2005). This interpretation on the constrained evolution is consistent with the phylogenetic signal values obtained in this study, all closer to the expectancy of a disparity described by BM, with size presenting a slightly stronger evidence for phylogenetic conservativeness than shape. The phylogenetic conservativeness is also evident with the concentration of disparity towards the root obtained for all datasets in *decdiv* analyses. Despite this overall consistent scenario about the phylogenetic signal, disparity distribution and selected model, we should be cautious not to go further and associate them with specific process, since their relationship is not always straightforward, with various processes being able to generate a similar pattern (Harmon et al. 2008, Harmon 2018).

A two-rate OU model (different rates between the two main clades) could not be discarded for skull shape, and is probably reflecting the high levels of shape disparity found for the *"Scapteromys"* lineage. The most morphologically disparate lineage is also the least diverse, indicating that a positive correlation between the two variables should not be steadily assumed (Alhajeri and Steppan 2018a). The pattern found for this lineage, of high disparity distributed in few species, may have arisen in three main ways. First, it could be due to higher rates of morphological evolution, causing species to become more distinct from one another in the same time interval of a lineage with relatively lower rates (Larsson et al. 2012, Hopkins 2016). Second, it could be reflecting the same amount of rates of morphological evolution of the other three main

lineages, but during longer time periods (Erwin 2007). Considering the dated tree, thelineage is indeed the oldest among the four, considering only their crown group, and had more time of independent evolution to diverge in the morphospace. The third option is that we see only part of the evolutionary history of the "*Scapteromys"* lineage, which could include more species that went extinct within that time frame (Foote 1997, Ciampaglio et al. 2001, Sidlauskas 2008). These species would fill the morphospace so that the ones we see today would not be so disparate between each other, and would actually form part of a morphological continuum, as seems to be the case for its sister lineage. The three scenarios are not mutually exclusive, and may have co-occurred in different levels.

Apparently, akodontine skull and mandible features are less evolutionary labile than ecological aspects like diet (Verde Arregoitia 2016), probably requiring higher selective pressures over longer timescales in order to diverge from their ancestral condition. Other studies found similar results concerning the importance of historical factors in shaping rodent skull (Renaud et al. 2007, Álvarez et al. 2011, 2013, 2017, Casanovas-Vilar and van Dam 2013). This may be explained in some part by the morphological versatility of the rodent cranial complex that can successfully exploit different resources, reflecting one-to-many relationships between form and function (Landry 1970, Wainwrigth et al. 2005, Zelditch et al. 2017). This versatility is what probably allows their opportunistic feeding behaviour (Rowe et al. 2011, Verde Arregoitia 2016, Zelditch et al. 2017), which may be partially responsible for their evolutionary success (Esselstyn et al. 2012). It is also noteworthy that models related to diet receive some non- negligible support, sometimes being the second best model, although still with a lower fit than the best models. This can be indicative that diet have some causal influence in the form of skull and mandible in Akodontini, but as a secondary factor, maybe related to some dietary classes butnot others (Maestri et al. 2017).

4.4.3. Convergence

The ancestral state reconstruction for diet shows a higher probability of insectivory at the root of Akodontini. Although derived, the convergent skull shape appears mainly in primitively insectivorous lineages, with the exception of *A. mimus* and *P. roraimae*, which seem to have gone through a dietary shift from omnivory to insectivory. The versatility of the skull allows an ecological diversity without an apparent morphological diversity (Maestri et al. 2017, Zelditch et

al. 2017), but morphological convergence of rodents related to diet shifts is well-documented (Samuels 2009, Rowe et al. 2016). Convergence of rodents that feed on animal matter involves changes in the masticatory apparatus related to the demands of catching prey (Samuels 2009). At the same time, high muscle forces are dispensable when little or no plant material needs to be processed (Samuels 2009, Maestri et al. 2016). Insectivory related skull convergence is described for several muroid lineages (Rowe et al. 2016, Fabre et al. 2017, Martinez et al. 2018), and evidence of a similar pattern for some Akodontini species was also found here. The frequency of convergent events was not significant for Akodontini as a whole, in agreement of our model selection results. However, the strength of convergence, which focus only on the convergent set of taxa, was significant. This further illustrates how different levels of analysis for the same data can offer different perspectives over evolutionary phenomena, allowing to diagnose patterns sometimes obscured by more general approaches (Hopkins and Smith 2015, Slater 2015, Burns and Sidlauskas 2019).

Some insectivorous species did not converge in the morphospace, which may indicate the prevalence of historical contingencies in their morphology. As stated above, morphology alone may not be a limiting factor due to the ecological versatility of the rodent skull. In addition, some species seems to be more dependent on invertebrates as resources, which is possibly reflected on their convergent specialized morphology for increasing hunting efficiency (Samuels 2009). This may not be the case for the species lacking insectivorous morphological specializations, which possibly have broader trophic niches and rely on other sources of energy (Landry 1970, Verde Arregoitia 2016).

4.5. Conclusion

Our knowledge about the diet of rodents is still limited in important ways (Verde Arregoitia 2016), and the diet categories used here are essentially a simplification of a complex ecological character (Baab et al. 2014, Pineda-Munoz and Alroy 2014). Rodents are mostly opportunistic on their eating behavior, with diet varying according to locality, season and presence of competitors (Landry 1970, Meserve et al. 1988, Verde Arregoitia 2016). It has been suggested that dietary categories should take morphological specializations that reflects mechanical challenges into account (Santana et al. 2010, Verde Arregoitia 2016). In addition, thecryptic nature of rodents

makes it difficult to obtain this kind of ecological data, and the diet of a species is often inferred from punctual and sparse information from few individuals (Pineda- Munoz and Alroy 2014, Verde Arregoitia 2016). Furthermore, other ecological factors that may be affecting the morphology of the cranial complex, like locomotory habits and habitat, were not evaluated here (Agrawal 1967, Álvarez et al. 2013, Becerra et al. 2014, Alhajeri and Steppan 2018b, Camargo et al. 2019).

It is important to consider that the choice of models that better describe trait evolution is limited to the options that are provided, which may reflect our own limitations on identifying major drivers of diversification (e.g. Pennel et al. 2015). In addition, the fact that some akodontine species were not sampled here should be taken into account, and its addition in futurestudies may have impacts on these results. Sampling limitation of the specimens should also be considered (Silvestro et al. 2015), and the results found here are limited to a small sample representing the variation of an entire species.

Our results show the importance of testing for historical factors when investigating adaptive scenarios, which is sometimes not considered. The cranial complex of akodontine rodents seems to be evolving according to historical contingencies, with size and shape presenting different modes of evolution. Feeding ecology apparently have a secondary role in shaping skull and mandible morphology, with the evolution of specialist insectivores appearing convergently in the tribe.

Acknowledgements

We would like to thank the curators from other mammal collections (AMNH, Robert Voss; USNM, Darrin Lunde; MCNM, Claudia Costa; MN, João Oliveira) who allowed access of specimens under their care. We also thank Daniela Rossoni, Fábio Machado, Renan Maestri, and Julien Clavel who kindly provided useful information concerning comparative methods and the mvMORPH package. Coordenação de Aperfeiçoamento de Pessoal de Nível Superior gave financial support (CAPES - Finance Code 0001) through regular (R.V.M. and D.M.C) and sandwich (R.V.M.) fellowships (88881.133833/2016-1).

4.6. References

Adams, D.C., 2014. A generalized K statistic for estimating phylogenetic signal from

shape and other high-dimensional multivariate data. Systematic Biology, 63(5), pp. 685-697.

Adams, D.C., M. L. Collyer, and Kaliontzopoulou, A., 2019. Geomorph: Software for geometric morphometric analyses. R package version 3.1.0. https://cran.r-project.org/package=geomorph.

Agrawal, V.C., 1967. Skull adaptations in fossorial rodents. Mammalia, 31(2), pp. 300-312.

Alhajeri, B.H. and Steppan, S.J., 2018a. Ecological and ecomorphological specialization are not associated with diversification rates in muroid rodents (Rodentia: Muroidea). Evolutionary Biology, 45(3), pp. 268-286.

Alhajeri, B.H. and Steppan, S.J., 2018b. A phylogenetic test of adaptation to deserts and aridity in skull and dental morphology across rodents. Journal of Mammalogy, 99(5), pp. 1197-1216.

Álvarez, A., Perez, S.I. and Verzi, D.H., 2011. Ecological and phylogenetic influence on mandible shape variation of South American caviomorph rodents (Rodentia: Hystricomorpha). Biological Journal of the Linnean Society, 102(4), pp. 828-837.

Álvarez, A., Perez, S.I. and Verzi, D.H., 2013. Ecological and phylogenetic dimensions of cranial shape diversification in South American caviomorph rodents (Rodentia: Hystricomorpha). Biological Journal of the Linnean Society, 110(4), pp. 898-913.

Álvarez, A., Arévalo, R.L.M. and Verzi, D.H., 2017. Diversification patterns and size evolution in caviomorph rodents. Biological Journal of the Linnean Society, 121(4), pp. 907-922.

Baab, K.L., Perry, J.M., Rohlf, F.J. and Jungers, W.L., 2014. Phylogenetic, ecological, and allometric correlates of cranial shape in Malagasy lemuriforms. Evolution, 68(5), pp. 1450-1468.

Becerra, F., Echeverría, A.I., Casinos, A. and Vassallo, A.I., 2014. Another one bites the dust: bite force and ecology in three caviomorph rodents (Rodentia, Hystricognathi). Journal of Experimental Zoology Part A: Ecological Genetics and Physiology, 321(4), pp. 220- 232.

Blomberg, S.P., Garland, T. and Ives, A.R., 2003. Testing for phylogenetic signal in comparative data: behavioral traits are more labile. Evolution, 57(4), pp. 717-745.

Burnham, K.P., and Anderson, D.R., 2002. Model selection and multimodel inference: A practical information-theoretic approach. New York: Springer-Verlag.

Burns, M.D. and Sidlauskas, B.L., 2019. Ancient and contingent body shape

diversification in a hyperdiverse continental fish radiation. Evolution, 73(3), pp. 569-587.

Butler, M.A. and King, A.A., 2004. Phylogenetic comparative analysis: a modeling approach for adaptive evolution. The American Naturalist, 164(6), pp. 683-695.

Camargo, N.F., Machado, L.F., Mendonça, A.F. and Vieira, E.M., 2019. Cranial shape predicts arboreal activity of Sigmodontinae rodents. Journal of Zoology, https://doi.org/10.1111/jzo.12659.

Cano, A.R.G., Fernández, M.H. and Álvarez-Sierra, M.Á., 2013. Dietary ecology of Murinae (Muridae, Rodentia): a geometric morphometric approach. PLoS One, 8(11), p. e79080.

Casanovas-Vilar, I. and van Dam, J., 2013. Conservatism and adaptability during squirrel radiation: what is mandible shape telling us? PLoS One, 8(4), p. e61298.

Ciampaglio, C.N., Kemp, M. and McShea, D.W., 2001. Detecting changes in morphospace occupation patterns in the fossil record: characterization and analysis of measures of disparity. Paleobiology, 27(4), pp. 695-715.

Clavel, J., Escarguel, G. and Merceron, G., 2015. mvMORPH: an R package for fitting multivariate evolutionary models to morphometric data. Methods in Ecology and Evolution, 6(11), pp. 1311-1319.

Cressler, C.E., Butler, M.A. and King, A.A., 2015. Detecting adaptive evolution in phylogenetic comparative analysis using the Ornstein–Uhlenbeck model. Systematic Biology, 64(6), pp. 953-968.

D'Elía, G. and Pardiñas, U.F.J., 2015. Tribe Akodontini Vorontsov 1959. Mammals of South America, Volume 2: Rodents, pp. 140-144. Chicago: University of Chicago Press.

Edwards, D.L., Melville, J. Joseph, L. and Keogh J.S., 2015. Ecological divergence, adaptive diversification, and the evolution of social signaling traits: an empirical study in arid Australian lizards. American Naturalist, 186, pp. E144–E161.

Erwin, D.H., 2007. Disparity: morphological pattern and developmental context. Palaeontology, 50(1), pp. 57-73.

Esselstyn, J.A., Achmadi, A.S. and Rowe, K.C., 2012. Evolutionary novelty in a rat with no molars. Biology Letters, 8(6), pp. 990-993.

Fabre, P.H., Herrel, A., Fitriana, Y., Meslin, L. and Hautier, L., 2017. Masticatory muscle architecture in a water-rat from Australasia (Murinae, Hydromys) and its implication for the evolution of carnivory in rodents. Journal of Anatomy, 231(3), pp. 380-397.

Felsenstein, J., 1985. Phylogenies and the comparative method. The American Naturalist, 125(1), pp.1-15.

Freeman, P.W., and Lemen, C.A., 2008. A simple morphological predictor of bite force in rodents. Journal of Zoology, 275(4), pp. 418-422.

Foote, M., 1997. The evolution of morphological diversity. Annual Review of Ecology and Systematics, 28(1), pp.129-152.

Garamszegi, L.Z. (ed), 2014. Modern phylogenetic comparative methods and their application in evolutionary biology. Berlin: Springer-Verlag.

Ginot, S., Claude, J., and Hautier, L., 2018. One skull to rule them all? Descriptive and comparative anatomy of the masticatory apparatus in five mouse species. Journal of Morphology 279(9), pp. 1234-1255.

Glor, R.E., 2010. Phylogenetic insights on adaptive radiation. Annual Review of Ecology, Evolution, and Systematics, 41, pp. 251-270.

Hansen, T. F., 1997. Stabilizing selection and the comparative analysis of adaptation. Evolution, 51, pp. 1341–1351.

Hansen, T.F. and Orzack, S.H., 2005. Assessing current adaptation and phylogenetic inertia as explanations of trait evolution: the need for controlled comparisons. Evolution, 59(10), pp. 2063-2072.

Harmon, L., 2018. Phylogenetic comparative methods: learning from trees. CreateSpace Independent Publishing Platform. https://lukejharmon.github.io/pcm/

Harmon, L.J., Schulte, J.A., Larson, A. and Losos, J.B., 2003. Tempo and mode of evolutionary radiation in iguanian lizards. Science, 301(5635), pp. 961-964.

Harmon, L.J., Weir, J.T., Brock, C.D., Glor, R.E. and Challenger, W., 2008. W: GEIGER: investigating evolutionary radiations. Bioinformatics, 24, pp. 129-131.

Harmon, L.J., Losos, J.B., Jonathan Davies, T., Gillespie, R.G., Gittleman, J.L., Bryan Jennings, W., Kozak, K.H., McPeek, M.A., Moreno-Roark, F., Near, T.J. and Purvis, A., 2010. Early bursts of body size and shape evolution are rare in comparative data. Evolution: International Journal of Organic Evolution, 64(8), pp. 2385-2396.

Harvey, P.H. and Pagel, M.D., 1991., The comparative method in evolutionary biology. Oxford: Oxford University Press.

Harvey, P.H. and Rambaut, A., 2000. Comparative analyses for adaptive radiations.

Philosophical Transactions of the Royal Society of London. Series B: Biological Sciences, 355(1403), pp. 1599-1605.

Hershkovitz, P., 1966. South American swamp and fossorial rats of the scapteromyine group (Cricetinae, Muridae) with comments on the glans penis in murid taxonomy. Zeitschrift für Säugetierkunde, 31, pp. 81-149.

Hopkins, M.J. and Smith, A.B., 2015. Dynamic evolutionary change in post-Paleozoic echinoids and the importance of scale when interpreting changes in rates of evolution. Proceedings of the National Academy of Sciences, 112(12), pp. 3758-3763.

Hopkins, M.J, 2016. Magnitude versus direction of change and the contribution of macroevolutionary trends to morphological disparity. Biological Journal of the Linnean Society, 118(1), 116-130.

Hopkins, M.J. and Gerber, S., 2018. Morphological disparity. Evolutionary developmental biology: a reference guide, pp. 1-12. Cham: Springer International Publishing.

Larsson, H.C., Dececchi, T.A., and Harrison, L.B., 2012. Morphological largess: can morphology offer more and be modeled as a stochastic evolutionary process. From clone to bone: the synergy of morphological and molecular tools in paleobiology, pp. 84-115. Cambridge: Cambridge University Press.

Landry Jr, S.O, 1970. The Rodentia as omnivores. The Quarterly Review of Biology, 45(4), pp. 351-372.

MacArthur, R., 1957. On the relative abundance of bird species. Proceedings of the National Academy of Sciences of the United States of America, 43, pp. 293-295.

Machado, F.A., Zahn, T.M.G. and Marroig, G., 2018. Evolution of morphological integration in the skull of Carnivora (Mammalia): changes in Canidae lead to increased evolutionary potential of facial traits. Evolution, 72(7), pp. 1399-1419.

Maestri, R., Patterson, B.D., Fornel, R., Monteiro, L.R., and de Freitas, T.R.O., 2016. Diet, bite force and skull morphology in the generalist rodent morphotype. Journal of Evolutionary Biology, 29(11), pp. 2191-2204.

Maestri, R., Monteiro, L.R., Fornel, R., Upham, N.S., Patterson, B.D. and de Freitas, T.R.O., 2017. The ecology of a continental evolutionary radiation: Is the radiation of sigmodontine rodents adaptive? Evolution, 71(3), pp. 610-632.

Maestri, R., Upham, N.S. and Patterson, B.D., 2019. Tracing the diversification history of

a Neogene rodent invasion into South America. Ecography, 42(4), pp. 683-695.

Martinez, Q., Lebrun, R., Achmadi, A.S., Esselstyn, J.A., Evans, A.R., Heaney, L.R., Miguez, R.P., Rowe, K.C. and Fabre, P.H., 2018. Convergent evolution of an extreme dietary specialisation, the olfactory system of worm-eating rodents. Scientific Reports, 8(1), p. 17806.

Meserve P.L., Lang B.K. and Patterson B.D., 1988. Trophic relationships of small mammals in a Chilean temperate rainforest. Journal of Mammalogy 69(4), pp. 721-730.

Missagia, R.V. and Perini, F.A., 2018. Skull morphology of the Brazilian shrew mouse Blarinomys breviceps (Akodontini; Sigmodontinae), with comparative notes on Akodontini rodents. Zoologischer Anzeiger 277, pp. 148-161.

Missagia, R.V., Patterson, B.D. and Perini, F.A., in press. Stable isotopic signatures and the trophic diversification of akodontine rodents. Manuscript submitted to Evolutionary Ecology.

Missagia, R.V., Patterson, B.D. and Perini, F.A., in prep. Jaw functional morphology reflects diet in akodontine rodents. Manuscript in preparation.

Monteiro, L.R. and Nogueira, M.R., 2011. Evolutionary patterns and processes in the radiation of phyllostomid bats. BMC Evolutionary Biology, 11(1), p. 137.

Pagel, M., 1994. Detecting correlated evolution on phylogenies: a general method for the comparative analysis of discrete characters. Proceedings of the Royal Society of London. Series B: Biological Sciences, 255(1342), pp. 37-45.

Pardiñas, U.F.J., Myers, P., León-Paniagua, L., Ordóñez-Garza, N., Cook, J., Kryštufek, B., Haslauer, R., Bradley, R., Shenbrot, G. and Patton, J., 2017. Family Cricetidae (true hamsters, voles, lemmings and New World rats and mice). Handbook of the Mammals of the World, Volume 7: Rodents II, pp. 204-279. Barcelona: Lynx Edicion.

Pavoine, S., Baguette, M. and Bonsall, M.B., 2010. Decomposition of trait diversity among the nodes of a phylogenetic tree. Ecological Monographs, 80(3), pp. 485-507.

Pavoine, S., 2018. adiv: Analysis of Diversity. R package version 1.2. https://CRAN.R-project.org/package=adiv

Pennell, M.W., FitzJohn, R.G., Cornwell, W.K. and Harmon, L.J., 2015. Model adequacy and the macroevolution of angiosperm functional traits. The American Naturalist, 186(2), pp. E33-E50.

Pineda-Munoz, S. and Alroy, J., 2014. Dietary characterization of terrestrial mammals. Proceedings of the Royal Society B: Biological Sciences, 281(1789), pp. 20141173.

R Core Team., 2017. R: A language and environment for statistical computing. R Foundation for Statistical Computing, Vienna, Austria. URL https://www.R-project.org/.

Reig, O.A., 1987. An assessment of the systematics and evolution of the Akodontini, with the description of new fossil species of Akodon (Cricetidae, Sigmodontinae). Fieldiana Zoology, 39, pp. 347-399.

Renaud, S., Chevret, P. and Michaux, J., 2007. Morphological vs. molecular evolution: ecology and phylogeny both shape the mandible of rodents. Zoologica Scripta, 36(5), pp. 525- 535.

Revell, L.J., 2012. phytools: an R package for phylogenetic comparative biology (and other things). Methods in Ecology and Evolution, 3(2), pp. 217-223.

Rohlf, F.J., 2007. tps serie softwares. http//life.bio.sunysb.edu/ morph/

Rossoni, D.M., Costa, B.M., Giannini, N.P. and Marroig, G., 2019. A multiple peak adaptive landscape based on feeding strategies and roosting ecology shaped the evolution of cranial covariance structure and morphological differentiation in phyllostomid bats. Evolution. https://doi.org/10.1111/evo.13715

Rowe, K.C., Aplin, K.P., Baverstock, P.R. and Moritz, C., 2011. Recent and rapid speciation with limited morphological disparity in the genus Rattus. Systematic Biology, 60(2), pp. 188-203.

Rowe, K.C., Achmadi, A.S. and Esselstyn, J.A., 2016. Repeated evolution of carnivory among Indo-Australian rodents. Evolution, 70(3), pp. 653-665.

Samuels, J.X., 2009. Cranial morphology and dietary habits of rodents. Zoological Journal of the Linnean Society, 156(4), pp. 864-888.

Santana, S.E., Dumont, E.R. and Davis, J.L., 2010. Mechanics of bite force production and its relationship to diet in bats. Functional Ecology, 24(4), pp. 776-784.

Satoh, K., 1999. Mechanical advantage of area of origin for the external pterygoid muscle in two murid rodents, Apodemus speciosus and Clethrionomys rufocanus. Journal of Morphology, 240(1), pp. 1-14.

Satoh, K. and Iwaku, F., 2006. Jaw muscle functional anatomy in northern grasshopper mouse, Onychomys leucogaster, a carnivorous murid. Journal of Morphology 267, pp. 987-999.

Sidlauskas, B., 2008. Continuous and arrested morphological diversification in sister clades of characiform fishes: a phylomorphospace approach. Evolution: International Journal of Organic Evolution, 62(12), pp. 3135-3156.

Silvestro, D., Kostikova, A., Litsios, G., Pearman, P.B. and Salamin, N., 2015. Measurement errors should always be incorporated in phylogenetic comparative analysis. Methods in Ecology and Evolution, 6(3), pp. 340-346.

Slater, G.J., Price, S.A., Santini, F. and Alfaro, M.E., 2010. Diversity versus disparity and the radiation of modern cetaceans. Proceedings of the Royal Society B: Biological Sciences, 277(1697), pp. 3097-3104.

Slater, G.J., 2015. Iterative adaptive radiations of fossil canids show no evidence for diversity- dependent trait evolution. Proceedings of the National Academy of Sciences, 112(16), pp. 4897-4902.

Stayton, C.T., 2015. The definition, recognition, and interpretation of convergent evolution, and two new measures for quantifying and assessing the significance of convergence. Evolution, 69(8), pp. 2140-2153.

Stayton, C.T. 2018. convevol: Analysis of Convergent Evolution. R package version 1.3. https://CRAN.R-project.org/package=convevol

Turnbull, W.D., 1970. Mammalian masticatory apparatus. Fieldiana Geology 18, pp. 147–356. Verde Arregoitia, L.D., 2016. Rethinking Omnivory in Rodents. doi:10.20944/preprints201609.0017.v1

Vorontsov, N.N., 1979. Evolution of the alimentary system in myomorph rodents. Washington: Smithsonian Institution and the National Science Foundation.

Wainwright, P.C., 2007. Functional versus morphological diversity in macroevolution. Annual Review of Ecology, Evolution, and Systematics, 38, pp. 381-401.

Wainwright, P.C., Alfaro, M.E., Bolnick, D.I. and Hulsey, C.D., 2005. Many-to-one mapping of form to function: a general principle in organismal design?. Integrative and Comparative Biology, 45(2), pp. 256-262.

Wickham, H. 2016. ggplot2: Elegant Graphics for Data Analysis. New York: Springer-Verlag. Wills, M.A., 2001. Morphological disparity: a primer. Fossils, phylogeny, and form, pp. 55-144. Boston: Springer.

Wood, A.E., 1965. Grades and clades among rodents. Evolution, 19, pp. 115-130.

Zelditch, M.L., Lundrigan, B.L. and Garland Jr, T., 2004. Developmental regulation of skull morphology. I. Ontogenetic dynamics of variance. Evolution & Development, 6(3), pp. 194-206.

Zelditch, M.L., Ye, J., Mitchell, J.S. and Swiderski, D.L., 2017. Rare ecomorphological convergence on a complex adaptive landscape: Body size and diet mediate evolution of jaw shape in squirrels (Sciuridae). Evolution, 71(3): 633-649.

4.7. Figures

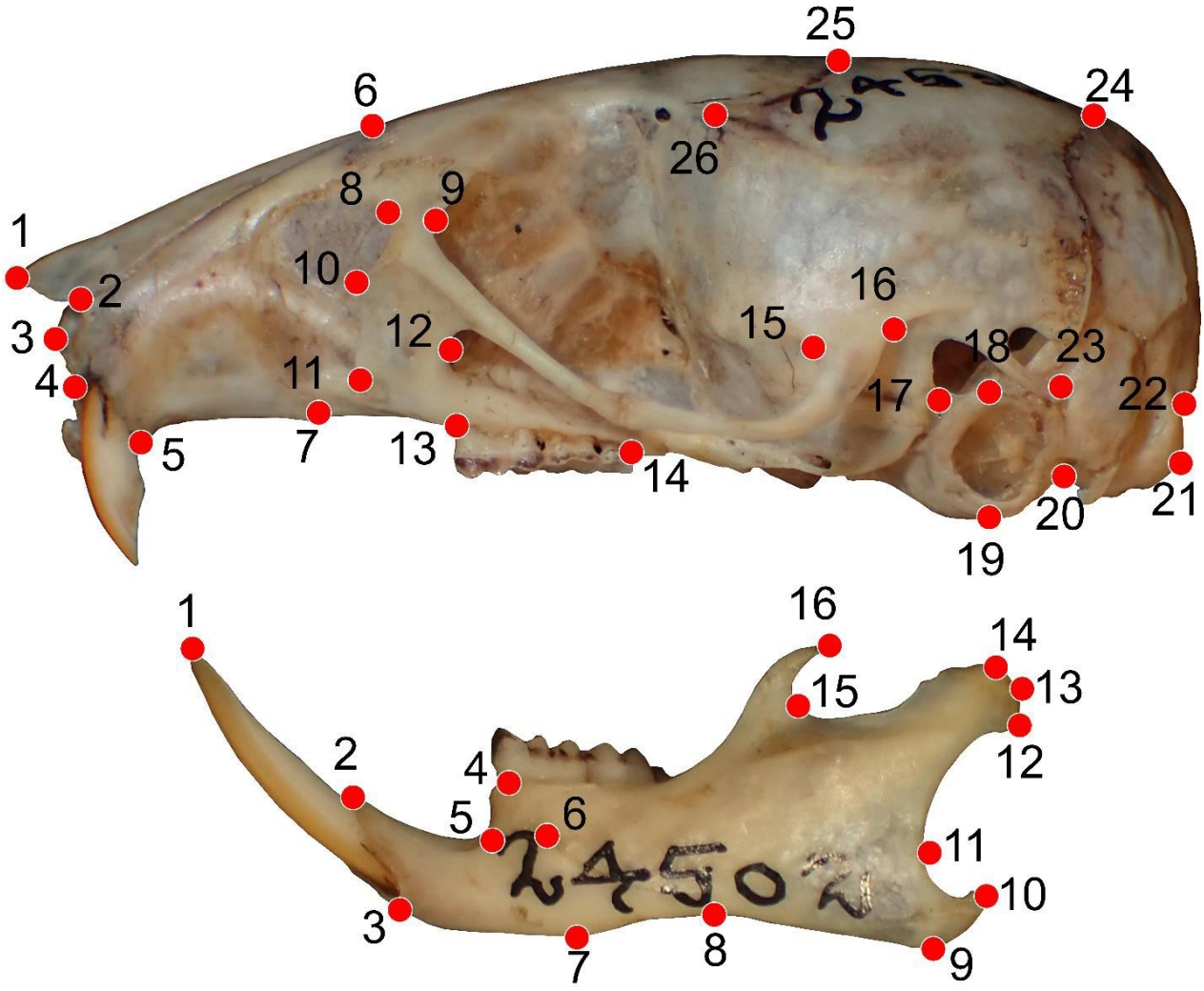

Figure 4.1. Landmark locations used in this study shown on *Akodon aerosus* skull (a; FMNH 24536) and mandible (b; FMNH 24502). See detailed descriptions of landmarks in Supplementary Material 4.S2.

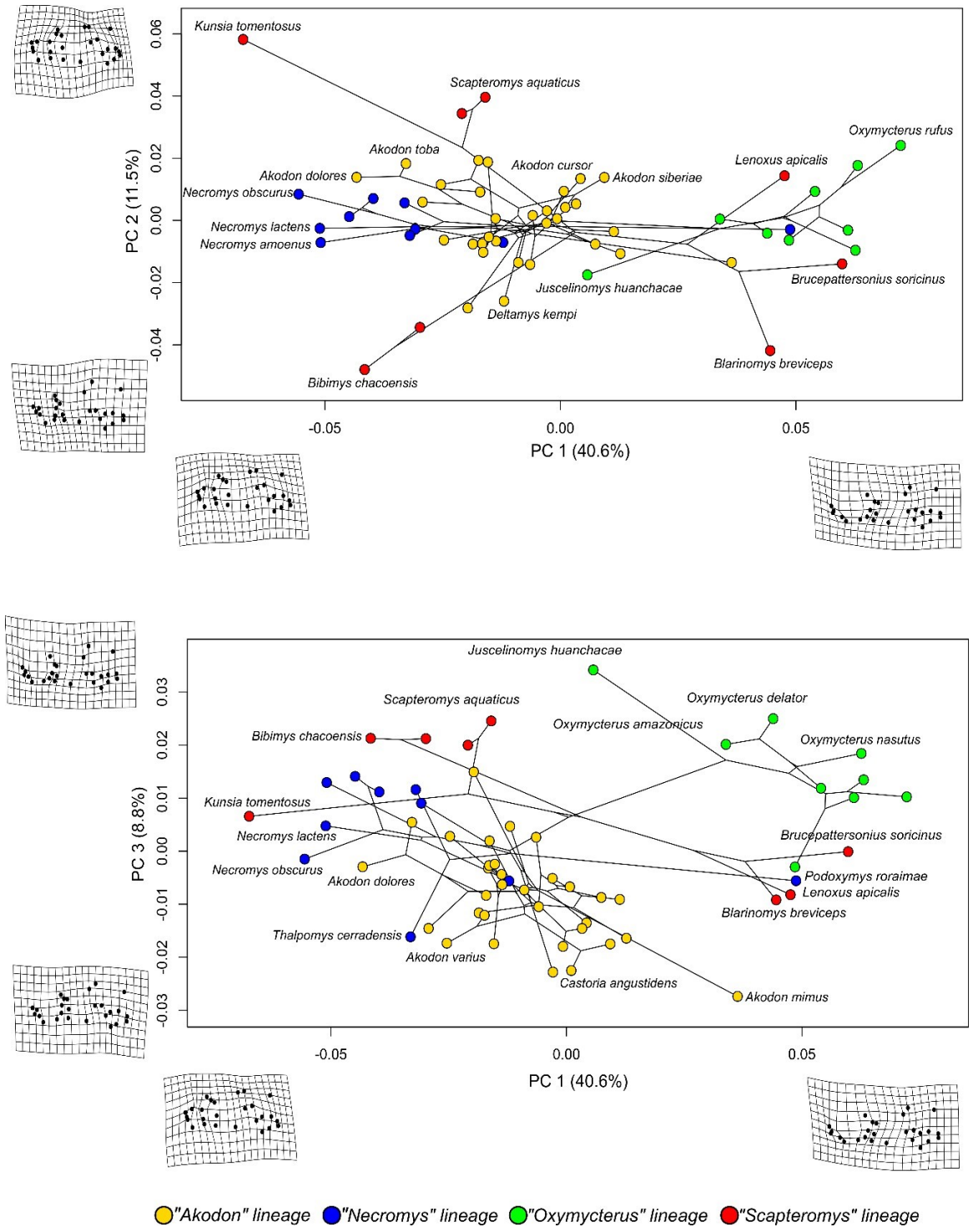

Figure 4.2. Phylomorphospace plots of the first principal component plotted with the second (above) and third (below) principal components for the skull dataset. Labels represent the four lineages.

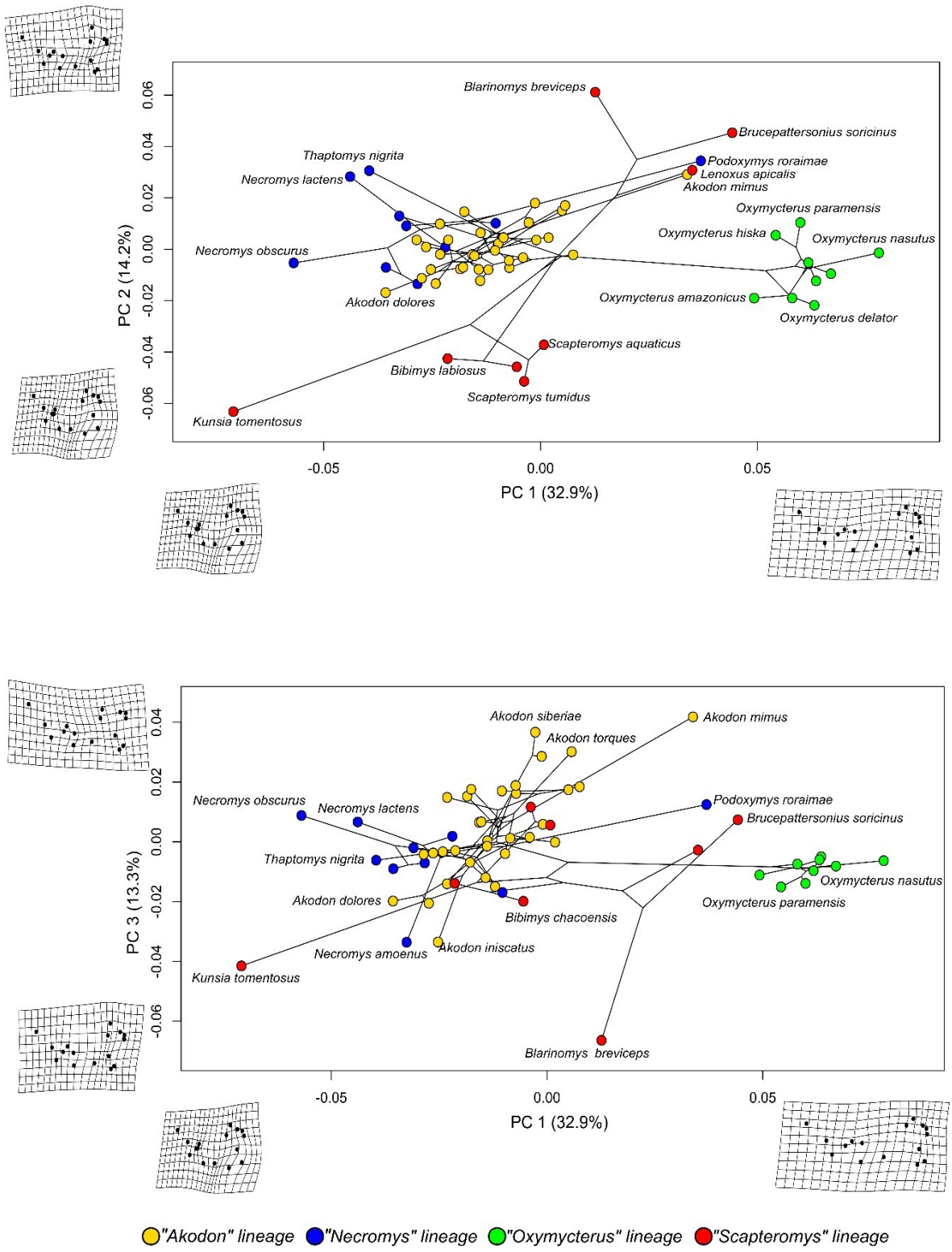

Figure 4.3. Phylomorphospace plots of the first principal component plotted with the second (above) and third (below) principal components for the mandible dataset. Labels represent the four lineages.

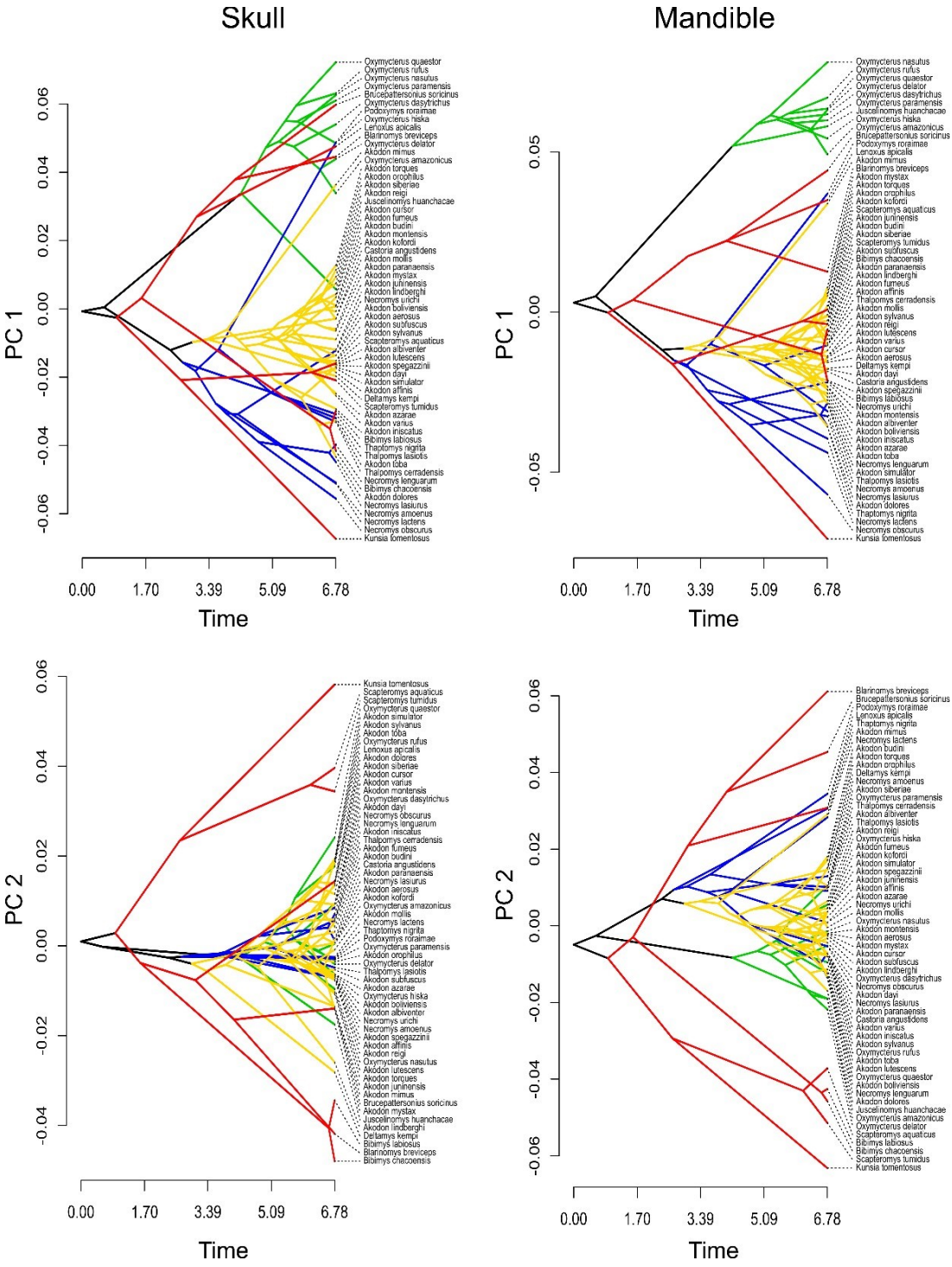

Figure 4.4. Traitgrams illustrating PC1 and PC2 values for the skull, at right, and mandible, at left. Tips of the phylogenies are arrayed along the x axis, showing the species trait values. Tree branches are colored according to the four main lineages (colors match those on Figures 4.2 and 4.3).

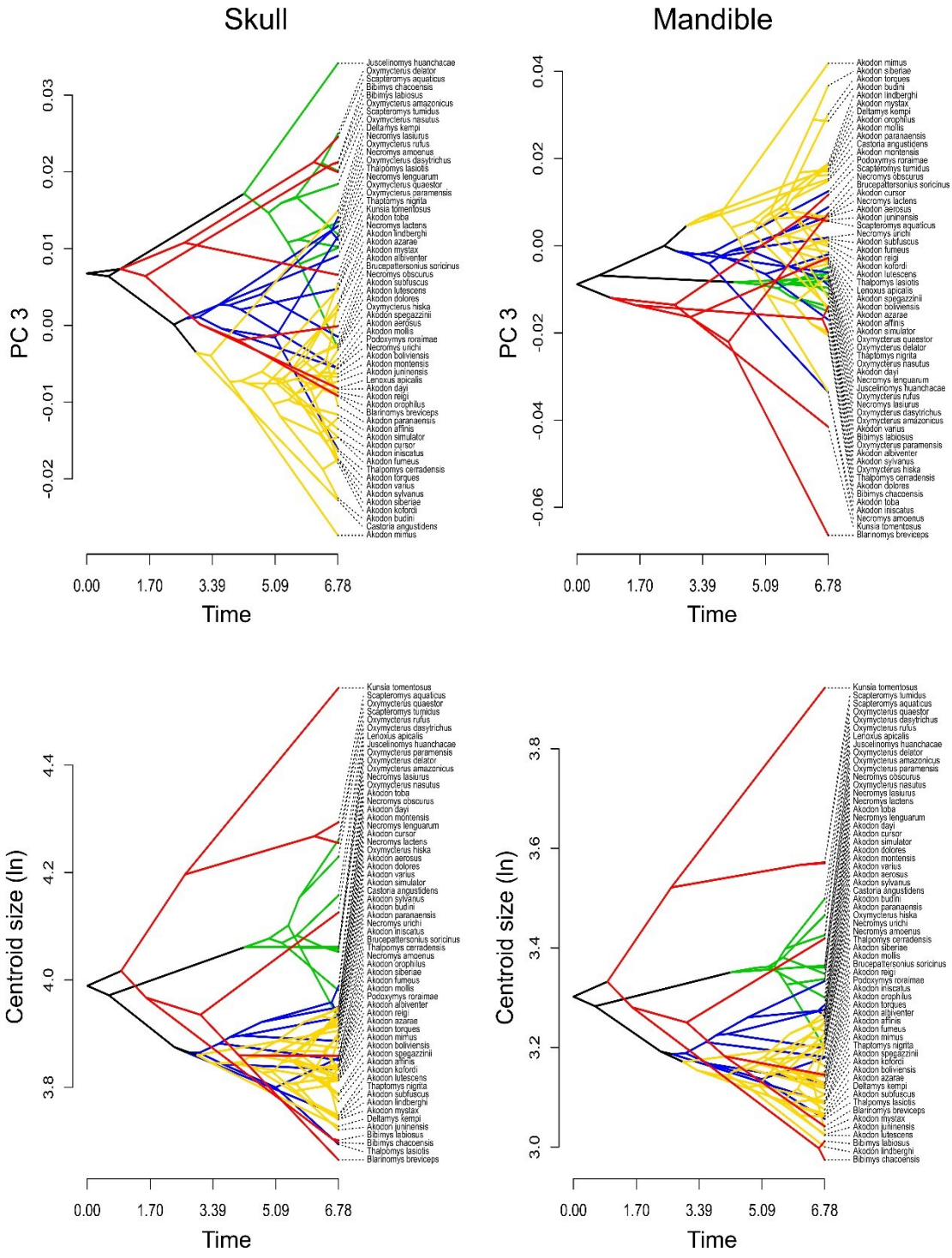

Figure 4.5. Traitgrams illustrating PC3 and logarithm of centroid size values for the skull, at right, and mandible, at left. Tips of the phylogenies are arrayed along the x axis, showing the species trait values. Tree branches are colored according to the four main lineages (colors match those on Figures 4.2 and 4.3).

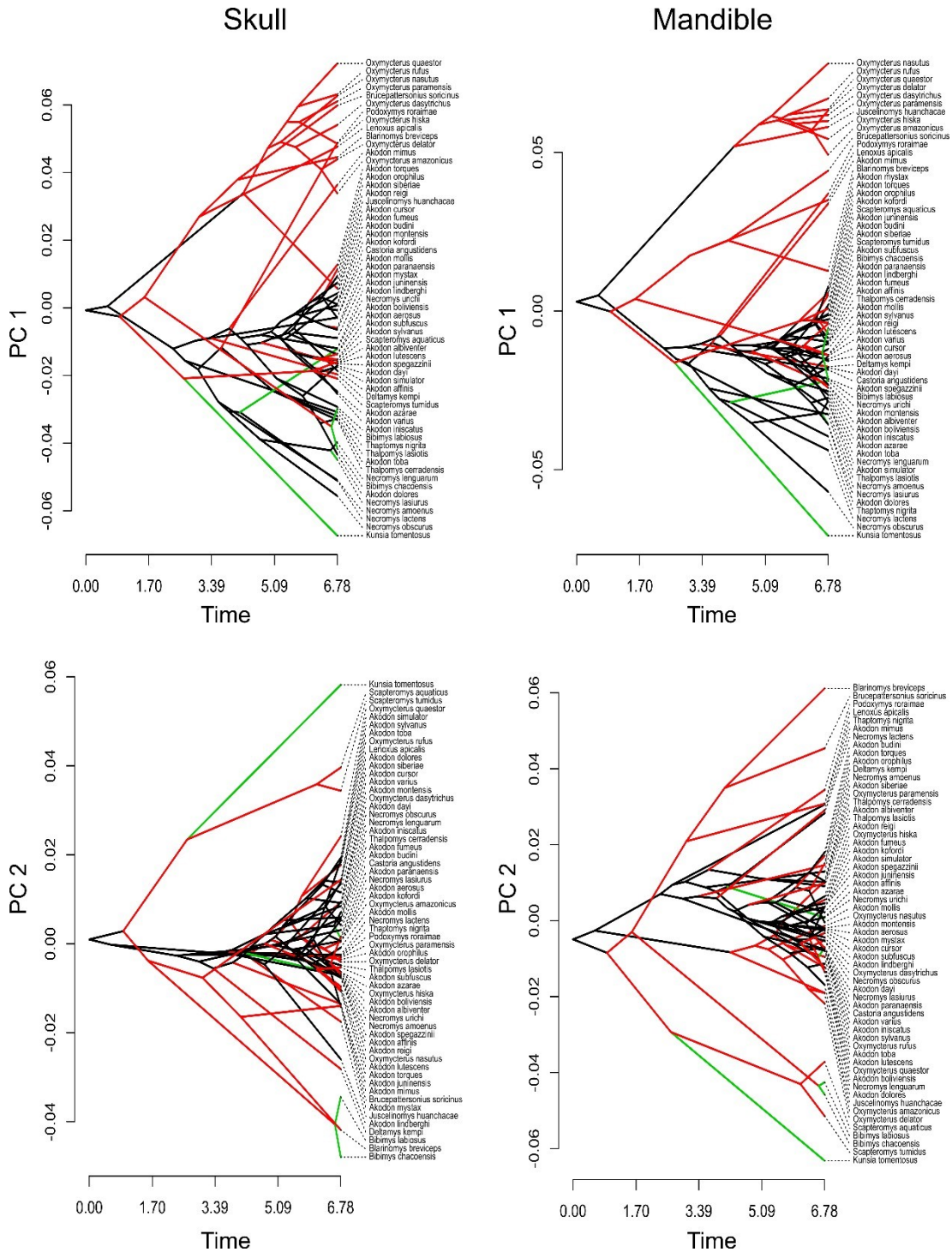

Figure 4.6. Traitgrams illustrating PC1 and PC2 values for the skull, at right, and mandible, at left. Tips of the phylogenies are arrayed along the x axis, showing the species trait values. Tree branches are colored according to the three diet categories (red: insectivores; green: herbivores; black: omnivores).

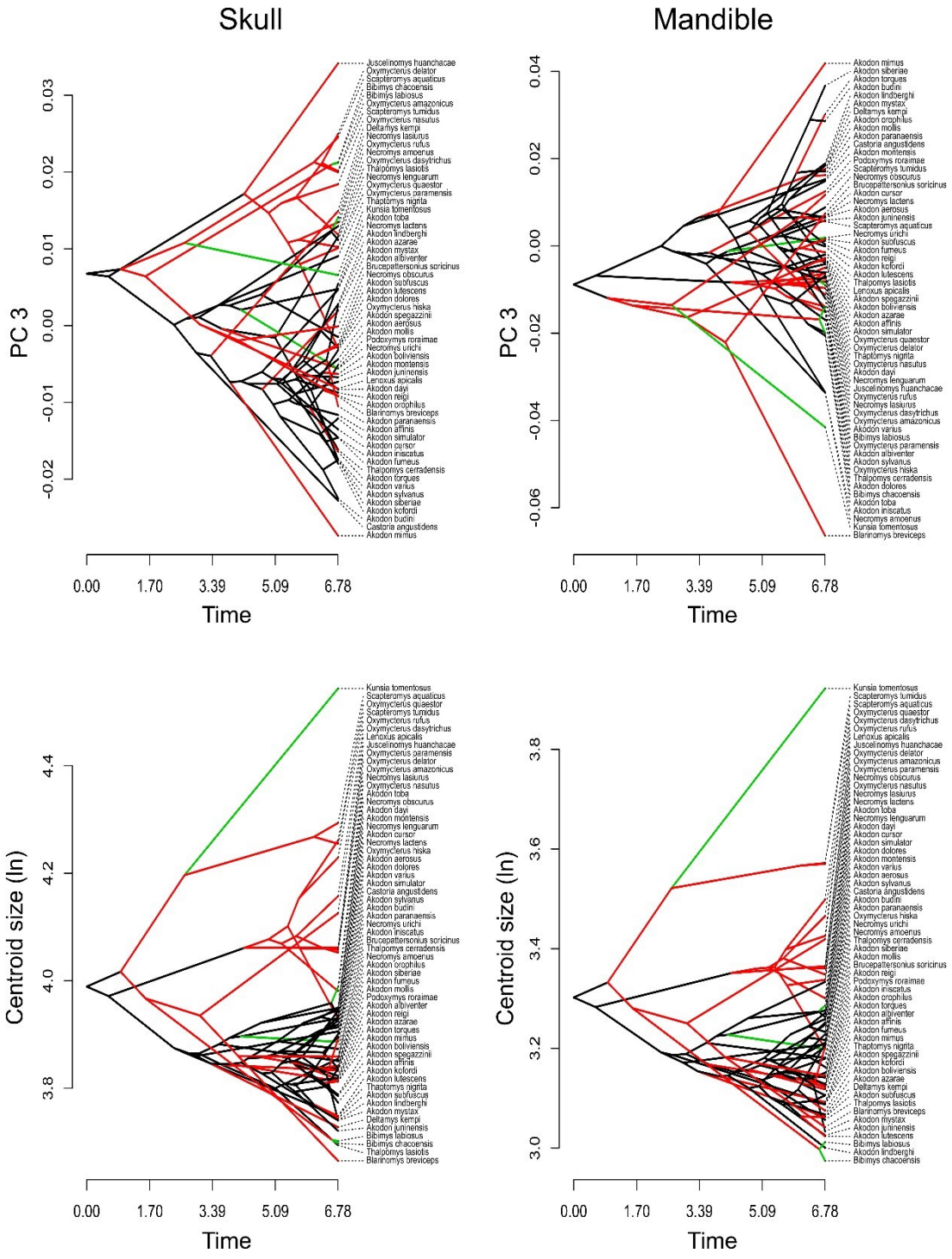

Figure 4.7. Traitgrams illustrating PC3 and logarithm of centroid size values for the skull, at right, and mandible, at left. Tips of the phylogenies are arrayed along the x axis, showing the species trait values. Tree branches are colored according to the three diet categories (red:insectivores; green: herbivores; black: omnivores).

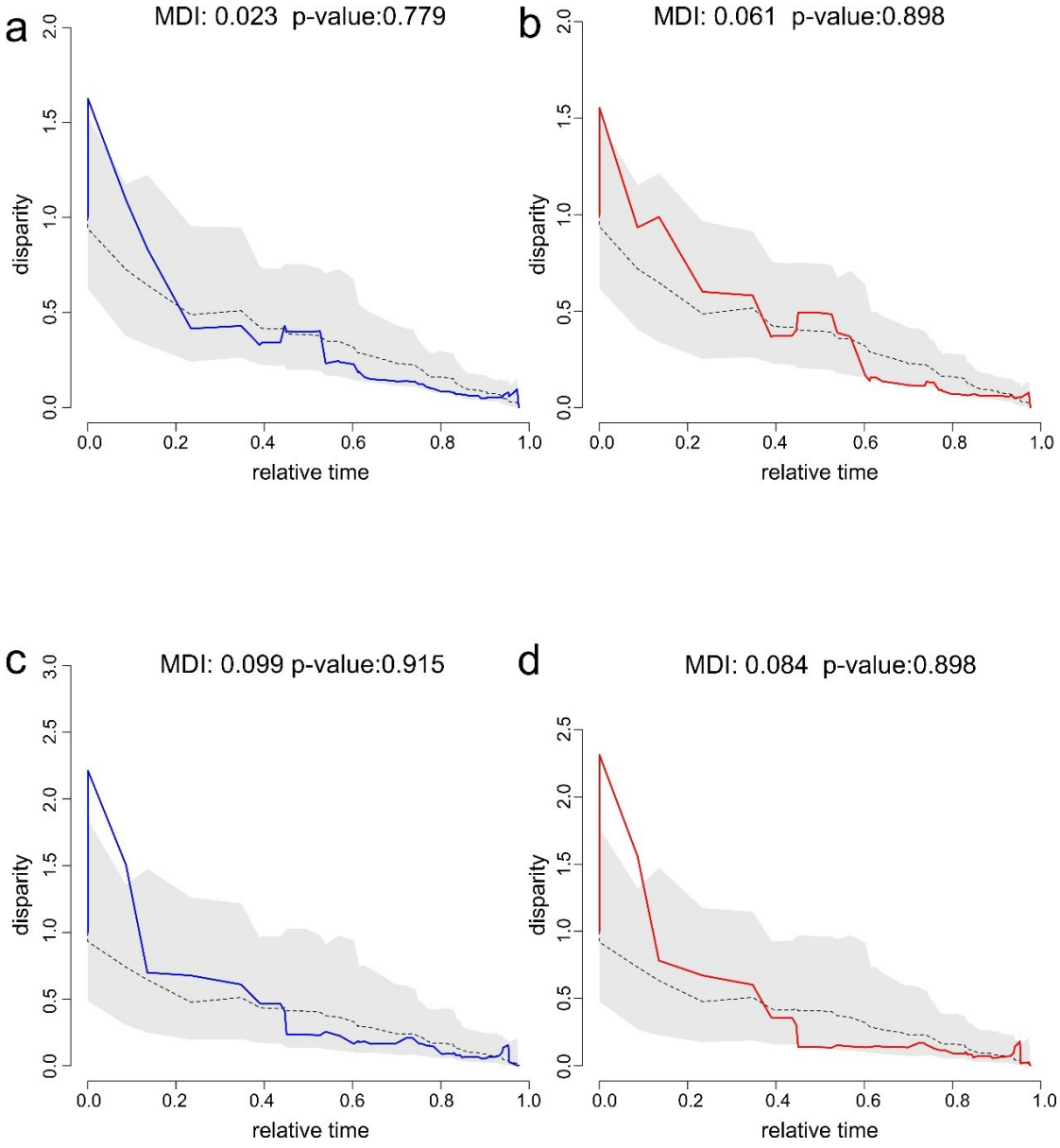

Figure 4.8. Disparity through time plots for skull shape (a), mandible shape (b), skull size (c),and mandible size (d). Blue (skull) and red (mandible) lines represent the empirical curve for disparity obtained from the three first principal components, dashed curves and gray envelopes representing, respectively, the median and 95% confidence interval for a null distribution simulated after 1000 replications, using Brownian motion. Disparity scale measures the relative within-clade disparity among nodes at each time slice, and time scale representing the relative time, from the root of the tree (0.0), to the present (1.0). Morphological disparity index (MDI) and respective p-values are represented above each plot.

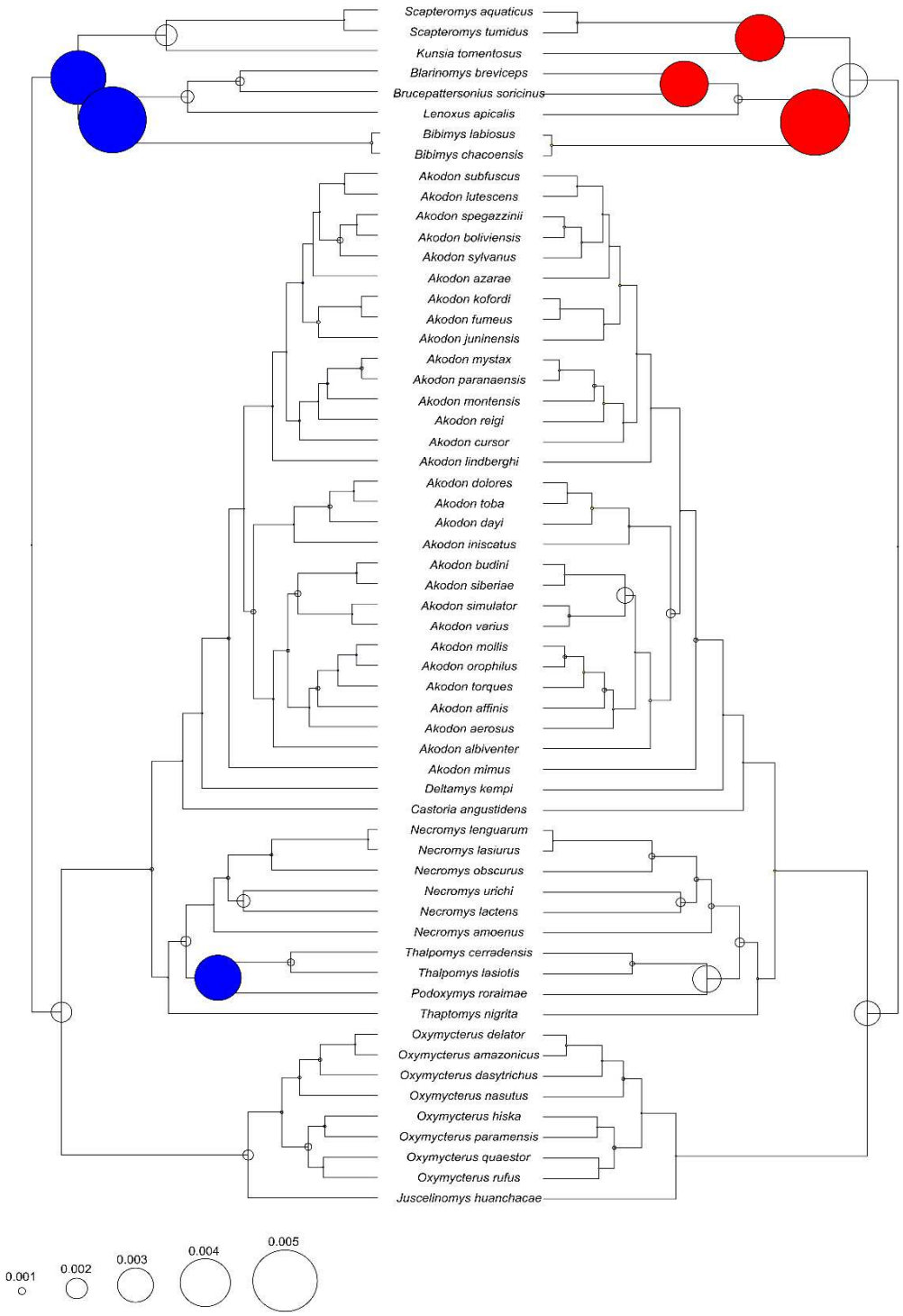

Figure 4.9. Disparity per nodes resulting from the analysis of decomposition of diversity (*decdiv*)for shape data (skull to the left, mandible to the right). Node sizes are proportional to the percentage of disparity explained by each node, and blue (skull) and red (mandible) nodes are those with a major contribution, accounting for more than 10% of the total disparity in the tree.

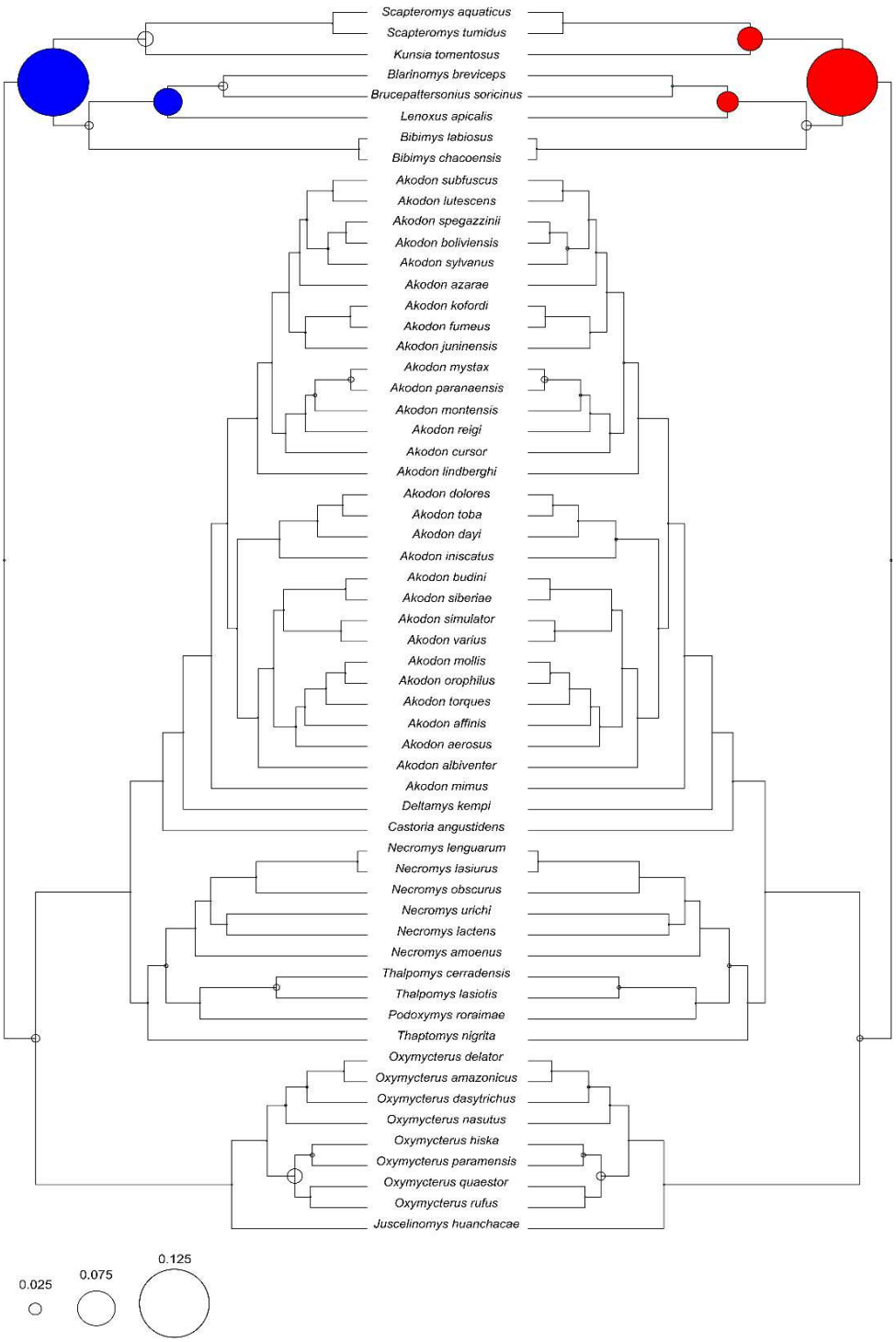

Figure 4.10. Disparity per nodes resulting from the analysis of decomposition of diversity (*decdiv*) for size data (skull to the left, mandible to the right). Node sizes are proportional to the percentage of disparity explained by each node, and blue (skull) and red (mandible) nodes are those with a major contribution, accounting for more than 10% of the total disparity in the tree.

4.8. Tables

Table 4.1. Observed disparity in phylogenetic decomposition analysis (*decdiv*) of Akodontini skull and mandible (size and shape). Asterisk for tests significant at α=0.05.

Test	Skull size	Skull shape	Mandible size	Mandible shape
Single node	0.3411739*	0.1818224*	0.3607772	0.1741992
Few nodes	0.6493863*	0.5467146*	0.637693	0.5828399*
Root skewness	0.5467618*	0.5496577*	0.5588859*	0.5087178*

Table 4.2. Results of *convevol* for each metric of convergence applied. Obs= Observed value for the metric in the data, Cutoff = estimated cutoff value for significance (do not apply to C5) and p-value relative to the null distribution, after 100 simulations.

Metric	Obs	Cutoff	P-value
C1	0.565675	0.182594	<0.01
C2	0.043601	0.0096	<0.01
C3	0.249774	0.104665	<0.01
C4	0.012713	0.008258	<0.01
C5	4	-	0.54

4.9. Supplementary Material

Supplementary Material 4.S1. Voucher numbers of specimens analyzed in this study. The analyzed specimens are deposited in the mammal collections of the Field Museum of Natural History (FMNH), American Museum of Natural History (AMNH), National Museum of Natural History (UMNH), Museu de História Natural of Pontifícia Universidade Católica of Minas Gerais (MCNM), Museu de Zoologia João Moojen (MZUFV), and Museu Nacional of Universidade Federal do Rio de Janeiro (MN, CAZ, PRG).

Skull

Akodon aerosus: FMNH 18180, FMNH 19265, FMNH 19266, FMNH 19268, FMNH 19757, FMNH 24502, FMNH 24506, FMNH 24510, FMNH 24536, FMNH 24538, FMNH 24540, FMNH 24542, FMNH 52494, FMNH 68614

Akodon affinis: AMNH 32991, AMNH 32992, AMNH 32994, AMNH 33005, AMNH 33007, AMNH 71208, AMNH 71215, AMNH 71218, AMNH 71226

Akodon albiventer: FMNH 107470, FMNH 107475, FMNH 107478, FMNH 107479, FMNH 107492, FMNH 107568, FMNH 107579, FMNH 107580, FMNH 107591, FMNH 107592, FMNH 107600, FMNH 107634, FMNH 107661, FMNH 162685, FMNH 162707, FMNH 162725

Akodon azarae: FMNH 23333, FMNH 23337, FMNH 23338, FMNH 23347, FMNH 27617, FMNH 27619, FMNH 27624, FMNH 27627, FMNH 27632, FMNH 27636, FMNH 27638, FMNH 29189, FMNH 29195

Akodon boliviensis: FMNH 107829, FMNH 107834, FMNH 107845, FMNH 107848, FMNH 107856, FMNH 107865, FMNH 107868, FMNH 107883, FMNH 107886, FMNH 107940, FMNH 107976, FMNH 162751, FMNH 43375, FMNH 49702, FMNH 52544, FMNH 52549

Akodon budini: FMNH 23351, FMNH 23355, FMNH 23356, FMNH 23357, FMNH 23359, FMNH 23360, FMNH 23361, FMNH 23362, FMNH 23363, FMNH 23364, FMNH 23365, FMNH 23369, FMNH 23370, FMNH 23371, USNM 259612

Akodon cursor: FMNH 123063, FMNH 141602, FMNH 141611, FMNH 145329, FMNH 145330, FMNH 145348, FMNH 145361, FMNH 145363, FMNH 94450, FMNH 94453, FMNH 94468, FMNH 94469, FMNH 94471, FMNH 94476, FMNH 94479, FMNH 94485

Akodon dayi: FMNH 140809, FMNH 140810, FMNH 21575, FMNH 21578, FMNH 21581, FMNH 21588, USNM 276609, USNM 390141, USNM 390699, USNM 584503, USNM 584504, USNM 584505, USNM 584506

Akodon dolores: FMNH 35243, USNM 364531

Akodon fumeus: FMNH 46143, FMNH 74874, FMNH 74875, FMNH 74876, FMNH 74878, FMNH 74881, FMNH 74882, USNM 290907, USNM 290927

Akodon iniscatus: FMNH 29127, FMNH 35248, FMNH 41285, USNM 236314

Akodon juninensis: AMNH 231329, AMNH 231334, AMNH 231337, AMNH 231338, AMNH 231340, FMNH 23671, FMNH 75561

Akodon kofordi: FMNH 18181, FMNH 52554, FMNH 52555, FMNH 52556, FMNH 75483

Akodon lindberghi: FMNH 128293, FMNH 128295, FMNH 128297, MN 33682, MN 33683, MN 33703, MN 48026, MN 67123

Akodon lutescens: FMNH 21559, FMNH 49696, FMNH 49697, FMNH 50975, FMNH 74884, FMNH 74886, FMNH 74887, FMNH 74890

Akodon mimus: AMNH 264911, AMNH 264913, AMNH 264914, AMNH 264915, AMNH 264918, AMNH 264919, AMNH 264920, AMNH 268823, AMNH 268826, AMNH 268828, AMNH 268829, AMNH 26883, AMNH 268831, AMNH 268832, AMNH 2754

Akodon mollis: FMNH 129216, FMNH 129219, FMNH 19285, FMNH 19287, FMNH 19288, FMNH 19318, FMNH 20909, FMNH 20910, FMNH 23660, FMNH 23686, FMNH 24491, FMNH 81348, FMNH 81349, FMNH 81350, FMNH 81351, FMNH 81368, FMNH 81374, FMNH 81375

Akodon montensis: FMNH 18185, FMNH 23844, FMNH 26817, FMNH 26834, FMNH 26838, FMNH 26845, FMNH 26846, FMNH 26847, FMNH 29437, FMNH 47956

Akodon mystax: FMNH 230333, FMNH 230335, MN 69605, MN 69606, MN 69609, MN 69613, MN 69623, MN 69627, MN 69628, MN 69629, MN 69644

Akodon orophilus: FMNH 19719, FMNH 19721, FMNH 19722, FMNH 19725, FMNH 19733, FMNH 19738, FMNH 19739, FMNH 19740, FMNH 19741, FMNH 19742, FMNH 19743, FMNH 19744, FMNH 19745, FMNH 19746, FMNH 19754, FMNH 23657

Akodon paranaensis: FMNH 232547, FMNH 232563, FMNH 232572, FMNH 232578, FMNH 232579, FMNH 232624, FMNH 232651, FMNH 232652, MN 48041, MN 48067, MN 69675, MN 69677, MN 69679

Akodon reigi: MN 62119, MN 62120

Akodon siberiae: AMNH 260423, AMNH 260424, AMNH 260425, AMNH 260426, AMNH 260427, AMNH 260428, AMNH 260430, AMNH 260431, AMNH 260434, AMNH 260578, AMNH 260579, AMNH 260594

Akodon simulator: FMNH 29134, FMNH 29137, FMNH 30110, FMNH 30112, FMNH 30117, FMNH 30119, FMNH 30120, FMNH 30131, FMNH 35249

Akodon spegazzinii: FMNH 29122, FMNH 29123, FMNH 30181, FMNH 30182, FMNH 30184, FMNH 30185, FMNH 34997, USNM 259279, USNM 259280, USNM 259632, USNM 259633

Akodon subfuscus: FMNH 107744, FMNH 107750, FMNH 107753, FMNH 107754, FMNH 107760, FMNH 107766, FMNH 107772, FMNH 75524, FMNH 75525, FMNH 75527, FMNH 75529, FMNH 75530, FMNH 75531, FMNH 75532, FMNH 75533, FMNH 75535, FMNH 75550

Akodon sylvanus: AMNH 264272

Akodon toba: FMNH 157165, FMNH 157179, FMNH 157182, FMNH 157186, FMNH 157187, FMNH 157188, FMNH 157195, FMNH 157209, FMNH 164136, FMNH 164159, FMNH 164168, FMNH 164170, FMNH 164179, FMNH 164182

Akodon torques: FMNH 170501, FMNH 170503, FMNH 170506, FMNH 170508, FMNH 170509, FMNH 170510, FMNH 170511, FMNH 170517, FMNH 170519, FMNH 172221, FMNH 172225, FMNH 172227, FMNH 43366, FMNH 43367, FMNH 43368

Akodon varius: AMNH 38667, AMNH 38670, AMNH 38674, AMNH 38675, FMNH 50160, FMNH 50978, FMNH 50980

Bibimys chacoensis: USNM 236239

Bibimys labiosus: MCNM 2198, MCNM 2827, MCNM 2829, MCNM 2833, MCNM 2838, MCNM 2839, MZUFV 753, PRG 1034, PRG 210

Blarinomys breviceps: MCNM 1377, MCNM 1472, MCNM 2534, MCNM 2983, MN 29457, MN 70223, MN 70224, MN 70225, MN 77786

Brucepattersonius soricinus: FMNH 230356, FMNH 94499, FMNH 94480

Castoria angustidens: FMNH 230337, FMNH 230338, FMNH 230340, FMNH 230342, FMNH 230345, FMNH 230346, FMNH 230348, FMNH 230349, FMNH 230350, FMNH 230351, FMNH 230352, FMNH 230353

Deltamys kempi: AMNH 206115, AMNH 206121, AMNH 206139, AMNH 206140, AMNH 206142, AMNH 206158, AMNH 206159, AMNH 206161, AMNH 206164, AMNH 206165, MN 42090, MN 42091, MN 42098, MN 42100

Juscelinomys huanchacae: USNM 584508, USNM 584509, USNM 584510, USNM 584511, USNM 584512, USNM 584513, USNM 584514

Kunsia tomentosus: FMNH 122710, FMNH 122711, MN 316, MN 53969, MN 62567, MN 62569, USNM 584516

Lenoxus apicalis: AMNH 16064, AMNH 16065, AMNH 16553, AMNH 16555, AMNH 16556, AMNH 16557, AMNH 16558, AMNH 16559, AMNH 264854, AMNH 264855, AMNH 264856, AMNH 264857, AMNH 72607, AMNH 72609, AMNH 72610, AMNH 72618, FMNH 52612, FMNH 52613

Necromys amoenus: FMNH 107665, FMNH 107680, FMNH 107699, FMNH 107702, FMNH 107728, FMNH 107838, FMNH 107862, FMNH 107864, FMNH 107875, FMNH 49671, FMNH 49672, FMNH 49676

Necromys lactens: FMNH 162771, FMNH 23366

Necromys lasiurus: FMNH 117120, FMNH 117122, FMNH 117124, FMNH 128331, FMNH 128335, FMNH 128337, FMNH 164214, FMNH 164235, FMNH 25196, FMNH 25197, FMNH 25198, FMNH 25200, FMNH 25201, FMNH 96114, FMNH 96115

Necromys lenguarum: FMNH 164229, FMNH 164324, FMNH 164325, FMNH 164352, FMNH 164378, FMNH 164385, FMNH 164392, FMNH 164403, FMNH 164421, FMNH 164441, USNM 584525, USNM 584531, USNM 584538, USNM 584541

Necromys obscurus: FMNH 122687, FMNH 35357

Necromys urichi: USNM 317731, USNM 317742, USNM 317743, USNM 317744, USNM 371199, USNM 371206, USNM 387978, USNM 406117, USNM 406122, USNM 409941, USNM 409946, USNM 409947, USNM 540711, USNM 560659

Oxymycterus amazonicus: USNM 519783, USNM 519784, USNM 519785, USNM 519786, USNM 519787, USNM 521481, USNM 521482, USNM 521485, USNM 521486, USNM 521487, USNM 521489, USNM 521494, USNM 544637, USNM 546017, USNM 546023, USNM 546028, USNM 546031

Oxymycterus dasytrichus: FMNH 145437, FMNH 145438, FMNH 145441, FMNH 145443, FMNH 53874, FMNH 53875, FMNH 94525, FMNH 94526, FMNH 94529, MCNM 1300, MCNM 1477, MCNM 3072, MCNM 3158, USNM 545060

Oxymycterus delator: FMNH 128320, FMNH 128321, FMNH 128322, FMNH 128323, FMNH 128324, MCNM 2482, MCNM 3073, MCNM 3076, MCNM 3126, MCNM 3259, MCNM 3260, MCNM 3333, MCNM 3512

Oxymycterus hiska: AMNH 91601, AMNH 91602

Oxymycterus nasutus: CAZ 100, CAZ 108, CAZ 118, CAZ 122, CAZ 125, CAZ 129, CAZ 133, CAZ 138, CAZ 63, FMNH 27652, FMNH 29253, MN 42435, MN 42436

Oxymycterus paramensis: FMNH 162839, FMNH 162841, FMNH 162851, FMNH 22234, FMNH 23316, FMNH 23319, FMNH 23320, FMNH 23322, FMNH 23324, FMNH 23325, FMNH 50985, FMNH 50986, FMNH 74894, FMNH 74898, FMNH 74900

Oxymycterus quaestor: FMNH 23843, FMNH 26586, FMNH 26595, FMNH 26754, FMNH 26756, FMNH 26757, FMNH 34377, FMNH 34380, USNM 259577, USNM 462123, USNM 484400, USNM 484404

Oxymycterus rufus: FMNH 122696, FMNH 122697, FMNH 136927, FMNH 136929, FMNH 26754, FMNH 26757, USNM 236328, USNM 309164

Podoxymys roraimae: AMNH 75584, AMNH 75585, AMNH 75586

Scapteromys aquaticus: FMNH 29160, FMNH 98286, FMNH 98287, FMNH 98289

Scapteromys tumidus: AMNH 206220, AMNH 206221, AMNH 206222, AMNH 206230, AMNH 206231, AMNH 206240, AMNH 206247, AMNH 206261, AMNH 206267, AMNH 206278, AMNH 206280, AMNH 235431, AMNH 235432, AMNH 235433

Thalpomys cerradensis: FMNH 128328

Thalpomys lasiotis: FMNH 128326, FMNH 128327, MN 60199, MN 60200, MN 60201, MN 61652, MN 61653, MN 62654, MN 62655, MN 62656, MN 62657, MN 62658, MN 62659, MN 75104, MN 75105

Thaptomys nigrita: FMNH 230387, FMNH 230389, FMNH 230390, USNM 460539, USNM 460541, USNM 484233, USNM 484234, USNM 484236, USNM 484237, USNM 484241, USNM 484243, USNM 484244

Mandible

Akodon aerosus: FMNH 18180, FMNH 19265, FMNH 19266, FMNH 19268, FMNH 19757, FMNH 24502, FMNH 24506, FMNH 24510, FMNH 24512, FMNH 24514, FMNH 24538, FMNH 24540, FMNH 52493, FMNH 52525, FMNH 52539

Akodon affinis: AMNH 181479, AMNH 32992, AMNH 32994, AMNH 33005, AMNH 33007, AMNH 33018, AMNH 71208, AMNH 71213, AMNH 71215, AMNH 71217, AMNH 71218, AMNH 71222, AMNH 71223, AMNH 71226, AMNH 71227, FMNH 107441

Akodon albiventer: FMNH 107453, FMNH 107475, FMNH 107478, FMNH 107479, FMNH 107488, FMNH 107491, FMNH 107492, FMNH 107497, FMNH 107532, FMNH 107554, FMNH 107568, FMNH 107578, FMNH 52575, FMNH 53622

Akodon azarae: FMNH 22233, FMNH 23329, FMNH 23333, FMNH 23336, FMNH 23337, FMNH 23338, FMNH 23340, FMNH 23341, FMNH 23344, FMNH 23345, FMNH 23346, FMNH 23347, FMNH 27612, FMNH 27614, FMNH 27617, FMNH 27624

Akodon boliviensis: FMNH 43375, FMNH 43377, FMNH 49684, FMNH 49699, FMNH 49700, FMNH 49701, FMNH 49702, FMNH 51290, FMNH 51293, FMNH 52542, FMNH 52544, FMNH 52545, FMNH 52547, FMNH 52548, FMNH 52551

Akodon budini: FMNH 23351, FMNH 23355, FMNH 23356, FMNH 23357, FMNH 23358, FMNH 23359, FMNH 23360, FMNH 23361, FMNH 23362, FMNH 23363, FMNH 23364, FMNH 23365, FMNH 23370, FMNH 23371, FMNH 35345

Akodon cursor: FMNH 141602, FMNH 141603, FMNH 141604, FMNH 141605, FMNH 141606, FMNH 141609, FMNH 141611, FMNH 141612, FMNH 141613, FMNH 145332, FMNH 145337, FMNH 145354, FMNH 145356, FMNH 145358, FMNH 145361, FMNH 145363,

Akodon dayi: FMNH 140809, FMNH 140810, FMNH 21588, FMNH 46145, USNM 276608, USNM 276609, USNM 390141, USNM 584503, USNM 584504, USNM 584505, USNM 584506

Akodon dolores: FMNH 35243

Akodon fumeus: FMNH 162755, FMNH 74874, FMNH 74876, FMNH 74877, FMNH 74882, USNM 290907, USNM 290927

Akodon iniscatus: FMNH 29127, FMNH 29128, FMNH 35248, FMNH 41284, FMNH 41285, USNM 236314

Akodon juninensis: AMNH 231329, AMNH 231334, AMNH 231337, AMNH 231338, AMNH 231340, FMNH 23673, FMNH 75561

Akodon kofordi: FMNH 18181, FMNH 52553, FMNH 52554, FMNH 52555, FMNH 52556, FMNH 75483, USNM 172966

Akodon lindberghi: FMNH 128293, FMNH 128297, MN 33681, MN 33682, MN 33683, MN 33684, MN 33685, MN 33686, MN 33687, MN 33703, MN 48026, MN 67123

Akodon lutescens: FMNH 21559, FMNH 49696, FMNH 49697, FMNH 74886, FMNH 74887, FMNH 74890, FMNH 74891

Akodon mimus: AMNH 264910, AMNH 264911, AMNH 264913, AMNH 264914, AMNH 264915, AMNH 264918, AMNH 264919, AMNH 264920, AMNH 268803, AMNH 268823, AMNH 268826, AMNH 268828, AMNH 268829, AMNH 268831, AMNH 268832

Akodon mollis: FMNH 19272, FMNH 19277, FMNH 19280, FMNH 19281, FMNH 19282, FMNH

19285, FMNH 19286, FMNH 19287, FMNH 19318, FMNH 19850, FMNH 19851, FMNH 20902, FMNH 20905, FMNH 20909, FMNH 20910

Akodon montensis: FMNH 18185, FMNH 23844, FMNH 26817, FMNH 26834, FMNH 26837, FMNH 26838, FMNH 26845, FMNH 26846, FMNH 26847, FMNH 29438, FMNH 34038, FMNH 47956

Akodon mystax: FMNH 230333, FMNH 230335, MN 69602, MN 69605, MN 69606, MN 69609, MN 69613, MN 69623, MN 69627, MN 69628, MN 69629, MN 69644

Akodon orophilus: FMNH 19719, FMNH 19721, FMNH 19722, FMNH 19725, FMNH 19726, FMNH 19729, FMNH 19731, FMNH 19732, FMNH 19733, FMNH 19734, FMNH 19737, FMNH 19738, FMNH 19739, FMNH 19740, FMNH 19741

Akodon paranaensis: FMNH 232547, FMNH 232563, FMNH 232572, FMNH 232578, FMNH 232579, FMNH 232624, FMNH 232651, FMNH 232652, MN 48041, MN 48067, MN 69675, MN 69676, MN 69677, MN 69679

Akodon reigi: MN 62119, MN 62120

Akodon siberiae: AMNH 260423, AMNH 260424, AMNH 260425, AMNH 260426, AMNH 260427, AMNH 260428, AMNH 260430, AMNH 260431, AMNH 260578, AMNH 260579, AMNH 260594

Akodon simulator: FMNH 29134, FMNH 29137, FMNH 30109, FMNH 30110, FMNH 30112, FMNH 30115, FMNH 30117, FMNH 30119, FMNH 30120, FMNH 30122, FMNH 30123, FMNH 30128, FMNH 30132, FMNH 35249

Akodon spegazzinii: FMNH 29122, FMNH 29123, FMNH 30181, FMNH 30182, FMNH 30184, FMNH 30185, FMNH 30189, FMNH 34997, USNM 259279, USNM 259280, USNM 259282, USNM 259633

Akodon subfuscus: FMNH 107754, FMNH 107772, FMNH 107777, FMNH 107793, FMNH 107794, FMNH 107810, FMNH 107814, FMNH 107817, FMNH 107820, FMNH 75527, FMNH 75531, FMNH 75533, FMNH 75550, FMNH 75551

Akodon sylvanus: AMNH 264272, AMNH 264274

Akodon toba: FMNH 157165, FMNH 157187, FMNH 157188, FMNH 157195, FMNH 157209, FMNH 164136, FMNH 164159, FMNH 164161, FMNH 164168, FMNH 164170, FMNH 164173, FMNH 164178, FMNH 164179, FMNH 164180, FMNH 46161

Akodon torques: FMNH 170501, FMNH 170503, FMNH 170506, FMNH 170509, FMNH 170510, FMNH 170517, FMNH 170519, FMNH 170523, FMNH 171861, FMNH 171862, FMNH 172221, FMNH 172225, FMNH 43366, FMNH 43367, FMNH 43368

Akodon varius: AMNH 38667, AMNH 38670, AMNH 38674, AMNH 38675, FMNH 50160, FMNH

50981

Bibimys chacoensis: USNM 236239

Bibimys labiosus: MCNM 2198, MCNM 2827, MCNM 2829, MCNM 2833, MCNM 2838, MN 62395, MN 62601, PRG 1034

Blarinomys breviceps: MCNM 1377, MCNM 1472, MCNM 2197, MCNM 2534, MCNM 2846, MCNM 3332, MN 13353, MN 29446, MN 29461, MN 29466, MN 37030, MN 71837, MN 77786

Brucepattersonius soricinus: FMNH 230356, FMNH 94480

Castoria angustidens: FMNH 230337, FMNH 230338, FMNH 230339, FMNH 230342, FMNH 230345, FMNH 230346, FMNH 230350, FMNH 230351, FMNH 230352, FMNH 230353

Deltamys kempi: AMNH 206097, AMNH 206102, AMNH 206115, AMNH 206117, AMNH 206118, AMNH 206119, AMNH 206120, AMNH 206121, AMNH 206139, AMNH 206140, AMNH 206142, AMNH 206157, AMNH 206158, AMNH 206159, AMNH 206161

Juscelinomys huanchacae: USNM 584508, USNM 584509, USNM 584510, USNM 584511, USNM 584512, USNM 584513, USNM 584514

Kunsia tomentosus: FMNH 122711, MN 53969, MN 62567, MN 62569, USNM 584516

Lenoxus apicalis: AMNH 16064, AMNH 16065, AMNH 16555, AMNH 16556, AMNH 16557, AMNH 16558, AMNH 16559, AMNH 264854, AMNH 264855, AMNH 264856, AMNH 264857, AMNH 72605, AMNH 72610, AMNH 72615, AMNH 72620

Necromys amoenus: FMNH 107665, FMNH 107680, FMNH 107699, FMNH 107702, FMNH 107728, FMNH 107838, FMNH 107861, FMNH 107862, FMNH 107864, FMNH 107875, FMNH 49671, FMNH 49672, FMNH 49676, FMNH 49677, FMNH 49750, USNM 194725

Necromys lactens: FMNH 162771, FMNH 23366

Necromys lasiurus: FMNH 117120, FMNH 117124, FMNH 128331, FMNH 128334, FMNH 128335, FMNH 128337, FMNH 128338, FMNH 164214, FMNH 164226, FMNH 164235, FMNH 164320, FMNH 25196, FMNH 25197, FMNH 25198, FMNH 25200, FMNH 25201, FMNH 96114

Necromys lenguarum: FMNH 164244, FMNH 164325, FMNH 164352, FMNH 164375, FMNH 164377, FMNH 164378, FMNH 164385, FMNH 164392, FMNH 164400, FMNH 164421, FMNH 164441, USNM 584523, USNM 584525, USNM 584531, USNM 584533

Necromys obscurus: FMNH 122687, FMNH 35357

Necromys urichi: USNM 280767, USNM 314184, USNM 317731, USNM 317743, USNM 317744, USNM 371198, USNM 371199, USNM 371206, USNM 406117, USNM 406122, USNM 409946, USNM 409947, USNM 442343, USNM 442350, USNM 540711, USNM 85567

Oxymycterus amazonicus: FMNH 94524, USNM 519783, USNM 519784, USNM 519785, USNM 519786, USNM 519787, USNM 521436, USNM 521481, USNM 521482, USNM 521484, USNM 521485, USNM 521486, USNM 521487, USNM 521489, USNM 521494

Oxymycterus dasytrichus: FMNH 145437, FMNH 145438, FMNH 145441, FMNH 145443, FMNH 53874, FMNH 53875, FMNH 94525, FMNH 94526, FMNH 94529, MCNM 1300, MCNM 1477, MCNM 3072, MCNM 3074, USNM 545060

Oxymycterus delator: FMNH 128321, FMNH 128322, FMNH 128323, FMNH 128324, MCNM 2482, MCNM 3073, MCNM 3075, MCNM 3076, MCNM 3126, MCNM 3256, MCNM 3259, MCNM 3260, MCNM 3333, MCNM 3512

Oxymycterus hiska: AMNH 72889, AMNH 91303, AMNH 91601, AMNH 91602

Oxymycterus nasutus: CAZ 100, CAZ 106, CAZ 108, CAZ 118, CAZ 122, CAZ 125, CAZ 129, CAZ 133, CAZ 138, FMNH 27652, MN 42436

Oxymycterus paramensis: FMNH 22234, FMNH 23316, FMNH 23319, FMNH 23320, FMNH 23322, FMNH 23324, FMNH 50985, FMNH 50987, FMNH 74892, FMNH 74893, FMNH 74894, FMNH 74895, FMNH 74896, FMNH 74898

Oxymycterus quaestor: FMNH 128321, FMNH 128322, FMNH 128323, FMNH 26586, FMNH 26595, FMNH 26754, FMNH 26756, FMNH 26757, FMNH 34377, FMNH 34380, FMNH 35354, USNM 259577, USNM 462120, USNM 462121, USNM 484404, USNM 484405

Oxymycterus rufus: FMNH 136923, FMNH 136927, FMNH 230386, FMNH 23843, FMNH 26754, FMNH 26757, FMNH 98285, MN 65522,MN 65523, MN 65525, MN 65526, MN 65531, MN 66193, USNM 282159, USNM 309164

Podoxymys roraimae: AMNH 75583, AMNH 75584, AMNH 75585, AMNH 75586

Scapteromys aquaticus: FMNH 29160, FMNH 98286, FMNH 98289, MN 62305, MN 62308, MN 62309, MN 62310, MN 62312

Scapteromys tumidus: AMNH 206209, AMNH 206220, AMNH 206221, AMNH 206222, AMNH 206230, AMNH 206231, AMNH 206240, AMNH 206247, AMNH 206248, AMNH 206261, AMNH 206267, AMNH 206272, AMNH 206278, AMNH 206280, AMNH 235431, AMNH 235432, AMNH 235433, MN 32855

Thalpomys cerradensis: FMNH 128328, FMNH 128329

Thalpomys lasiotis: FMNH 128326, FMNH 128327, MN 24361, MN 60201, MN 61652, MN 61653, MN 62654, MN 62655, MN 62656, MN 62657, MN 62658, MN 62659, MN 66008, MN 75104, MN 75105, MN 81597, MN 82159

Thaptomys nigrita: FMNH 220012, FMNH 230387, FMNH 26820, USNM 460539, USNM 460541, USNM 484233, USNM 484235, USNM 484236, USNM 484237, USNM 484239, USNM 484240, USNM 484241, USNM 484243, USNM 484244, USNM 484245

Supplementary Material 4.S2. Landmark descriptions for the ventral view of the skull and jaw of Akodontini rodents used in this study.

Lateral view: (1) anterior-most point of nasal; (2) anterior-most point of suture between nasal and premaxillae; (3) anterior-most point of premaxilla, (4) anterior-most point of incisive alveolus; (5) posterior-most point of incisive alveolus, (6) posterior-most point of suture between nasal and premaxilla; (7) inferior-most point of suture between premaxilla and maxilla; (8) point of origin of superior root of zygomatic plate; (9) point of maximum posterior constriction of anterorbital bridge; (10) anterior-most point of zygomatic plate; (11) point of origin of inferior root of zygomatic plate; (12) point of maximum posterior constriction of maxillary root of zygomatic plate; (13) anterior-most point of the first molar alveolus; (14) posterior-most point of the third molar alveolus; (15) point of maximal anterior constrictionof squamosal root of zygomatic arch; (16) point of maximum posterior constriction of squamosal root of zygomatic arch; (17) suture between squamosal, alisphenoid and auditory bulla; (18) superior-most point of auditory bulla; (19) inferior-most point of auditory bulla; (20) suture between auditory bulla and mastoid; (21) posterior-most point of occipital condyle; (22) point of maximum constriction of occipital plate; (23) suture between parietal, squamosal and occipital; (24) superior-most point of occipital plate; (25) superior-most point of suture between frontals and parietals; (26) point of suture between frontal, parietal and squamosal.

Mandible: (1) tip of the incisor; (2) ventral-most point of alveolus of the incisor; (3) dorsal-most point of alveolus of the incisor; (4) ventral-most point between the incisor origin and the lower first molar; (5) anterior-most point of the alveolar margin of the tooth row; (6) anterior edge of the masseteric ridge; (7) intersection between the ascending ramus of the mandible and the tooth row; (8) ventral-most point of the front lower part of the mandible; (9) dorsal-most point between the angular process and the front lower part of the mandible. (10) ventral-most point of the angular process; (11) posterior-most point of the angular process; (12) point at the maximum of concavity between the articular and the angular processes; (13) ventral-most point of the articular condyle; (14) posterior-most point of the articular condyle; (15) dorsal-most point of the articular condyle; (16) point at the maximum of concavity between the coronoid and the articular processes; (17) dorsal-most point of the coronoid process.

Supplementary Material 4.S3. Evolutionary hypotheses for testing the association ofphylogenetic history and diet with skull and mandible morphology.

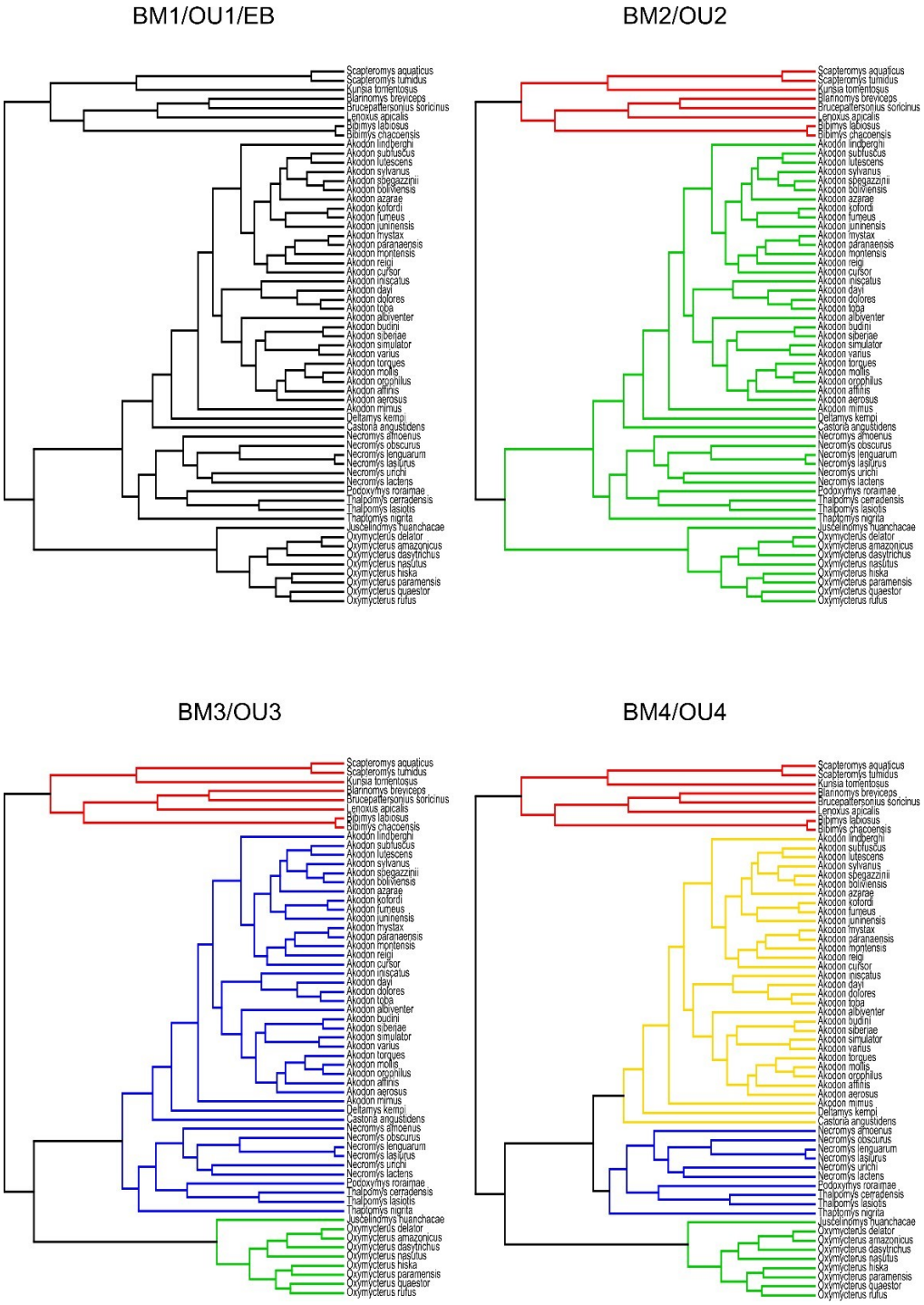

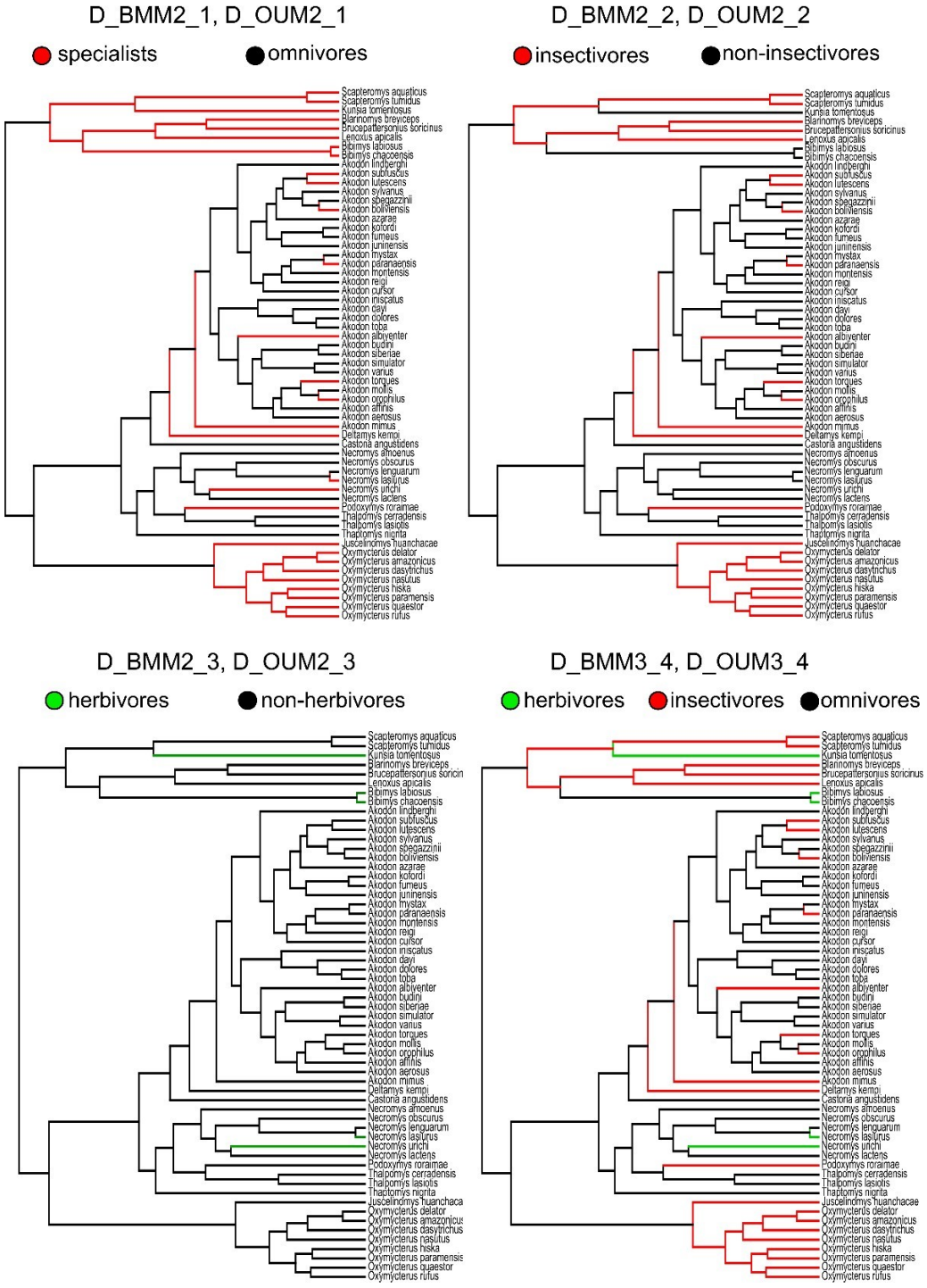
D_BMM2_1, D_OUM2_1
specialists
omnivores
D_BMM2_2, D_OUM2_2
insectivores
non-insectivores
D_BMM2_3, D_OUM2_3
herbivores
non-herbivores
D_BMM3_4, D_OUM3_4
herbivores
insectivores
omnivores
Scapteromys aquaticus
Scapteromys tumidus
Kunsia tomentosus
Blarinomys breviceps
Brucepattersonius soricinus
Lenoxus apicalis
Bibimys labiosus
Bibimys chacoensis
Akodon lindberghi
Akodon subfuscus
Akodon lutescens
Akodon sylvanus
Akodon spegazzinii
Akodon boliviensis
Akodon azarae
Akodon kofordi
Akodon fumeus
Akodon juninensis
Akodon mystax
Akodon paranaensis
Akodon montensis
Akodon reigi
Akodon cursor
Akodon iniscatus
Akodon dayi
Akodon dolores
Akodon toba
Akodon albiventer
Akodon budini
Akodon siberiae
Akodon simulator
Akodon varius
Akodon torques
Akodon mollis
Akodon orophilus
Akodon affinis
Akodon aerosus
Akodon mimus
Deltamys kempi
Castoria angustidens
Necromys amoenus
Necromys obscurus
Necromys lenguarum
Necromys lasiurus
Necromys urichi
Necromys lactens
Podoxymys roraimae
Thalpomys cerradensis
Thalpomys lasiotis
Thaptomys nigrita
Juscelinomys huanchacae
Oxymycterus delator
Oxymycterus amazonicus
Oxymycterus dasytrichus
Oxymycterus nasutus
Oxymycterus hiska
Oxymycterus paramensis
Oxymycterus quaestor
Oxymycterus rufus

Supplementary Material S4: Standard deviation (SD), proportion of variance (PV), and cumulative proportion (CP) of each principal component for skull and mandible of akodontine rodents used in this study.

Skull_Importance of components:
PC1 PC2 PC3 PC4 PC5 PC6 PC7 SD0.03322 0.01766 0.01547 0.01169 0.01110 0.008747 0.008314
PV 0.40594 0.11470 0.08804 0.05022 0.04529 0.028140 0.025420
CP 0.40594 0.52064 0.60868 0.65890 0.70419 0.732330 0.757750 PC8 PC9 PC10 PC11 PC12 PC13
SD 0.008044 0.00768 0.007436 0.007108 0.006606 0.006209
PV 0.023800 0.02169 0.020340 0.018580 0.016050 0.014180
CP 0.781550 0.80324 0.823580 0.842160 0.858210 0.872390 PC14 PC15 PC16 PC17 PC18 PC19
SD 0.005951 0.005336 0.004967 0.004831 0.004516 0.004289
PV 0.013030 0.010470 0.009080 0.008590 0.007500 0.006770
CP 0.885420 0.895890 0.904960 0.913550 0.921050 0.927820 PC20 PC21 PC22 PC23 PC24 PC25
SD 0.004221 0.003983 0.003687 0.003532 0.003366 0.003311
PV 0.006550 0.005840 0.005000 0.004590 0.004170 0.004030
CP 0.934370 0.940200 0.945200 0.949790 0.953960 0.957990 PC26 PC27 PC28 PC29 PC30 PC31
SD 0.003047 0.002966 0.002953 0.002847 0.002784 0.002571
PV 0.003410 0.003230 0.003210 0.002980 0.002850 0.002430
CP 0.961410 0.964640 0.967850 0.970830 0.973680 0.976110 PC32 PC33 PC34 PC35 PC36 PC37
SD 0.002532 0.002488 0.002373 0.002289 0.002251 0.002137
PV 0.002360 0.002280 0.002070 0.001930 0.001860 0.001680
CP 0.978470 0.980740 0.982810 0.984740 0.986610 0.988280 PC38 PC39 PC40 PC41 PC42 PC43
SD 0.002097 0.001968 0.001927 0.001844 0.001757 0.001693
PV 0.001620 0.001420 0.001370 0.001250 0.001140 0.001050
CP 0.989900 0.991330 0.992690 0.993940 0.995080 0.996130 PC44 PC45 PC46 PC47 PC48 PC49
SD 0.001653 0.001588 0.001543 0.00134 0.001042 1.111e-16
PV 0.001010 0.000930 0.000880 0.00066 0.000400 0.000e+00
CP 0.997140 0.998060 0.998940 0.99960 1.000000 1.000e+00 PC50 PC51 PC52
SD 1.054e-16 3.555e-17 2.325e-17 PV 0.000e+00 0.000e+00 0.000e+00 CP 1.000e+00 1.000e+00 1.000e+00

Mandible_Importance of components:
PC1 PC2 PC3 PC4 PC5 PC6 PC7 SD0.03432 0.02253 0.02185 0.01504 0.01320 0.01217 0.01126
PV 0.32875 0.14169 0.13333 0.06314 0.04862 0.04136 0.03542
CP 0.32875 0.47044 0.60377 0.66692 0.71554 0.75690 0.79233 PC8 PC9 PC10 PC11 PC12 PC13
SD 0.009815 0.009582 0.008551 0.007753 0.007707 0.007213
PV 0.026890 0.025630 0.020410 0.016780 0.016580 0.014520
CP 0.819220 0.844850 0.865260 0.882040 0.898620 0.913150
PC14 PC15 PC16 PC17 PC18 PC19 PC20 SD 0.00682 0.006493 0.005838 0.005674 0.005526 0.004849 0.00447
PV 0.01298 0.011770 0.009520 0.008990 0.008530 0.006560 0.00558
CP 0.92613 0.937900 0.947420 0.956410 0.964930 0.971490 0.97707 PC21 PC22 PC23 PC24 PC25 PC26
SD 0.004424 0.003837 0.003528 0.003097 0.002887 0.002565
PV 0.005460 0.004110 0.003470 0.002680 0.002330 0.001840
CP 0.982540 0.986650 0.990120 0.992800 0.995130 0.996960 PC27 PC28 PC29 PC30 PC31 PC32
SD 0.00238 0.002284 1.802e-16 1.699e-16 3.246e-17 2.645e-17 PV 0.00158 0.001460 0.000e+00 0.000e+00 0.000e+00 0.000e+00 CP 0.99854 1.000000 1.000e+00 1.000e+00 1.000e+00 1.000e+00

Supplementary Material S5. Disparity decomposed by tree nodes for skull and mandible shape and size. Tree nodes depicted below.

Node	skull_size_disparity	%	skull_shape_disparity	%	jaw_size_disparity	%	jaw_shape_disparity	%
60	3.89E-03	1%	3.09E-05	0%	4.68E-03	1%	1.02E-04	0%
61	1.68E-02	4%	1.30E-03	6%	1.31E-02	3%	1.79E-03	6%
62	1.72E-04	0%	6.52E-04	3%	1.06E-06	0%	3.40E-05	0%
63	1.70E-03	0%	1.83E-04	1%	5.76E-06	0%	5.79E-05	0%
64	3.14E-02	7%	4.46E-04	2%	1.88E-02	4%	2.42E-04	1%
65	5.01E-04	0%	6.76E-05	0%	2.66E-03	1%	1.47E-05	0%
66	8.64E-03	2%	1.69E-04	1%	9.53E-03	2%	2.89E-05	0%
67	4.40E-03	1%	1.81E-04	1%	3.10E-03	1%	2.25E-04	1%
68	4.67E-03	1%	2.08E-04	1%	5.50E-03	1%	1.18E-04	0%
69	1.31E-05	0%	7.26E-05	0%	7.57E-05	0%	1.13E-04	0%
70	2.15E-04	0%	2.14E-04	1%	1.23E-03	0%	1.40E-04	1%
71	3.17E-03	1%	8.18E-06	0%	2.68E-03	1%	1.33E-04	0%
72	7.40E-03	2%	6.46E-04	3%	8.05E-03	2%	6.56E-04	2%
73	1.55E-03	0%	2.95E-03	**12%**	5.67E-05	0%	1.96E-03	7%
74	1.29E-02	3%	4.41E-04	2%	7.55E-03	2%	3.25E-04	1%
75	2.08E-03	0%	6.86E-05	0%	2.26E-03	1%	3.67E-04	1%
76	1.13E-03	0%	1.95E-04	1%	1.54E-03	0%	3.05E-04	1%
77	9.62E-04	0%	8.22E-04	3%	3.01E-03	1%	6.29E-04	2%
78	5.34E-05	0%	1.75E-04	1%	1.55E-03	0%	4.13E-04	1%
79	1.57E-03	0%	3.45E-05	0%	2.55E-04	0%	4.87E-05	0%
80	2.59E-04	0%	1.66E-05	0%	2.88E-04	0%	1.48E-05	0%
81	8.54E-04	0%	9.25E-05	0%	3.92E-04	0%	2.61E-05	0%
82	6.61E-05	0%	1.78E-04	1%	1.71E-04	0%	2.94E-04	1%
83	2.06E-03	0%	4.86E-05	0%	2.89E-03	1%	1.45E-05	0%
84	1.63E-03	0%	3.03E-04	1%	1.29E-03	0%	6.19E-04	2%
85	1.75E-04	0%	8.11E-05	0%	5.27E-04	0%	1.75E-04	1%
86	1.23E-03	0%	1.86E-04	1%	2.03E-03	0%	2.25E-05	0%
87	3.58E-03	1%	9.13E-05	0%	2.29E-03	1%	1.16E-04	0%
88	7.92E-04	0%	2.49E-04	1%	2.80E-04	0%	3.05E-04	1%
89	2.10E-04	0%	1.03E-04	0%	1.14E-04	0%	1.48E-04	1%
90	1.74E-05	0%	1.14E-04	0%	3.02E-04	0%	2.39E-04	1%
91	1.24E-03	0%	3.87E-04	2%	1.22E-03	0%	1.15E-03	4%
92	1.13E-05	0%	7.62E-05	0%	4.58E-04	0%	1.99E-04	1%
93	1.65E-03	0%	9.31E-05	0%	8.26E-04	0%	6.25E-05	0%
94	1.68E-03	0%	8.40E-05	0%	5.97E-03	1%	1.26E-04	0%
95	2.93E-05	0%	2.58E-04	1%	2.02E-05	0%	1.85E-04	1%
96	2.92E-04	0%	9.98E-05	0%	7.19E-04	0%	5.07E-05	0%
97	7.88E-04	0%	9.48E-05	0%	1.62E-03	0%	3.52E-05	0%

(continued)

98	2.41E-03	1%	7.17E-05	0%	3.65E-03	1%	8.29E-05	0%
99	2.15E-03	0%	1.11E-04	0%	3.23E-03	1%	2.30E-05	0%
100	4.89E-04	0%	6.93E-05	0%	6.62E-05	0%	1.51E-04	1%
101	7.24E-03	2%	1.34E-04	1%	5.42E-03	1%	2.48E-04	1%
102	1.16E-02	3%	2.10E-04	1%	1.43E-02	3%	1.23E-04	0%
103	2.82E-04	0%	1.30E-04	1%	9.41E-05	0%	1.52E-04	1%
104	3.16E-03	1%	2.03E-04	1%	2.23E-03	1%	1.55E-05	0%
105	2.02E-03	0%	2.52E-05	0%	1.65E-04	0%	5.47E-05	0%
106	1.17E-04	0%	5.22E-05	0%	1.63E-04	0%	5.14E-05	0%
107	3.69E-03	1%	6.17E-05	0%	3.15E-03	1%	7.57E-05	0%
108	4.51E-03	1%	3.68E-04	2%	7.20E-03	2%	1.17E-04	0%
109	3.08E-04	0%	9.49E-06	0%	8.30E-05	0%	1.48E-04	1%
110	7.98E-06	0%	1.28E-05	0%	7.43E-04	0%	9.35E-05	0%
111	1.48E-01	**34%**	3.51E-03	**15%**	1.56E-01	**36%**	2.44E-03	9%
112	1.65E-02	4%	4.29E-03	**18%**	2.12E-02	5%	4.82E-03	**17%**
113	9.10E-06	0%	1.61E-04	1%	7.10E-04	0%	1.50E-04	1%
114	5.93E-02	**14%**	8.10E-04	3%	4.72E-02	**11%**	5.63E-04	2%
115	1.88E-02	4%	5.47E-04	2%	5.33E-03	1%	3.35E-03	**12%**
116	3.23E-02	7%	1.37E-03	6%	5.48E-02	**13%**	3.41E-03	**12%**
117	7.49E-04	0%	3.64E-05	0%	1.05E-06	0%	1.30E-04	0%
TOTAL	4.33E-01	100%	2.36E-02	100%	4.33E-01	100%	2.77E-02	100%

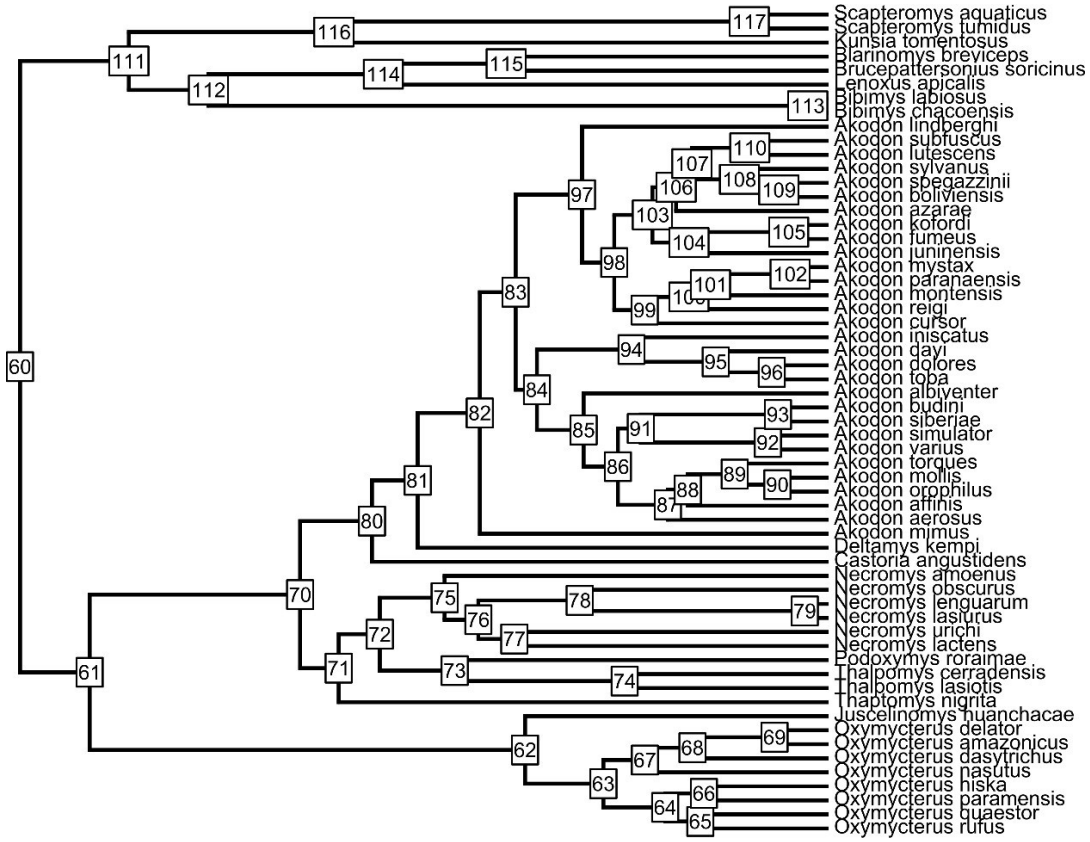
Scapteromys aquaticus
Scapteromys tumidus
Kunsia tomentosus
Blarinomys breviceps
Brucepattersonius soricinus
Lenoxus apicalis
Bibimys labiosus
Bibimys chacoensis
Akodon lindbergh
Akodon subfuscus
Akodon lutescens
Akodon sylvanus
Akodon spegazzinii
Akodon boliviensis
Akodon azarae
Akodon kofordi
Akodon fumeus
Akodon juninensis
Akodon mystax
Akodon paranaensis
Akodon montensis
Akodon reigi
Akodon cursor
Akodon iniscatus
Akodon dayi
Akodon dolores
Akodon toba
Akodon albiventer
Akodon budini
Akodon siberiae
Akodon simulator
Akodon varius
Akodon torques
Akodon mollis
Akodon orophilus
Akodon affinis
Akodon aerosus
Akodon mimus
Deltamys kempi
Castoria angustidens
Necromys amoenus
Necromys obscurus
Necromys lenguarum
Necromys lasiurus
Necromys urichi
Necromys lactens
Podoxymys roraimae
Thalpomys cerradensis
Thalpomys lasiotis
Thaptomys nigrita
Juscelinomys huanchacae
Oxymycterus delator
Oxymycterus amazonicus
Oxymycterus dasytrichus
Oxymycterus nasutus
Oxymycterus hiska
Oxymycterus paramensis
Oxymycterus quaestor
Oxymycterus rufus
60
61
62
63
64
65
66
67
68
69
70
71
72
73
74
75
76
77
78
79
80
81
82
83
84
85
86
87
88
89
90
91
92
93
94
95
96
97
98
99
101
102
103
104
105
106
107
108
109
110
111
112
113
114
115
116
117

Supplementary Material S6. Summary of model test results for skull and mandible shape and size of Akodontini rodents analyzed in this study.

Dataset	Model	Δ_AICc_mean	Δ_AICc_median	Δ_AICc_stder	Weights_mean	Weights_median	Weights_stder
Skull_size	BM1	6.93E+00	5.85E+00	5.60E-01	3.21E-02	3.24E-02	1.31E-03
	BMM2	8.52E+00	7.52E+00	5.63E-01	1.45E-02	1.49E-02	5.94E-04
	BMM3	5.47E+00	4.63E+00	5.70E-01	7.12E-02	6.57E-02	4.05E-03
	BMM4	7.24E-01	0.00E+00	5.35E-01	6.64E-01	6.68E-01	1.54E-02
	OU1	8.22E+00	7.13E+00	5.60E-01	1.68E-02	1.70E-02	6.86E-04
	OUM2	8.36E+00	7.29E+00	5.60E-01	1.57E-02	1.60E-02	6.51E-04
	OUM3	1.07E+01	9.58E+00	5.60E-01	4.96E-03	5.02E-03	2.02E-04
	OUM4	1.23E+01	1.12E+01	5.60E-01	2.17E-03	2.21E-03	8.85E-05
	EB	9.15E+00	8.07E+00	5.60E-01	1.06E-02	1.07E-02	4.30E-04
	D_BMM2_1	6.83E+00	6.14E+00	5.86E-01	4.41E-02	3.15E-02	6.45E-03
	D_OUM2_1	1.02E+01	9.15E+00	5.61E-01	6.44E-03	6.53E-03	3.69E-04
	D_BMM2_2	7.03E+00	6.56E+00	5.87E-01	4.47E-02	2.51E-02	7.02E-03
	D_OUM2_2	1.02E+01	9.12E+00	5.63E-01	6.51E-03	6.26E-03	3.35E-04
	D_BMM2_3	8.65E+00	7.73E+00	5.57E-01	1.42E-02	1.40E-02	7.47E-04
	D_OUM2_3	9.75E+00	8.90E+00	5.72E-01	8.38E-03	7.40E-03	4.97E-04
	D_BMM3_4	7.97E+00	8.22E+00	2.38E-01	4.10E-02	9.63E-03	1.43E-02
	D_OUM3_4	1.20E+01	1.11E+01	5.76E-01	3.02E-03	2.42E-03	3.49E-04
Skull_shape	BM1	2.52E+01	2.47E+01	2.55E-01	2.46E-06	2.65E-06	5.97E-08
	BMM2	2.75E+01	2.72E+01	2.50E-01	8.03E-07	7.79E-07	3.62E-08
	BMM3	2.25E+01	2.21E+01	3.49E-01	2.39E-05	9.02E-06	5.47E-06
	BMM4	1.89E+01	1.89E+01	4.76E-01	2.91E-04	4.53E-05	5.19E-05
	OU1	4.57E-01	0.00E+00	2.55E-01	5.76E-01	6.19E-01	1.40E-02
	OUM2	2.58E+00	2.15E+00	2.56E-01	2.00E-01	2.14E-01	5.00E-03
	OUM3	8.25E+00	7.80E+00	2.56E-01	1.17E-02	1.26E-02	2.84E-04
	OUM4	1.47E+01	1.43E+01	2.56E-01	4.64E-04	4.96E-04	1.16E-05
	EB	2.76E+01	2.71E+01	2.55E-01	7.34E-07	7.90E-07	1.78E-08
	D_BMM2_1	1.74E+01	1.92E+01	7.22E-01	4.75E-02	3.98E-05	1.78E-02
	D_OUM2_1	6.16E+00	6.07E+00	2.66E-01	3.91E-02	2.98E-02	3.30E-03
	D_BMM2_2	1.78E+01	1.85E+01	5.00E-01	1.94E-03	5.83E-05	7.46E-04
	D_OUM2_2	6.81E+00	6.61E+00	2.46E-01	2.53E-02	2.24E-02	1.26E-03
	D_BMM2_3	3.40E+01	3.46E+01	4.26E-01	3.14E-04	1.81E-08	2.48E-04
	D_OUM2_3	4.94E+00	5.13E+00	3.08E-01	8.48E-02	4.89E-02	9.25E-03
	D_BMM3_4	2.63E+01	2.80E+01	6.22E-01	9.32E-03	5.45E-07	9.22E-03
	D_OUM3_4	1.15E+01	1.16E+01	3.14E-01	4.19E-03	1.85E-03	7.36E-04

Skull size

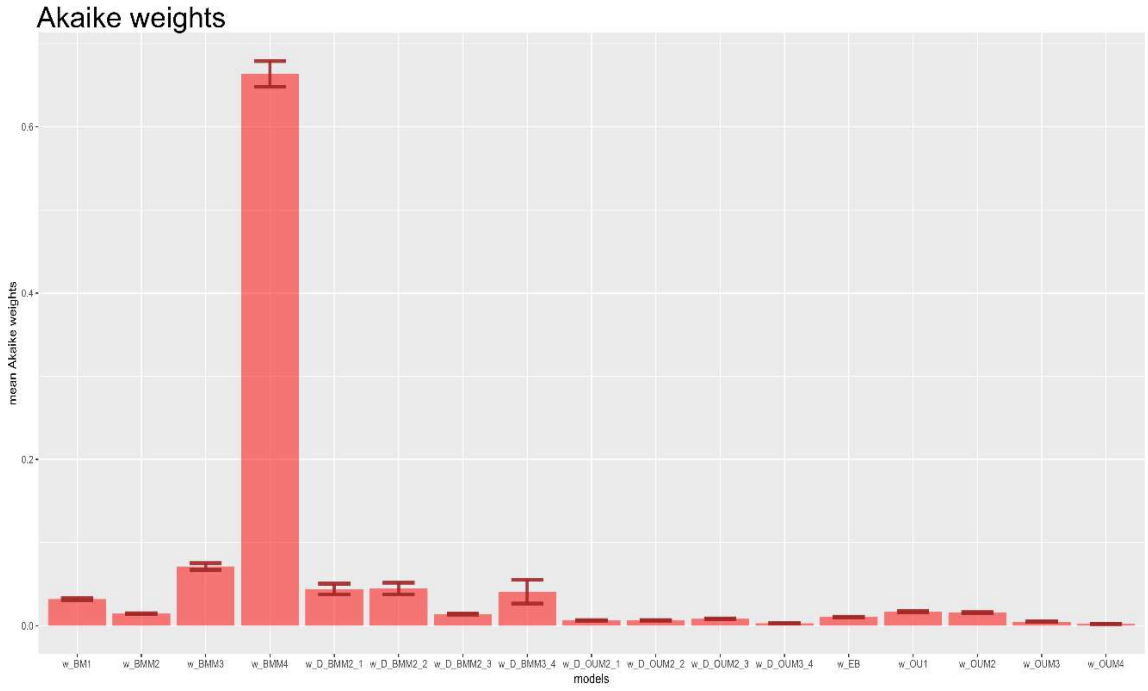
Akaike weights
mean Akaike weights
0.6
0.4
0.2
0.0
w_BM1
w_BMM2
w_BMM3
w_BMM4
w_D_BMM2_1
w_D_BMM2_2
w_D_BMM2_3
w_D_BMM3_4
w_D_OUM2_1
w_D_OUM2_2
w_D_OUM2_3
w_D_OUM3_4
w_EB
w_OU1
w_OUM2
w_OUM3
w_OUM4
models

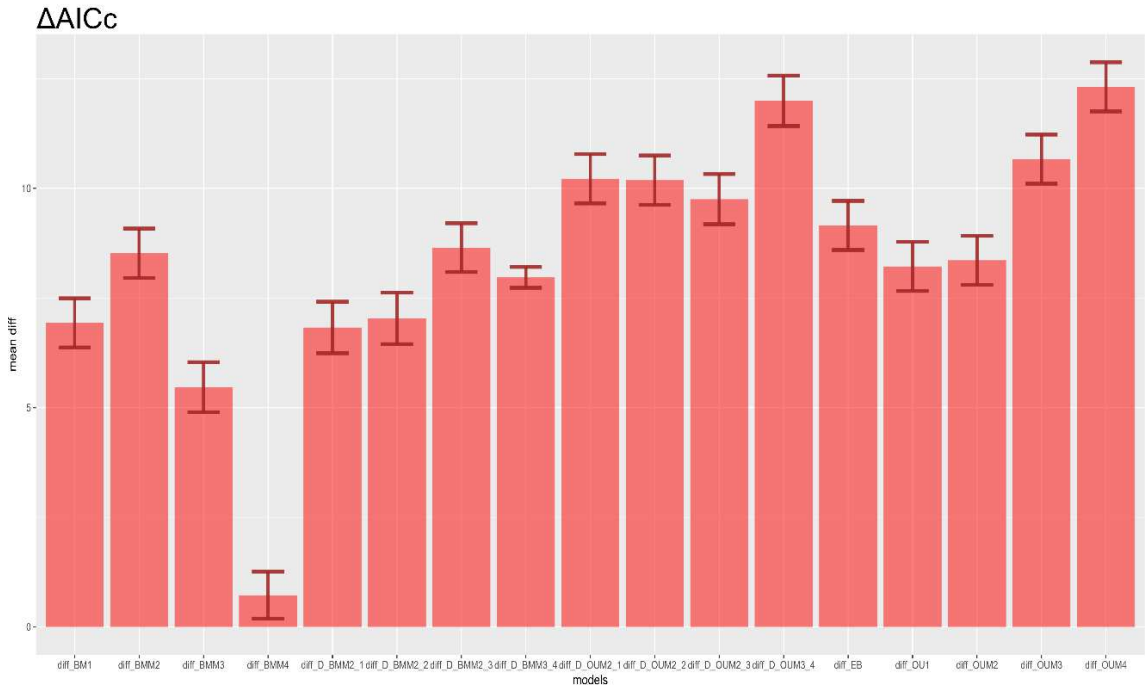
ΔAICc
mean diff
10
5
0
diff_BM1
diff_BMM2
diff_BMM3
diff_BMM4
diff_D_BMM2_1
diff_D_BMM2_2
diff_D_BMM2_3
diff_D_BMM3_4
diff_D_OUM2_1
diff_D_OUM2_2
diff_D_OUM2_3
diff_D_OUM3_4
diff_EB
diff_OU1
diff_OUM2
diff_OUM3
diff_OUM4
models

Skull shape

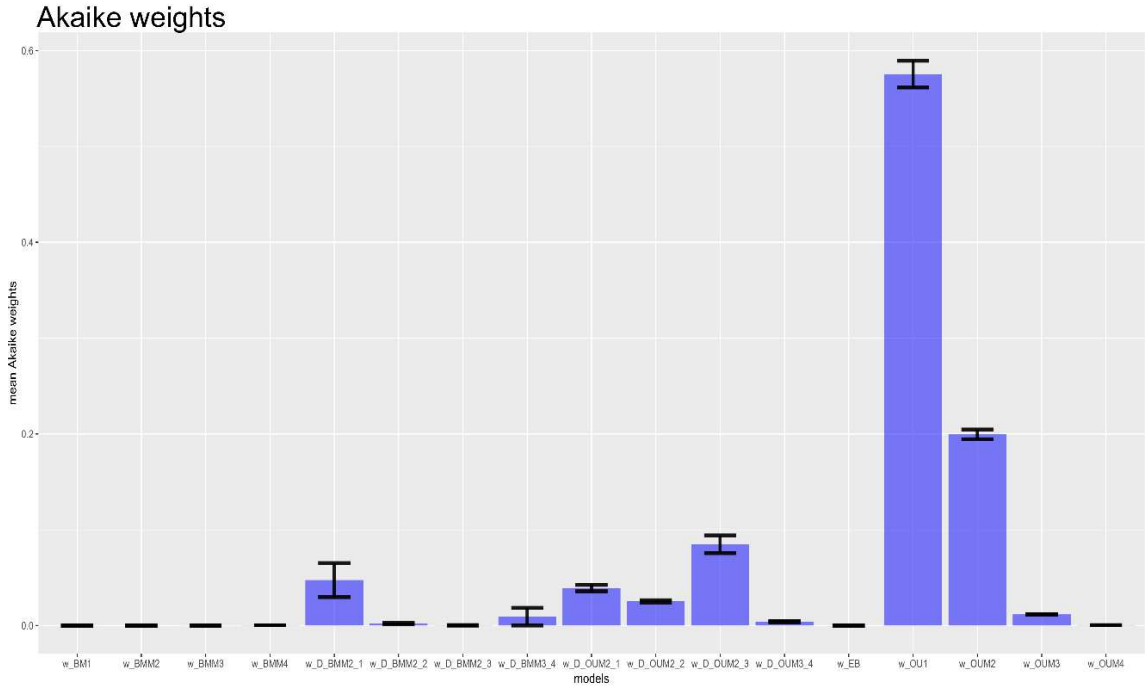
Akaike weights
mean Akaike weights
0.6
0.4
0.2
0.0
w_BM1
w_BMM2
w_BMM3
w_BMM4
w_D_BMM2_1
w_D_BMM2_2
w_D_BMM2_3
w_D_BMM3_4
w_D_OUM2_1
w_D_OUM2_2
w_D_OUM2_3
w_D_OUM3_4
w_EB
w_OU1
w_OUM2
w_OUM3
w_OUM4
models

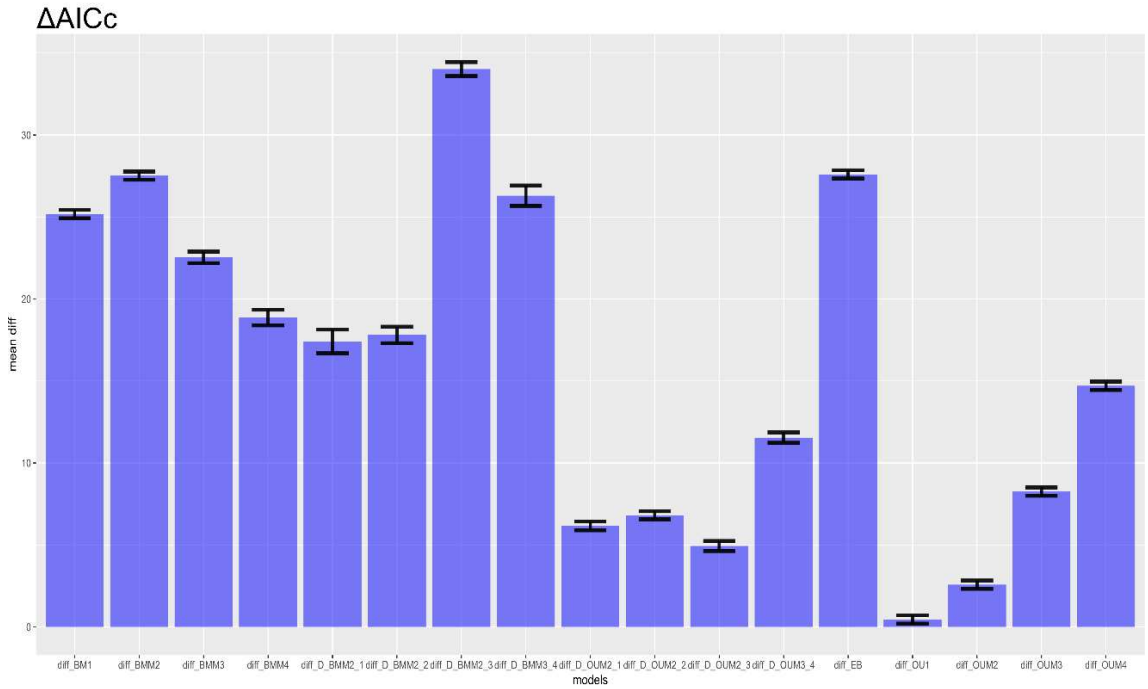
ΔAICc
mean diff
30
20
10
0
diff_BM1
diff_BMM2
diff_BMM3
diff_BMM4
diff_D_BMM2_1
diff_D_BMM2_2
diff_D_BMM2_3
diff_D_BMM3_4
diff_D_OUM2_1
diff_D_OUM2_2
diff_D_OUM2_3
diff_D_OUM3_4
diff_EB
diff_OU1
diff_OUM2
diff_OUM3
diff_OUM4
models

Dataset	Models	Δ_AICc_mean	Δ_AICc_median	Δ_AICc_stder	Weights_mean	Weights_median	Weights_stder
Mandible_size	BM1	6.14E+00	6.17E+00	9.04E-02	2.90E-02	2.84E-02	7.85E-04
	BMM2	8.36E+00	8.39E+00	9.04E-02	9.57E-03	9.42E-03	2.59E-04
	BMM3	6.63E+00	6.56E+00	1.05E-01	2.36E-02	2.16E-02	9.46E-04
	BMM4	7.93E-02	0.00E+00	4.94E-02	5.95E-01	6.08E-01	1.25E-02
	OU1	5.60E+00	5.63E+00	9.04E-02	3.81E-02	3.72E-02	1.03E-03
	OUM2	5.01E+00	5.04E+00	9.04E-02	5.11E-02	4.99E-02	1.38E-03
	OUM3	7.32E+00	7.34E+00	9.08E-02	1.61E-02	1.58E-02	4.41E-04
	OUM4	7.79E+00	7.82E+00	9.05E-02	1.28E-02	1.25E-02	3.46E-04
	EB	8.37E+00	8.40E+00	9.04E-02	9.56E-03	9.35E-03	2.59E-04
	D_BMM2_1	4.96E+00	5.19E+00	1.81E-01	7.04E-02	4.38E-02	7.16E-03
	D_OUM2_1	7.64E+00	7.59E+00	9.37E-02	1.39E-02	1.40E-02	4.37E-04
	D_BMM2_2	5.93E+00	5.93E+00	1.50E-01	3.86E-02	3.01E-02	3.31E-03
	D_OUM2_2	7.58E+00	7.54E+00	1.09E-01	1.51E-02	1.33E-02	1.06E-03
	D_BMM2_3	7.56E+00	7.54E+00	1.08E-01	1.50E-02	1.34E-02	6.34E-04
	D_OUM2_3	7.38E+00	7.36E+00	1.03E-01	1.63E-02	1.49E-02	6.90E-04
	D_BMM3_4	7.07E+00	7.41E+00	1.74E-01	3.57E-02	1.52E-02	1.08E-02
	D_OUM3_4	9.51E+00	9.67E+00	1.37E-01	9.90E-03	4.83E-03	4.49E-03
Mandible_shape	BM1	4.59E+01	4.46E+01	3.74E-01	1.16E-10	1.37E-10	5.12E-12
	BMM2	5.21E+01	5.14E+01	3.95E-01	6.19E-12	4.72E-12	5.23E-13
	BMM3	3.30E+01	3.44E+01	9.20E-01	1.97E-02	2.24E-08	1.37E-02
	BMM4	1.79E+01	2.07E+01	1.02E+00	7.07E-02	1.98E-05	2.04E-02
	OU1	1.29E+00	0.00E+00	3.74E-01	5.66E-01	6.72E-01	2.50E-02
	OUM2	7.49E+00	6.35E+00	3.73E-01	2.56E-02	2.98E-02	1.16E-03
	OUM3	1.41E+01	1.28E+01	3.73E-01	9.52E-04	1.08E-03	4.22E-05
	OUM4	1.80E+01	1.67E+01	3.74E-01	1.34E-04	1.54E-04	6.11E-06
	EB	4.82E+01	4.69E+01	3.74E-01	3.77E-11	4.47E-11	1.67E-12
	D_BMM2_1	3.05E+01	3.19E+01	1.17E+00	2.87E-02	9.51E-08	1.58E-02
	D_OUM2_1	6.37E+00	5.52E+00	3.82E-01	5.02E-02	4.37E-02	3.62E-03
	D_BMM2_2	2.42E+01	2.63E+01	1.20E+00	6.55E-02	1.21E-06	2.06E-02
	D_OUM2_2	6.70E+00	5.56E+00	3.70E-01	3.89E-02	4.11E-02	2.11E-03
	D_BMM2_3	5.67E+01	5.59E+01	4.15E-01	1.62E-12	4.89E-13	7.76E-13
	D_OUM2_3	5.48E+00	5.01E+00	4.52E-01	1.12E-01	5.90E-02	1.21E-02
	D_BMM3_4	3.28E+01	3.47E+01	1.26E+00	1.33E-02	2.06E-08	9.49E-03
	D_OUM3_4	1.10E+01	1.03E+01	4.40E-01	7.52E-03	3.75E-03	1.14E-03

Mandible size

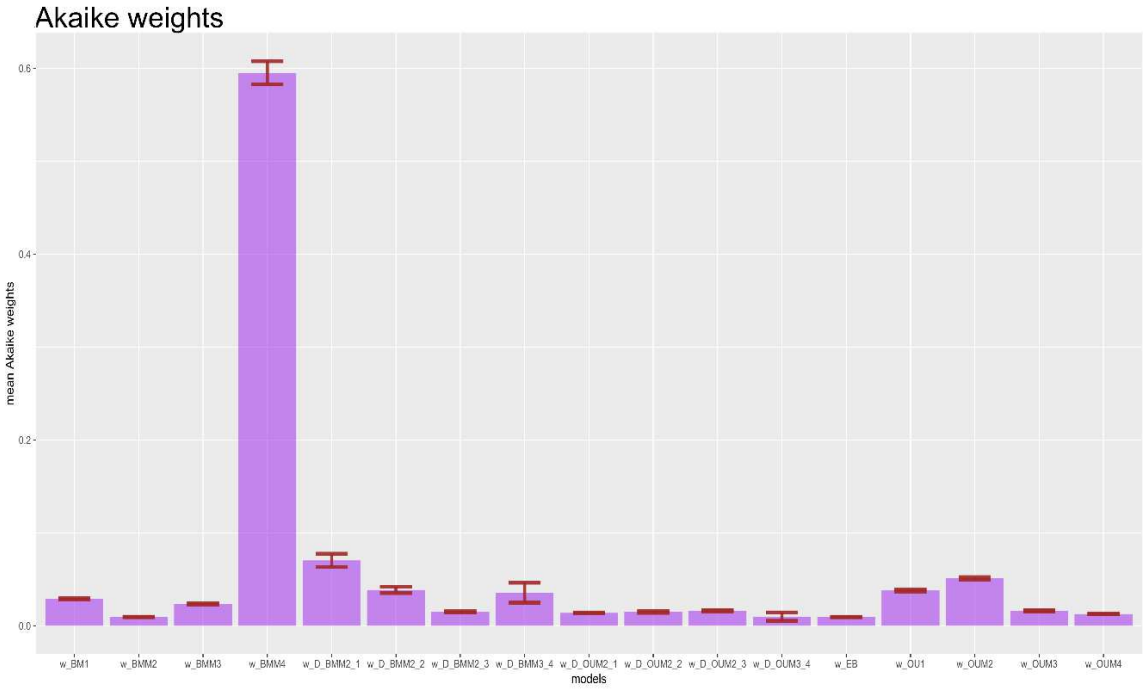

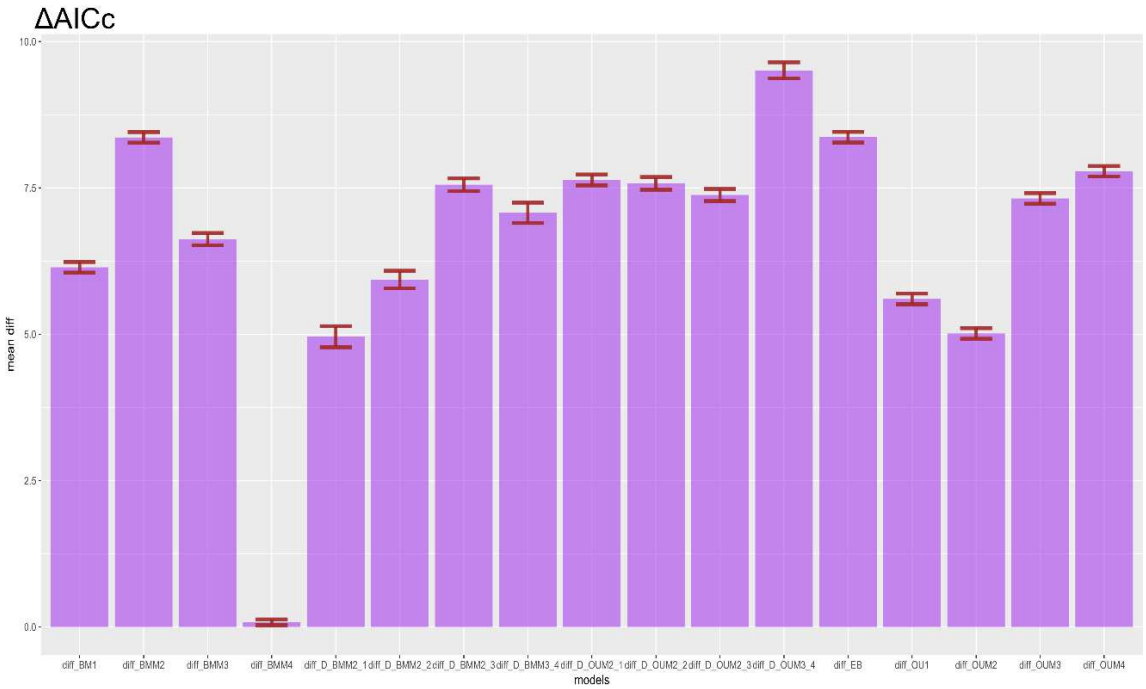

Mandible shape

Akaike weights

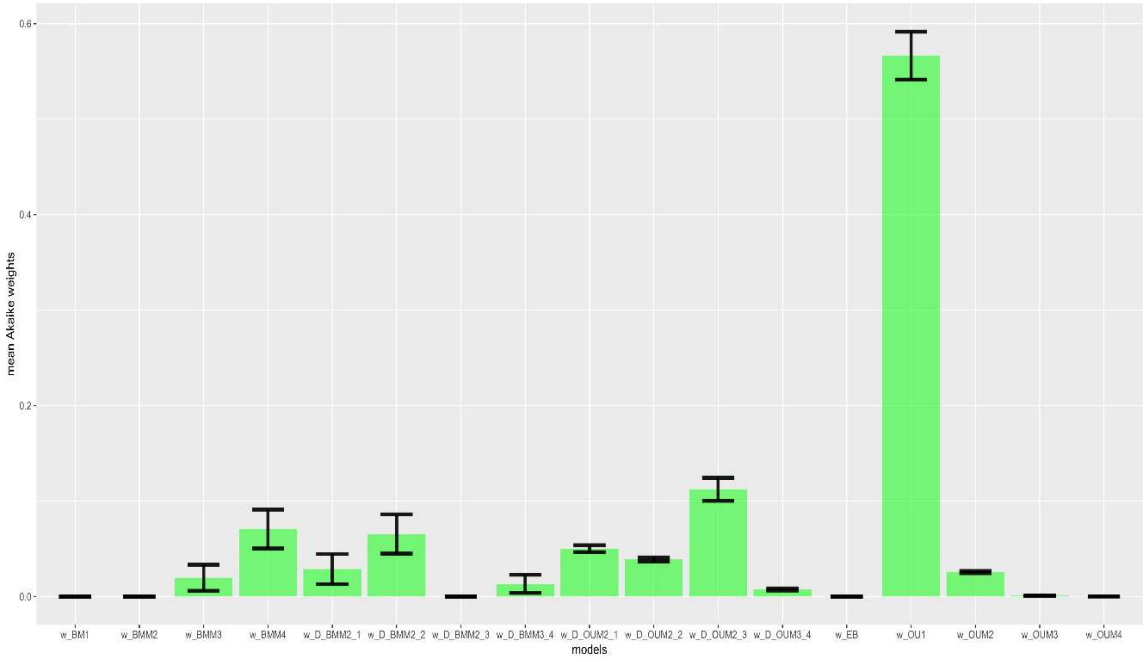

ΔAICc

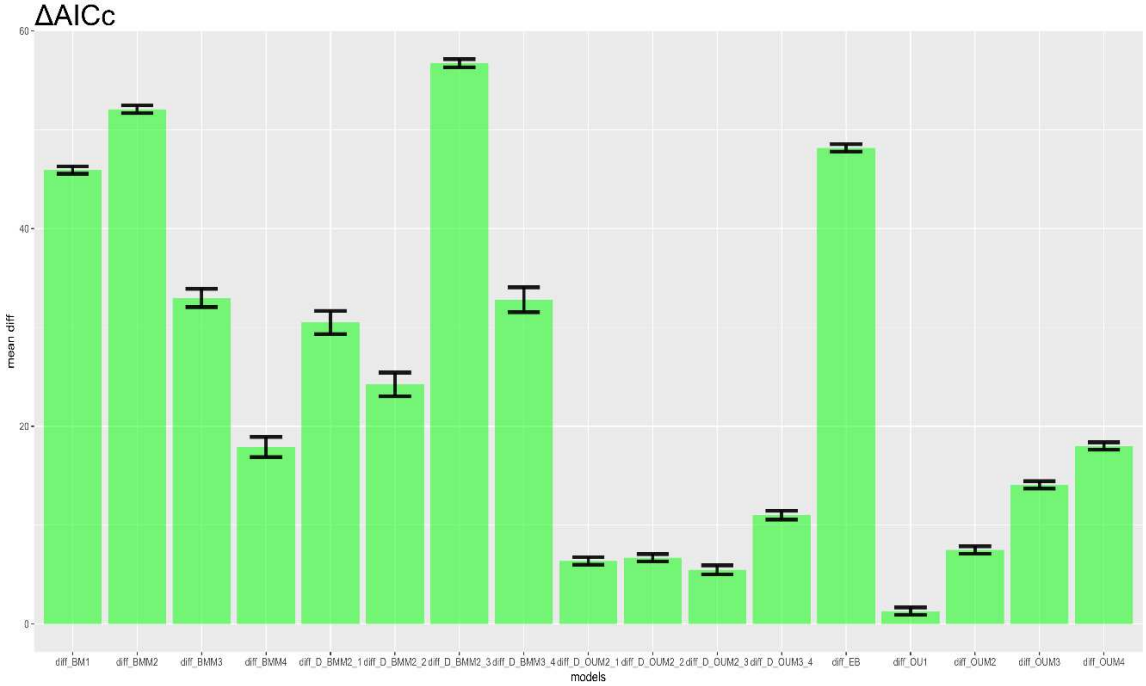

Supplementary Material S7. ASR of diet of akodontine rodents, under the ER (top) and SYM (bottom) models.

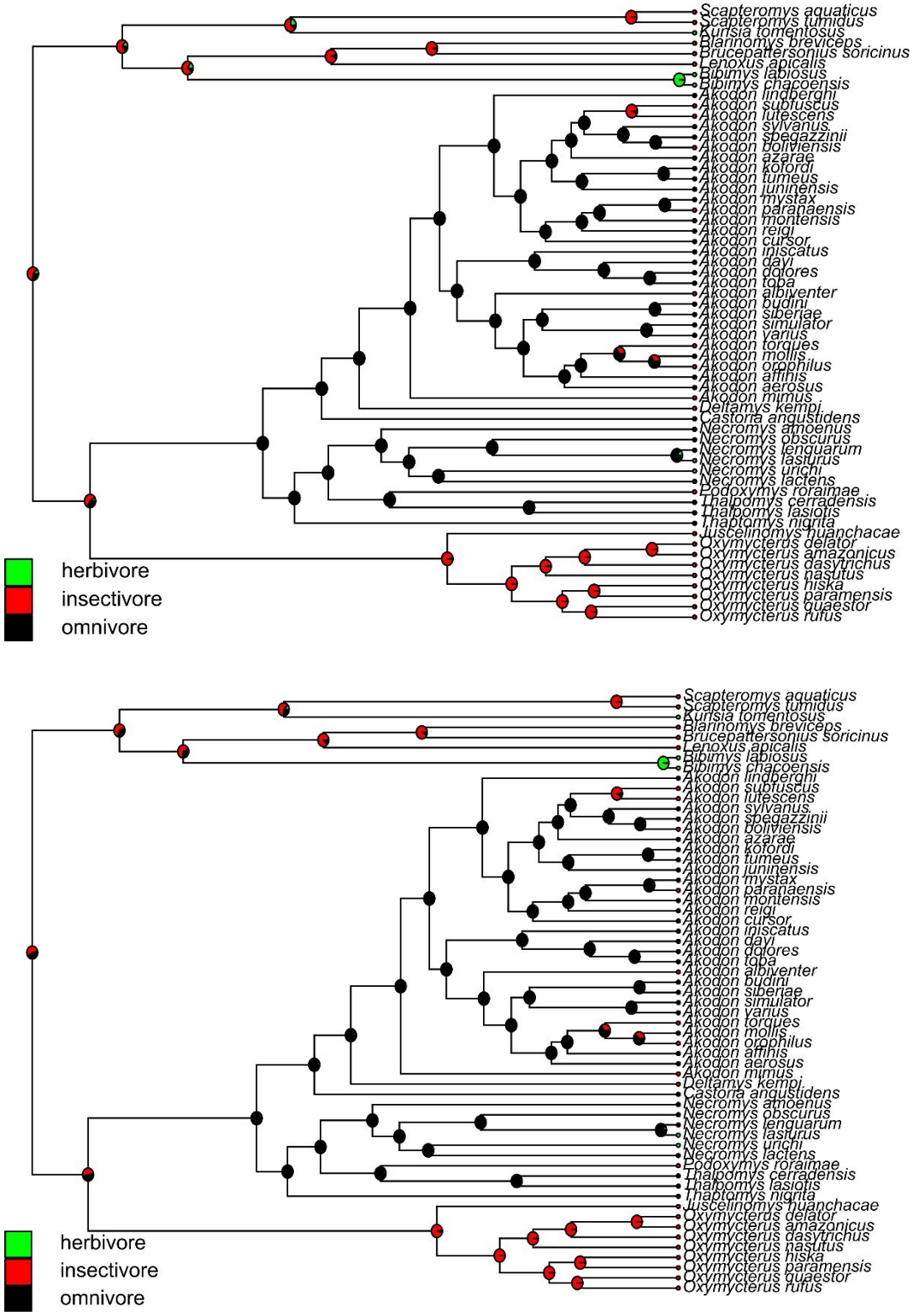

Supplementary Material S8. ASR for PC1 of skull shape of akodontine rodents.

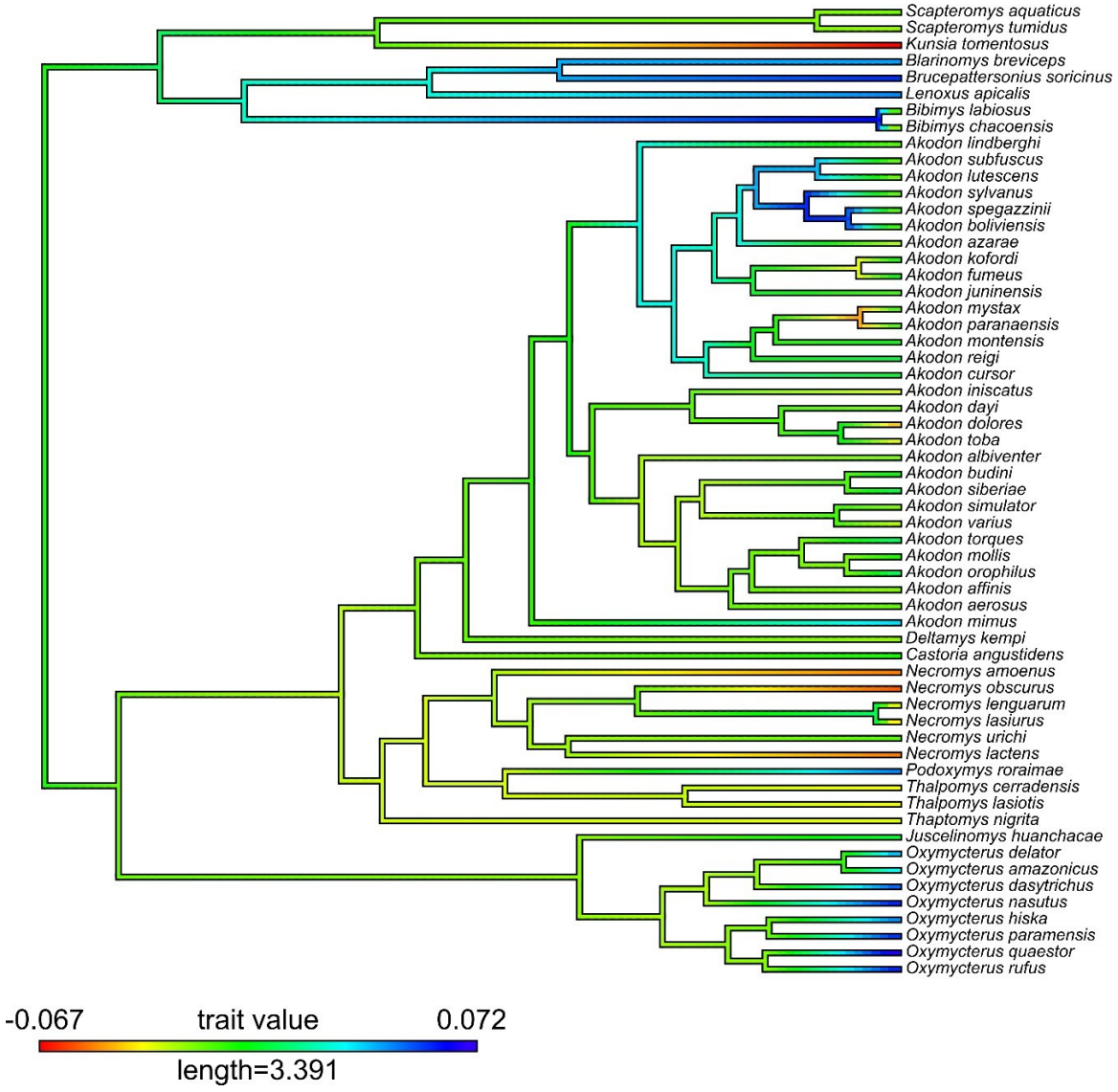

Supplementary Material S9. Convergence plot from *convevol*. Red ellipse delimits the convergent area defined by taxa defined as convergent. Red arrows indicating the path of convergence for the four convergent lineages.

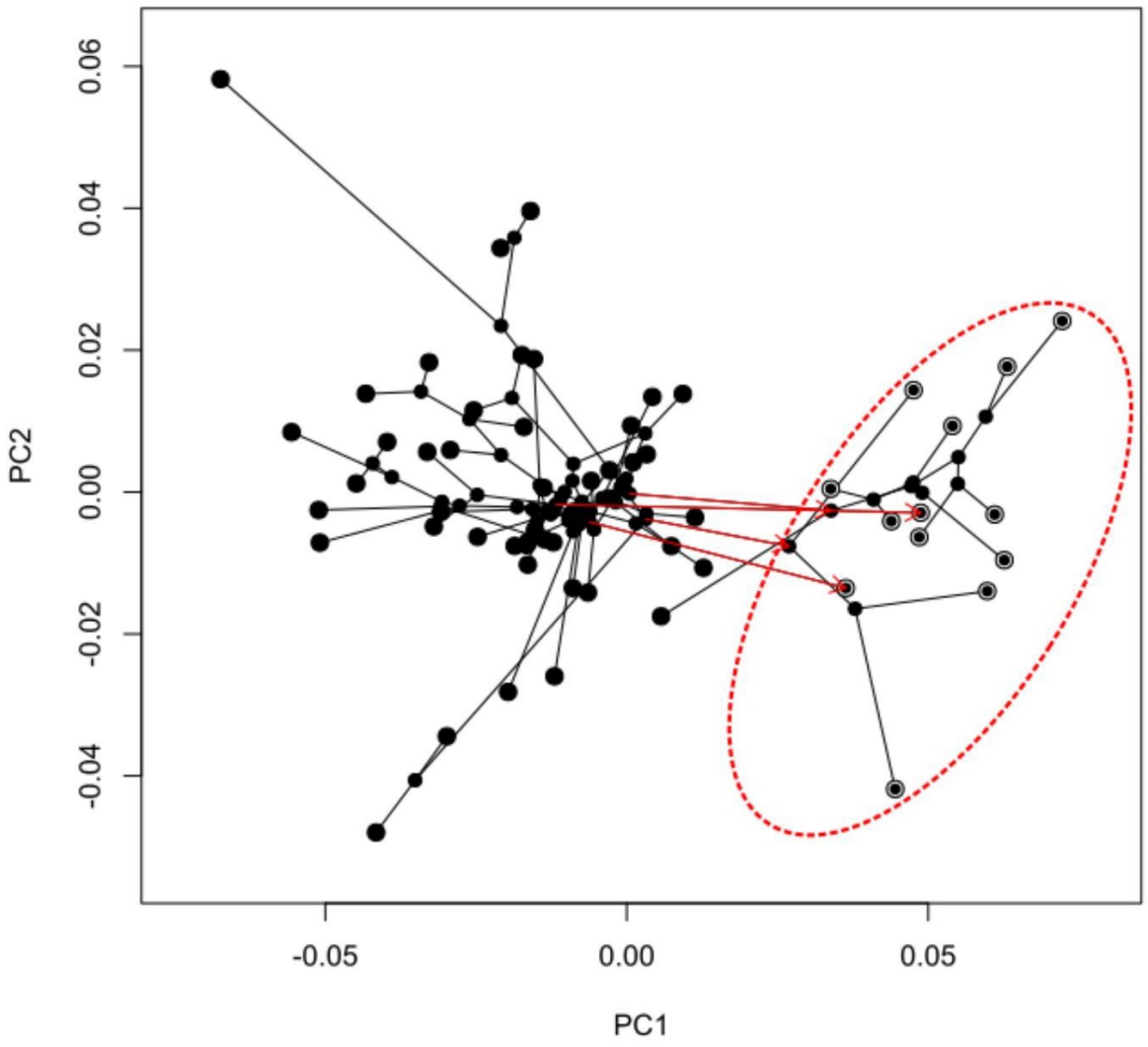

CONCLUDING REMARKS

Akodontini rodents represent an important part of the Neotropical rodent fauna. They can be found from the lowlands of eastern South America to the tepuis on the Guiana shields and grassfields of the Andes. Their ecological versatility is clearly reflected in their morphology, and some akodontines represent a radiation of insectivores that add up to the other lineages of faunivorous species that appeared convergently within rodents.

The tribe is divided into two mais lineages that differ on their patterns of taxonomic and morphological diversity. While one lineage comprises the majority of species of the tribe and do not present high levels of morphological disparity, the other lineage presents a set of few species that appear to have acquired a specialized morphology partly in response to different feeding habits. Stable isotopes gave insights about the narrowing of the trophic niche of these species, which present correspondly specialized morphologies. This pattern could appear in response to higher rates of trait evolution, causing species to diverge on cranial morphology; or due to high extinction rates, when compared to its sister lineage, which would erase part of their evolutionaryhistory, leaving only some species that occupy morphological extremes.

Feeding ecology seems to have a secondary, but important, role in shaping cranial morphology of Akodontini rodents. The different diets are reflected on jaw functional traits, with short and higher mandibles representing species that consume more abrasive diets, contrasting with the slender and long mandibles of invertebrate feeders. Considering the relationship between carbon isotope values and functional measures of the mandible, it seems that the consumption of more fibrous plants is limited by functional properties related to masticatory efficiency. On the other hand, some species may occasionally rely on invertebrate consumption depending on the availability of resources, and the consumption of invertebrates does not seems to be limited by the presence of morphofunctional characteristics that favor the capture of prey.

This feeding specialization seems to have given rise to an insectivorous convergent morphology at least four times in the evolutionary history of akodontines. Insectivorous placentals, like shrews and moles, are absent in most of South America, and this niche is mainly occupied by marsupials and some rodents. Although some Akodontini species may only occasionally consume invertebrates, others seem remarkably specialized for this task, and their widespread distribution across South America may represent a successful occupation of the insectivorous niche on the

continent. Considering the trade-off between bite force and jaw closing speed, this relationship between form and function may depend on crossing a threshold where a species gives up its bite force in favor of a configuration that increases hunting efficiency, allowing a species to base its diet almost entirely on invertebrates. While maybe moresubject to seasonal variations, this kind of resources are more energetically rich and its consumption may provide an evolutionary advantage for these species.

In a group as diverse as rodents, the latest computational tools have helped us reach a better understanding of their evolution. New data on natural history will always be welcome to refine these results. It has become clear that, to understand why species are morphologically different, it is necessary to understand how selective factors and phylogenetic history affect their evolutionary history. We hope that this work will allow discussions about how multidisciplinary approaches are useful when we want to have a clearer picture of macroevolutionary patterns.